

UNIVERSITE DE LILLE
FACULTE DE PHARMACIE DE LILLE
Ecole Doctorale Biologie-Santé

In vitro drug release from 3D printed biodegradable dosage forms

**Libération in vitro de substance active à partir de formes
galéniques biodégradables imprimées en 3D**

THESE DE DOCTORAT

Soutenue le 04 février 2022 à Lille

Par **Céline BASSAND**

Dirigée par Pr. Juergen SIEPMANN

*Laboratoire INSERM U1008, Médicaments et biomatériaux à libération contrôlée :
mécanismes et optimisation*

JURY :

Professeur Yann PELLEQUER

Professeur Abdul BASIT

Professeur Jérémie SOULESTIN

Professeur Juergen SIEPMANN

Rapporteur

Rapporteur

Président de jury

Directeur de thèse

« Merci pour les roses, merci pour les épines. »

Jean d'Ormesson

Remerciements

En premier lieu je tiens à remercier mon directeur de thèse, le **Pr Juergen Siepmann** ; pour la confiance qu'il m'a accordé tout au long de ces trois années, ainsi que les précieux et nombreux conseils qu'il a su me prodiguer et qui m'ont aidé à me développer. Travailler au sein de l'unité qu'il dirige a été une aventure heureuse.

Mes remerciements vont au **Pr Jérémie Soulestin**, qui me fait l'honneur de présider ce jury. Je tiens également à le remercier pour son soutien et son ouverture à la collaboration durant ces trois années à travers le projet 3D med.

Je tiens également à remercier vivement le **Pr. Abdul Basit**, qui me fait l'honneur de juger et d'évaluer ces trois années de travail.

Merci également au **Pr. Yann Pellequer**, qui a su dès ma première année d'étude supérieure me transmettre sa passion pour la galénique et la biopharmacie. Il y a 10 ans il me donnait mes premiers cours de pharmacie galénique, aujourd'hui il me fait l'honneur d'évaluer mes travaux de thèse, c'est une belle façon de clôturer ce dernier chapitre de ma vie étudiante.

Je tiens également à remercier le **Pr Florence Siepmann** pour son partage, son savoir, ses qualités scientifiques et aussi humaines, ainsi que pour sa présence pendant ces trois années de thèse.

Tous mes remerciements aux **Dr. Sébastien Charlon**, et **Dr. Cédric Samuel**, pour m'avoir accueilli quelques fois au sein de l'IMT Lille-Douai, et pour avoir pris le temps de partager avec moi leurs connaissances.

Un grand merci également à **Jérémy Vérin**, pour son aide, son support, et pour toujours avoir répondu présent en cas de problème. Je garderais en mémoire les longues journées passées ensemble pour les photos SEM, mais aussi ton humour et les moments de partage autour d'un verre, d'un repas ou d'un café.

Travailler pendant ces trois années au sein de l'INSERM U 1008 m'a permis de rencontrer des personnes sans lesquelles cette aventure aurait eu une saveur bien différente.

Mes coéquipiers de l'ancienne vague qui m'ont vu passer par toutes sortes d'émotions : **Youcef, Martin L., Coco, Adam**. Et surtout mes deux coéquipières, qui avec le temps sont devenues de véritables amies, des oreilles attentives, des épaules sur lesquelles me reposer, des rires à partager : **Fahima** et **Doha**, avoir croisés vos chemins a été un véritable cadeau. Il y a également mes collègues de la nouvelle vague : **Yanis, Fabiana, Lise-Anne, Filipa, Charline** et **Samuel**, vous êtes chacun à votre façon venu ajouter votre touche de couleur et de bonne humeur dans cette aventure. Je vous souhaite à tous beaucoup de réussite à venir, et espère avoir

encore de belles occasions de partager des moments avec vous autour d'un « *thé* », d'un gâteau, d'une petite blague ou bien de la suite de « *la dernière série* » hollywoodienne.

Je remercie également tous les stagiaires que j'ai eu la chance d'encadrer : ***Célia, Clotilde, Martin, Hanna, Jana, Cédric et Lydia***, j'espère avoir réussi à vous transmettre autant que j'ai pu apprendre à vos côtés. Ainsi que ceux que je n'ai pas encadré, mais dont la présence m'a marqué, je pense particulièrement à ***Synthia et Nina***.

Un grand merci à ***Laurence***, et ***Alexandra*** avec lesquelles j'ai adoré partager discuter du quotidien, de nos vies, de nos vacances etc.

Merci également à tous les membres de l'U 1008, avec lesquels j'ai eu l'occasion d'échanger des moments agréables : ***Dr. Susanne Muschert, Dr. Younes Karrouit, Dr. Kevimy Agossa, Mickael Maton, Hugues Florin, Muriel Deudon***.

Cette thèse n'aurait pas pu aboutir non plus sans le soutien de ma famille et de mes amis. C'est pourquoi je tiens à les remercier tout particulièrement.

Mes parents, qui ont su me transmettre le goût d'aller au bout des choses, de ne jamais baisser les bras et de toujours se relever, qui ont toujours fait tout ce qu'ils pouvaient pour me permettre de mener à bien mes études. J'espère pouvoir vous rendre au centuple tout ce que vous avez fait pour nous.

Ma sœur, qui a su très tôt alimenter en moi la flamme de la curiosité scientifique. Qui a toujours été pour moi un modèle et un exemple, et dont le soutien a été essentiel durant ces trois dernières années mais pas uniquement.

Mes neveux, et ***ma nièce***, qui me donnent chaque jour envie de participer à ma manière à créer un meilleur monde pour demain, et qui m'aident à leur manière à garder mon âme d'enfant.

Mes amis, ceux qui sont là depuis près de 20 ans maintenant, ceux que j'ai connu au lycée, à la faculté, ou bien encore plus récemment en arrivant à Lille.

Et plutôt deux fois qu'une : *last but not least* ***Jad***, mon partenaire au quotidien, mon meilleur ami, mon plus grand soutien, mes meilleurs fou rires et mes plus beaux souvenirs. Après avoir traversé ensemble, nos études de pharmacie et notre vie lilloise, à nous d'écrire le prochain chapitre. Et je suis sûre qu'il sera magique puisqu'on l'écrit ensemble.

Table des matières

Abbreviation list	i
Charts list	xi
I. GENERAL INTRODUCTION	1
I.1. Control drug delivery.....	3
I.1.1. Definitions	3
I.1.2. Long-acting injectables	4
I.1.3. Testing <i>in vitro</i> drug release from dosage forms designed to subcutis	6
I.2. Poly(lactic-co-glycolic) acid	13
I.2.1. General characteristics and synthesis	13
I.2.2. Molecular weight.....	13
I.2.3. Crystallinity and glass transition temperatures	14
I.2.4. Hydrophilic properties and solubility.....	15
I.2.5. Biodegradation	15
I.2.6. Biocompatibility	17
I.2.7. Use in control drug delivery	17
I.2.8. Release mechanisms and release pattern.....	19
I.3. Three-dimensional printing technologies.....	25
I.3.1. Generalities.....	25
I.3.2. Classification.....	26
I.3.3. Use in the pharmaceutical field	37
I.4. Research objectives	45
I.5. References	47
II. HOW HYDROGELS SURROUNDING PLGA IMPLANTS LIMIT SWELLING AND SLOW DOWN DRUG RELEASE	63
II.1. Abstract.....	65
II.2. Introduction.....	67
II.3. Materials and methods	71
II.3.1. Materials.....	71
II.3.2. Implant preparation	71
II.3.3. Practical drug loading.....	71
II.3.4. In vitro drug release.....	71
II.3.5. Implant swelling	73
II.3.6. Implant erosion and PLGA degradation.....	73
II.3.7. Differential scanning calorimetry (DSC)	74
II.3.8. Scanning electronic microscopy (SEM).....	74
II.4. Results and discussion	75
II.4.1. In vitro release set-ups.....	75
II.4.2. Drug release and implant swelling	77
II.4.3. Implant erosion and PLGA degradation.....	83
II.5. Conclusion	90
II.6. Acknowledgements	90
II.7. Authors statement.....	90
II.8. References	91
III. HOT MELT EXTRUDED IBUPROFEN-LOADED PLGA IMPLANTS: IMPORTANCE OF HEAT EXPOSURE	95
III.1. Abstract.....	97
III.2. Introduction.....	99

III.3. Materials and methods	101
III.3.1. Materials.....	101
III.3.2. Implant preparation	101
III.3.3. Practical drug loading.....	102
III.3.4. In vitro drug release.....	102
III.3.5. Implant swelling	102
III.3.6. Implant erosion and PLGA degradation.....	103
III.3.7. Differential scanning calorimetry (DSC)	103
III.3.8. X ray powder diffraction	104
III.3.9. Scanning electronic microscopy (SEM).....	104
III.4. Results and discussion	105
III.4.1. Implants before exposure to the release medium	105
III.4.2. Implants after exposure to the release medium	109
III.5. Conclusions.....	116
III.6. Acknowledgments	116
III.7. Author statement	116
III.8. References	118
IV. PLGA IMPLANTS FOR CONTROLLED DRUG RELEASE: IMPACT OF THE DIAMETER.....	123
IV.1. Abstract.....	125
IV.2. Introduction.....	127
IV.3. Materials and methods	129
IV.3.1. Materials.....	129
IV.3.2. Implant preparation	129
IV.3.3. Optical macroscopy.....	129
IV.3.4. Practical drug loading.....	129
IV.3.5. Differential scanning calorimetry (DSC)	130
IV.3.6. In vitro drug release.....	130
IV.3.7. Implant swelling	132
IV.3.8. Implant erosion and PLGA degradation.....	132
IV.3.9. Scanning electronic microscopy (SEM).....	133
IV.4. Results and discussion	134
IV.4.1. Implants before exposure to the release medium	134
IV.4.2. Implants after exposure to the release medium	138
IV.5. Conclusions.....	146
IV.6. Acknowledgments	146
IV.7. Authors statement	146
IV.8. References	147
V. HOW BULK FLUID RENEWAL CAN AFFECT DRUG RELEASE FROM PLGA IMPLANTS.....	151
V.1. Abstract.....	153
V.2. Introduction	155
V.3. Materials and methods.....	158
V.3.1. Materials.....	158
V.3.2. Implant preparation	158
V.3.3. Optical macroscopy and implant dimensions.....	158
V.3.4. Practical drug loading.....	158
V.3.5. Drug solubility measurements.....	159
V.3.6. In vitro drug release.....	159
V.3.7. Implant swelling	161

V.3.8. Implant erosion and PLGA degradation.....	161
V.3.9. Scanning electronic microscopy (SEM).....	162
V.4.Results and discussion.....	163
V.4.1. In vitro drug release and implant swelling	163
V.4.2. PLGA degradation and implant erosion	168
V.5.Conclusions	171
V.6.Acknowledgments.....	171
V.7.Author statement.....	171
V.8.References	172
VI. 3D PRINTING OF IBUPROFEN LOADED CONTROLLED RELEASE IMPLANTS WITH PLGA – PROOF OF CONCEPT AND IMPACT FILLING PATTERN ON DRUG RELEASE	175
VI.1. Abstract.....	177
VI.2. Introduction.....	179
VI.3. Materials and methods	181
VI.3.1. Materials.....	181
VI.3.2. Differential scanning calorimetry (DSC)	181
VI.3.3. Thermogravimetric analysis (TGA).....	181
VI.3.4. Disc preparation	181
VI.3.5. Melt rheology	182
VI.3.6. Hot-melt extrusion.....	182
VI.3.7. 3D printing test.....	183
VI.3.8. Practical drug loading.....	184
VI.3.9. Gel permeation chromatography (GPC)	184
VI.3.10. In vitro drug release.....	184
VI.3.11. Implant swelling	185
VI.4. Results and discussion	186
VI.4.1. Raw materials characterization	186
VI.4.2. Melt rheology studies	187
VI.4.3. Preliminary printing test.....	188
VI.4.4. In vitro drug release performance	191
VI.5. Conclusion	193
VI.6. Acknowledgments	194
VI.7. Author statement	194
VI.8. References	195
VII. PLGA BASED 3D PRINTED IMPLANT – IMPACT OF THE 3D PRINTED TECHNOLOGY ON DRUG RELEASE	199
VII.1. Abstract.....	201
VII.2. Introduction.....	203
VII.3. Materials and methods	205
VII.3.1. Materials.....	205
VII.3.2. Implants preparation.....	205
VII.3.3. Optical microscopy	207
VII.3.4. Practical drug loading.....	207
VII.3.5. Differential scanning calorimetry (DSC)	208
VII.3.6. Gel permeation chromatography (GPC)	208
VII.3.7. In vitro drug release.....	208
VII.3.8. Implants swelling	209
VII.3.9. Implants erosion and PLGA degradation	209
VII.3.10. . Scanning electronic microscopy (SEM)	210

VII.4. Results and discussion	211
VII.4.1. Characterization of the implants before exposure to the release medium.....	211
VII.4.2. Characterization of the implants after exposure to the release medium	216
VII.5. Conclusion	220
VII.6. Acknowledgments	221
VII.7. Author statement	221
VII.8. References	222
VIII. PLGA BASED 3D PRINTED IMPLANTS – IMPACT OF FILLING DENSITY ON DRUG RELEASE	228
VIII.1. Abstract	230
VIII.2. Introduction	232
VIII.3. Materials and methods.....	234
VIII.3.1. Materials	234
VIII.3.2. Pellets preparation	234
VIII.3.3. 3D printing of the implant	234
VIII.3.4. Optical microscopy	235
VIII.3.5. Practical drug loading.....	235
VIII.3.6. Differential scanning calorimetry (DSC)	235
VIII.3.7. Gel permeation chromatography (GPC)	236
VIII.3.8. In vitro drug release.....	236
VIII.3.9. Implant swelling	236
VIII.3.10. Implant erosion and PLGA degradation	237
VIII.3.11. Scanning electronic microscopy (SEM)	237
VIII.4. Results and discussion.....	238
VIII.4.1. Characterization of the implants before exposure to the release medium.....	238
VIII.4.2. Characterization of the implant after exposure to the release medium	241
VIII.5. Conclusion.....	245
VIII.6. Acknowledgements.....	245
VIII.7. Author statement.....	245
VIII.8. References	247
IX. GENERAL CONCLUSION AND DISCUSSION	252
IX.1. General conclusion.....	254
IX.2. Future perspectives	257
SUMMARY.....	258
RESUME.....	262
LIST OF PUBLICATIONS.....	266
CURRICULUM VITAE	272

Abbreviation list

3D	Three dimension
AM	Additive manufacturing
API	Active pharmaceutical ingredient
BJ	Binder Jetting
CBAM	Composite Based Additive Manufacturing
CLIP	Continuous Liquid Interface Production
DDM	Droplet Deposition Modeling
DED	Direct Energy Deposition
DLP	Digital Light processing
DMLS	Direct Metal Laser Sintering
DOD	Drop On Demand
DPE	Direct Powder Extrusion
DPP	Daylight Polymer Printing
DSC	Differential scanning calorimetry
EBAM	Electron Beam Additive Manufacturing
EBM	Electron Beam Melting
EDQM	European Directorate for Quality of Medicines & HealthCare
FDA	Food and Drug Administration
FDM	Fused Deposition Modeling
FFF	Fused Filament Fabrication
GA	Glycolic acid
GA	Glycolic Acid
LA	Lactic acid
LA	Lactic Acid
LCD	Liquid Crystal Display
LDW	Laser Deposition Welding
LOM	Laminated Object Manufacturing
ME	Material extrusion
MJ	Material Jetting
MJF	Multi Jet Fusion
Mw	Average molecular weight
NPJ	NanoParticle Jetting
PBF	Powder Bed Fusion
PE/SE	Pneumatic or Syringe Extrusion
PLGA	Poly (lactic-co-glycolic acid)
SEM	Scanning electronic microscopy
SHS	Selective Heat Sintering
SL	Sheet Lamination
SLA	Stereolithography
SLCOM	Selective Lamination Composite Object Manufacturing
SLM	Selective Laser Melting
SLS	Selective Laser Sintering
T _g	Glass transition temperature
T _m	Melting temperature
UC	Ultrasonic Additive Manufacturing
USP	United State Pharmacopeia

Figures list

Figure I-1. Active pharmaceutical ingredient plasmatic concentration, after repeated administration of conventional drug delivery systems (green lines) and administration from an "ideal" controlled drug delivery system (blue line).....	3
Figure I-2. Requirement for long-acting injectables formulations. Mandatory attributes are reported in black and desirable ones in grey. Adapted from Selmin et al. 2020.....	5
Figure I-3. Schematic illustration of sample and separate in vitro drug release method. Figure created using (20).....	6
Figure I-4. Schematic illustration of the United States Pharmacopeia apparatus (A) I: basket, and (B) II: paddle.....	7
Figure I-5. Schematic illustration of the United States Pharmacopeia apparatus IV: continuous flow-through method.....	7
Figure I-6. Schematic illustration of the dialysis-based in vitro drug release method. Figure created using (20).	8
Figure I-7. Synthesis of Poly (lactic-co-glycolic acid) by (A) polycondensation and (B) ring-opening polymerization.	13
Figure I-8. Summary of the main characteristics, and schematic arrangement of molecular chains in crystalline, semi-crystalline, and amorphous polymers.	15
Figure I-9. The acid-catalyzed ester hydrolysis of poly (lactic-co-glycolic acid). Adapted from Ford Versypt et al. 2013.	16
Figure I-10. Illustration of the size-dependent autocatalytic effect. Adapted from Ford Versypt et al. 2013.	16
Figure I-11. Schematic representation of the elimination and metabolization of the poly (lactic-co-glycolic) degradation products. Adapted from Maurus et al. 2004.....	17
Figure I-12. The number of publications referring to PLGA per year from 1965 (1 publication) to 2020 (1127 publications).....	19
Figure I-13. Schematic representation of the active pharmaceutical ingredient release mechanisms from a poly (lactic-co-glycolic acid) device: (A) diffusion through water-filled pores, (B) diffusion through the polymer matrix, and (C) degradation or erosion of the polymer matrix. Adapted from Fredenberg et al. 2011.	20
Figure I-14. Change of dry mass and molecular weight of the polymer in the case of (A) surface erosion and (B) bulk erosion. Adapted from Grund et al. 2011.....	21
Figure I-15. Schematic representation of the different release patterns of a drug substance from a poly (lactic-co-glycolic acid) device.	22
Figure I-16. Timeline of three-dimensional printing technologies.	25
Figure I-17. Schematic representation of photopolymerization-based three-dimensional printing technologies.	26
Figure I-18. Schematic representation of powder bed fusion-based three-dimensional printing technologies. ...	28
Figure I-19. Schematic representation of fused deposition modeling or fused filament fabrication three-dimensional printing technologies.	30
Figure I-20. Schematic representation of “Arburg Plastic Freeforming [®] ” technology - a proprietary droplet deposition modeling process.	31
Figure I-21. Schematic representation of material jetting-based three-dimensional printing technologies.	32
Figure I-22. Schematic representation of binder jetting-based three-dimensional printing technologies.	34

Figure I-23. Schematic representation of direct energy deposition-based three-dimensional printing technologies.	35
Figure I-24. Schematic representation of sheet lamination-based three-dimensional printing technologies.	36
Figure I-25. Different classes of 3D printing technologies, the ones used in pharmaceutical field have been colored in green, and the other ones in dark blue. Adapted from Lim et al 2018.	38
Figure I-26. Illustration of the different possibilities to modulate the structure to control the drug release from 3D printed devices. Adapted from Patel et al 2021.....	40
Figure I-27. Examples of reported studies on the effect of the external structure of 3D printed devices on drug release. Adapted from (A) Goyanes et al.(135) and (B) Fu et al.(180).	41
Figure I-28. Examples of reported studies on the effect of the internal structure of 3D printed devices on drug release. Adapted from (A) Yang et al. (181), (B) Zhang et al.(182), and (C) Welsh et al. (138).....	42
Figure I-29. Examples of reported studies on the effect of size and structure of 3D printed devices on drug release. Adapted from (A) Xu et al. (183), (B) Tan et al.(184), and (C) Russi et al. (185).....	43
Figure II-1. Schematic presentations of the experimental set-ups used to monitor drug release from PLGA-based implants in: A) well agitated phosphate buffer pH 7.4 (in metal baskets) in Eppendorf tubes, B) agarose gels in Eppendorf tubes, the gels being exposed to well agitated phosphate buffer pH 7.4, C) agarose gels in transwell plates, the receptor compartment containing well agitated phosphate buffer pH 7.4. In all cases, sink conditions were provided throughout the experiments in the well agitated bulk fluids. Optionally, pH indicators were added to the phosphate buffer. Details are described in the text. The diagram in D) shows the rates at which an ibuprofen solution (200 µg/mL) was “released” from the donor compartment in a transwell plate free of gel, or from a gel in an Eppendorf tube or from a gel in a transwell plate.	77
Figure II-2. Ibuprofen release from and swelling of PLGA implants upon exposure to phosphate buffer pH 7.4, observed using 3 experimental set-ups: In bulk fluids in Eppendorf tubes, in agarose gels exposed to the release medium in Eppendorf tubes, and in agarose gels in transwell plates (the acceptor compartment containing the release medium). Please note the different scaling of the x-axes on the left versus the right hand side.	78
Figure II-3. SEM pictures of surfaces and cross sections of ibuprofen-loaded PLGA implants before and after exposure to phosphate buffer pH 7.4 using the 3 experimental set-ups. The type of set-up and exposure times are indicated on the left hand side. Please note that after exposure to the release medium the implants were freeze-dried prior to analysis. Thus, caution must be paid due to artefact creation.	80
Figure II-4. Optical macroscopy pictures of surfaces and cross sections of ibuprofen-loaded PLGA implants before and after exposure to phosphate buffer pH 7.4 using 3 experimental set-ups: In bulk fluids in Eppendorf tubes, in agarose gels exposed to the release medium in Eppendorf tubes, and in agarose gels in transwell plates (the acceptor compartment containing the release medium). The exposure times are indicated at the top, the type of set-up is indicated on the left hand side	82
Figure II-5. Simplified schematic presentation of the mass transport mechanisms controlling ibuprofen release from the investigated PLGA implants. Initially, limited amounts of water diffuse into the system, leading to polyester degradation throughout the implants (“bulk erosion”). As soon as a critical polymer molecular weight is reached, substantial amounts of water penetrate into the device, facilitating subsequent drug release. Details are described in the text.	83

Figure II-6. Dynamic changes in the pH of the well agitated bulk fluids, dry mass (%) of the implants and PLGA polymer molecular weight (Mw) upon exposure of the implants to phosphate buffer pH 7.4 in the 3 experimental set-ups: In bulk fluids in Eppendorf tubes, in agarose gels exposed to the release medium in Eppendorf tubes, and in agarose gels in transwell plates (the acceptor compartment containing the release medium). Please note the different scaling of the x-axes on the left versus the right hand side. The Asterix indicates that the average polymer molecular weight (Mw) was below 5 kDa. 85

Figure II-7. Optical macroscopy pictures of ibuprofen-loaded PLGA implants embedded in agarose gels (“gel – Eppendorf” and “gel – transwell” set-ups) before and after exposure to phosphate buffer pH 7.4, optionally containing 0.0025 % phenol red (PR), bromothymol blue (BTB), or bromocresol green (BCG), as indicated.... 86

Figure II-8. Optical macroscopy pictures of surfaces and cross sections of ibuprofen-loaded PLGA implants before and after exposure to phosphate buffer pH 7.4 containing 0.0025 % phenol red (PR), bromothymol blue (BTB), bromocresol green (BCG) or bromophenol blue (BPB). Three experimental set-ups were used: Bulk fluids in Eppendorf tubes, agarose gels exposed to the release medium in Eppendorf tubes, and in agarose gels in transwell plates (the acceptor compartment containing the release medium). The type of set-up and exposure times are indicated at the top, the type of pH indicator is given on the left hand side. The Asterix indicates that the respective samples were too fragile to be cut. 88

Figure III-1. Schematic presentations of the experimental set-ups used to: (A) prepare ibuprofen-loaded PLGA implants by hot melt extrusion, and (B) monitor drug release from the implants upon exposure to phosphate buffer pH 7.4 in well agitated Eppendorf tubes. Details are described in the text. 101

Figure III-2. Optical macroscopy pictures and SEM pictures of surfaces and cross sections of ibuprofen-loaded implants before exposure to release medium. The PLGA-ibuprofen blends were heated for 3 to 15 min during implant preparation (as indicated). Drug crystals are highlighted by dotted red circles. 106

Figure III-3. DSC thermograms of the: (A) investigated ibuprofen-loaded PLGA implants (before exposure to the release medium), and (B) raw materials (PLGA & ibuprofen). During implant preparation, ibuprofen-PLGA blends were heated for 3 to 15 min (as indicated). The dashed orange oval highlights ibuprofen melting events in the implants. Please note the different scaling of the y-axes in (A) and (B). 107

Figure III-4. X-ray diffraction patterns of the: (A) investigated ibuprofen-loaded PLGA implants, and (B) raw materials (PLGA & ibuprofen) (for reasons of comparison). During implant preparation, ibuprofen-PLGA blends were heated for 3 to 15 min (as indicated). The orange ovals highlight specific peaks. Please note the different scaling of the y-axes in (A) and (B). 108

Figure III-5. Ibuprofen release and swelling behavior of the investigated PLGA-based implants upon exposure to phosphate buffer pH 7.4. The diagram on the right-hand side at the top is a zoom on the first 10 h. The heating times of the ibuprofen-PLGA blends during implant preparation are indicated in the diagrams. 110

Figure III-6. Optical macroscopy pictures of the investigated ibuprofen-loaded PLGA implants upon exposure to phosphate buffer pH 7.4. At the top, the time periods of implant exposure to the release medium are shown. On the left-hand side, the heating times of the ibuprofen-PLGA blends during implant preparation are indicated. The pictures on the right-hand side were obtained with light coming from the bottom. 112

Figure III-7. SEM pictures (surfaces and cross sections) of the investigated ibuprofen-loaded PLGA implants after 2, 6 and 8 days exposure to phosphate buffer pH 7.4. The heating times (in min) of the ibuprofen-PLGA blends during implant preparation are indicated on the left-hand side. The dotted red circles highlight drug crystals,

the dotted red rectangles surface-near regions including a highly swollen surface layer and the “not yet swollen” inner implant region. 114

Figure III-8. Dynamic changes in the: (A) average polymer molecular weight (Mw) of the PLGA, and (B) dry mass of the investigated ibuprofen-loaded implants upon exposure of the systems to phosphate buffer pH 7.4. The heating times of the ibuprofen-PLGA blends during implant preparation are indicated in the diagrams. 115

Figure IV-1. Schematic presentations of the experimental set-ups used to monitor drug release from the PLGA-based implants: (A) In well-agitated release medium in Eppendorf tubes (with metal baskets), (B) In agarose gels in Eppendorf tubes, the gels being exposed to well-agitated release medium, (C) In agarose gels in transwell plates, the receptor compartment containing well-agitated release medium. In all cases, sink conditions were provided throughout the experiments in the well-agitated bulk fluids. Details are described in the text. 131

Figure IV-2. Optical macroscopy pictures of implants before exposure to release medium. The diameter of the die used for hot melt extrusion is indicated at the top. 134

Figure IV-3. DSC thermograms of: (A) PLGA raw material and the investigated ibuprofen-loaded implants (the diameter of the implants are indicated on the left hand-side), and (B) ibuprofen raw material. 135

Figure IV-4. Scanning electronic microscopy pictures of surfaces and cross sections of implants before exposure to release medium. The diameters of the implants are indicated on the left hand-side. 137

Figure IV-5. Implant behavior of the ibuprofen-loaded PLGA implants upon exposure to phosphate buffer pH 7.4 using the 3 experimental set-ups: Relative (%) and absolute (mg) ibuprofen release kinetics (top and bottom), dynamic changes in the implant volume and pH of the well agitated bulk fluids (middle rows). The implant diameters are indicated in the diagrams. 139

Figure IV-6. Optical macroscopy pictures ibuprofen-loaded PLGA implants upon exposure to phosphate buffer pH 7.4 in the 3 experimental set-ups: In bulk fluids in Eppendorf tubes, in agarose gels exposed to the release medium in Eppendorf tubes, and in agarose gels in transwell plates containing the release medium in the acceptor compartment. In the case of the bulk fluids, the implants became too fragile after 8 or 10 d to allow sample withdrawal for imaging. 141

Figure IV-7. Zoom on the first 10 d of implant exposure to phosphate buffer pH 7.4 using the 3 experimental set-ups: Relative drug release, dynamic changes in the wet mass & dry mass of the systems and in the average polymer molecular weight of the PLGA. The implant diameters are indicated in the diagrams. 142

Figure IV-8. SEM pictures of surfaces and cross sections of ibuprofen-loaded PLGA implants after exposure for 2, 4 or 8 d to phosphate buffer pH 7.4 (as indicated on the left hand-side). Please note that the implants were freeze-dried prior to analysis, creating artefacts. The implant diameters are also indicated in the diagrams. 144

Figure V-1. Schematic presentations of the experimental set-ups used to monitor drug release from the PLGA-based implants: (A) In well-agitated release medium in Eppendorf tubes, (B) In agarose gels in Eppendorf tubes, the gels being exposed to well-agitated release medium, (C) In agarose gels in transwell plates, the receptor compartment containing well-agitated release medium. Details are given in the text. 160

Figure V-2. Drug release, increase in volume and change in wet mass of ibuprofen-loaded PLGA implants upon exposure to phosphate buffer pH 7.4 using the 3 experimental set-ups. The implants were placed in well agitated bulk fluids in Eppendorf tubes, in agarose gels exposed to well agitated bulk fluid in Eppendorf tubes, or in agarose gels in transwell plates (the receptor compartment containing well-agitated bulk fluid). At pre-determined time points, the entire bulk fluid, or 1 or 3 mL thereof, was renewed (as indicated). 164

Figure V-3. Optical macroscopy pictures of ibuprofen-loaded PLGA implants after different exposure times to phosphate buffer pH 7.4 using the 3 experimental set-ups. The implants were placed in well agitated bulk fluids in Eppendorf tubes, in agarose gels exposed to well agitated bulk fluid in Eppendorf tubes, or in agarose gels in transwell plates (the receptor compartment containing well-agitated bulk fluid). At pre-determined time points, the entire bulk fluid, or 1 or 3 mL thereof, was renewed (as indicated).....	166
Figure V-4. SEM pictures of surfaces and cross-sections of ibuprofen-loaded PLGA implants before and after 8 days exposure to phosphate buffer pH 7.4 using the 3 experimental set-ups. The implants were placed in well agitated bulk fluids in Eppendorf tubes, in agarose gels exposed to well agitated bulk fluid in Eppendorf tubes, or in agarose gels in transwell plates (the receptor compartment containing well-agitated bulk fluid). At pre-determined time points, the entire bulk fluid, or 1 or 3 mL thereof, was renewed (as indicated). Please note that after exposure to the release medium, the implants were freeze-dried prior to analysis. Thus, caution must be paid due to artefact creation.	168
Figure V-5. Dynamic changes in the pH of the well agitated bulk fluid, in the implants' dry mass and PLGA polymer molecular weight (Mw) upon exposure of ibuprofen-loaded implants to phosphate buffer pH 7.4 using the 3 experimental set-ups. The implants were placed in well agitated bulk fluids in Eppendorf tubes, in agarose gels exposed to well agitated bulk fluid in Eppendorf tubes, or in agarose gels in transwell plates (the receptor compartment containing well-agitated bulk fluid). At pre-determined time points, the entire bulk fluid, or 1 or 3 mL thereof, was renewed (as indicated).....	169
Figure V-6. Dependence of the solubility of ibuprofen as a function of the pH at 37 °C. Phosphate buffer pH 7.4 USP 42 served as bulk fluid. Its pH was adjusted using of 10 N lactic acid or 0.05 N NaOH (final pH values are reported).....	170
Figure VI-1. Schematic representation of the method used to prepare the polymer discs for melt rheology studies.	182
Figure VI-2. Thermograms of (A) the raw materials, (B) their physical mixture, (C) impact of the ibuprofen content on PLGA glass transition temperature measured by differential scanning calorimetry, and (D) PLGA, ibuprofen, and PLGA/ibuprofen physical mixture loss of mass upon heating, obtained by thermogravimetric analysis.....	186
Figure VI-3. Effect of temperature on (A) PLGA and PLGA: ibuprofen (85:15) complex viscosity and (B) storage G' and loss G'' modulus.	188
Figure VI-4. Effect of printing temperature on (A) ibuprofen content and (B) PLGA molecular weight.	189
Figure VI-5. Optical macroscopic pictures of the surface of ibuprofen PLGA-implants printed with the three different filling patterns.....	190
Figure VI-6. Thermograms of the ibuprofen loaded PLGA filaments, and the ibuprofen loaded PLGA 3D printed implants.....	191
Figure VI-7. (A) Relative (%) and (B) absolute (mg) ibuprofen release from 3D printed PLGA implants, (C) pH changes of the release medium upon exposure to phosphate buffer pH 7.4, and (D) increase in wet mass (%) of the implants after exposure to the release medium.	192
Figure VI-8. Optical macroscopy pictures ibuprofen-loaded PLGA implants upon exposure to phosphate buffer pH 7.4 37°C 80 RPM.	193

Figure VII-1. Schematic representation of (A) droplet deposition modeling by Arburg® Freeformer, and (B) fused filament fabrication by Volumic®.	207
Figure VII-2. (A) Optical macroscopic pictures of the surface of ibuprofen PLGA-implants obtained either with DDM with the Arburg Freeformer® technology, or FFF with the Volumic® printer, before exposure to the release medium and (B) schematic representation of the deposited lines of PLGA-ibuprofen loaded implants obtained either with DDM with the Arburg Freeformer® technology, or FFF with the Volumic® printer.	212
Figure VII-3. Scanning electronic microscopic pictures of the surface and cross-section of ibuprofen PLGA-implants obtained either with DDM with the Arburg Freeformer® technology, or FFF with the Volumic® printer, before exposure to the release medium.	214
Figure VII-4. Impact of the 3D printing technology used on (A) PLGA molecular weight and (B) the ibuprofen content.	214
Figure VII-5. Impact of the 3D printing technology used on the thermograms of the obtained PLGA-ibuprofen loaded implants and intermediate products (pellets and filaments).	215
Figure VII-6. (A) Relative (%) and (B) absolute (mg) ibuprofen release from PLGA implants, and (C) pH changes upon exposure to phosphate buffer pH 7.4, 37°C, 80 RPM.	216
Figure VII-7. (A) Change in wet mass (%), (B) dry mass (%), and (C) molecular weight (Mw) of ibuprofen-loaded PLGA implants upon exposure to phosphate buffer pH 7.4 37°C 80 RPM.	218
Figure VII-8. Optical macroscopy pictures ibuprofen-loaded PLGA implants upon exposure to phosphate buffer pH 7.4, 37°C, 80 RPM.	218
Figure VII-9. SEM pictures of surfaces and cross-sections of ibuprofen-loaded PLGA implants after exposure to phosphate buffer pH 7.4, 37°C, 80 RPM. Please note that after exposure to the release medium the implants were freeze-dried before analysis. Thus, caution must be paid due to artefact creation.	220
Figure VIII-1. Schematic presentation of the Arburg Freeformer® technology.	235
Figure VIII-2. Optical macroscopic pictures of the surface of ibuprofen PLGA-implant obtained with the Arburg Freeformer® technology, with a filling density of either 10 %, or 100 % before exposure to the release medium.	238
Figure VIII-3. Scanning electronical microscopic pictures of the surface and cross section of ibuprofen PLGA-implant obtained with the Arburg Freeformer® technology, with a filling density of either 10 %, or 100 % before exposure to the release medium.	239
Figure VIII-4. DSC thermograms of: (A) the raw materials (PLGA & ibuprofen), and (B) pellets and ibuprofen loaded PLGA implant obtained with Arburg freeformer ® technology.	240
Figure VIII-5. PLGA polymer molecular weight as: raw material, hot-melt extruded pellets and 3D printed ibuprofen loaded PLGA implant.	241
Figure VIII-6. (A) Relative (%), (B) absolute (mg) ibuprofen release for the 3D printed PGLA implants, and (C) increase in wet mass, upon exposure to phosphate buffer pH 7.4.	241
Figure VIII-7. Optical macroscopy pictures of surfaces of ibuprofen loaded PLGA implant after exposure to phosphate buffer pH 7.4.	243
Figure VIII-8. Dynamic changes in the (A) dry mass (%) of the implant and (B) PLGA polymer molecular weight (Mw) upon exposure of the implant to phosphate buffer pH 7.4.	244

Figure VIII-9. SEM pictures of surfaces and cross-sections of ibuprofen loaded PLGA implant after 3 days exposure to phosphate buffer pH 7.4. Please note that after exposure to the release medium the implants were freeze-dried prior to analysis. Thus, caution must be paid due to artefact creation. 244

Charts list

Table I-1. Differences between quality control in vitro drug release testing, and biorelevant in vitro drug release testing methods.	5
Table I-2. Examples of reported studies on the impact of instrument-based parameters on in vitro drug release.	10
Table I-3. Examples of reported studies on the impact of medium based parameters on in vitro drug release.	12
Table I-4. Summary of the FDA-approved products containing poly (lactic-co-glycolic acid). Adapted from Ochi et al. 2021.	18
Table I-5. Principal photopolymerization based 3D printed technologies, operating mode, advantages, and disadvantages.	27
Table I-6. Principal powder bed fusion-based 3D printed technologies, operating mode, advantages, and disadvantages.	29
Table I-7. Principal material extrusion based-3D printed technologies, operating mode, advantages, and disadvantages.	31
Table I-8. Principal material jetting based 3D printed technologies, operating mode, advantages, and disadvantages.	33
Table I-9. Principal binder jetting 3D printing technology advantages and disadvantages.	34
Table I-10. Principal direct energy deposition-based 3D printed technologies, operating mode, advantages, and disadvantages.	35
Table I-11. Principal sheet lamination-based 3D printed technologies, operating mode, advantages, and disadvantages.	37
Table I-12. Examples of 3D printing technologies in pharmaceutical field.	39
Table II-1. Physical key properties of the investigated ibuprofen-loaded PLGA implants (Tg: glass transition temperature). Mean values \pm standard deviations are indicated (n=3).	75
Table III-1. Physical key properties of the investigated ibuprofen-loaded PLGA implants (Tg: glass transition temperature, Mw: average polymer molecular weight). The heating time applied during implant manufacturing is indicated in the top row. Mean values \pm standard deviations are indicated (n = 3).	105
Table IV-1. Key properties of the investigated ibuprofen-loaded PLGA implants (Tg: glass transition temperature, Mw: average polymer molecular weight). Mean values \pm standard deviations are indicated (n = 3).	138
Table V-1. Key properties of the investigated ibuprofen-loaded PLGA implants before exposure to the release medium (Tg: glass transition temperature, Tm: melting temperature). Mean values \pm standard deviations are indicated (n=3).	163
Table VI-1. Preparation method of polymer discs for melt rheology studies.	182
Table VI-2. Printing parameters used to obtain the ibuprofen loaded PLGA-implant.	183
Table VI-3. Key properties of the ibuprofen loaded PLGA-implants. (Tg: glass transition temperature, Mw: molecular weight). Mean values \pm standard deviations are indicated (Weight, Length, Width, Practical drug loading n=6, Thickness, Tg, Mw n=3).	190
Table VII-1. Printing parameters used to obtain the ibuprofen-loaded PLGA-implants.	205

Table VII-2. Key properties of the obtained ibuprofen-loaded PLGA-implants. (Tg: glass transition temperature, Mw: molecular weight). Mean values \pm standard deviations are indicated (Weight, Length, Width, Implants pore size n=36, Practical drug loading n=6, Thickness, Tg, Mw n=3).	213
Table VIII-1. Printing parameters used to obtain the ibuprofen loaded PLGA-implants of different density...	234
Table VIII-2. Key properties of the obtained ibuprofen loaded PLGA-implants. (Tg: glass transition temperature, Mw: molecular weight). Mean values \pm standard deviations are indicated (Weight, Length, Width, Implant pore size n=36, Practical drug loading n=6, Tg, Mw n=3).....	239

I. GENERAL INTRODUCTION

I.1. Control drug delivery

I.1.1. Definitions

The success of many therapies requires a minimum concentration of active pharmaceutical ingredients (API). Thus, to ensure pharmacological activity, without reaching the toxicity threshold causing adverse effects. For conventional drug delivery systems (immediate-release), plasmatic drug concentration can be kept constant by repeated administration of small doses of API. However, these frequent administrations may lead to lack of compliance and failure of the medical treatment. Moreover, these significant variations in the plasmatic drug concentration may be critical when the API has a narrow therapeutic window (1).

To optimize the therapeutic response, controlled drug delivery systems allow compensating elimination of the API by the body, by providing the API at an appropriate rate (1). Thus, optimal plasmatic drug concentration can be reached after one administration and kept constant during a certain period, as illustrated in *Figure I-1*.

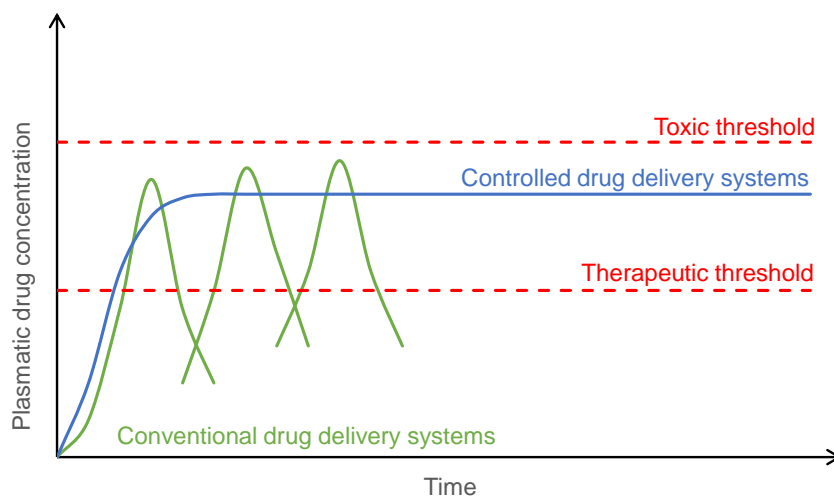


Figure I-1. Active pharmaceutical ingredient plasmatic concentration, after repeated administration of conventional drug delivery systems (green lines) and administration from an "ideal" controlled drug delivery system (blue line).

A lot of oral controlled drug delivery systems have been developed, allowing optimum concentrations to be reached at a determined speed (2). However, these are not always suitable due to the hostile environment along the gastrointestinal tract (pH, enzymes, low absorption capacity, hepatic first-pass effect, etc.) (3,4). To overcome these limitations, parenteral control drug delivery systems are a good alternative. Their advantages are numerous including (i) release of the API at a speed adapted to in vivo needs and (ii) release of the API directly at the

site of action, thus allowing to reach normally undistributed sites or to limit systemic adverse effects (3,4).

I.1.2. Long-acting injectables

I.1.2.1. Definitions

According to O'Brien *et al.*, “long-acting injectables are parenteral drug products designed to release an API at a controlled rate to achieve prolonged therapeutic exposure”(5). As stated by the European Directorate for Quality of Medicines & HealthCare (EDQM), polymeric based long-acting injectables include (6):

- Implants,
- Pellets,
- Rods,
- Stents,
- Powder and solvent for suspension for injection,
- Microspheres,
- Resorbable microparticles,
- In situ gelling systems.

They have been developed for use via various administration routes such as subcutaneous, intramuscular, epidural, intra articular, and surgical insertion directly at the tissue of interest (3).

I.1.2.2. Requirements and regulations

Long-acting injectables are complex formulations requiring dedicated regulations to assure their quality, safety, and efficacy as illustrated in Figure I-2 (6,7). According to European and United States pharmacopeias, there is a different requirement for parenteral preparations depending on the type of formulation including (8–10):

- Sterility
- Biocompatibility
- Uniformity of dosage units
- Uniformity of content
- Uniformity of mass
- Release of the active substance(s)

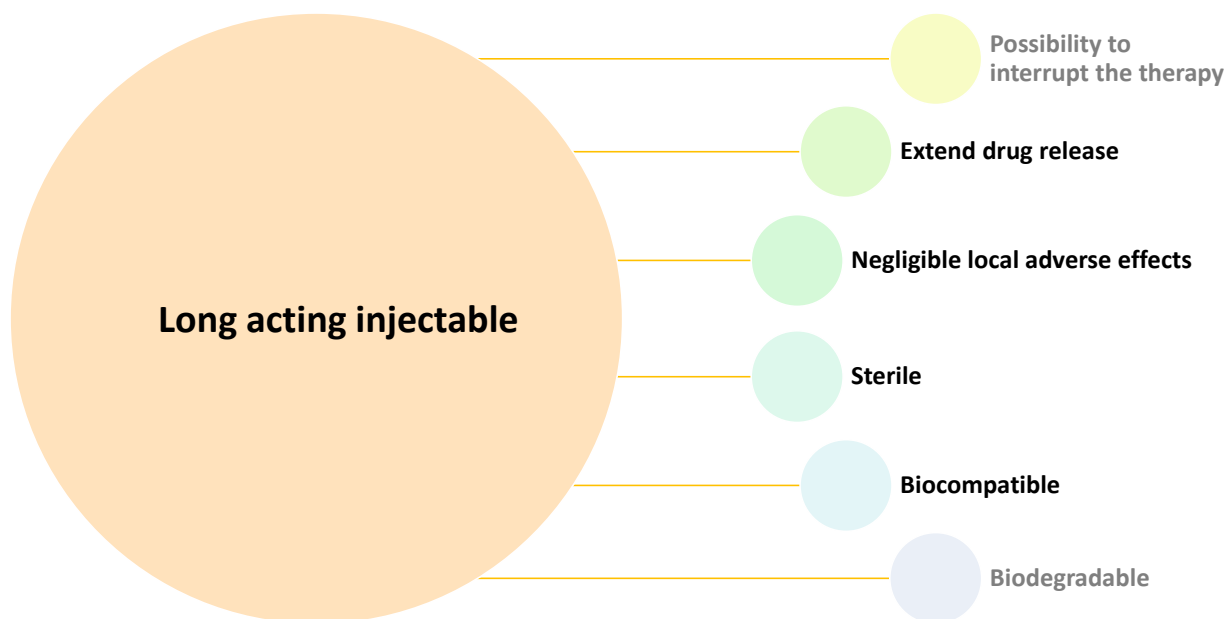


Figure I-2. Requirement for long-acting injectables formulations. Mandatory attributes are reported in black and desirable ones in grey. Adapted from Selmin et al. 2020.

Procedures for uniformity, sterility, and biocompatibility tests are well described for the parenteral formulations, unlike the release of the active substance (8,9).

It has been reported that the type of in vitro release method depends on the test objectives (11). Two types of in vitro release methods should be distinguished: (i) quality control methods and (ii) biorelevant methods. Both methods have different aims which are summarized in *Table I-1*.

Table I-1. Differences between quality control in vitro drug release testing, and biorelevant in vitro drug release testing methods.

Type of in vitro drug release method	Quality control methods	Biorelevant methods
Aim	Discriminate changes in the drug product characteristics	Establishment of an in vitro in vivo correlation
Type of medium	Do not necessarily use a medium that has the same characteristics as the administration site	Should have the same key characteristics as the administration site
Type of apparatus	Usually, pharmacopeia is referred apparatus	Not necessarily a pharmacopeia apparatus

Therefore, quality control and biorelevant methods used to predict *in vivo* performance should be developed separately (11–13). Due to the complexity of parenteral formulations the *in vitro* drug release test methods should be developed case-by-case (14). In fact, instrument and release medium should be chosen carefully as the release profile is directly impacted by: type of instrument, release medium composition, and temperature (3,15–18). To do so, key product attributes need to be known as well as, the release mechanism, and *in vivo* environment that influences drug release to successfully develop *in vitro* methods (3). The development of the *in vitro* method may require the use of modified compendial or non-compendial equipment (Varying volume, medium, agitation, etc.) (14,19).

I.1.3. Testing *in vitro* drug release from dosage forms designed to subcutis

I.1.3.1. Referenced methods

I.1.3.1.1. Sample and separate method

The sample and separate method consist in the for replenishment of the release medium either via filtration or centrifugation to maintain all the formulation in the release equipment as illustrated in *Figure I-3*.

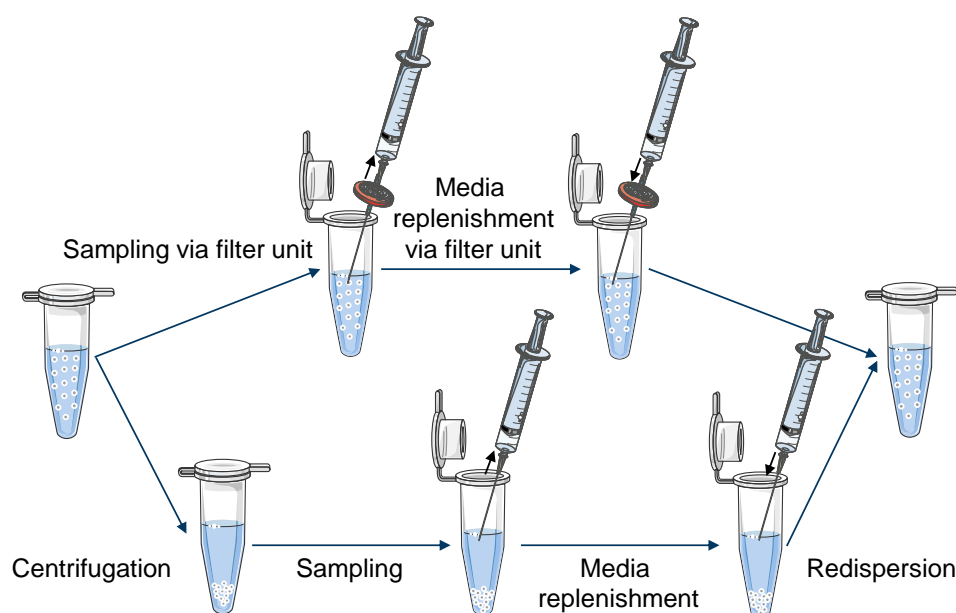


Figure I-3. Schematic illustration of sample and separate *in vitro* drug release method. Figure created using (20).

The sample and separate method could be used with a different container, from small recipients, if small release medium is needed (16,21–25), to United State Pharmacopeia apparatus 1 or 2 (*Figure I-4*) if larger medium volume is required.

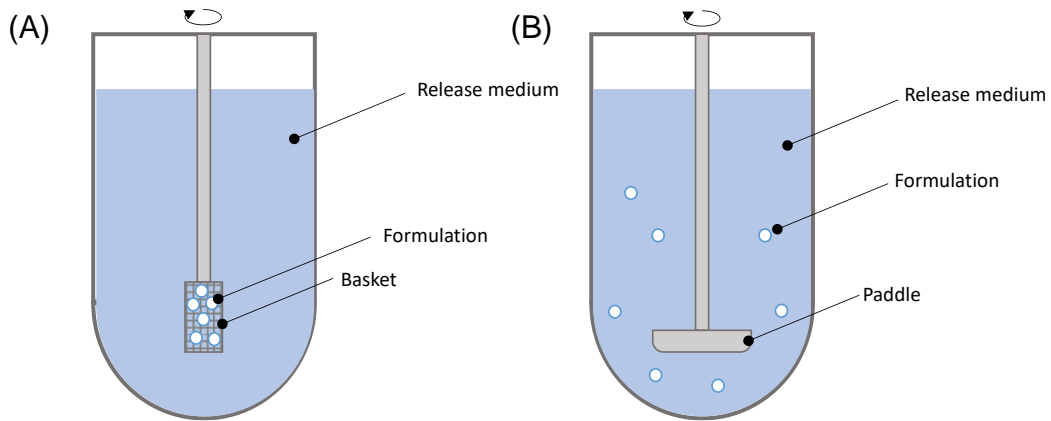


Figure I-4. Schematic illustration of the United States Pharmacopeia apparatus (A) I: basket, and (B) II: paddle.

This method is easy to implement, but it should be taken into consideration that, aggregation if the formulation or potential loss of formulation pieces after degradation (if the formulation is biodegradable) could occur during the separation step leading to erroneous release profiles (13).

I.1.3.1.2. Continuous flow through method

The continuous flow-through method referred to as apparatus IV in the United State pharmacopeia is illustrated in *Figure I-5*.

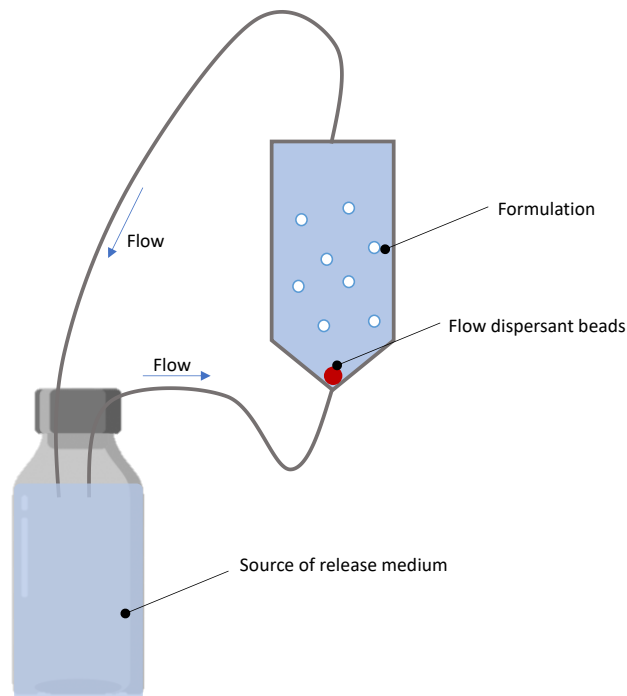


Figure I-5. Schematic illustration of the United States Pharmacopeia apparatus IV: continuous flow-through method.

In this method, the formulation is contained in the cell and the release medium is pumped from the reservoir through the cell. The apparatus can work either in an open or closed loop and present many advantages such as: do not need a sample and separate and easy adjustment of the release medium volume (13,19).

I.1.3.1.3. Dialysis membrane technics

In the dialysis-based technics, the formulation is dispersed in the release medium in a dialysis bag, immersed in the release medium. In some cases, it has been reported that the formulation is dispersed in the chamber, and the dialysis bag contains a release medium as illustrated in *Figure I-6* (13).

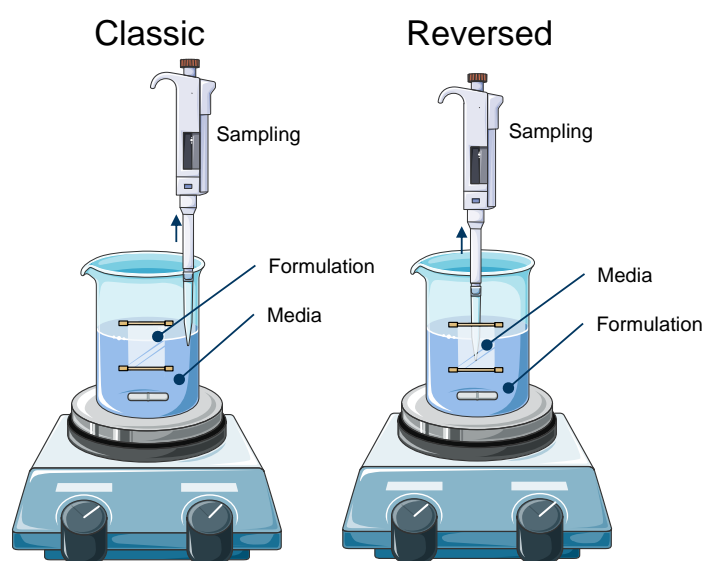


Figure I-6. Schematic illustration of the dialysis-based in vitro drug release method. Figure created using (20).

In the case of the classic dialysis-based technic, the main disadvantages are (i) the potential aggregation of the formulation in the dialysis bag due to lack of agitation, and (ii) the potential violation of sink condition in the dialysis bag. The reversed dialysis-based technics have been developed to overcome the limitation of the sink condition in the dialysis bag (13).

In some cases, dialysis membranes have been used for mimicking in vivo compartments using United States pharmacopeia referred apparatus such as apparatus I or IV (26,27).

The environment of the site of administration plays a key role in the in vivo drug release from long-acting injectables. Among the factors impacting drug release, some are of particular importance: barriers to drug diffusion (viscosity); drug partitioning at the site (uptake into

tissue); the fluid volume available at the site; and in the case of intramuscular injection muscle movement may also be an important factor (13).

I.1.3.2. Development of a suitable *in vitro* drug release testing method

I.1.3.2.1. Instrument based parameters

According to the *in vivo* site of administration, some parameters can be adjusted depending on the *in vitro* setup used. Instrument based parameters can be listed as:

- Flow rate
- Sampling
- Dialysis membrane
- Recipient
- Agitation ...

Reported studies that investigated the variation of these parameters have been reported in *Table I-2*.

If instruments based have been demonstrated to play a key role in the development of an *in vitro* drug release testing method (28–31), the composition and the choice of the release medium are also of great importance.

Table I-2. Examples of reported studies on the impact of instrument-based parameters on in vitro drug release.

Investigated parameter	Effect on drug release	Explanation	Ref
Flow rate	It was observed that flow rate did not have a significant effect on the release of triamcinolone acetonide from the microspheres.	In this case, the flow rate was not a key parameter impacting in vitro drug release mechanisms.	(28)
Dialysis	Comparison of release profile obtained from microparticles with USP II, IV apparatus, and dialysis method, shows that all the profiles had a sigmoidal shape, and complete drug release was achieved after 6 days for all methods. However, for the dialysis method, the lag phase could not be distinguished from the erosion phase.	It might be due to a decrease in drug diffusion of the API through the membrane in comparison with the diffusion from the microparticles.	(29)
Recipient	Drug release was studied in Eppendorf tubes, and glass flasks, and customized flow-through cells. The impact of the different methods on drug release was moderate.	In the investigated field, the type of recipient did not seem to be a key parameter controlling the drug release from microparticles.	(30)
Agitation	The drug release rate was decreased in tubes without agitation compared to agitated tubes in a sample and separate method.	In the case of “non-agitated” tubes convective bulk fluid transport through the implant matrix can be considered negligible	(30)
	Greater agitation provided by USP II apparatus compared to shaking bath lead to differences in drug release rate from microparticles.	Agitation may prevent aggregation by continually dispersing microparticles in the release medium, resulting in a faster release	(31)

I.1.3.2.2. Medium based parameters

Depending on the *in vivo* site of administration, some release medium parameters can be adjusted such as:

- Osmolarity,
- pH
- Surfactant,
- Ionic strength,
- Additive components,
- Viscosity,
- Temperature.

Reported studies that investigated the impact of these parameters have been reported in *Table I-3*. Development of a suitable *in vitro* drug release method by modulating instrument-based and medium based parameters to be as close as possible to the parameters controlling the release rate *in vivo* is of great importance(16,17,28–34). Especially for poly (lactic-co-glycolic) acid-based devices, due to the numerous mechanisms involved in the drug release from such a polymer (35) as described in the following sections.

Table I-3. Examples of reported studies on the impact of medium based parameters on in vitro drug release.

Investigated parameter	Effect on drug release	Explanation	Ref
Osmolarity	Drug release rate decreased with increasing osmolarity of the release medium	Probably due to a decrease in water uptake rate	(17)
Buffer concentration	Drug release rate slightly decreased when increasing the buffer concentration	Might be due to an increase in the concentration of bases in the release medium, leading to potential diminution au autocatalytic effect of PLGA	(17)
	When increasing buffer concentration, release rate significantly increases	Increasing ionic strength of the release medium, reduce interaction between API end polymer end-groups	(32)
	When the buffer concentration was decreased from 0.02 M to 0.01 M a significant increase in drug release rate was observed. The release profile was also changed from tri-phasic to bi-phasic.	Might be due to the difference in osmotic pressure leading to different water uptake.	(29)
pH	A similar trend in drug release during burst and lag phases at pH 2 and pH 4. Release rate during erosion phase was faster at pH 2 than pH4	It indicates that burst and lag phases are not dependent on pH while the erosion phase is.	(29)
Temperature	Release rate significantly increases when temperature increases from 37°C to 65°C	Probably due to the increase of the mobility (drug mobility, but also polymer chains mobility) with temperature	(17)
	Release rate decreases when temperature decreases from 37°C to 5°C	Due to decrease in mobility, water uptake, and degradation rate of the polymer	(16,33)
	The time to achieve complete peptide release was reduced from 18 to 6 days by increasing the temperature from 40°C to 45°C.	Within the first two phases (burst and lag), the drug release is accelerated by diffusion as a higher temperature softens polymer chains and increases their mobility, while during the third phase, such a temperature enhances hydration and polymer erosion.	(29)
	By increasing temperature from 35°C to 39°C drug release rate decreases	Might be due to polymer plasticization, leading to drug entrapment	(28)
Surfactants	With decreasing sodium dodecyl sulfate concentrations, the cumulative triamcinolone acetonide release decreased	The triamcinolone release observed in different decreasing sodium dodecyl sulfate-containing media correlated well with the solubility of the drug in the respective media	(28)
Viscosity	Release rate during the 3 rd phase of poly(lactic-co-glycolic) acid-based implant and microparticles, is decreased when the systems are exposed to agarose gel instead of bulk fluid	The viscosity of the agarose gel limits the swelling and the water uptake of the implant during the 3 rd release phase.	(34)
	The release rate is increased when microparticles are exposed to agarose gel compared to phosphate buffer pH 7.4	It might be explained as follows: when surrounded by bulk fluid, the acids generated by the hydrolysis of the polyester are more rapidly neutralized than in the case of the agarose gel technique, in which rapid convective mass transport is effectively suppressed.	(18)

I.2. Poly(lactic-co-glycolic) acid

I.2.1. General characteristics and synthesis

Poly (lactic-co-glycolic acid) (PLGA) is a copolymer composed of lactic acid (LA; levogyre or dextrogyre) and glycolic acid (GA) (36,37). PLGA can be synthesized either by polycondensation or ring-opening polymerization. As described in *Figure I-7*, in the case of polycondensation, linear polymers of low average molecular weight (Mw) are obtained by intramolecular esterification of alpha-hydroxy acids, while ring-opening polymerization allows obtaining linear polymer of higher Mw by ring polymerization of the cyclic monomers (38). In the latter case, the use of a catalyst is necessary.

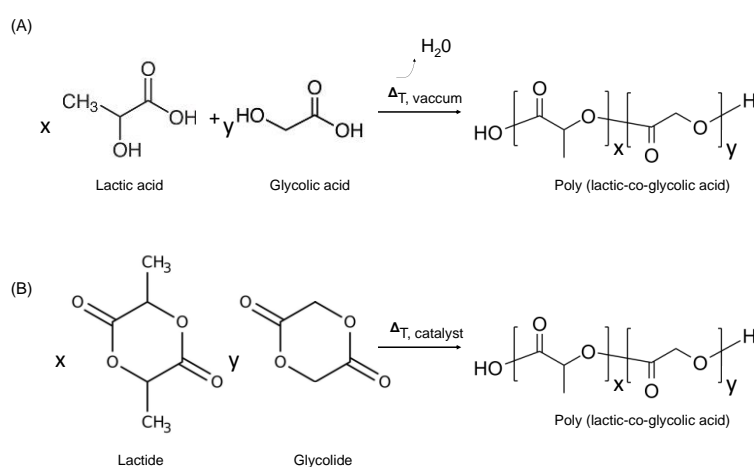


Figure I-7. Synthesis of Poly (lactic-co-glycolic acid) by (A) polycondensation and (B) ring-opening polymerization.

Different PLGA grades can be obtained by controlling polymerization conditions such as temperature, time, type and concentration of catalyst, nature, and quantity of monomer. These different grades are distinguished by the choice of the monomer ratio, the molecular weight, and the nature of the end-group of the copolymer (36,38,37).

These characteristics influence the physicochemical properties of the copolymer and therefore the mechanical properties, thermoplastic behavior, rate of degradation, and release of the associated API (37).

I.2.2. Molecular weight

When the Mw increase, the polymer has longer polymeric chains and so higher intrinsic viscosity. This leads to a lower degradation rate (39). As described in *section I.2.1* depending on PLGA synthesis, different PLGA Mw could be obtained.

PLGA Mw is known to have an impact on drug release, from devices composed of this polymer. Some studies reported that with higher Mw not only a longer release is reached but also a lower burst effect (40,41). Moreover, it has been recently reported that drug release depends on both the molecular weight and polydispersity of the polymer (42). They observed an increase of the initial burst release when increasing the amount of low molecular weight PLGA in microparticles.

However, Kohno *et al.*, previously reported that in some cases Mw is not a critical formulation parameter regarding drug release compared to other parameters such as glass transition temperature, or API-polymer interactions (43)

I.2.3. Crystallinity and glass transition temperatures

In some cases, PLGA copolymers composed of less than 85% of GA have been reported to be amorphous (37). In fact, due to the coexistence of two enantiomeric isomers of LA (D or L, depending on the position of the methyl group on the alpha carbon), the crystalline organization is made difficult. While GA doesn't have the methyl group, this makes it highly subject to crystallinity (44). P_(L)LGA composed from 75:25 to 30:70 (LA:GA) and P_(D,L)LGA composed from 100:0 to 30:70 (LA:GA) have been reported to be amorphous copolymers (45,44).

Crystalline, semi-crystalline, and amorphous materials have different properties as illustrated in *Figure I-8*. The amorphous grades of PLGA are characterized by their glass transition temperature (T_g). T_gs are defined as a range of temperature, in which the polymer goes from a glassy to a rubbery state. T_gs are impacted by both the ratio between LA and GA, and the Mw of the PLGA (37,44). It has been reported that depending on PLGA composition and Mw, their T_gs range between 40°C and 60°C (44).

On the other side, some substances, of low molecular weight, called plasticizers have the property of being interposed between the polymer chains, enhancing their mobility, and their T_gs. Water, but also some API have been reported to have a plasticizing effect on PLGA (46–49,24).

Crystalline	Semi-crystalline	Amorphous
Regular, repeating arrangement of components in a solid	Alternating between regular and irregular pattern of components in a solid	Irregular pattern of components in a solid
Have a sharp melting point (T_m)		Melt over a range of temperature (T_g)
Definite heat fusion	Have both a sharp melting point and melt over a range of temperature ($T_m + T_g$)	No definite heat fusion
Isotropic		Anisotropic

Figure I-8. Summary of the main characteristics, and schematic arrangement of molecular chains in crystalline, semi-crystalline, and amorphous polymers.

I.2.4. Hydrophilic properties and solubility

By modulating the ratio between its two constitutive monomers: LA and GA, a more or less hydrophilic polymer can be obtained. LA methyl group makes it more hydrophobic than GA, thus increasing the proportion of LA leads to a less hydrophilic copolymer (40,50). Due to this ability to varying PLGA hydrophilicity, it is possible to find PLGA grade that has affinity either with hydrophobic or hydrophilic API (39).

Many different solvents including chlorinated solvents, tetrahydrofuran, acetone, or ethyl acetate can dissolve PLGA, whatever the ratio between its constituting monomers (51,39).

I.2.5. Biodegradation

PLGA degradation occurs through hydrolysis of the polyester backbones. Biodegradation takes place by chemical hydrolysis and induces erosion of the polymer matrix. The water molecules diffuse into the polymer matrix and break the ester bonds of the main chain, leading to the production of oligomers, and its constituting monomers: LA and GA. Hydrolysis is a reaction catalyzed either by acidic or basic products (52). The acid catalyst can come either from a strong acid in the medium, or the carboxylic acid end groups of the PLGA. In the latter case, it is called autocatalytic reaction, as illustrated in *Figure I-9* where n , m , and $n - m$ represent different degrees of polymerization, and H^+ the acidic catalyst coming from the carboxylic end group of the polymer.

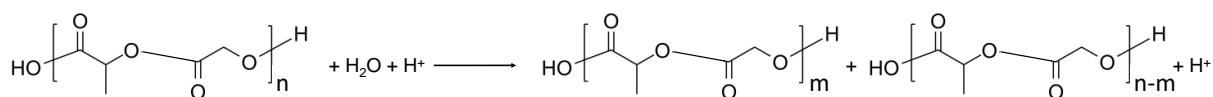


Figure I-9. The acid-catalyzed ester hydrolysis of poly (lactic-co-glycolic acid). Adapted from Ford Versypt et al. 2013.

The degradation products present free carboxyl groups which decrease the micro-environmental pH (25,53,54). However, the chemical hydrolysis reaction is catalyzed by the presence of protons (25,36). This phenomenon is important because it determines the degradation and erosion regime of the polymer matrix (52,55). This lowering of pH can also influence the stability of a formulation, in particular when it is composed of API sensitive to acidic media or proteins (56).

After exposition to the release medium, porosity and size of the system will impact the degradation. Higher degradation rates have been reported for the largest devices (57–64). Indeed, *Figure I-10* illustrates the size-dependent autocatalytic effect. For larger devices, there is a region (illustrated in dark orange) in which acidic degradation products can freely diffuse through the polymer matrix (blue arrow). Thus, leading to an acceleration of the hydrolysis reaction in the light orange region, due to autocatalysis (52,63,65).

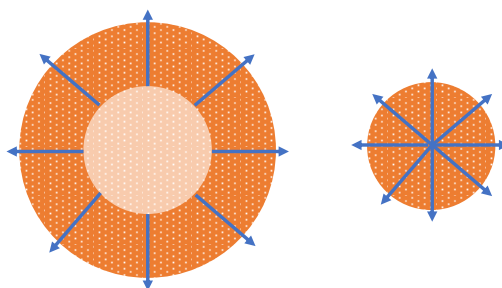


Figure I-10. Illustration of the size-dependent autocatalytic effect. Adapted from Ford Versypt et al. 2013.

The degradation rate is also directly influenced by the ratio of monomers. As mentioned above, GA is more hydrophilic than LA, making it more prone to hydrolysis than LA. But several publications reported that the rate of degradation is highest when the ratio LA:GA is 50:50 (36,44).

Other factors must also be considerate such as the pH, the addition of API with plasticizing or anti-plasticizing effect, the addition of acidic or basic API, mechanical constraints, manufacturing process, and sterilization of the system (49,66,67).

I.2.6. Biocompatibility

Food and Drug Administration (FDA) use the definition of biocompatibility gave by J. Black in 2006 as a reference, where it is defined as the ability of a device material to perform with an appropriate host response in a specific situation (68,69).

PLGA has been reported to have excellent biocompatibility (70–73). Indeed, as illustrated in *Figure I-11* the metabolites produced by hydrolysis are safely eliminated by the human body, either by the urine or directly integrated into the citric acid cycle and transformed in water and carbon dioxide.

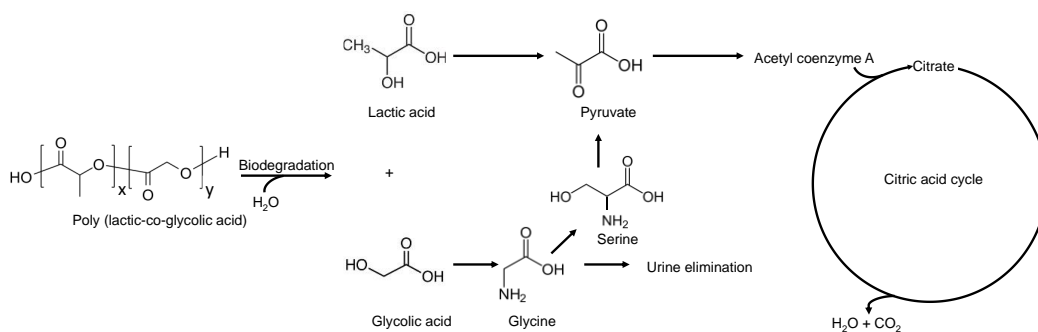


Figure I-11. Schematic representation of the elimination and metabolization of the poly(lactic-co-glycolic) degradation products. Adapted from Maurus et al. 2004.

Thus, leads to a very low systemic toxicity, and makes PLGA an excellent polymer for drug delivery and biomaterial application (74,71).

I.2.7. Use in control drug delivery

PLGA is frequently used as a polymer matrix in controlled release systems such as microparticles, nanofibers, or implants (63,72,75). These offer many advantages: a minimal inflammatory response, an appropriate release rate depending on the application, an in-situ degradation compatible with the healing and/or regeneration process (63,72,75).

Since 1989, the first approval of a product containing PLGA by the FDA, many specialties of parenteral products composed of PLGA have been approved for human use, such as microspheres, implants, or *in situ* forming implants. These products, the API delivered, the dosage form, the duration of drug release, and the company are summarized in *Table I-4*.

Table I-4. Summary of the FDA-approved products containing poly (lactic-co-glycolic acid).
Adapted from Ochi et al. 2021.

Product	Active pharmaceutical ingredient	Formulation	Drug released for	Company	Year of approval
Lupron Depot	Luprolide acetate	Microspheres	1,3,4,6 months	Abbvie	1989
Zoladex Depot	Gosereline acetate	Implant	1,3 months	AstraZeneca	1989
Sandostatin LAR	Octreotide acetate	Microspheres	1 month	Novartis	1998
Atridox	Doxyclyne hyclate	<i>In situ</i> forming implant	1 week	Zila Therapeutics	1998
Nutropin Depot	Somatotropin	Microspheres	1 month	Genentech	1999
Trelstar	Triptorelin pamoate	Microspheres	1,3,6 months	Allergan	2000
Somatuline Depot	Lanreotide	Microspheres	1 month	IPSEN	2000
Arestin	Minocycline HCl	Microspheres	2 weeks	OraPharma	2001
Eligard	Leuprolide acetate	<i>In situ</i> forming implant	1,3,4,6 months	Sanofi	2002
Risperdal Consta	Risperdone	Microspheres	2 weeks	Janssen	2003
Vivitrol	Naltrexone	Microspheres	1 month	Alkermes	2006
Ozurdex	Dexamethasone	Implant	3 months	Allergan	2009
Propel mini	Mometasone furoate	Implant	1 month	Intersect	2011
Bydureon	Xenatide	Microspheres	1 week	AstraZeneca	2012
Lupaneta pack	Leuprolide acetate	Microspheres	3 months	Abbvie	2012
Signifor LAR	Pasireotide	Microspheres	1 month	Novartis	2014
Zilretta	Triamcinolone	Microspheres	3 months	Flexion Therapeutics	2017
Sublocade	Buprenorphine	<i>In situ</i> forming implant	1 month	Indivior	2017
Perseris	Risperdone	<i>In situ</i> forming implant	1 month	Indivior	2018

Along with the commercialization of these products, in the literature, there is a constant increasing interest of devices based on PLGA. As illustrated in *Figure I-12*, the number of publications referring to PLGA per year is constantly increasing (Figure created using the number of references per year using the key word PLGA on PubMed).

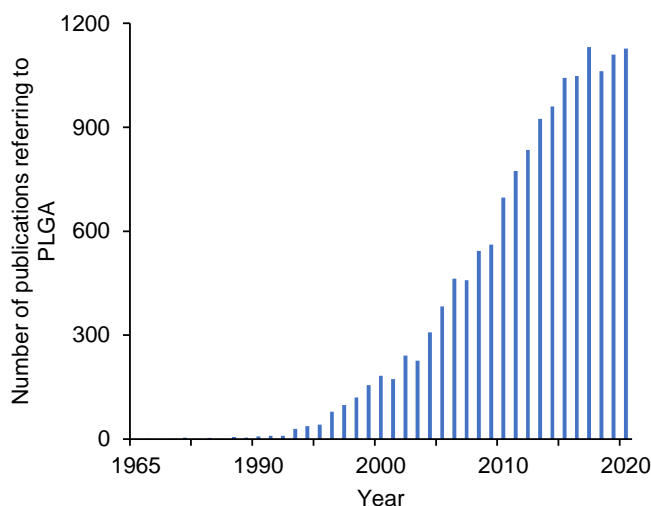


Figure I-12. *The number of publications referring to PLGA per year from 1965 (1 publication) to 2020 (1127 publications).*

Indeed, the interpretation of the observed results is not straightforward, and the underlying mass transport phenomena controlling drug release are often difficult to elucidate (35).

I.2.8. Release mechanisms and release pattern

I.2.8.1. Definitions

Understanding the mechanisms that control the release of API from PLGA based systems is far from trivial. Indeed, some hypotheses are described in the literature but many physicochemical phenomena are involved and remain to be elucidated.

API release mechanisms could be defined either as: (i) how the API is released from the system, or (ii) the phenomenon that controls its release rate (76,77). So far, several phenomena controlling the release rate of an API from PLGA devices have been reported such as (78–91,35,92,48,49,93,94,33,25,54,16)

- API dissolution,
- API diffusion through water-filled pores,
- API diffusion through the polymer matrix,
- Polymer hydrolysis,

- Polymer erosion,
- Osmotic effect,
- Water absorption / Swelling,
- API-Polymer, API-API interactions,
- Pore closing,
- Heterogeneous polymer degradation,
- Formation of cracks, deformation of the device,
- The collapse of the polymer structure.

In addition, as illustrated in *Figure I-13*, Fredenberg *et al.* identified three-way for an API to be released from PLGA-based systems: diffusion through water-filled pores, diffusion through the polymer matrix, and degradation or erosion of the polymer matrix (35).

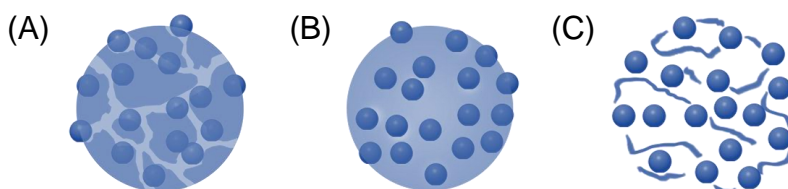


Figure I-13. Schematic representation of the active pharmaceutical ingredient release mechanisms from a poly (lactic-co-glycolic acid) device: (A) diffusion through water-filled pores, (B) diffusion through the polymer matrix, and (C) degradation or erosion of the polymer matrix. Adapted from Fredenberg *et al.* 2011.

I.2.8.2. Diffusion throughout a porous network

This mechanism describes the first release step, before the erosion of the polymer begins. It is very dependent on the porous structure of the device and is therefore dependent on the processes that promote pore formation (95). These must be continuous and large enough for the API to pass through (35). Transport through water-filled pores can be achieved either by diffusion when the concentration gradient controls transport, and/or convection when osmotic pressure controls the transport (35).

I.2.8.3. Diffusion throughout the polymer matrix

This mechanism concerns low molecular weight hydrophobic API (96,35). The diffusion rate is very dependent on the physical state of the polymer. It can increase as the polymer changes from a glassy state to a rubbery state and unlike diffusion through water-filled pores, it is not

dependent on the pore structure (46). Diffusion is often higher in low molecular weight polymers, due to higher mobility of polymer chains (97).

I.2.8.4. Degradation of polymer matrix

Matrix degradation/erosion is the process of cleavage of polymer chains into oligomers and monomers (98). Faisant *et al.* identified two types of erosion: surface erosion and mass erosion as illustrated in *Figure I-14* (72,97).

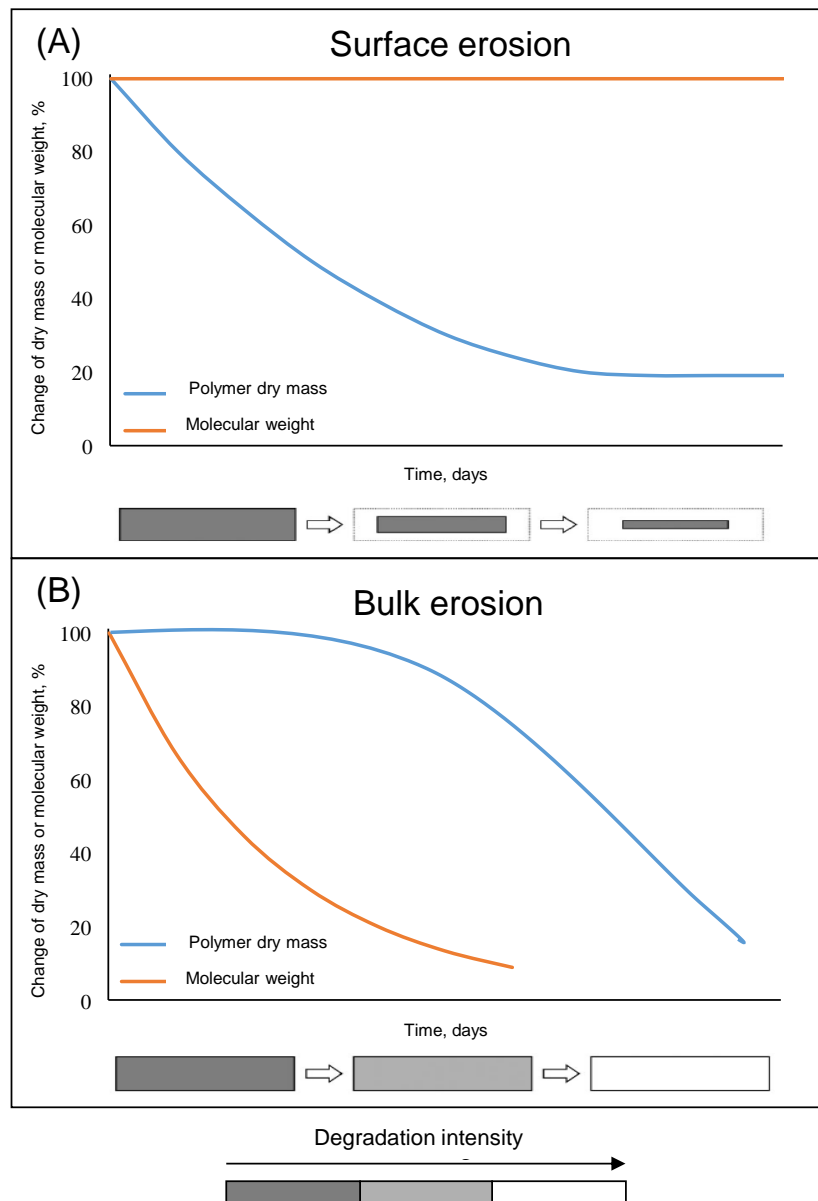


Figure I-14. Change of dry mass and molecular weight of the polymer in the case of (A) surface erosion and (B) bulk erosion. Adapted from Grund *et al.* 2011.

In the first case, erosion occurs only at the surface, due to a weak diffusion of water into the polymer (99). In contrast, in the second case, degradation occurs more slowly and throughout

the system. PLGA-based devices are generally considered to be systems undergoing erosion mass (62,72).

I.2.8.5. Release pattern

Different types of release profiles can be observed from PLGA devices. *Figure I-15* describes the three types of release patterns: mono-phasic, bi-phasic, or tri-phasic.

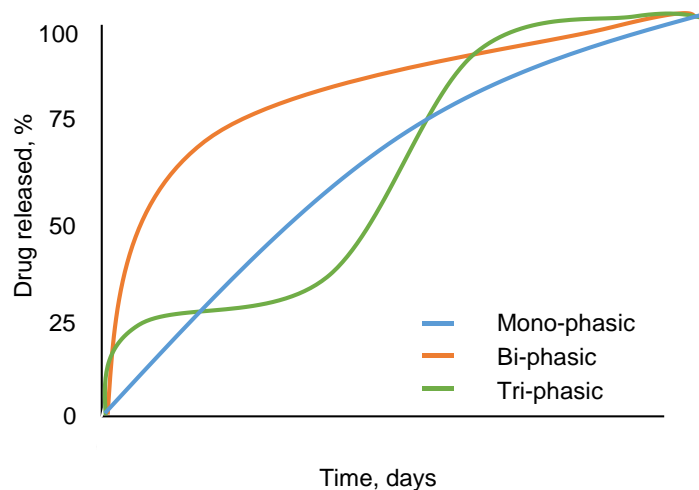


Figure I-15. Schematic representation of the different release patterns of a drug substance from a poly (lactic-co-glycolic acid) device.

It is not always obvious to know which are the mechanisms of release which dominate during the phases previously described (35,100). Indeed, the release profiles are often due to the combination of several of the mechanisms described above.

I.2.8.5.1. Monophasic release pattern

This profile consists of, one single release phase, sought after in most applications to avoid the "burst" effect that can cause toxic effects. In most cases the release of API is constant and is only controlled by a diffusion process. Wang *et al.* have shown that zero-order kinetics can be obtained from microparticles prepared by the simple solvent evaporation emulsion technique (101). Monophasic release of API from PLGA devices is rare. It is mainly done in a biphasic or triphasic way (35).

I.2.8.5.2. Bi-phasic release pattern

This profile consists of two release phases. In most of the cases it is divided in: (i) the first phase called the "burst" effect, (ii) followed by a plateau, or in (i) zero order release, follow by a (ii) second phase of rapid release (102,103).

- Phase I:

For many formulations, an initial rapid release of API is observed before the release rate reaches a plateau (102). This phenomenon is generally called the “burst” effect. This can be defined as the amount of API released by the device before polymer erosion begins (103).

- Phase II:

Then follows a phase where the release rate of API is constant, called a plateau, during which the slowing of the release due to the increase in diffusion paths is compensated by the erosion of the polymer. The water which has penetrated inside the matrix induces the hydrolysis of the polymer chains into oligomers and water-soluble monomers (35,39,97).

I.2.8.5.3. Tri-phasic release pattern

This release profile also exhibits a "burst" effect followed by a second phase which corresponds to slow diffusion of the API through the polymer matrix and the pores. The third phase is the result of the degradation and/or the swelling of the polymer matrix which results in a rapid release of the API (48,49,33,25,16).

- Phase I:

As described above, the “burst” effect is mainly attributed to the diffusion of the SA which is adsorbed on the surface of the particle, or to the diffusion of the API through pores filled with water in contact directly with the surface of the latter (33). Previous work suggests that the “burst” period ends when the pores close (87,88,104).

- Phase II:

This phase, also called the lag phase, is characterized by slow diffusion of the API through the polymer matrix and the few pores filled with water (105). During this period, hydration of the device as well as degradation of the polymer takes place. This phase may also be due to pore closure and polymer-API interactions, which could limit the release of API. Several factors have been reported to induce pore closure, among them: degradation of the polymer, plasticizers, and high temperatures (106,107). In some systems, this lag phase is negligible due to the rapid degradation of the PLGA. The duration of this phase depends mainly on the characteristics of the polymer, the size, and the geometry of the device (57,60,62,64).

Gasmi et al. showed that this second phase of release depended mainly on the initial SA content. They explained that at high levels, part of the API which does not have direct access to the

surface of the device is trapped by the PLGA and takes time to diffuse through the polymer matrix (93). In other studies, API is released by the swelling of the device due to the diffusion of water. Indeed, water diffuses inside the device causing the dissolution of the API and its diffusion into the release medium (108).

- Phase III:

This phase is characterized by a faster release of AS. The release during this phase is mainly due to massive erosion of the polymer and swelling and/or deformation of PM (35). The beginning of this phase is when an entirely continuous porous network is formed inside the particle. The large swelling observed at the end of the second phase can result from the osmotic pressure built up in the system and begins as soon as the polymeric structure reaches a sufficiently molecular weight low (48,49,25,54,58,35,33,16)

In this thesis, the work will mainly focus on PLGA based implants for subcutaneous delivery. Several techniques for manufacturing implants have been reported, such as compression, solvent casting, injection molding, hot-melt extrusion, and more recently, three-dimensional (3D) printing (109).

I.3. Three-dimensional printing technologies

I.3.1. Generalities

I.3.1.1. Definition

3D printing technologies are additive manufacturing (AM) technics able to produce various 3D products (110). The final object is formed either by deposition, binding, or polymerization of materials in successive layers (110,111).

I.3.1.2. Timeline

As illustrated in *Figure I-16*, in 1980, the concept of 3D printing was first reported by Hideo Kodama which described a process of solidification of polymers using a beam of UV light. In 1986, the first additive manufacturing technology, known as stereolithography, was patented by Charles Hull (112–116). Around the same time, selective laser sintering was invented by Carl Deckard (117). In 1989 the company Stratasys was funded by L. Crump and S. Scott, who filed the patent for fused deposition modeling (FDM) (116,118). In the 1990s other 3D printing technologies have been investigated (116). In 2005, the patent for FDM expired, leading to democratization and an increase of interest for the 3D printing technologies (112,116,119).

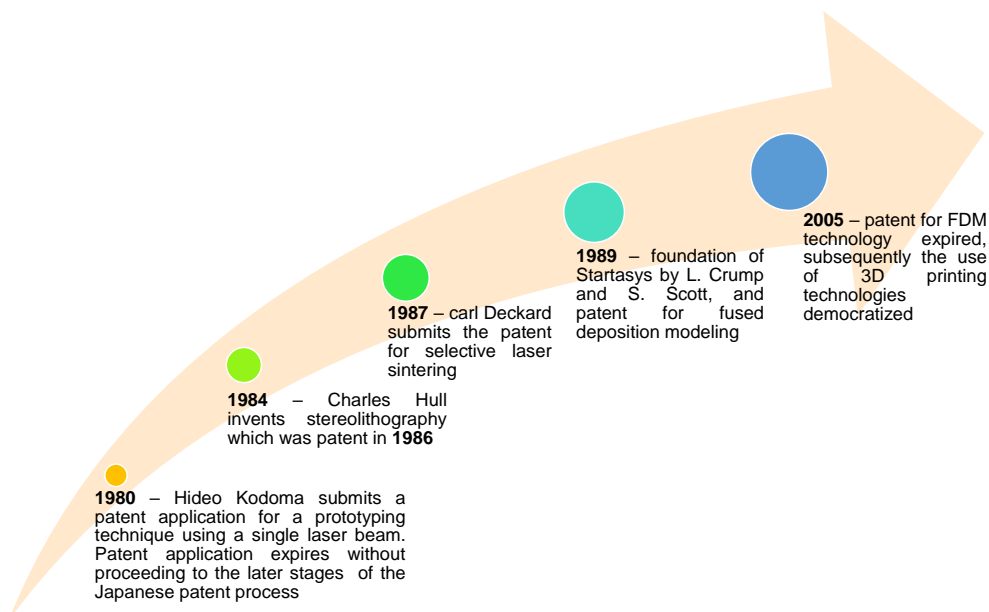


Figure I-16. Timeline of three-dimensional printing technologies.

The 3D printing technologies invented since the 1980s can be classified into seven categories further developed below: photopolymerization, powder bed fusion, material jetting, direct energy deposition, binder jetting, selective deposition lamination, and material extrusion (110,111).

I.3.2. Classification

I.3.2.1. Photopolymerization

Photopolymerization-based 3D printing technologies work as described in *Figure I-17*. Indeed, a mobile platform serving as support is immersed in a vat of liquid photopolymer at a certain depth. This resin is generally a mixture of acrylate or epoxy monomers and a photoinitiator which will initiate the polymerization under the effect of UV or visible light directed using deflectors. The model gradually sinks during manufacturing and is finally cut, washed, and baked to harden it (115,120,121).

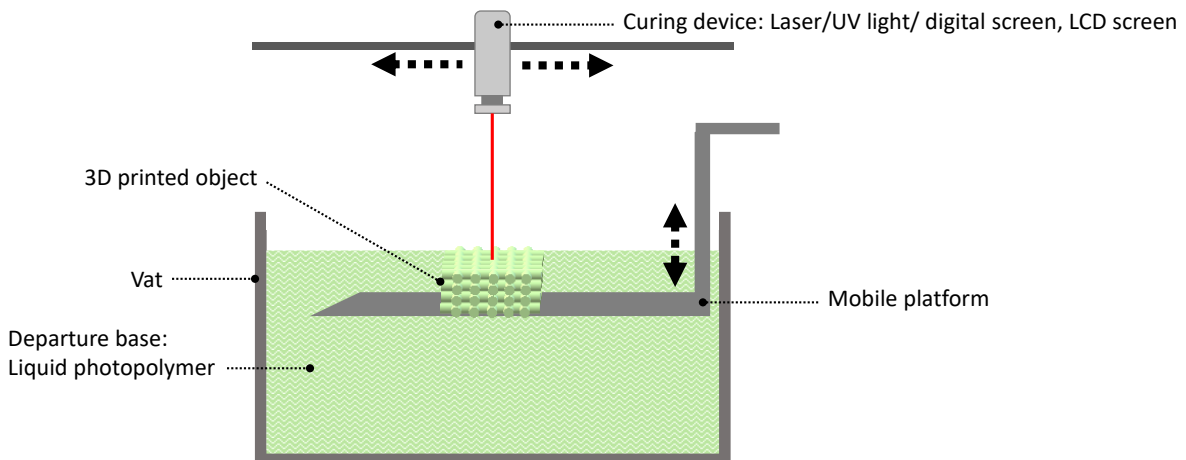


Figure I-17. Schematic representation of photopolymerization-based three-dimensional printing technologies.

Four methods are based on this principle, stereolithography (SLA), Digital Light Processing (DLP), Continuous Liquid Interface Production (CLIP), and Daylight Polymer Printing (DPP), their operating mode are summarized in *Table I-5*(115,121–125).

Table I-5. *Principal photopolymerization based 3D printed technologies, operating mode, advantages, and disadvantages.*

Name	Operating mode	Advantage	Disadvantages	Ref
SLA	A concentrated beam of UV or laser beam is projected onto the surface of a tank filled with liquid photopolymer. The beam is focused, creating the 3D object layer by layer by crosslinking of the polymer.	High precision, high quality, smooth finish.	Not suitable for mass production. Limited choice of materials (photopolymerization).	(115)
DLP	A digital projection screen illuminates a single image of each layer in a single operation.	Faster print times (each layer is exposed all at once instead of being drawn).	The layers are formed of small rectangular bricks (the layer is made up of square pixels). Limited choice of materials (photopolymerization).	(122,126)
CLIP	The bottom part of the tank allows UV light to pass through. UV beam passes through this window, and illuminates a precise cross-section of the object, leading to cross-linking of the polymer resin. The object rises slowly enough to allow the resin to flow underneath and remain in contact with the bottom of the object.	Print continually (up to 100 times faster than traditional printing technologies).	Limited choice of materials (photopolymerization).	(123,124)
DPP	A Liquid crystal display (LCD) is used to cure the polymer.	Faster than traditional printing technologies.	Limited choice of materials (photopolymerization). Need specially formulated natural light polymer.	(125)

I.3.2.2. Powder bed fusion

Powder Bed Fusion (PBF) 3D printing technologies generate precision products. The powder particles are fused using a heat source (generally a laser beam or electron beam). Thus, layer by layer the 3D object is formed as illustrated in *Figure I-18* (117,120,121,127–133).

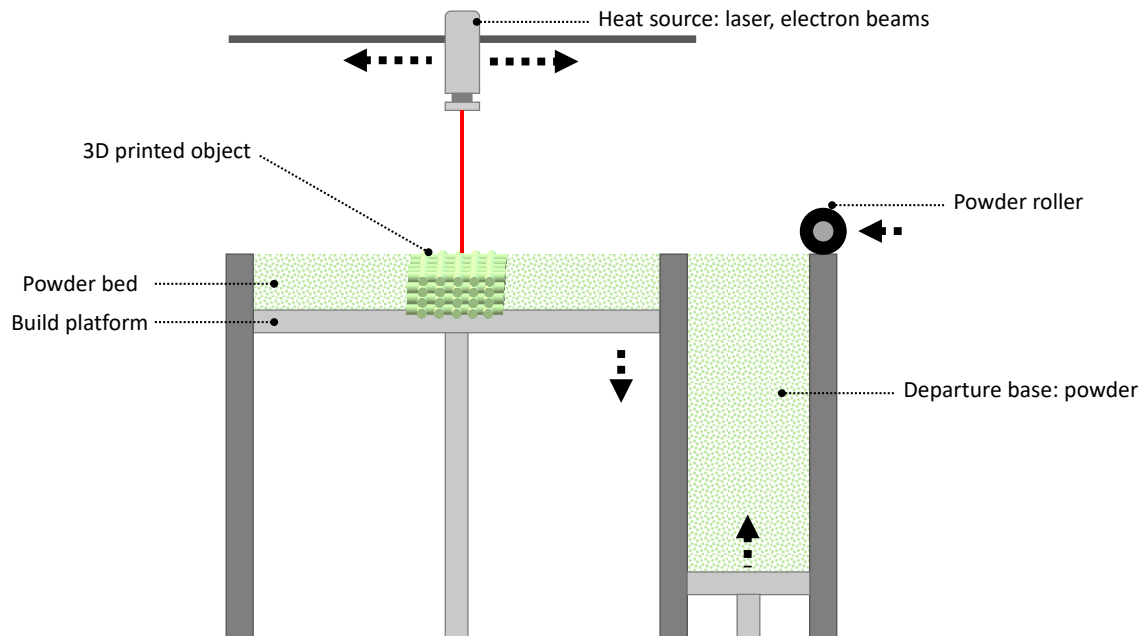


Figure I-18. Schematic representation of powder bed fusion-based three-dimensional printing technologies.

Several techniques can be cited such as Selective Laser Sintering (SLS), Electron Beam Melting (EBM), Selective Heat Sintering (SHS), Direct Metal Laser Sintering (DMLS), Selective Laser Melting (SLM), Multi Jet Fusion (MJF). Their operating mode, advantage, and disadvantages are summarized in *Table I-6*.

Table I-6. *Principal powder bed fusion-based 3D printed technologies, operating mode, advantages, and disadvantages.*

Name	Operating mode	Advantage	Disadvantages	Ref
SLS	Use laser beams to sinter, or agglomerate, powdered materials, layer after layer to create a 3D object Laser power up to 0.04 kW	Several materials can be used. Powder recycling.	Possible shrinkage and warping of thin parts when designing. High power usage.	(117)
EBM	The material is fused by a high-energy electron beam.	Use less energy and can produce layers faster than SLS. Powder recycling.	Requires post-processing	(128)
SHS	Use a thermal print head to selectively fuse material powder	Low cost. Powder recycling	High power usage	(129)
DMLS/SLM	Agglomerates powders and is limited to alloys, including those composed of titanium. Laser power up to 1 kW	Powder recycling.	Require additional work to compensate for the high residual stress and limit the occurrence of distortion. Work only with metals.	(130)
MJF	Infrared lamp acts as the energy source to consolidate powder particles	improved printing efficiency, accuracy and speed.	requires two additional agents: a fusion agent and a detailing agent	(132,133)

I.3.2.3. Material extrusion

Material Extrusion (ME) based 3D printing technologies can be divided into two parts: (i) extrusion of low melting point past or gel and (ii) extrusion of high melting point thermoplastic polymer (111). In both cases, it consists of dispensing molten or semi-solid material through the orifice of a nozzle, deposited layers by layers in order to obtain a 3D object (120). Nowadays, these printing technologies are considered the simplest and are the most widely used.

When it comes to extrude a low melting point past or gel, Pneumatic or Syringe Extrusion (PE/SE) are the referenced technics (111,134). It consists of filling pastes into ink cartridges for extrusion through a nozzle. The past or gel, is then deposited layer by layer in order to form the desired object. The obtained 3D object is then under vacuum and heating for complete drying (134).

Concerning the high melting point thermoplastic polymers, several technologies have been reported such as Fused Deposition Modeling (FDM) also known as Fused Filament Fabrication

(FFF), Direct Powder Extrusion (DPE), and Droplet Deposition Modeling (DDM) (111,120,121,135–139).

FDM or FFF technologies are illustrated in *Figure I-19*. This is the technologies are based on the one developed and patented by L. Crump and S. Scott in 1989 (116,118). These technologies use a continuous filament of thermoplastic material as the base material. Filament is fed by a spool, via a heated, mobile printer extrusion head, often referred to as an extruder. The molten material is expelled from the extrusion nozzle and deposited first on a 3D printing platform, which can be heated to ensure good adhesion. Once the first layer is complete, the extruder and the platform move away simultaneously and the second layer can then be directly deposited on the part being manufactured (111,120,121,135).

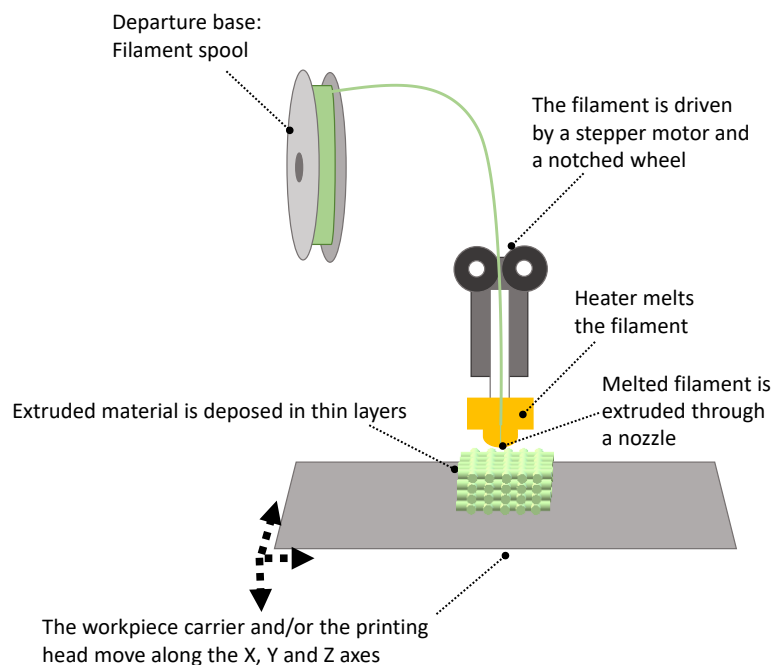


Figure I-19. Schematic representation of fused deposition modeling or fused filament fabrication three-dimensional printing technologies.

Development of a suitable filament for FDM/FFF printer can be challenging (140,141). To overcome this limitation, new 3D printing technologies, for which departure base material can be either a powder mixture (DPE) or pellets (DDM) have been developed (136–139).

The “Arburg Plastic Freeforming[®]” technology is a thermoplastic DDM technology, capable to process a wide range of granulated polymer feedstocks commonly used in injection molding processes (137,138). This technology is illustrated in *Figure I-20*.

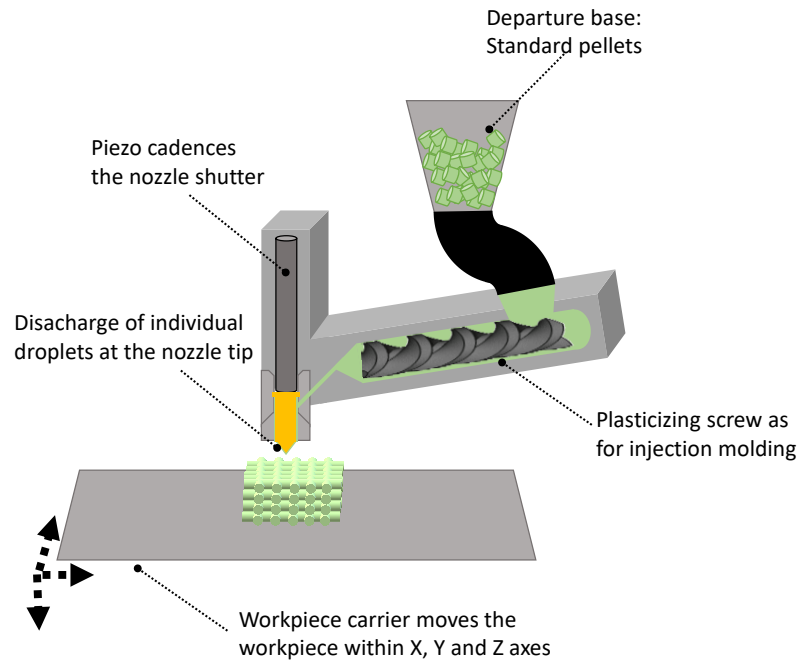


Figure I-20. Schematic representation of “Arburg Plastic Freeforming[®]” technology - a proprietary droplet deposition modeling process.

Operating mode, advantages and disadvantages of the ME technologies have been summarized in Table I-7.

Table I-7. Principal material extrusion based-3D printed technologies, operating mode, advantages, and disadvantages.

Name	Operating mode	Advantage	Disadvantages	Ref
SE/PE	A past or gel, is extruded then deposited layer by layer in order to form the desired object. The obtained 3D object is then under vacuum and heating for complete drying	Low heating, or no heating	Post treatment	(120,134)
FDM/FFF	Molten filament is extruded deposited Layer by layer to form 3D object.	Low cost, easily usable.	Need to develop a suitable filament if working with non-commercial polymer	(120,135)
DPE	Powder are loaded into a screw similar to hot melt extrusion, material is extruded and deposited layer by layer.	Avoid development of filament Ingle step process		(136)
DDM	Pellets are loaded into a screw similar to injection modeling, material is extruded and deposited layer by layer.	Avoid development of filament	Mechanical stress (up to 600 bar) can lead to polymer degradation	(138,139)

I.3.2.4. Material jetting

The Material Jetting (MJ) 3D printing technique is often compared to the standard 2D inkjet process. The use of photopolymers, metals, or waxes that solidify when exposed to light or heat (like SLA) leads to the manufacturing of 3D objects layer by layer. MJ, allows to 3D prints different materials(120,121,142–147).

The printer simultaneously projects material and another so-called “support” soluble material in the form of micro-droplets. These could be cured by UV light and then form the first layer. The operation is repeated to form the entire object as illustrated in *Figure I-21* (120,121,142–147).

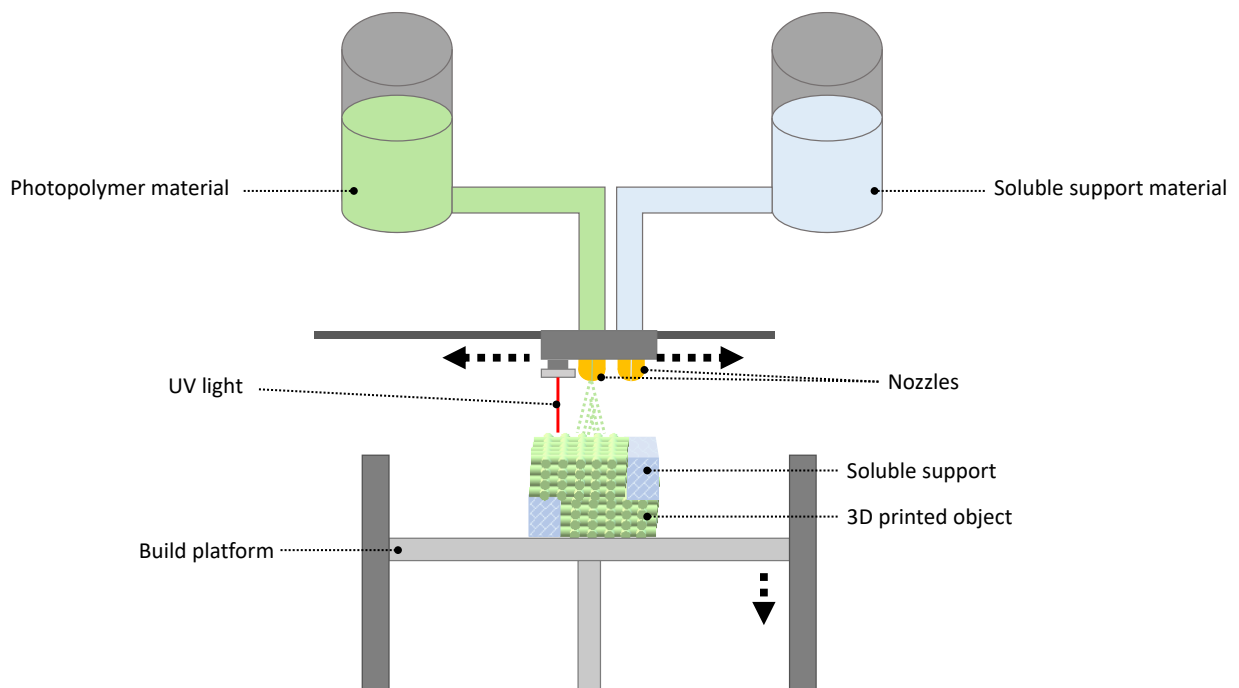


Figure I-21. Schematic representation of material jetting-based three-dimensional printing technologies.

Material jetting encompasses several techniques, the most common are Drop On Demand (DOD), Polyjet, NanoParticle Jetting (NPJ), and are summarized in *Table I-8*.

Table I-8. *Principal material jetting based 3D printed technologies, operating mode, advantages, and disadvantages.*

Name	Operating mode	Advantage	Disadvantages	Ref
DOP	Two printing jets: build material and soluble support material. A leveling blade skims the build area after each layer (flat surface before the next layer).	Good accuracy	A limited number of materials. Slow process, high cost.	(142,143)
Polyjet	Photopolymer materials are sprayed in ultra-thin layers. Each photopolymer layer is cured by UV. The gel-like carrier material can easily be removed manually or by water jet.	Good dimensional performance.	A limited number of materials. Slow process, high cost.	(144–146)
NPJ	Liquid-containing building nanoparticles or carrier nanoparticles are sprayed in layers. High temperatures inside the building area lead to evaporation of the liquid. Only the parts created from the building material remain.	Suitable for metals and ceramics.	A limited number of materials. Slow process, high cost.	(147)

I.3.2.5. Binder jetting

As illustrated in *Figure I-22* Binder Jetting (BJ) printers spray a binder solution or liquid formulation in thin layers of powder material (121,131,148,149). The powder is then bound by the formation of binding bridges, by dissolution or recrystallization. The unbound powder serves as a support for the printed object (121,131,148,149). When one layer is complete, the powder bed moves downward and a new layer of powder is sprayed onto the build surface. The process is repeated until all parts are completed. It is also possible to place the parts in the raw state inside an oven to obtain the sintering of the grains.

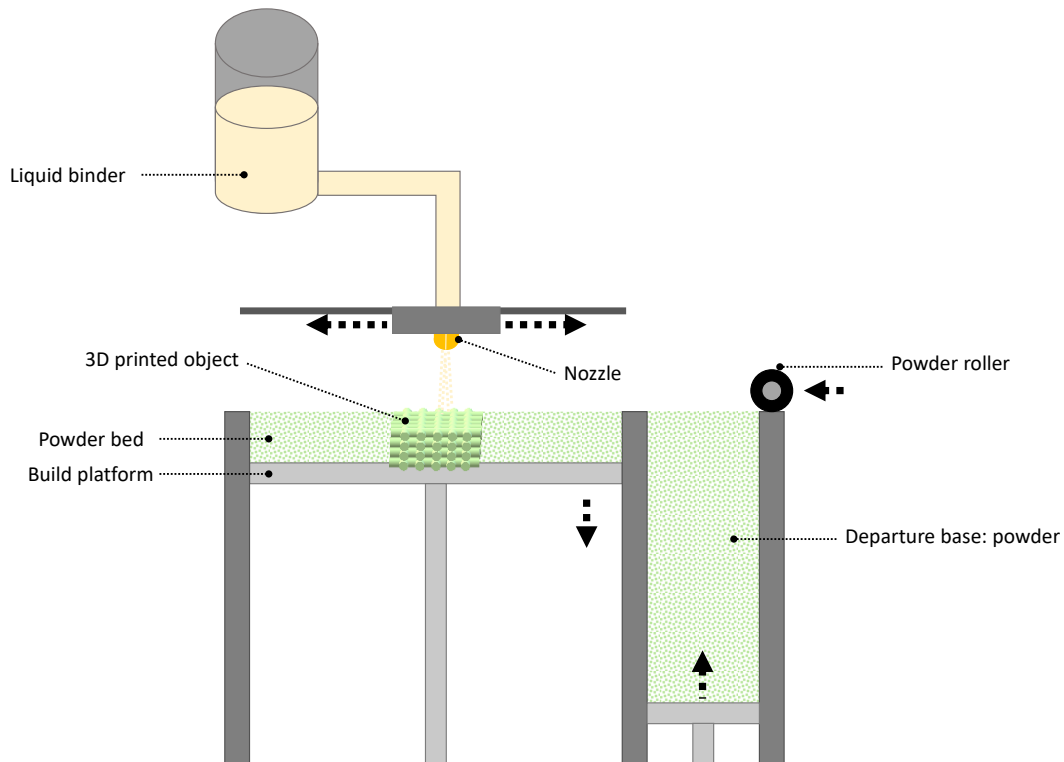


Figure I-22. Schematic representation of binder jetting-based three-dimensional printing technologies.

The main advantages and disadvantages of BJ 3D printing technologies are summarized in Table I-9.

Table I-9. Principal binder jetting 3D printing technology advantages and disadvantages.

Name	Advantage	Disadvantages	Ref
BJ	Don't use heat. Low cost. Suitable for a wild range of materials.	Weak mechanical properties (compared to fused based technologies)	(121,148,149)

I.3.2.6. Direct energy deposition

Direct Energy Deposition (DED) are 3D printing technologies in which an energy source (usually a laser beam) is focused on an area where material deposition is occurring simultaneously. This material, which may be in the form of a filament or a powder, is then melted and deposited at the same time as illustrated in Figure I-23 (120,121). This process is mainly used with metallic powder or stranded materials (131,150).

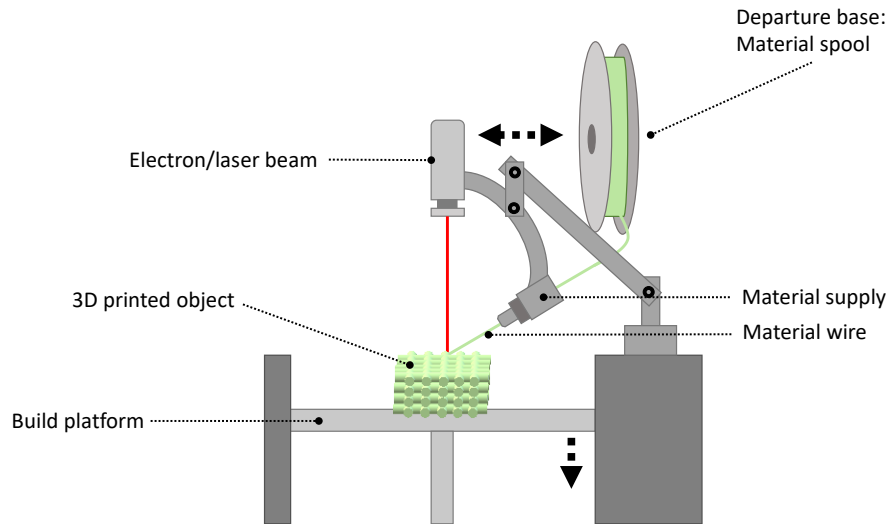


Figure I-23. Schematic representation of direct energy deposition-based three-dimensional printing technologies.

This technic encompasses several technologies such as LENS, Electron Beam Additive Manufacturing (EBAM), and Laser Deposition Welding (LDW). They are distinguished from each other by the way the material is melted, and each is tailored to specific purposes (120,121,150–153). *Table I-10* summarized the operating mode, advantages, and disadvantages of the main DED technologies.

Table I-10. Principal direct energy deposition-based 3D printed technologies, operating mode, advantages, and disadvantages.

Name	Operating mode	Advantage	Disadvantages	Ref
LENS	Laser construct object layer by layer directly from powdered metals, alloys, ceramics, or composites.	Process (argon gas chamber) prevents oxidation and ensures cleanliness.	As to take place in a sealed chamber filled with argon gas. Need post-treatment (heat-treated, hot isostatic pressing).	(151)
EBAM	Electron beam gun deposits metal via a weld head, layer by layer, until the part takes shape near the final dimension and is ready for finished machining	Large scale (3 to 9 kg of metal/hours).	Need post-treatment.	(152)
LDW	Deposits metal using a powder nozzle, combined with a 5-axis milling machine.	Fast printing. High precision metal parts of various size.	Need post-treatment.	(153)

I.3.2.7. Sheet lamination

Sheet Lamination (SL) 3D printing technology is different from all the previously described 3D printing strategies (121). This type of printer does not incorporate conventional 3D printing materials but sheets of paper, plastic, or metal as illustrated in *Figure I-24*. It consists of adding layer by layer an iron-on sheet cut by a laser or a blade. Between each cutting, the plate descends and a new sheet, glued by a binding agent, is unwound. A roller then exerts pressure to make it adhere to the surface. These steps are repeated until the 3D object is obtained. The new sheet can be bonded to the previous one by adhesive bonding, heat sealing, clamping, or ultrasound technique (121,131,154,155).

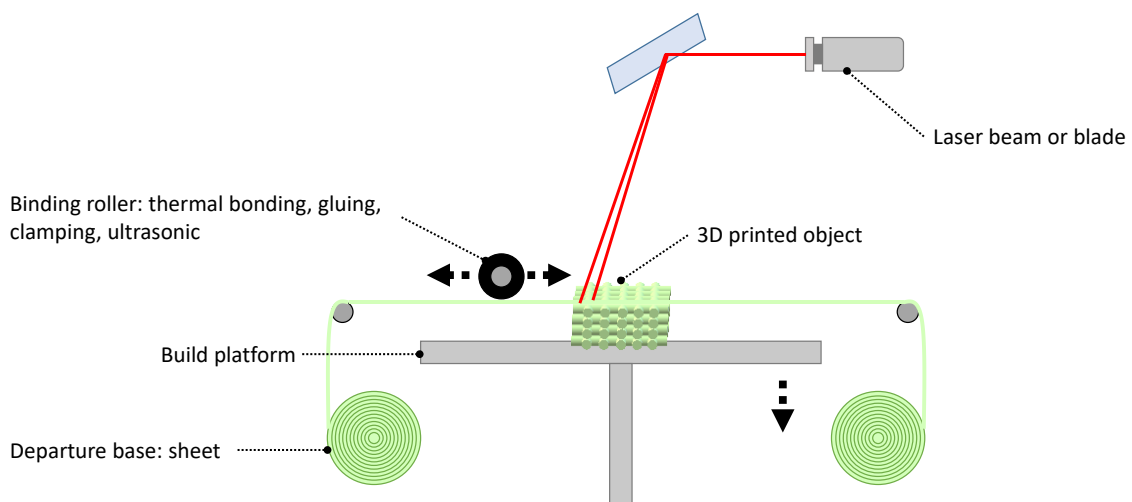


Figure I-24. Schematic representation of sheet lamination-based three-dimensional printing technologies.

Several technologies work on the principles of sheet lamination, such as Laminated Object Manufacturing (LOM), Ultrasonic Additive Manufacturing (UC), Composite Based Additive Manufacturing (CBAM), and Selective Lamination Composite Object Manufacturing (SLCOM). *Table I-11* summarized their operating mode and main advantages and disadvantages.

Table I-11. Principal sheet lamination-based 3D printed technologies, operating mode, advantages, and disadvantages.

Name	Operating mode	Advantage	Disadvantages	Ref
LOM	The bonding of the new sheet on the top of the other one is thermal		Post operating treatment	(121,154)
UC	The bonding of the new sheet on top of the other ones are ultrasonic	Speed, low cost, ease of material handling	Post operating treatment	(121,155)
CBAM	Fiber-reinforced composites fuse with a thermoplastic.		Post operating treatment	(121,131)
SLCOM	Use of thermoplastics as base material and composites of woven fibers.		Post operating treatment	(121,131)

I.3.3. Use in the pharmaceutical field

I.3.3.1. State of art

Among the 3D printing technologies described in *section I.3.2*, Five have been used for pharmaceutical application, either in actual product, or in research as illustrated in *Figure I-25* (111):

- Photopolymerization (126,156–158),
- Powder bed fusion (132,159–162),
- Material extrusion (135,136,138,163–165),
- Material jetting (166,167),
- Binder jetting (168–170).

The efforts and advances of 3D printing technology in the field of pharmaceuticals has recently culminated in 2015 with the US Food and Drug Administration approval of the world's first 3D printed orodispersible tablet SPRITAM[®] (168,169).

Some examples of the used of these technologies in the pharmaceutical field have been summarized in *Figure I-25* and *Table I-12*.

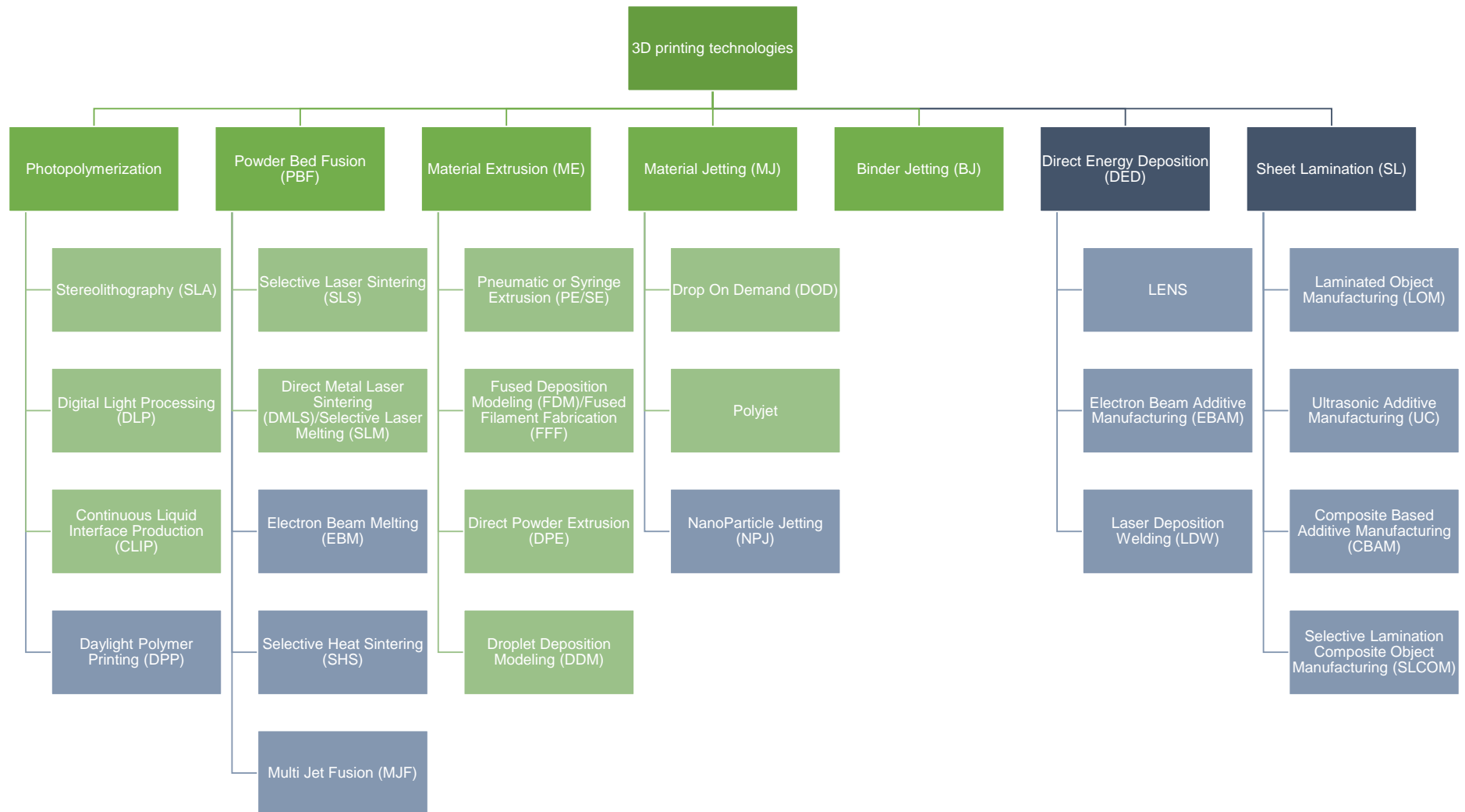


Figure I-25. Different classes of 3D printing technologies, the ones used in pharmaceutical field have been colored in green, and the other ones in dark blue. Adapted from Lim et al 2018.

Table I-12. Examples of 3D printing technologies in pharmaceutical field.

	Used technology	Results	Ref
Photopolymerization	SLA	SLA printing was used to prepare ibuprofen-loaded hydrogels of cross-linked polyethylene glycol diacrylate. Dissolution profiles showed that drug release rates were dependent on water content, with higher water content hydrogels releasing drug faster.	(156)
	SLA	SLA was used to create custom tablet geometries using a novel biocompatible photochemistry consisting of ascorbic acid encapsulated in a poly(ethylene glycol) dimethacrylate-based polymer network and polymerized using riboflavin as a photoinitiator. Different geometries were printed with different surface area to volume ratios. After 1 h of release, honeycomb and coaxial annulus tablet gels exhibit higher release rates at approximately 80%.	(157)
	DLP	Silk fibroin-based microneedles were fabricated using DLP 3D printing using riboflavin, a vitamin that acts as a photoinitiator. Delivery of molecules to the skin is verified using rhodamine B fluorescence dye.	(126)
	CLIP	CLIP technology is used to fabricate biocompatible and drug-loaded devices with controlled release properties, using liquid resins containing rhodamine B-base, docetaxel and dexamethasone-acetate. Formulations were shown to be biocompatible over the course of 175 days of in vitro degradation and the clinically-relevant drugs could be encapsulated and released in a controlled fashion.	(158)
PBF	SLS	SLS printing is used for manufacturing medicines with two thermoplastic pharmaceutical grade polymer, and three different drug loading of paracetamol. One of the polymers showed, showed pH-independent release characteristics, while the other showed pH-dependent, modified-release profiles independent of drug loading, with complete release being achieved over 12h.	(159)
	SLM	SLM was employed to manufacture Ti-6Al-4 V samples, with internal reservoirs and releasing Micro-channels (MCs) to simulate what could be a drug-delivering orthopedic or dental implant.	(160)
	SLM	Drug release of Vancomycin is enabled by manufacturing of integrated permeable structures possessing high porosity through application of selective laser melting technology.	(161)
ME	SLM	Titanium components fabricated using SLM were functionalized with Paracetamol using phosphonic acid based self-assembled monolayers. Thus, the proposed method has the potential to incorporate drugs to titanium coated surfaces and improve their biocompatibility and reduce post-implant complications.	(162)
	PE/SE	Bi-layered tablets containing Guaifenesin, Polyacrylic acid, microcrystalline cellulose, and sodium starch glycolate were printed using semi solid extrusion. Drug was release following a Fickian diffusion release pattern through hydrated polymer gel layer.	(163)
	PE/SE	Multi-active tablets (nifedipine, glipizide,captopril) mixed hydroxypropyl methylcellulose were printed using semisolid extrusion. Both nifedipine and glipizide showed sustained-release.	(164)
	FDM/FFF	FDM/FFF 3DP technology allow to manufacture tablet shapes of different geometries, that would be challenging to manufacture by conventional pharmaceutical technologies. Drug release from the tablets was not dependent on the surface area but on surface area to volume ratio.	(135)
	FDM/FFF	3D scanning was used to construct 3D models of a nose and ear to provide the opportunity to customize shape and size of a wound dressing to an individual patient.	(165)
	DPE	3D printing by avoiding the need for preparation of filaments by hot melt extrusion. This novel single-step technology could revolutionize the preparation of amorphous solid dispersions as final formulations and it may be especially suited for preclinical studies, where the quantity of drugs is limited and without the need of using traditional hot melt extrusion.	(136)
MJ	DDM	DDM can be used to manufacture drug delivery devices of varying geometries, densities and surface areas to control the drug release. This work presents a new opportunity to increase the release of Dapivirine.	(138)
	DOD	The functions of the bioprinter have been demonstrated by using a high-throughput drug-delivery model; and by bioprinting micro-tissues using a variety of different cell types, DOD demonstrates a promising platform for generating many types of tissues and drug-delivery models.	(166)
	Polyjet	The tablets produced consist of a cross-linked poly(ethylene glycol diacrylate) hydrogel matrix containing the drug, photoinitiated in a low oxygen environment using an aqueous solution.	(167)
BJ	ZipDose®	A high dose rapidly dispersing three-dimensionally printed dosage form comprising a high dose of levetiracetam in a porous matrix that disperses in water within a period of less than about 10 seconds.	(168,169)
	BJ	Fabrication of donut shaped tablets based on mixture of paracetamol and polymer powder by BJ technology. A monophasic release kinetic was obtained	(170)

I.3.3.2. Interest in control release

3D printing technologies offer high flexibility in the preparation of dosage forms such as combining different APIs or reaching complex release profiles (171). This is making 3D printing promising technologies for revolutionizing controlled drug delivery systems (172). As previously described the gain of interest of 3D printing technologies in the pharmaceutical field is extensive. The rise of these new technologies opened an infinite range of possibilities for modulating drug release. The conventional pharmaceutical technologies allowed to modulate the release pattern by modulating the size of classical shape devices (spheres, cylinders, etc.), or the selection of the appropriate carriers (polymer grade, molecular weight, etc.) (42,43,60–62,64). 3D printing technologies have revolutionized the way to develop new devices for the controlled release of API. With the appropriate choice of polymer and technology, it could be possible to precisely modulate drug release by precisely modulating either external structure (innovative geometry), the internal structure of the device (infill percentage or pattern), or size and structure of the device, as illustrated in *Figure I-26* (134,135,164,173–179).

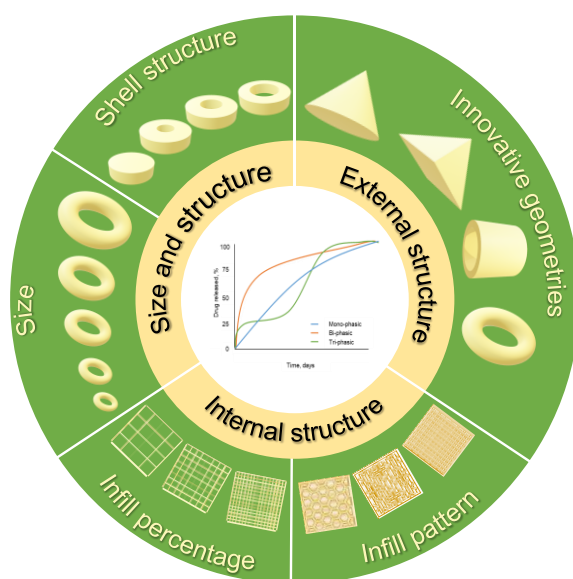


Figure I-26. Illustration of the different possibilities to modulate the structure to control the drug release from 3D printed devices. Adapted from Patel *et al* 2021.

I.3.3.2.1. Effect of the external structure

Two examples of the impact of the external structure were summarized in *Figure I-27*. In the first one, Goyanes *et al.* studied the impact of 5 different tablets geometries obtained by 3D printing, on the release of paracetamol. They show that drug release from the tablets was not dependent on the surface area but instead on the surface area to volume ratio (135). The second

study conducted by Fu *et al.* focuses on the impact of the shape of vaginal rings obtained by 3D printing for the controlled release of progesterone. They concluded that the dissolution rate of progesterone was higher for the vaginal ring exhibiting the higher surface area/volume ratio (180)

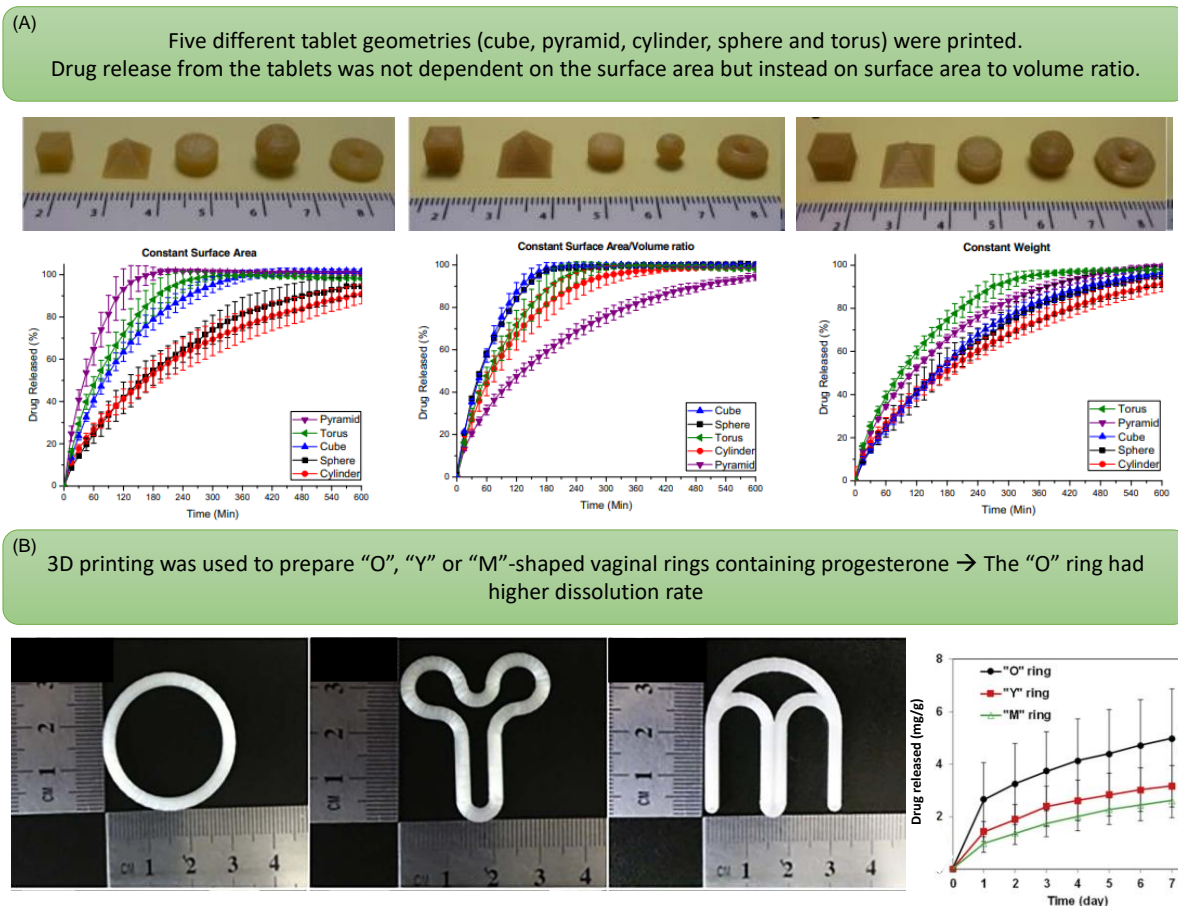
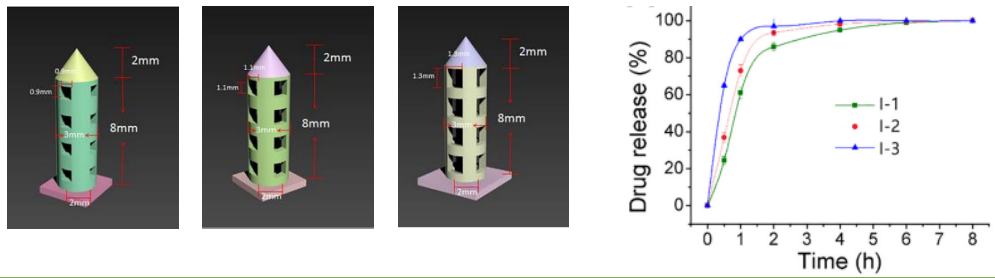


Figure I-27. Examples of reported studies on the effect of the external structure of 3D printed devices on drug release. Adapted from (A) Goyanes *et al.*(135) and (B) Fu *et al.*(180).

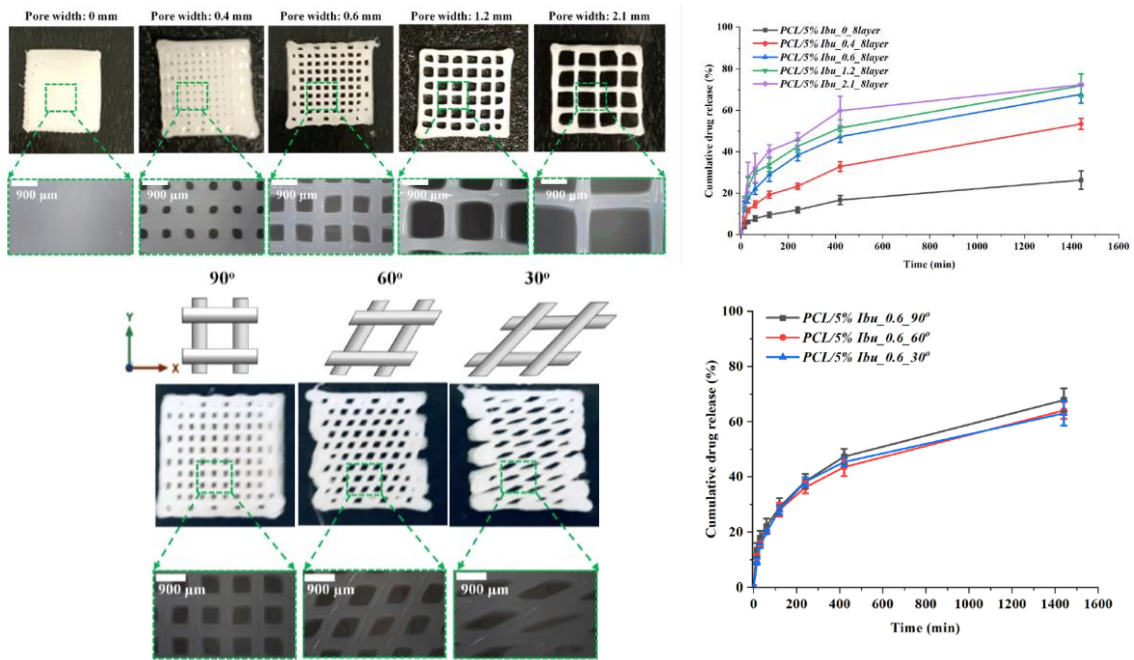
I.3.3.2.2. Effect of the internal structure

Examples of the effect of the internal structure on drug release are illustrated in *Figure I-28*. In these studies, the authors investigated the impact of porosity (percentage, and shape of the pore) on drug release rate. They exhibited that higher porosity leads to a quicker drug release rate by modulating the surface volume ratio (138,181,182).

(A) 3D printing was used to prepare hollow bullet-shaped implant with different porous surface for controlled cytoxin release



(B) The impact of geometrical parameters of 3D printed constructs (i.e., porosity, pore shape) on drug release was investigated → Porosity modulates the surface/volume ratio, and higher porosities lead to quicker drug release rates



(C) 10% density vaginal ring exhibited a 7 times fold increase in daprivine release compared to 100% density

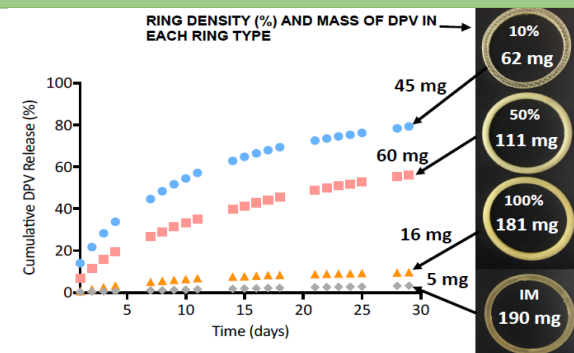
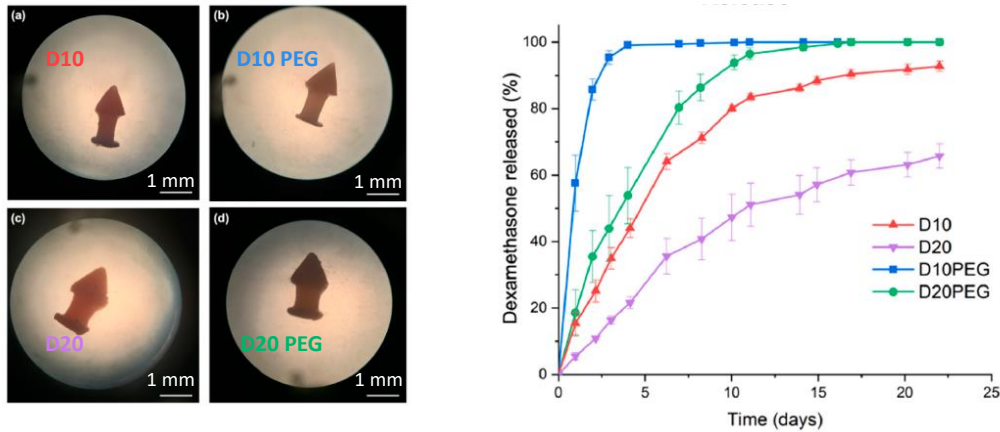


Figure I-28. Examples of reported studies on the effect of the internal structure of 3D printed devices on drug release. Adapted from (A) Yang et al. (181), (B) Zhang et al.(182), and (C) Welsh et al. (138).

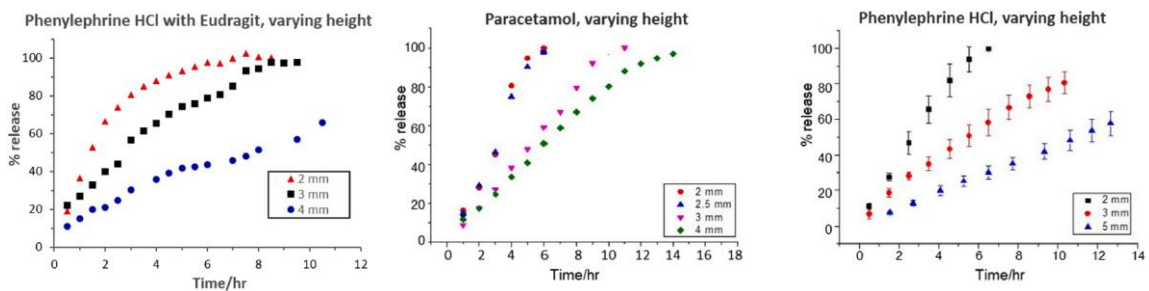
I.3.3.2.3. Effect of size and structure

Examples of the effect of the size and structure of the devices on drug release are illustrated in *Figure I-29*. Modulating both the size and the internal structure of the device by 3D printing is of great interest in modulating drug release rate (183–185).

(A) 3D printing was employed to develop dexamethasone-loaded punctal plugs which showed sustained release of dexamethasone for up to 7 days → it was shown that size has a significant impact on release rate



(B) Customization of the release duration by tuning different tablet height with 3 different API



(C) Multicompartmental capsules were 3D printed → allow to modulate drug release.

Temporal dissolution of the 3D printed capsules.

	Starting dissolution [min]	Ending dissolution [min]
One compartment capsule	70 ± 10	183 ± 6
Two compartment capsules	81 ± 2	233 ± 6
Three compartment capsules	83 ± 21	373 ± 23

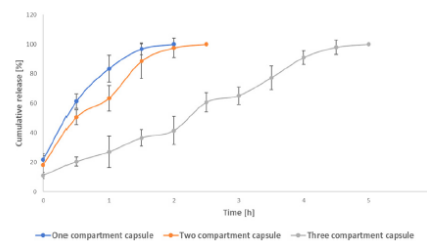


Figure I-29. Examples of reported studies on the effect of size and structure of 3D printed devices on drug release. Adapted from (A) Xu et al. (183), (B) Tan et al.(184), and (C) Russi et al. (185).

I.3.3.3. Poly(lactic-co-glycolic) acid

Among all the studies conducted on the suitability of 3D printing technologies in developing new controlled drug delivery devices, only a few of them focus on PLGA as a potential carrier.

Some studies have been published on the investigation of the interest of the use of PLGA and 3D printing technologies for bones repair (186–189). Yang *et al.* investigated the potential of a quaternized chitosan grafted PLGA hydroxyapatite scaffold obtained by 3D printing to improve antimicrobial activity and osteoconductive properties. They observed that this type of scaffold exhibited an improvement in anti-infection and bone regeneration capabilities (190). PLGA based scaffold for tissues engineering obtained by 3D printing have also been investigated by Rasoulianboroujeni *et al.* and Mironov *et al.* (191,192).

In 2017 Guo *et al.* investigated the impact of printing parameters on printing resolution of PLGA scaffolds obtained by 3D printing with different PLGA grade (193). They built a model that correlate the predominant factors determining the printing precision. Recently, Carlier *et al.* developed 3D printed implantable devices loaded with monoclonal antibodies obtained by FDM (194). They demonstrated the suitability of FDM for producing monoclonal antibody-loaded devices with good stability, affinity and sustained-release profiles of the monoclonal antibody with PLGA.

I.4. Research objectives

PLGA based devices are a first category choice for polymer-based long-acting injectables due to their good biocompatibility, biodegradability, and use in several FDA-approved products. However, establishing an *in vitro* *in vivo* correlation regarding drug release of such devices is challenging as many different mechanisms are involved in drug release. Thus, it is of great importance to properly characterize the devices, to identify the release mechanism by which the API is released from the device.

In the past few years, 3D printing technologies have revolutionized the development of new controlled drug release devices. These technologies allow to precisely control the size, shape, internal and external porosity of the device, and so the release rate of the API.

In this context the research objectives of this thesis were divided into two parts:

- (i) Development of experimental set-ups for *in vitro* drug release measurement for implants administrated to the subcutis, and investigation on the impact of several implants attribute on *in vitro* drug release;
- (ii) Development of PLGA based controlled drug release implants using 3D printing technologies, and investigation of the impact of the structure of the implant on *in vitro* drug release.

The research results of this Ph.D. thesis will be described in seven parts corresponding to scientific papers that have either been submitted in scientific journals or plan to be:

1. How hydrogels surrounding PLGA implants limit swelling and slow down drug release
2. Hot-melt extruded ibuprofen-loaded PLGA implants: Importance of heat exposure
3. PLGA implants for controlled drug release: Impact of the diameter
4. How bulk fluid renewal can affect drug release from PLGA implants
5. 3D printing of ibuprofen loaded controlled release implants with PLGA – Proof of concept and impact filling pattern
6. PLGA based 3D printed mesh – the impact of the 3D printed technology on drug release
7. PLGA based 3D printed mesh – the impact of filling density on drug release

I.5. References

1. Siepmann J, Siegel RA, Rathbone MJ, editors. Fundamentals and Applications of Controlled Release Drug Delivery [Internet]. Springer US; 2012 [cited 2021 Jul 12]. (Advances in Delivery Science and Technology). Available from: <https://www.springer.com/gp/book/9781461408802>
2. Mrsny RJ. Oral drug delivery research in Europe. *J Controlled Release*. 2012 Jul 20;161(2):247–53.
3. Nkanga CI, Fisch A, Rad-Malekshahi M, Romic MD, Kittel B, Ullrich T, et al. Clinically established biodegradable long acting injectables: An industry perspective. *Adv Drug Deliv Rev*. 2020 Dec 1;167:19–46.
4. Uhrich KE, Cannizzaro SM, Langer RS, Shakesheff KM. Polymeric systems for controlled drug release. *Chem Rev*. 1999 Nov 10;99(11):3181–98.
5. O'Brien MN, Jiang W, Wang Y, Loffredo DM. Challenges and opportunities in the development of complex generic long-acting injectable drug products. *J Control Release Off J Control Release Soc*. 2021 Aug 10;336:144–58.
6. Selmin F, Musazzi UM, Magri G, Rocco P, Cilurzo F, Minghetti P. Regulatory aspects and quality controls of polymer-based parenteral long-acting drug products: the challenge of approving copies. *Drug Discov Today*. 2020 Feb 1;25(2):321–9.
7. Burgess DJ, Crommelin DJA, Hussain AS, Chen M-L. Assuring quality and performance of sustained and controlled release parenterals: EUFEPS workshop report. *AAPS PharmSci*. 2015 Jul 10;6(1):100–11.
8. Parenteral preparations - European Pharmacopoeia 10.0 [Internet]. [cited 2021 Mar 17]. Available from: <https://pheur-edqm-eu.ressources-electroniques.univ-lille.fr/app/10-0/content/10-0/0520E.htm?highlight=on&terms=implants&terms=implants&terms=implants&terms=implants>
9. USP. <1> Injections and implanted drug products (parenterals) - Product quality tests. 2021.
10. USP. <1034> The biocompatibility of materials used in drug containers, medical devices, and implants. 2021.
11. Rawat A, Bhardwaj U, Burgess DJ. Comparison of in vitro-in vivo release of Risperdal(®) Consta(®) microspheres. *Int J Pharm*. 2012 Sep 15;434(1–2):115–21.
12. Andhariya JV, Jog R, Shen J, Choi S, Wang Y, Zou Y, et al. Development of Level A in vitro-in vivo correlations for peptide loaded PLGA microspheres. *J Control Release Off J Control Release Soc*. 2019 Aug 28;308:1–13.
13. Zolnik BS, Burgess DJ. Evaluation of in vivo–in vitro release of dexamethasone from PLGA microspheres. *J Controlled Release*. 2008 Apr 21;127(2):137–45.

14. Gray V, Cady S, Curran D, DeMuth J, Eradiri O, Hussain M, et al. In Vitro Release Test Methods for Drug Formulations for Parenteral Applications. *Dissolution Technol.* 2018 Jan 1;25:8–13.
15. Zolnik BS, Leary PE, Burgess DJ. Elevated temperature accelerated release testing of PLGA microspheres. *J Control Release Off J Control Release Soc.* 2006 May 30;112(3):293–300.
16. Tamani F, Bassand C, Hamoudi MC, Siepmann F, Siepmann J. Mechanistic explanation of the (up to) 3 release phases of PLGA microparticles: Monolithic dispersions studied at lower temperatures. *Int J Pharm.* 2021 Mar 1;596:120220.
17. Faisant N, Akiki J, Siepmann F, Benoit JP, Siepmann J. Effects of the type of release medium on drug release from PLGA-based microparticles: Experiment and theory. *Int J Pharm.* 2006 May 18;314(2):189–97.
18. Klose D, Azaroual N, Siepmann F, Vermeersch G, Siepmann J. Towards More Realistic In Vitro Release Measurement Techniques for Biodegradable Microparticles. *Pharm Res.* 2008 Oct 29;26(3):691.
19. USP. <1092> The dissolution procedure: development and validation. 2021.
20. SMART [Internet]. Servier Medical Art. [cited 2020 Nov 26]. Available from: <https://smart.servier.com/>
21. Ghalanbor Z, Körber M, Bodmeier R. Interdependency of protein-release completeness and polymer degradation in PLGA-based implants. *Eur J Pharm Biopharm.* 2013 Nov 1;85(3, Part A):624–30.
22. Gosau M, Müller BW. Release of gentamicin sulphate from biodegradable PLGA-implants produced by hot melt extrusion. *Pharm.* 2010 Jul;65(7):487–92.
23. Li L, Li C, Zhou J. Effective sustained release of 5-FU-loaded PLGA implant for improving therapeutic index of 5-FU in colon tumor. *Int J Pharm.* 2018 Oct 25;550(1):380–7.
24. Lizambard M, Menu T, Fossart M, Bassand C, Agossa K, Huck O, et al. In-situ forming implants for the treatment of periodontal diseases: Simultaneous controlled release of an antiseptic and an anti-inflammatory drug. *Int J Pharm.* 2019 Dec 15;572:118833.
25. Bode C, Kranz H, Fizez A, Siepmann F, Siepmann J. Often neglected: PLGA/PLA swelling orchestrates drug release: HME implants. *J Controlled Release.* 2019 Jul 28;306:97–107.
26. Abdel-Mottaleb MMA, Lamprecht A. Standardized in vitro drug release test for colloidal drug carriers using modified USP dissolution apparatus I. *Drug Dev Ind Pharm.* 2011 Feb;37(2):178–84.
27. Sterner B, Harms M, Weigandt M, Windbergs M, Lehr CM. Crystal suspensions of poorly soluble peptides for intra-articular application: a novel approach for biorelevant assessment of their in vitro release. *Int J Pharm.* 2014 Jan 30;461(1–2):46–53.

28. Tipnis NP, Shen J, Jackson D, Leblanc D, Burgess DJ. Flow-through cell-based in vitro release method for triamcinolone acetonide poly (lactic-co-glycolic) acid microspheres. *Int J Pharm.* 2020 Apr 15;579:119130.
29. Tomic I, Vidis-Millward A, Mueller-Zsigmondy M, Cardot J-M. Setting accelerated dissolution test for PLGA microspheres containing peptide, investigation of critical parameters affecting drug release rate and mechanism. *Int J Pharm.* 2016 May 30;505(1–2):42–51.
30. Delplace C, Kreye F, Klose D, Danède F, Descamps M, Siepmann J, et al. Impact of the experimental conditions on drug release from parenteral depot systems: From negligible to significant. *Int J Pharm.* 2012 Aug 1;432(1–2):11–22.
31. Bain DF, Munday DL, Smith A. Modulation of rifampicin release from spray-dried microspheres using combinations of poly-(DL-lactide). *J Microencapsul.* 1999 Jun;16(3):369–85.
32. Shameem M, Lee H, DeLuca PP. A short term (accelerated release) approach to evaluate peptide release from PLGA depot-formulations. *AAPS PharmSci.* 1999;1(3):E7.
33. Tamani F, Bassand C, Hamoudi MC, Danede F, Willart JF, Siepmann F, et al. Mechanistic explanation of the (up to) 3 release phases of PLGA microparticles: Diprophylline dispersions. *Int J Pharm.* 2019 Dec 15;572:118819.
34. Kožák J, Rabišková M, Lamprecht A. In-vitro drug release testing of parenteral formulations via an agarose gel envelope to closer mimic tissue firmness. *Int J Pharm.* 2021 Feb 1;594:120142.
35. Fredenberg S, Wahlgren M, Reslow M, Axelsson A. The mechanisms of drug release in poly(lactic-co-glycolic acid)-based drug delivery systems--a review. *Int J Pharm.* 2011;415(1–2):34–52.
36. Ramchandani M, Robinson D. In vitro and in vivo release of ciprofloxacin from PLGA 50:50 implants. *J Controlled Release.* 1998 Jul 31;54(2):167–75.
37. Erbetta CDC, Alves RJ, Resende JM, Freitas RF de S, Sousa RG de. Synthesis and Characterization of Poly(D,L-Lactide-co-Glycolide) Copolymer. *J Biomater Nanobiotechnology.* 2012 Apr 28;3(2):208–25.
38. Bendix D. Chemical synthesis of polylactide and its copolymers for medical applications. *Polym Degrad Stab.* 1998 Jan 3;59(1):129–35.
39. Makadia HK, Siegel SJ. Poly Lactic-co-Glycolic Acid (PLGA) as Biodegradable Controlled Drug Delivery Carrier. *Polymers.* 2011 Sep 1;3(3):1377–97.
40. Ogawa Y, Yamamoto M, Takada S, Okada H, Shimamoto T. Controlled-Release of Leuprolide Acetate from Polylactic Acid or Copoly(Lactic/Glycolic) Acid Microcapsules : Influence of Molecular Weight and Copolymer Ratio of Polymer. *Chem Pharm Bull (Tokyo).* 1988;36(4):1502–7.

41. Zilberman M, Grinberg O. HRP-Loaded Bioresorbable Microspheres: Effect of Copolymer Composition and Molecular Weight on Microstructure and Release Profile. *J Biomater Appl*. 2008 Mar 1;22(5):391–407.
42. Ochi M, Wan B, Bao Q, Burgess DJ. Influence of PLGA molecular weight distribution on leuprolide release from microspheres. *Int J Pharm*. 2021 Apr 15;599:120450.
43. Kohno M, Andhariya JV, Wan B, Bao Q, Rothstein S, Hezel M, et al. The effect of PLGA molecular weight differences on risperidone release from microspheres. *Int J Pharm*. 2020 May 30;582:119339.
44. Gentile P, Chiono V, Carmagnola I, Hatton PV. An Overview of Poly(lactic-co-glycolic) Acid (PLGA)-Based Biomaterials for Bone Tissue Engineering. *Int J Mol Sci*. 2014 Feb 28;15(3):3640–59.
45. Gilding DK, Reed AM. Biodegradable polymers for use in surgery—polyglycolic/poly(lactic acid) homo- and copolymers: 1. *Polymer*. 1979 Dec 1;20(12):1459–64.
46. Blasi P, D'Souza SS, Selmin F, DeLuca PP. Plasticizing effect of water on poly(lactide-co-glycolide). *J Controlled Release*. 2005 Nov 2;108(1):1–9.
47. Albertini B, Iraci N, Schoubben A, Giovagnoli S, Ricci M, Blasi P, et al. β -cyclodextrin hinders PLGA plasticization during microparticle manufacturing. *J Drug Deliv Sci Technol*. 2015 Dec 1;30:375–83.
48. Gasmi H, Danede F, Siepmann J, Siepmann F. Does PLGA microparticle swelling control drug release? New insight based on single particle swelling studies. *J Control Release*. 2015 Sep 10;213:120–7.
49. Gasmi H, Willart J-F, Danede F, Hamoudi MC, Siepmann J, Siepmann F. Importance of PLGA microparticle swelling for the control of prilocaine release. *J Drug Deliv Sci Technol*. 2015 Dec 1;30:123–32.
50. Hines DJ, Kaplan DL. Poly(lactic-co-glycolic) Acid-Controlled-Release Systems: Experimental and Modeling Insights. *Crit Rev Ther Drug Carrier Syst*. 2013;30(3):257–76.
51. Rowe RC, Sheskey PJ, Quinn ME. *Handbook of Pharmaceutical Excipients*. Pharmaceutical Press; 2009. 888 p.
52. Ford Versypt AN, Pack DW, Braatz RD. Mathematical modeling of drug delivery from autocatalytically degradable PLGA microspheres — A review. *J Controlled Release*. 2013 Jan 10;165(1):29–37.
53. Ding AG, Shenderova A, Schwendeman SP. Prediction of Microclimate pH in Poly(lactic-co-glycolic Acid) Films. *J Am Chem Soc*. 2006 Apr 1;128(16):5384–90.
54. Bode C, Kranz H, Siepmann F, Siepmann J. Coloring of PLGA implants to better understand the underlying drug release mechanisms. *Int J Pharm*. 2019 Oct 5;569:118563.

55. Antheunis H, van der Meer J-C, de Geus M, Heise A, Koning CE. Autocatalytic equation describing the change in molecular weight during hydrolytic degradation of aliphatic polyesters. *Biomacromolecules*. 2010 Apr 12;11(4):1118–24.
56. Dumetz AC, Chockla AM, Kaler EW, Lenhoff AM. Effects of pH on protein-protein interactions and implications for protein phase behavior. *Biochim Biophys Acta*. 2008 Apr;1784(4):600–10.
57. Grizzi I, Garreau H, Li S, Vert M. Hydrolytic degradation of devices based on poly(DL-lactic acid) size-dependence. *Biomaterials*. 1995 Mar;16(4):305–11.
58. Witt C, Kissel T. Morphological characterization of microspheres, films and implants prepared from poly(lactide-co-glycolide) and ABA triblock copolymers: is the erosion controlled by degradation, swelling or diffusion? *Eur J Pharm Biopharm Off J Arbeitsgemeinschaft Pharm Verfahrenstechnik EV*. 2001 May;51(3):171–81.
59. Schliecker G, Schmidt C, Fuchs S, Wombacher R, Kissel T. Hydrolytic degradation of poly(lactide-co-glycolide) films: effect of oligomers on degradation rate and crystallinity. *Int J Pharm*. 2003 Nov 6;266(1–2):39–49.
60. Siepmann J, Faisant N, Akiki J, Richard J, Benoit JP. Effect of the size of biodegradable microparticles on drug release: experiment and theory. *J Control Release Off J Control Release Soc*. 2004 Apr 16;96(1):123–34.
61. Siepmann J, Elkharraz K, Siepmann F, Klose D. How autocatalysis accelerates drug release from PLGA-based microparticles: a quantitative treatment. *Biomacromolecules*. 2005 Aug;6(4):2312–9.
62. Klose D, Siepmann F, Elkharraz K, Krenzlin S, Siepmann J. How porosity and size affect the drug release mechanisms from PLGA-based microparticles. *Int J Pharm*. 2006 May 18;314(2):198–206.
63. Kapoor DN, Bhatia A, Kaur R, Sharma R, Kaur G, Dhawan S. PLGA: a unique polymer for drug delivery. *Ther Deliv*. 2015 Jan;6(1):41–58.
64. Chen W, Palazzo A, Hennink WE, Kok RJ. Effect of Particle Size on Drug Loading and Release Kinetics of Gefitinib-Loaded PLGA Microspheres. *Mol Pharm*. 2017 Feb 6;14(2):459–67.
65. Klose D, Siepmann F, Elkharraz K, Siepmann J. PLGA-based drug delivery systems: importance of the type of drug and device geometry. *Int J Pharm*. 2008 Apr 16;354(1–2):95–103.
66. Hamoudi-Ben Yelles MC, Tran Tan V, Danede F, Willart JF, Siepmann J. PLGA implants: How Poloxamer/PEO addition slows down or accelerates polymer degradation and drug release. *J Control Release Off J Control Release Soc*. 2017 May 10;253:19–29.
67. Casalini T, Bassas-Galia M, Girard H, Castrovinci A, De Carolis A, Brianza S, et al. A Systematic Experimental and Computational Analysis of Commercially Available Aliphatic Polyesters. *Appl Sci*. 2019 Jan;9(16):3397.

68. Black J, Black J. *Biological Performance of Materials: Fundamentals of Biocompatibility*, Fourth Edition. 4th ed. Boca Raton: CRC Press; 2005. 520 p.
69. Health C for D and R. Use of International Standard ISO 10993-1, 'Biological evaluation of medical devices - Part 1: Evaluation and testing within a risk management process' [Internet]. U.S. Food and Drug Administration. FDA; 2020 [cited 2021 Jun 30]. Available from: <https://www.fda.gov/regulatory-information/search-fda-guidance-documents/use-international-standard-iso-10993-1-biological-evaluation-medical-devices-part-1-evaluation-and>
70. Nair LS, Laurencin CT. Biodegradable polymers as biomaterials. *Prog Polym Sci*. 2007 Aug 1;32(8):762–98.
71. Kumari A, Yadav SK, Yadav SC. Biodegradable polymeric nanoparticles based drug delivery systems. *Colloids Surf B Biointerfaces*. 2010 Jan 1;75(1):1–18.
72. Grund S, Bauer M, Fischer D. Polymers in Drug Delivery—State of the Art and Future Trends. *Adv Eng Mater*. 2011;13(3):B61–87.
73. Zhao D, Zhu T, Li J, Cui L, Zhang Z, Zhuang X, et al. Poly(lactic-co-glycolic acid)-based composite bone-substitute materials. *Bioact Mater*. 2021 Feb 1;6(2):346–60.
74. Maurus PB, Kaeding CC. Bioabsorbable implant material review. *Oper Tech Sports Med*. 2004 Jul 1;12(3):158–60.
75. Anderson JM, Shive MS. Biodegradation and biocompatibility of PLA and PLGA microspheres. *Adv Drug Deliv Rev*. 2012 Dec 1;64:72–82.
76. Sansdrap P, Moës AJ. In vitro evaluation of the hydrolytic degradation of dispersed and aggregated poly(dl-lactide-co-glycolide) microspheres. *J Controlled Release*. 1997 Jan 3;43(1):47–58.
77. Kranz H, Ubrich N, Maincent P, Bodmeier R. Physicomechanical properties of biodegradable poly(D,L-lactide) and poly(D,L-lactide-co-glycolide) films in the dry and wet states. *J Pharm Sci*. 2000;89(12):1558–66.
78. Shah NH, Railkar AS, Chen FC, Tarantino R, Kumar S, Murjani M, et al. A biodegradable injectable implant for delivering micro and macromolecules using poly (lactic-co-glycolic) acid (PLGA) copolymers. *J Controlled Release*. 1993 Nov 1;27(2):139–47.
79. Park TG. Degradation of poly(lactic-co-glycolic acid) microspheres: effect of copolymer composition. *Biomaterials*. 1995 Oct 1;16(15):1123–30.
80. Gasper MM, Blanco D, Cruz ME, Alonso MJ. Formulation of L-asparaginase-loaded poly(lactide-co-glycolide) nanoparticles: influence of polymer properties on enzyme loading, activity and in vitro release. *J Control Release Off J Control Release Soc*. 1998 Mar 2;52(1–2):53–62.
81. Zhu G, Mallery SR, Schwendeman SP. Stabilization of proteins encapsulated in injectable poly (lactide- co-glycolide). *Nat Biotechnol*. 2000 Jan;18(1):52–7.

82. Jonnalagadda S, Robinson DH. A bioresorbable, polylactide reservoir for diffusional and osmotically controlled drug delivery. *AAPS PharmSciTech*. 2000 Dec 1;1(4):26–34.
83. Wong HM, Wang JJ, Wang C-H. In Vitro Sustained Release of Human Immunoglobulin G from Biodegradable Microspheres. *Ind Eng Chem Res*. 2001 Feb 1;40(3):933–48.
84. Friess W, Schlapp M. Release mechanisms from gentamicin loaded poly(lactic-co-glycolic acid) (PLGA) microparticles. *J Pharm Sci*. 2002 Mar;91(3):845–55.
85. Bishara A, Domb AJ. PLA stereocomplexes for controlled release of somatostatin analogue. *J Control Release Off J Control Release Soc*. 2005 Oct 20;107(3):474–83.
86. Matsumoto A, Matsukawa Y, Suzuki T, Yoshino H. Drug release characteristics of multi-reservoir type microspheres with poly(dl-lactide-co-glycolide) and poly(dl-lactide). *J Control Release Off J Control Release Soc*. 2005 Aug 18;106(1–2):172–80.
87. Kim HK, Chung HJ, Park TG. Biodegradable polymeric microspheres with ‘open/closed’ pores for sustained release of human growth hormone. *J Control Release Off J Control Release Soc*. 2006 May 15;112(2):167–74.
88. Kang J, Schwendeman SP. Pore closing and opening in biodegradable polymers and their effect on the controlled release of proteins. *Mol Pharm*. 2007 Feb;4(1):104–18.
89. Sun Y, Wang J, Zhang X, Zhang Z, Zheng Y, Chen D, et al. Synchronic release of two hormonal contraceptives for about one month from the PLGA microspheres: in vitro and in vivo studies. *J Control Release Off J Control Release Soc*. 2008 Aug 7;129(3):192–9.
90. Mochizuki A, Niikawa T, Omura I, Yamashita S. Controlled release of argatroban from PLA film—Effect of hydroxyesters as additives on enhancement of drug release. *J Appl Polym Sci*. 2008;108(5):3353–60.
91. Gagliardi M, Silvestri D, Cristallini C, Guadagni M, Crifaci G, Giusti P. Combined drug release from biodegradable bilayer coating for endovascular stents. *J Biomed Mater Res B Appl Biomater*. 2010;93B(2):375–85.
92. Siepmann J, Siepmann F. Mathematical modeling of drug delivery. *Int J Pharm*. 2008;364(2):328–43.
93. Gasmi H, Siepmann F, Hamoudi MC, Danede F, Verin J, Willart J-F, et al. Towards a better understanding of the different release phases from PLGA microparticles: Dexamethasone-loaded systems. *Int J Pharm*. 2016 Nov 30;514(1):189–99.
94. Bode C, Kranz H, Siepmann F, Siepmann J. In-situ forming PLGA implants for intraocular dexamethasone delivery. *Int J Pharm*. 2018 Sep 5;548(1):337–48.
95. Zidan AS, Sammour OA, Hammad MA, Megrab NA, Hussain MD, Khan MA, et al. Formulation of anastrozole microparticles as biodegradable anticancer drug carriers. *AAPS PharmSciTech*. 2006 Jul 1;7(3):61.
96. Wischke C, Schwendeman SP. Principles of encapsulating hydrophobic drugs in PLA/PLGA microparticles. *Int J Pharm*. 2008 Dec 8;364(2):298–327.

97. Faisant N, Siepmann J, Benoit JP. PLGA-based microparticles: elucidation of mechanisms and a new, simple mathematical model quantifying drug release. *Eur J Pharm Sci Off J Eur Fed Pharm Sci.* 2002 May;15(4):355–66.
98. Göpferich A. Mechanisms of polymer degradation and erosion. *Biomaterials.* 1996 Jan 1;17(2):103–14.
99. Li S, McCarthy S. Further investigations on the hydrolytic degradation of poly (DL-lactide). *Biomaterials.* 1999 Jan;20(1):35–44.
100. Xu Y, Kim C-S, Saylor DM, Koo D. Polymer degradation and drug delivery in PLGA-based drug-polymer applications: A review of experiments and theories. *J Biomed Mater Res B Appl Biomater.* 2017 Aug;105(6):1692–716.
101. Wang J, Wang BM, Schwendeman SP. Characterization of the initial burst release of a model peptide from poly(D,L-lactide-co-glycolide) microspheres. *J Control Release Off J Control Release Soc.* 2002 Aug 21;82(2–3):289–307.
102. Huang X, Brazel CS. On the importance and mechanisms of burst release in matrix-controlled drug delivery systems. *J Control Release Off J Control Release Soc.* 2001 Jun 15;73(2–3):121–36.
103. Allison SD. Analysis of initial burst in PLGA microparticles. *Expert Opin Drug Deliv.* 2008 Jun;5(6):615–28.
104. Huang J, Mazzara JM, Schwendeman SP, Thouless MD. Self-healing of pores in PLGAs. *J Controlled Release.* 2015 May 28;206:20–9.
105. Luan X, Bodmeier R. Modification of the tri-phasic drug release pattern of leuprolide acetate-loaded poly(lactide-co-glycolide) microparticles. *Eur J Pharm Biopharm.* 2006 Jun 1;63(2):205–14.
106. Viswanathan NB, Patil SS, Pandit JK, Lele AK, Kulkarni MG, Mashelkar RA. Morphological changes in degrading PLGA and P(DL)LA microspheres: implications for the design of controlled release systems. *J Microencapsul.* 2001 Dec;18(6):783–800.
107. Bouissou C, Rouse JJ, Price R, van der Walle CF. The influence of surfactant on PLGA microsphere glass transition and water sorption: remodeling the surface morphology to attenuate the burst release. *Pharm Res.* 2006 Jun;23(6):1295–305.
108. Xu Q, Czernuszka JT. Controlled release of amoxicillin from hydroxyapatite-coated poly(lactic-co-glycolic acid) microspheres. *J Control Release Off J Control Release Soc.* 2008 Apr 21;127(2):146–53.
109. Stewart SA, Domínguez-Robles J, Donnelly RF, Larrañeta E. Implantable Polymeric Drug Delivery Devices: Classification, Manufacture, Materials, and Clinical Applications. *Polymers.* 2018 Dec 12;10(12):E1379.
110. Pravin S, Sudhir A. Integration of 3D printing with dosage forms: A new perspective for modern healthcare. *Biomed Pharmacother Biomedecine Pharmacother.* 2018 Nov;107:146–54.

111. Lim SH, Kathuria H, Tan JJY, Kang L. 3D printed drug delivery and testing systems - a passing fad or the future? *Adv Drug Deliv Rev.* 2018 May 18;
112. Hofmann M. 3D Printing Gets a Boost and Opportunities with Polymer Materials. *ACS Macro Lett.* 2014 Apr 15;3(4):382–6.
113. Jamróz W, Szafranec J, Kurek M, Jachowicz R. 3D Printing in Pharmaceutical and Medical Applications - Recent Achievements and Challenges. *Pharm Res.* 2018 Jul 11;35(9):176.
114. Mohammed A, Elshaer A, Sareh P, Elsayed M, Hassanin H. Additive Manufacturing Technologies for Drug Delivery Applications. *Int J Pharm.* 2020 Apr 30;580:119245.
115. Hull CW. Method of and apparatus for production of three dimensional objects by stereolithography [Internet]. US5236637A, 1993 [cited 2021 Jul 1]. Available from: <https://patents.google.com/patent/US5236637A/en>
116. Su A, Al'Aref SJ. Chapter 1 - History of 3D Printing. In: Al'Aref SJ, Mosadegh B, Dunham S, Min JK, editors. *3D Printing Applications in Cardiovascular Medicine* [Internet]. Boston: Academic Press; 2018 [cited 2021 Jul 1]. p. 1–10. Available from: <https://www.sciencedirect.com/science/article/pii/B9780128039175000018>
117. Deckard CR. Method and apparatus for producing parts by selective sintering [Internet]. US4863538A, 1989 [cited 2021 Jul 1]. Available from: <https://patents.google.com/patent/US4863538/en>
118. Crump SS. Modeling apparatus for three-dimensional objects [Internet]. US5340433A, 1994 [cited 2021 Jul 1]. Available from: <https://patents.google.com/patent/US5340433/en>
119. Banks J. Adding value in additive manufacturing: researchers in the United Kingdom and Europe look to 3D printing for customization. *IEEE Pulse.* 2013 Dec;4(6):22–6.
120. Madla CM, Trenfield SJ, Goyanes A, Gaisford S, Basit AW. 3D Printing Technologies, Implementation and Regulation: An Overview. In: Basit AW, Gaisford S, editors. *3D Printing of Pharmaceuticals* [Internet]. Cham: Springer International Publishing; 2018 [cited 2021 Jul 6]. p. 21–40. (AAPS Advances in the Pharmaceutical Sciences Series). Available from: https://doi.org/10.1007/978-3-319-90755-0_2
121. Stavropoulos P, Foteinopoulos P. Modelling of additive manufacturing processes: a review and classification. *Manuf Rev.* 2018;5:2.
122. Zhang Y, Li S, Zhao Y, Duan W, Liu B, Wang T, et al. Digital light processing 3D printing of AlSi10Mg powder modified by surface coating. *Addit Manuf.* 2021 Mar 1;39:101897.
123. Tumbleston JR, Shirvanyants D, Ermoshkin N, Januszewicz R, Johnson AR, Kelly D, et al. Continuous liquid interface production of 3D objects. *Science.* 2015 Mar 20;347(6228):1349–52.
124. He H, Yang Y, Pan Y. Machine learning for continuous liquid interface production: Printing speed modelling. *J Manuf Syst.* 2019 Jan 1;50:236–46.

125. Malas A, Isakov D, Couling K, Gibbons GJ. Fabrication of High Permittivity Resin Composite for Vat Photopolymerization 3D Printing: Morphology, Thermal, Dynamic Mechanical and Dielectric Properties. *Materials*. 2019 Jan;12(23):3818.
126. Shin D, Hyun J. Silk fibroin microneedles fabricated by digital light processing 3D printing. *J Ind Eng Chem*. 2021 Mar 25;95:126–33.
127. Zhai Y, Lados DA, LaGoy JL. Additive Manufacturing: Making Imagination the Major Limitation. *JOM*. 2014 May 1;66(5):808–16.
128. Murr L, Gaytant S, Ramirez D, Martinez E, Hernandez J, Amato K, et al. Metal Fabrication by Additive Manufacturing Using Laser and Electron Beam Melting Technologies. *J Mater Sci Technol*. 2012 Jan 1;28(1):1–14.
129. Shishkovsky IV, Kuznetsov MV, Morozov YuG. Porous titanium and nitinol implants synthesized by SHS/SLS: Microstructural and histomorphological analyses of tissue reactions. *Int J Self-Propagating High-Temp Synth*. 2010 Jun 1;19(2):157–67.
130. Simchi A, Petzoldt F, Pohl H. On the development of direct metal laser sintering for rapid tooling. *J Mater Process Technol*. 2003 Nov 1;141(3):319–28.
131. Zhang Y, Wu L, Guo X, Kane S, Deng Y, Jung Y-G, et al. Additive Manufacturing of Metallic Materials: A Review. *J Mater Eng Perform*. 2018 Jan 1;27(1):1–13.
132. Awad A, Fina F, Goyanes A, Gaisford S, Basit AW. Advances in powder bed fusion 3D printing in drug delivery and healthcare. *Adv Drug Deliv Rev*. 2021 Jul 1;174:406–24.
133. Sillani F, Kleijnen RG, Vetterli M, Schmid M, Wegener K. Selective laser sintering and multi jet fusion: Process-induced modification of the raw materials and analyses of parts performance. *Addit Manuf*. 2019 May 1;27:32–41.
134. Khaled SA, Burley JC, Alexander MR, Yang J, Roberts CJ. 3D printing of five-in-one dose combination polypill with defined immediate and sustained release profiles. *J Controlled Release*. 2015 Nov 10;217:308–14.
135. Goyanes A, Robles Martinez P, Buanz A, Basit AW, Gaisford S. Effect of geometry on drug release from 3D printed tablets. *Int J Pharm*. 2015 Oct 30;494(2):657–63.
136. Goyanes A, Allahham N, Trenfield SJ, Stoyanov E, Gaisford S, Basit AW. Direct powder extrusion 3D printing: Fabrication of drug products using a novel single-step process. *Int J Pharm*. 2019 Aug 15;567:118471.
137. Guessasma S, Nouri H, Roger F. Microstructural and Mechanical Implications of Microscaled Assembly in Droplet-based Multi-Material Additive Manufacturing. *Polymers*. 2017 Aug 18;9(8):372.
138. Welsh NR, Malcolm RK, Devlin B, Boyd P. Dapivirine-releasing vaginal rings produced by plastic freeforming additive manufacturing. *Int J Pharm*. 2019 Dec 15;572:118725.
139. Gradwohl M, Chai F, Payen J, Guerreschi P, Marchetti P, Blanchemain N. Effects of Two Melt Extrusion Based Additive Manufacturing Technologies and Common Sterilization

- Methods on the Properties of a Medical Grade PLGA Copolymer. *Polymers*. 2021 Jan;13(4):572.
140. Feuerbach T, Callau-Mendoza S, Thommes M. Development of filaments for fused deposition modeling 3D printing with medical grade poly(lactic-co-glycolic acid) copolymers. *Pharm Dev Technol*. 2019 Apr 21;24(4):487–93.
 141. Melocchi A, Parietti F, Maroni A, Foppoli A, Gazzaniga A, Zema L. Hot-melt extruded filaments based on pharmaceutical grade polymers for 3D printing by fused deposition modeling. *Int J Pharm*. 2016 Jul 25;509(1):255–63.
 142. Fayazfar H, Liravi F, Ali U, Toyserkani E. Additive manufacturing of high loading concentration zirconia using high-speed drop-on-demand material jetting. *Int J Adv Manuf Technol*. 2020 Aug 1;109(9):2733–46.
 143. Simonelli M, Aboulkhair N, Rasa M, East M, Tuck C, Wildman R, et al. Towards digital metal additive manufacturing via high-temperature drop-on-demand jetting. *Addit Manuf*. 2019 Dec 1;30:100930.
 144. Singh R. Process capability study of polyjet printing for plastic components. *J Mech Sci Technol*. 2011 Apr 1;25(4):1011–5.
 145. Salmi M, Paloheimo K-S, Tuomi J, Wolff J, Mäkitie A. Accuracy of medical models made by additive manufacturing (rapid manufacturing). *J Cranio-Maxillo-fac Surg Off Publ Eur Assoc Cranio-Maxillo-fac Surg*. 2013 Oct;41(7):603–9.
 146. Haghghi A, Yang Y, Li L. Dimensional Performance of As-Built Assemblies in Polyjet Additive Manufacturing Process. In American Society of Mechanical Engineers Digital Collection; 2017 [cited 2021 Jul 6]. Available from: <https://asmedigitalcollection.asme.org/MSEC/proceedings/MSEC2017/50732/V002T01A039/269501>
 147. Dilberoglu UM, Gharehpapagh B, Yaman U, Dolen M. The Role of Additive Manufacturing in the Era of Industry 4.0. *Procedia Manuf*. 2017 Jan 1;11:545–54.
 148. Goole J, Amighi K. 3D printing in pharmaceuticals: A new tool for designing customized drug delivery systems. *Int J Pharm*. 2016 Feb 29;499(1–2):376–94.
 149. Ziaee M, Crane NB. Binder jetting: A review of process, materials, and methods. *Addit Manuf*. 2019 Aug 1;28:781–801.
 150. Shim D-S, Baek G-Y, Seo J-S, Shin G-Y, Kim K-P, Lee K-Y. Effect of layer thickness setting on deposition characteristics in direct energy deposition (DED) process. *Opt Laser Technol*. 2016 Dec 1;86:69–78.
 151. Onuikwe B, Heer B, Bandyopadhyay A. Additive manufacturing of Inconel 718—Copper alloy bimetallic structure using laser engineered net shaping (LENSTM). *Addit Manuf*. 2018 May 1;21:133–40.
 152. Gong X, Anderson T, Chou K. Review on Powder-Based Electron Beam Additive Manufacturing Technology. In American Society of Mechanical Engineers Digital Collection; 2013 [cited 2021 Jul 7]. p. 507–15. Available from:

<https://journals.asmedigitalcollection.asme.org/ISFA/proceedings/ISFA2012/45110/507/267104>

153. Kaierle S, Barroi A, Noelke C, Hermsdorf J, Overmeyer L, Haferkamp H. Review on Laser Deposition Welding: From Micro to Macro. *Phys Procedia*. 2012 Jan 1;39:336–45.
154. Park J, Tari MJ, Hahn HT. Characterization of the laminated object manufacturing (LOM) process. *Rapid Prototyp J*. 2000 Jan 1;6(1):36–50.
155. Friel RJ, Harris RA. Ultrasonic Additive Manufacturing – A Hybrid Production Process for Novel Functional Products. *Procedia CIRP*. 2013 Jan 1;6:35–40.
156. Martinez PR, Goyanes A, Basit AW, Gaisford S. Fabrication of drug-loaded hydrogels with stereolithographic 3D printing. *Int J Pharm*. 2017 Oct 30;532(1):313–7.
157. Karakurt I, Aydoğdu A, Çıkrıkçı S, Orozco J, Lin L. Stereolithography (SLA) 3D printing of ascorbic acid loaded hydrogels: A controlled release study. *Int J Pharm*. 2020 Jun 30;584:119428.
158. Bloomquist CJ, Mecham MB, Paradzinsky MD, Januszewicz R, Warner SB, Luft JC, et al. Controlling release from 3D printed medical devices using CLIP and drug-loaded liquid resins. *J Controlled Release*. 2018 May 28;278:9–23.
159. Fina F, Goyanes A, Gaisford S, Basit AW. Selective laser sintering (SLS) 3D printing of medicines. *Int J Pharm*. 2017 Aug 30;529(1):285–93.
160. Hassanin H, Finet L, Cox SC, Jamshidi P, Grover LM, Shepherd DET, et al. Tailoring selective laser melting process for titanium drug-delivering implants with releasing micro-channels. *Addit Manuf*. 2018 Mar 1;20:144–55.
161. Bezuidenhout MB, Booysen E, van Staden AD, Uheida EH, Hugo PA, Oosthuizen GA, et al. Selective Laser Melting of Integrated Ti6Al4V ELI Permeable Walls for Controlled Drug Delivery of Vancomycin. *ACS Biomater Sci Eng*. 2018 Dec 10;4(12):4412–24.
162. Vaithilingam J, Kilsby S, Goodridge RD, Christie SDR, Edmondson S, Hague RJM. Functionalisation of Ti6Al4V components fabricated using selective laser melting with a bioactive compound. *Mater Sci Eng C*. 2015 Jan 1;46:52–61.
163. Khaled SA, Burley JC, Alexander MR, Roberts CJ. Desktop 3D printing of controlled release pharmaceutical bilayer tablets. *Int J Pharm*. 2014 Jan 30;461(1):105–11.
164. Khaled SA, Burley JC, Alexander MR, Yang J, Roberts CJ. 3D printing of tablets containing multiple drugs with defined release profiles. *Int J Pharm*. 2015 Oct 30;494(2):643–50.
165. Muwaffak Z, Goyanes A, Clark V, Basit AW, Hilton ST, Gaisford S. Patient-specific 3D scanned and 3D printed antimicrobial polycaprolactone wound dressings. *Int J Pharm*. 2017 Jul 15;527(1):161–70.
166. Grottkau BE, Hui Z, Pang Y. A Novel 3D Bioprinter Using Direct-Volumetric Drop-On-Demand Technology for Fabricating Micro-Tissues and Drug-Delivery. *Int J Mol Sci*. 2020 Jan;21(10):3482.

167. Clark EA, Alexander MR, Irvine DJ, Roberts CJ, Wallace MJ, Sharpe S, et al. 3D printing of tablets using inkjet with UV photoinitiation. *Int J Pharm.* 2017 Aug 30;529(1–2):523–30.
168. Spritam--a new formulation of levetiracetam for epilepsy. *Med Lett Drugs Ther.* 2016 Jun 20;58(1497):78–9.
169. Jacob J, COYLE N, West TG, Monkhouse DC, Surprenant HL, Jain NB. Rapid disperse dosage form containing levetiracetam [Internet]. WO2014144512A1, 2014 [cited 2021 Jul 8]. Available from: <https://patents.google.com/patent/WO2014144512A1/en>
170. Yu D-G, Branford-White C, Ma Z-H, Zhu L-M, Li X-Y, Yang X-L. Novel drug delivery devices for providing linear release profiles fabricated by 3DP. *Int J Pharm.* 2009 Mar 31;370(1–2):160–6.
171. Prasad LK, Smyth H. 3D Printing technologies for drug delivery: a review. *Drug Dev Ind Pharm.* 2016;42(7):1019–31.
172. Kotta S, Nair A, Alsabeelah N. 3D Printing Technology in Drug Delivery: Recent Progress and Application. *Curr Pharm Des.* 2018;24(42):5039–48.
173. Patel SK, Khoder M, Peak M, Alhnan MA. Controlling drug release with additive manufacturing-based solutions. *Adv Drug Deliv Rev.* 2021 Jul 1;174:369–86.
174. Shi K, Tan DK, Nokhodchi A, Maniruzzaman M. Drop-On-Powder 3D Printing of Tablets with an Anti-Cancer Drug, 5-Fluorouracil. *Pharmaceutics.* 2019 Apr;11(4):150.
175. Khaled SA, Alexander MR, Wildman RD, Wallace MJ, Sharpe S, Yoo J, et al. 3D extrusion printing of high drug loading immediate release paracetamol tablets. *Int J Pharm.* 2018 Mar 1;538(1):223–30.
176. Li P, Jia H, Zhang S, Yang Y, Sun H, Wang H, et al. Thermal Extrusion 3D Printing for the Fabrication of Puerarin Immediate-Release Tablets. *AAPS PharmSciTech.* 2019 Dec 1;21(1):20.
177. Dores F, Kuźmińska M, Soares C, Bohus M, A Shervington L, Habashy R, et al. Temperature and solvent facilitated extrusion based 3D printing for pharmaceuticals. *Eur J Pharm Sci.* 2020 Sep 1;152:105430.
178. Sadia M, Arafat B, Ahmed W, Forbes RT, Alhnan MA. Channelled tablets: An innovative approach to accelerating drug release from 3D printed tablets. *J Control Release Off J Control Release Soc.* 2018 Jan 10;269:355–63.
179. Maroni A, Melocchi A, Parietti F, Foppoli A, Zema L, Gazzaniga A. 3D printed multi-compartment capsular devices for two-pulse oral drug delivery. *J Controlled Release.* 2017 Dec 1;268:10–8.
180. Fu J, Yu X, Jin Y. 3D printing of vaginal rings with personalized shapes for controlled release of progesterone. *Int J Pharm.* 2018 Mar 25;539(1–2):75–82.

181. Yang N, Chen H, Han H, Shen Y, Gu S, He Y, et al. 3D printing and coating to fabricate a hollow bullet-shaped implant with porous surface for controlled cytoxan release. *Int J Pharm.* 2018 Sep 19;552(1–2):91–8.
182. Zhang B, Gleadall A, Belton P, Mcdonagh T, Bibb R, Qi S. New insights into the effects of porosity, pore length, pore shape and pore alignment on drug release from extrusionbased additive manufactured pharmaceuticals. *Addit Manuf.* 2021 Oct 1;46:102196.
183. Xu X, Awwad S, Diaz-Gomez L, Alvarez-Lorenzo C, Brocchini S, Gaisford S, et al. 3D Printed Punctal Plugs for Controlled Ocular Drug Delivery. *Pharmaceutics.* 2021 Sep;13(9):1421.
184. Tan YJN, Yong WP, Low HR, Kochhar JS, Khanolkar J, Lim TSE, et al. Customizable drug tablets with constant release profiles via 3D printing technology. *Int J Pharm.* 2021 Apr 1;598:120370.
185. Russi L, Del Gaudio C. 3D printed multicompartmental capsules for a progressive drug release. *Ann 3D Print Med.* 2021 Sep 1;3:100026.
186. Lai Y, Li Y, Cao H, Long J, Wang X, Li L, et al. Osteogenic magnesium incorporated into PLGA/TCP porous scaffold by 3D printing for repairing challenging bone defect. *Biomaterials.* 2019 Mar 1;197:207–19.
187. Kwon B-J, Seon GM, Lee MH, Koo M-A, Kim MS, Kim D, et al. Locally delivered ethyl-2,5-dihydroxybenzoate using 3D printed bone implant for promotion of bone regeneration in a osteoporotic animal model. *Eur Cell Mater.* 2018 12;35:1–12.
188. Lin S, Cui L, Chen G, Huang J, Yang Y, Zou K, et al. PLGA/ β -TCP composite scaffold incorporating salvianolic acid B promotes bone fusion by angiogenesis and osteogenesis in a rat spinal fusion model. *Biomaterials.* 2019 Mar 1;196:109–21.
189. Jakus AE, Geisendorfer NR, Lewis PL, Shah RN. 3D-printing porosity: A new approach to creating elevated porosity materials and structures. *Acta Biomater.* 2018 May 1;72:94–109.
190. Yang Y, Chu L, Yang S, Zhang H, Qin L, Guillaume O, et al. Dual-functional 3D-printed composite scaffold for inhibiting bacterial infection and promoting bone regeneration in infected bone defect models. *Acta Biomater.* 2018 Oct 1;79:265–75.
191. Rasoulianboroujeni M, Fahimipour F, Shah P, Khoshroo K, Tahriri M, Eslami H, et al. Development of 3D-printed PLGA/TiO₂ nanocomposite scaffolds for bone tissue engineering applications. *Mater Sci Eng C.* 2019 Mar 1;96:105–13.
192. Mironov AV, Mironova OA, Syachina MA, Popov VK. 3D printing of polylactic-co-glycolic acid fiber scaffolds using an antisolvent phase separation process. *Polymer.* 2019 Nov 7;182:121845.
193. Guo T, Holzberg TR, Lim CG, Gao F, Gargava A, Trachtenberg JE, et al. 3D printing PLGA: a quantitative examination of the effects of polymer composition and printing parameters on print resolution. *Biofabrication.* 2017 12;9(2):024101.

194. Carlier E, Marquette S, Peerboom C, Amighi K, Goole J. Development of mAb-loaded 3D-printed (FDM) implantable devices based on PLGA. *Int J Pharm.* 2021 Mar 15;597:120337.

**II. HOW HYDROGELS SURROUNDING
PLGA IMPLANTS LIMIT SWELLING AND
SLOW DOWN DRUG RELEASE**

II. HOW HYDROGELS SURROUNDING PLGA IMPLANTS LIMIT SWELLING AND SLOW DOWN DRUG RELEASE

Research article – Submitted in Journal of Controlled Release

How hydrogels surrounding PLGA implants limit swelling and slow down drug release

C. Bassand, J. Verin, M. Lamatsch, F. Siepmann, J. Siepmann

Univ. Lille, Inserm, CHU Lille, U1008, F-59000 Lille, France

II.1. Abstract

The aim of this study was to better understand to which extent the presence of an agarose gel (mimicking living tissue) around a PLGA [poly(lactic-co-glycolic acid)] implant affects the resulting drug release kinetics. Ibuprofen-loaded implants were prepared by hot melt extrusion. Drug release was measured upon exposure to phosphate buffer pH 7.4 in Eppendorf tubes and upon inclusion into an agarose gel which was exposed to phosphate buffer pH 7.4 in Eppendorf tubes or in transwell plates. Dynamic changes in the implants' dry and wet mass as well as dimensions were monitored by optical macroscopy and gravimetrically. SEM and GPC were used to follow system erosion and polymer degradation. Different pH indicators were applied to measure pH changes in the bulk fluids, gels and within the implants during drug release. Ibuprofen release was bi-phasic in all cases: A zero order release phase (~20 % of the dose) was followed by a more rapid, final drug release phase. Interestingly, the presence of the hydrogel delayed the onset of the 2nd release phase. This could be attributed to the sterical hindrance of implant swelling: After a certain lag time, the degrading PLGA matrix becomes sufficiently hydrophilic and mechanically instable to allow for the penetration of substantial amounts of water into the system. This fundamentally changes the conditions for drug release: The latter becomes much more mobile and is more rapidly released. A gel surrounding the implant mechanically hinders system swelling and, thus, slows down drug release. These observations strengthen the hypothesis of the “orchestrating” role of PLGA swelling for the control of drug release and can help developing more realistic in vitro release set-ups.

Key words: PLGA implant; release mechanism; swelling; ibuprofen; hydrogel

II. HOW HYDROGELS SURROUNDING PLGA IMPLANTS LIMIT SWELLING AND SLOW DOWN DRUG RELEASE

II.2.Introduction

Poly(lactic-co-glycolic acid) (PLGA) offers an interesting potential as matrix former for controlled parenteral drug delivery (1–3). In particular, PLGA microparticles and implants have been proposed in the literature (4–6). Several drug products are on the market since decades. The great success of this polymer for this type of applications can be attributed to its good biocompatibility (7), complete biodegradability (avoiding the removal of empty remnants upon drug exhaust) and the possibility to provide desired drug release kinetics during flexible periods of time (8–11). The resulting drug release kinetics depend on a variety of factors, including the type of PLGA (e.g., average polymer molecular weight, type of end groups), composition of the system as well as the type of manufacturing method and parameters used during processing (12–14).

Despite the great practical importance of PLGA-based drug delivery systems, yet the underlying mass transport mechanisms controlling drug release are generally not fully understood. This can be explained by the potential complexity of the involved physico-chemical processes (15,16), including for example water penetration into the systems, polymer degradation (17), drug dissolution, drug diffusion, polymer – drug interactions (18), water – polymer interactions (19), the creation of a local acidic micro-environment *within* the dosage form (20–22) causing autocatalytic effects (23), the closure of surface pores (24), substantial system swelling (25), limited drug solubility effects and system disintegration. The relative importance of these phenomena can strongly depend on the specific composition and inner & outer structure of the delivery system. For instance, the extent of local drops in the micro-pH can be altered by the addition of basic excipients or by varying the initial device porosity (determining at which rate acids and bases can diffuse into and out of the system).

Often, mono-, bi-, or tri-phasic drug release profiles are observed from PLGA-based drug delivery systems, irrespective of their geometry and size (e.g., implants, microparticles and films) (26–28). In the case of tri-phasic drug release, the following phases can generally be distinguished: An initial burst release phase (frequently limited to the first few hours or 1-2 days) is followed by a “zero order drug release phase” (with an about constant release rate), and a final, again rapid release phase leading to complete drug exhaust. It has recently been proposed that PLGA swelling might play a decisive, “orchestrating” role for these different release phases (29–31), although PLGA swelling is often neglected in the literature for the explanation of drug release patterns. The initial burst release might be attributable to the release of drug particles which come into direct contact with water once the system is exposed to an

aqueous fluid, because they are located directly at the system's surface, or very close to it. Eventually, this contact is assured via tiny pores with direct surface access or via an interconnected drug particle network. Since drug dissolution is rapid (as well as diffusion through short, water-filled pores), this release phase often ends during the first 1-2 days. Potentially, (limited) PLGA swelling can also close surface pores, terminating the initial burst release phase (32).

It is well known that water penetration into PLGA-based drug delivery systems is relatively rapid, so that the entire device is wetted and polymer degradation occurs *throughout* the system ("bulk erosion") (33). The possible root causes for the second (zero order release) phase are often less well understood. It has been suggested that in the case of microparticles consisting of a PLGA matrix into which tiny diphosphylline crystals were dispersed, the continuous growth of a highly swollen surface layer plays a crucial role (34): Since the PLGA at the system's surface is in contact with very high amounts of water, polymer degradation can be expected to be accelerated in this region. Upon ester bond cleavage shorter chain acids and alcohols are generated, rendering especially the matrix in the outmost layer more and more hydrophilic. At a certain time point, the latter undergoes substantial swelling. With time its thickness increases, because also "deeper" polymer layers get exposed to very high water concentrations. As long as a diphosphylline particle is surrounded by a dense PLGA matrix, it cannot dissolve (lack of water) and diffuse out (lack of mobility). However, once the steadily growing, highly swollen surface layer reaches the particle, the latter can dissolve and dissolved drug molecules can rather rapidly move through the highly swollen PLGA gel. This phenomenon was evidenced for *single* microparticles, occurring at random time points: Each particle has its own structure and its own way to release the drug. Since the drug was homogeneously distributed throughout the system, the numerous occasional individual drug release events summed up to an about constant drug release rate.

The final, again rapid drug release phase (3rd phase) observed with certain PLGA microparticles and implants could be attributed to the onset of substantial system swelling occurring after a lag time. Due to PLGA degradation, the entanglement of the polymer chains decreases with time and the concentration of water-soluble degradation products increases (creating a continuously increasing osmotic pressure inside the device). In addition, the system becomes more and more hydrophilic (due to the newly created -COOH and -OH end groups). At a certain time point, the mechanical stability of the macromolecular network becomes insufficient and

II. HOW HYDROGELS SURROUNDING PLGA IMPLANTS LIMIT SWELLING AND SLOW DOWN DRUG RELEASE

substantial amounts of water penetrate into the *entire* device, allowing for drug particle dissolution and significantly increased drug mobility.

In certain cases, only bi- or mono-phasic drug release patterns are observed from PLGA-based drug delivery systems. This might be due to the fact that no drug has direct initial access to the system's surface (absence of a burst release); or all drug is already released before the substantial entire system swelling sets on (no 3rd drug release phase).

If the hypothesis of an “orchestrating role” of PLGA swelling for the control of drug release is correct, the presence of a hydrogel surrounding the device might have a non-negligible effect on drug release, since it might hinder the onset of substantial system swelling. In vivo, the living tissue surround the implant can be expected to have a similar effect. However, in most cases experimental set-ups used for in vitro drug release measurements from PLGA-based drug delivery systems expose the dosage form directly to a bulk fluid. In the literature only relatively few studies address the potential impact of the presence of a gel. For example, in an interesting recent report, the group of Lamprecht measured the release of flurbiprofen, lidocaine and risperidone from ethylcellulose or PLGA-based films, microparticles and cylindrical implants in the presence and absence of a surrounding gel (35). In many cases, the presence of the gel led to slower drug release from PLGA-based devices. However, in the case of certain flurbiprofen-loaded films the release rate became faster during most of the release period, the gel hindering the films to deform. And for some other systems, the impact of the presence of a surrounding gel was negligible. The same group proposed the use of components of muscle tissue to better mimic intramuscular environments and addressed the potential role of lipids for drug release from a variety of controlled release microparticles (36). Allababidi and Sha (37) investigated the release of cefazolin from *glycerol monostearate*-based implants into an agar gel or phosphate buffer pH 7.4 bulk fluid, and did not observe major differences. Furthermore, the release of profiles of ciprofloxacin hydrochloride and vancomycin hydrochloride from different types of *hydroxyapatite* implants functionalized with hydroxypropyl- β -cyclodextrin were measured into agarose gels or well agitated phosphate buffer pH 7.4. Drug release was much faster in the agitated bulk fluid, which was at least in part attributed to accelerated matrix erosion. Hydrogels have also been proposed by the group of Ostergaard as surrogates for subcutaneous tissue when studying controlled release implants (38,39)

The aim of this study was to investigate ibuprofen-loaded PLGA implants using 3 different experimental set-ups: (i) Upon exposure to well agitated bulk fluid in Eppendorf tubes,

(ii) Embedded in agarose gels, which are exposed to bulk fluid in Eppendorf tubes, and
(iii) Embedded in agarose gels, which are exposed to bulk fluid in transwell plates. The observed drug release kinetics were to be explained based on the monitoring of dynamic changes in the systems' wet and dry mass (gravimetrically), average polymer molecular weight (GPC), inner and outer morphology (by optical and scanning electron microscopy) and pH measurements in the bulk fluids, gels and implants.

II. HOW HYDROGELS SURROUNDING PLGA IMPLANTS LIMIT SWELLING AND SLOW DOWN DRUG RELEASE

II.3. Materials and methods

II.3.1. Materials

Poly (D,L lactic-co-glycolic acid) (PLGA, 50:50 lactic acid: glycolic acid; Resomer RG 503H; Evonik, Darmstadt; Germany); ibuprofen (BASF, Ludwigshafen, Germany); agarose (genetic analysis grade), bromocresol green (BCG), bromothiol blue (BTB), bromophenol blue (BPB), phenol red (PR) and tetrahydrofuran (HPLC grade) (Fisher Scientific, Illkirch, France); potassium dihydrogen orthophosphate and sodium hydroxide (Acros Organics, Geel, Belgium); acetonitrile (VWR, Fontenoy-sous-Bois, France); sodium hydrogen phosphate (Na_2HPO_4 , Panreac Quimica, Barcelona, Spain).

II.3.2. Implant preparation

PLGA was milled for 4 x 30 s in a grinder (Valentin, Seb, Ecully, France). Appropriate amounts of PLGA and drug powders were blended for 5 min at 20 rpm in a Turbula T2C Shaker-Mixer (Willy A Bachofen, Basel, Switzerland). Three hundred mg mixture were filled into a 1 mL syringe (Henke Sass Wolf, Tuttlingen, Germany), followed by heating at 105 °C for 15 min in an oven (FP115, Binder, Tuttlingen, Germany). The molten blend was manually extruded using the syringe. The obtained extrudate was cut with a hot scalpel into cylindrical implants of approximately 5 mm length.

II.3.3. Practical drug loading

Implants were dissolved in acetonitrile (1 implant in 5 mL), followed by filtering (PVDF syringe filters, 0.45 μm ; Agilent Technologies, Santa Clara, USA) and drug content determination by HPLC-UV analysis using a Thermo Fisher Scientific Ultimate 3000 Series HPLC, equipped with a LPG 3400 SD/RS pump, an auto sampler (WPS-3000 SL) and a UV-Vis detector (VWD-3400RS) (Thermo Fisher Scientific, Waltham, USA). A reversed phase column C18 (Gemini 5 μm ; 110 Å; 150 x 4.6 mm; Phenomenex, Le Pecq, France) was used. The mobile phase was a mixture of 30 mM Na_2HPO_4 pH 7.0: acetonitrile (60:40, v:v). The detection wavelength was 264 nm, the flow rate was set at 0.5 mL/min. Ten microliter samples were injected.

II.3.4. In vitro drug release

Ibuprofen release from the PLGA implants was measured using 3 different experimental setups:

II.3.4.1. In well agitated bulk fluids

Implants were placed in metal baskets in 5 mL Eppendorf tubes (1 implant per basket/tube), filled with 5 mL phosphate buffer pH 7.4 USP 42 (*Figure II-1 A*). Optionally, one of the following pH indicators was added: bromocresol green, bromothylol blue, bromophenol blue or phenol red (0.0025 % w:v). The tubes were placed in a horizontal shaker (80 rpm, 37°C; GFL 3033; Gesellschaft fuer Labortechnik, Burgwedel, Germany). At predetermined time points, the entire bulk fluid was replaced by fresh (pre-heated) release medium. The withdrawn samples were filtered (PVDF syringe filter, 0.45 µm; Agilent, Santa Clara, California, USA) and analyzed for their ibuprofen contents by HPLC-UV, as described in *section II.3.3*.

II.3.4.2. In agarose gels in Eppendorf tubes

Implants were embedded in agarose gels in 5 mL Eppendorf tubes, as illustrated in *Figure II-1 B* (1 implant per tube). The gel was prepared with 0.5% w:v agarose and 1 mL phosphate buffer pH 7.4 USP 42 (optionally containing 0.0025 % w:v bromocresol green, bromothylol blue, bromophenol blue or phenol red as pH indicator). An agarose dispersion in the respective buffer solution was heated to 100 °C under magnetic stirring (250 rpm) until a clear solution was obtained. The latter was cooled to 47°C and continuously stirred (to prevent gelation). 0.5 mL of the solution was placed into the bottom of an Eppendorf tube and cooled in a refrigerator for 5 min to allow for gelation. An implant was carefully placed on top of the gel, and covered with second layer of 0.5 mL agarose solution (47 °C), followed by cooling in a refrigerator for 5 min. Four mL phosphate buffer pH 7.4 USP 42 (optionally containing a pH indicator) were added on top of the gel, and the tube was placed in a horizontal shaker (80 rpm, 37°C; GFL 3033). At predetermined time points, the entire bulk fluid was replaced by fresh (pre-heated) release medium. The withdrawn samples were treated as in the case of drug release measurements in well agitated bulk fluids.

II.3.4.3. In agarose gels in transwell pates

Implants were embedded in agarose gels in transwell plates (1 implant per insert, 1 mL gel, membranes: 1.13 cm², 11 µm, 0.4 µm pore size; Nunc, Roskilde, Denmark), as illustrated in *Figure II-1 C*. The agarose gels were prepared as described above, and the implants included accordingly (placed between 2 “layers” of 0.5 mL gel). The well plates were filled with 4 mL phosphate buffer pH 7.4 USP 42 (optionally containing 0.0025 % pH indicator, as described above), covered with lids and Parafilm to minimize evaporation, and placed in a horizontal shaker (80 rpm, 37°C; GFL 3033). At predetermined time points, the entire bulk fluid was

II. HOW HYDROGELS SURROUNDING PLGA IMPLANTS LIMIT SWELLING AND SLOW DOWN DRUG RELEASE

replaced by fresh (pre-heated) release medium. The withdrawn samples were treated as in the case of drug release measurements in well agitated bulk fluids.

In all cases, the pH of the release medium was measured at pre-determined time points using a pH meter (InoLab pH Level 1; WTW, Weilheim, Germany). Furthermore, in all cases, sink conditions were provided throughout the experiments in all agitated bulk fluids. All experiments were conducted in triplicate. Mean values +/- standard deviations are reported.

II.3.5. Implant swelling

Implants were treated as for the *in vitro* drug release measurements described in *section II.3.4*. At pre-determined time points:

- (i) Pictures of the implants were taken with an a SZN-6 trinocular stereo zoom microscope (Optika, Ponteranica, Italy), equipped with an optical camera (Optika Vison Lite 2.1 software). Cross-sections were obtained by cutting with a scalpel. The lengths and diameters of the implants were determined using the ImageJ software (US National Institutes of Health). Dynamic changes in the systems' volume were calculated considering cylindrical geometry.
- (ii) Implant samples were withdrawn and excess water was carefully removed using Kimtech precision wipes (Kimberly-Clark, Rouen, France). The samples were weighed [*wet mass (t)*], and the *change in wet mass (%) (t)* was calculated as follows:

$$\text{change in wet mass } (\%)(t) = \frac{\text{wet mass } (t) - \text{mass } (t = 0)}{\text{mass } (t = 0)} \times 100 \%$$

where *mass (t = 0)* denotes the implant mass before exposure to the release medium.

All experiments were conducted in triplicate. Mean values +/- standard deviations are reported.

II.3.6. Implant erosion and PLGA degradation

Implant samples were treated as for the *in vitro* drug release studies described in *section II.3.4*. At pre-determined time points, implant samples were withdrawn and freeze dried (freezing at -45°C for 2 h 35 min, primary drying at -20 °C/0.940 mbar for 35 h 10 min, secondary drying at +20 °C/0.0050 mbar for 35 h; Christ Alpha 2-4 LSC+; Martin Christ, Osterode, Germany).

The *dry mass (%) (t)* was calculated as follows:

$$\text{dry mass } (\%)(t) = \frac{\text{dry mass } (t)}{\text{mass } (t = 0)} \times 100 \%$$

where $\text{mass } (t = 0)$ denotes the implant mass before exposure to the release medium. All experiments were conducted in triplicate. Mean values +/- standard deviations are reported.

The average polymer molecular weight (Mw) of the PLGA was determined by gel permeation chromatography (GPC) as follows: Freeze-dried implant samples were dissolved in tetrahydrofuran (3 mg/mL). One hundred μL samples were injected into an Alliance GPC (refractometer detector: 2414 RI, separation module e2695, Empower GPC software; Waters, Milford, USA), equipped with a Phenogel 5 μm column (kept at 35°C, 7.8 \times 300 mm; Phenomenex). Tetrahydrofuran was the mobile phase (flow rate: 1 mL/min). Polystyrene standards with molecular weights between 5,120 and 70,950 Da (Polymer Laboratories, Varian, Les Ulis, France) were used to prepare the calibration curve. All experiments were conducted in triplicate. Mean values +/- standard deviations are reported.

II.3.7. Differential scanning calorimetry (DSC)

DSC thermograms of PLGA (raw material) and implants were recorded using a DCS1 Star System (Mettler Toledo, Greifensee, Switzerland). Approximately 5 mg PLGA and around 10 mg implant samples were heated in perforated aluminum pans as follows: from -70 to 120 °C, cooling to -70 °C, re-heating to 120 °C (heating/cooling rate = 10 °C/min). The reported glass temperatures (T_{gs}) were determined from the 1st heating cycles in the case of implants (the thermal history being of interest), and from the 2nd heating cycle in the case of the PLGA raw material (the thermal history not being of interest). All experiments were conducted in triplicate. Mean values +/- standard deviations are reported.

II.3.8. Scanning electronic microscopy (SEM)

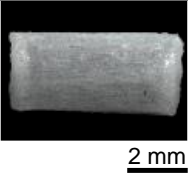
The internal and external morphology of the implants before and after exposure to the release medium was studied using a JEOL Field Emission Scanning Electron Microscope (JSM-7800F, Japan), equipped with the Aztec 3.3 software (Oxford Instruments, Oxfordshire, UK). Samples were fixed with a ribbon carbon double-sided adhesive and covered with a fine chrome layer. In the case of implants which had been exposed to the release medium, the systems were treated as described for the in vitro release studies in *section II.3.4*. At predetermined time points, implant samples were withdrawn, optionally cut using a scalpel and freeze-dried (as described in *section II.3.6*).

II. HOW HYDROGELS SURROUNDING PLGA IMPLANTS LIMIT SWELLING AND SLOW DOWN DRUG RELEASE

II.4. Results and discussion

The image in *Table II-1* shows an optical macroscopy picture of an ibuprofen-loaded PLGA implant before exposure to the release medium. The practical drug loading was $6.6 \pm 0.3 \%$. The glass transition temperature (T_g) of the implants was determined to be $34.5 \pm 0.3 \text{ }^\circ\text{C}$, while the T_g of the PLGA raw material was $47.1 \pm 0.1 \text{ }^\circ\text{C}$. This indicates that ibuprofen acts as a plasticizer for PLGA.

Table II-1. Physical key properties of the investigated ibuprofen-loaded PLGA implants (T_g : glass transition temperature). Mean values \pm standard deviations are indicated ($n=3$).

Practical loading (%)	Weight (mg)	Length (mm)	Diameter (mm)	T_g ($^\circ\text{C}$)	Picture
6.6 ± 0.3	33.7 ± 4.4	5.1 ± 0.3	2.6 ± 0.2	34.5 ± 0.3	

II.4.1. In vitro release set-ups

The schemes in *Figure II-1* illustrate the 3 experimental set-ups, which were used to monitor ibuprofen release. The idea was to evaluate the potential impact of the presence of a hydrogel around the implants (mimicking living tissue) on the resulting drug release kinetics.

Figure II-1 A shows the “Bulk fluid” set-up, in which an implant is placed into a metal basket in an Eppendorf tube filled with 5 mL phosphate buffer pH 7.4. The tubes are placed into a horizontal shaker (80 rpm) and kept at $37 \text{ }^\circ\text{C}$. At pre-determined time points, the entire bulk fluid is replaced by fresh (pre-heated) release medium. The metal basket assured that the implant did not sink to the bottom of the tube. Its meshes were sufficiently large ($250 \text{ }\mu\text{m}$) to allow for convective flow and rapid medium exchange between the liquid inside and outside the basket.

Figure II-1 B illustrates the “gel – Eppendorf” set-up: In this case, an implant is surrounded by a 0.5 % agarose gel prepared with 1 mL phosphate buffer pH 7.4. Four mL phosphate buffer pH 7.4 are carefully added on top of the gel, and the Eppendorf tube is placed into a horizontal shaper (80 rpm) at $37 \text{ }^\circ\text{C}$. At pre-determined time points, the entire bulk fluid is replaced by fresh (pre-heated) phosphate buffer pH 7.4, and the drug content in the withdrawn samples is measured. Thus, to be “detected as released”, drug molecules/ions released from the implant also have to cross the gel. To evaluate the impact of the presence of this additional mass

transport step on the observed ibuprofen release kinetics, the following reference experiment was conducted: Drug release from a 0.5 % agarose gel, which was prepared with a 200 $\mu\text{g}/\text{mL}$ *solution* of ibuprofen in phosphate buffer pH 7.4, was measured with the same set-up. The black circles in *Figure II-1 D* show the obtained results: More than 50 % of the drug was released after 10 h. This is rapid compared to the ibuprofen release rate from the investigated PLGA implants (which was of the order of 10 d).

The “gel – transwell” set-up is schematically shown in *Figure II-1 C*. In this case, an implant is placed in the donor compartment of a transwell plate, being embedded in a 0.5 % agarose gel prepared with 1 mL phosphate buffer pH 7.4. Four mL phosphate buffer pH 7.4 are placed into the acceptor compartment. The transwell plate is horizontally shaken (80 rpm) at 37 °C. At pre-determined time points, the entire bulk fluid in the acceptor compartment is replaced by fresh (pre-heated) release medium. From a practical point of view, this is easier than replacing the release medium in the “gel – Eppendorf” set-up. The drug content in the withdrawn samples is determined by HPLC-UV analysis. Thus, also in this case, the presence of the agarose gel can be expected to slow down ibuprofen release to a certain degree. In addition, the presence of the membrane of the transwell plate might impact the rate at which the ibuprofen reaches the acceptor compartment. To evaluate the relative importance of these 2 phenomena, the following reference experiments were conducted: (i) The “release rate” of an ibuprofen solution in phosphate buffer pH 7.4 (200 $\mu\text{g}/\text{mL}$) from the donor compartment (free of agarose gel) into the acceptor compartment was measured. The black triangles in *Figure II-1 D* show that the entire drug amount was released in less than 10 h under these conditions. This is very rapid compared to the release periods from the investigated implants in this study (≥ 10 d). Thus, the impact of the transwell plate membrane can likely be neglected. (ii) Ibuprofen release from a 0.5 % agarose gel, prepared with an ibuprofen *solution* in phosphate buffer pH 7.4 (200 $\mu\text{g}/\text{mL}$) was measured using this set-up. The open squares in *Figure II-1 D* illustrate the obtained results, indicating that the impact of the presence of the gel was similar to the impact of the gel in the “gel – Eppendorf” set-up. This is fully sound, since the compositions of the gels are identical and the distances to be overcome similar. Hence, again, the observed delay in drug release due to ibuprofen transport through the agarose gel is relatively small compared to the much longer release periods from the investigated PLGA implants.

Importantly, all 3 experimental set-ups guaranteed sink conditions throughout the experiments in this study in the agitated bulk fluids.

II. HOW HYDROGELS SURROUNDING PLGA IMPLANTS LIMIT SWELLING AND SLOW DOWN DRUG RELEASE

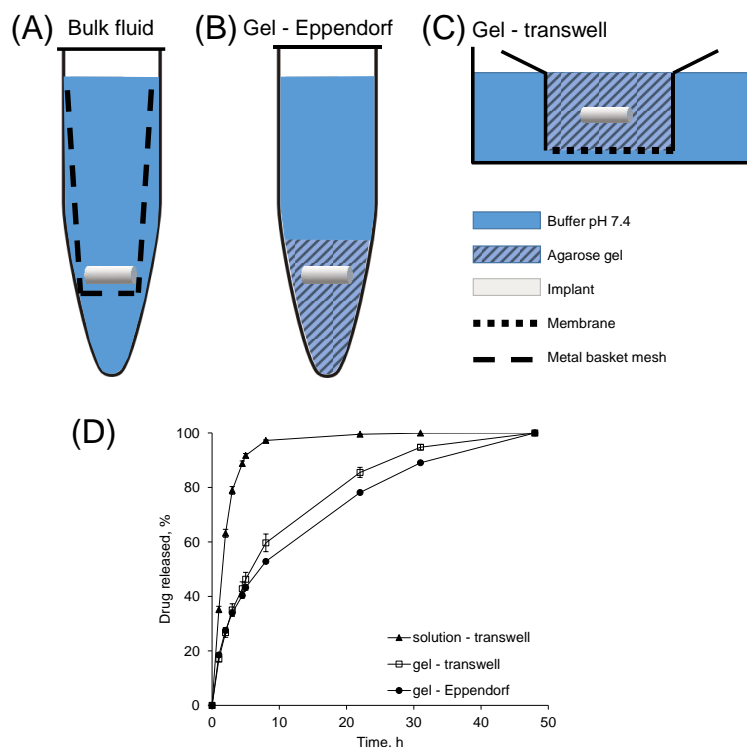


Figure II-1. Schematic presentations of the experimental set-ups used to monitor drug release from PLGA-based implants in: A) well agitated phosphate buffer pH 7.4 (in metal baskets) in Eppendorf tubes, B) agarose gels in Eppendorf tubes, the gels being exposed to well agitated phosphate buffer pH 7.4, C) agarose gels in transwell plates, the receptor compartment containing well agitated phosphate buffer pH 7.4. In all cases, sink conditions were provided throughout the experiments in the well agitated bulk fluids. Optionally, pH indicators were added to the phosphate buffer. Details are described in the text. The diagram in D) shows the rates at which an ibuprofen solution (200 $\mu\text{g}/\text{mL}$) was “released” from the donor compartment in a transwell plate free of gel, or from a gel in an Eppendorf tube or from a gel in a transwell plate.

II.4.2. Drug release and implant swelling

The diagrams at the top of *Figure II-2* show the experimentally measured ibuprofen release kinetics from the investigated PLGA implants using the 3 different set-ups. The diagram on the right-hand side shows a zoom on the first 10 d. As it can be seen, drug release was faster when using the “bulk fluid” set-up compared to the “gel – Eppendorf” and “gel – transwell” set-ups. For instance, complete released was observed after about 11 d versus 17 d and 21 d. This can only in part be explained by the additional drug transport step through the agarose gels, as discussed above.

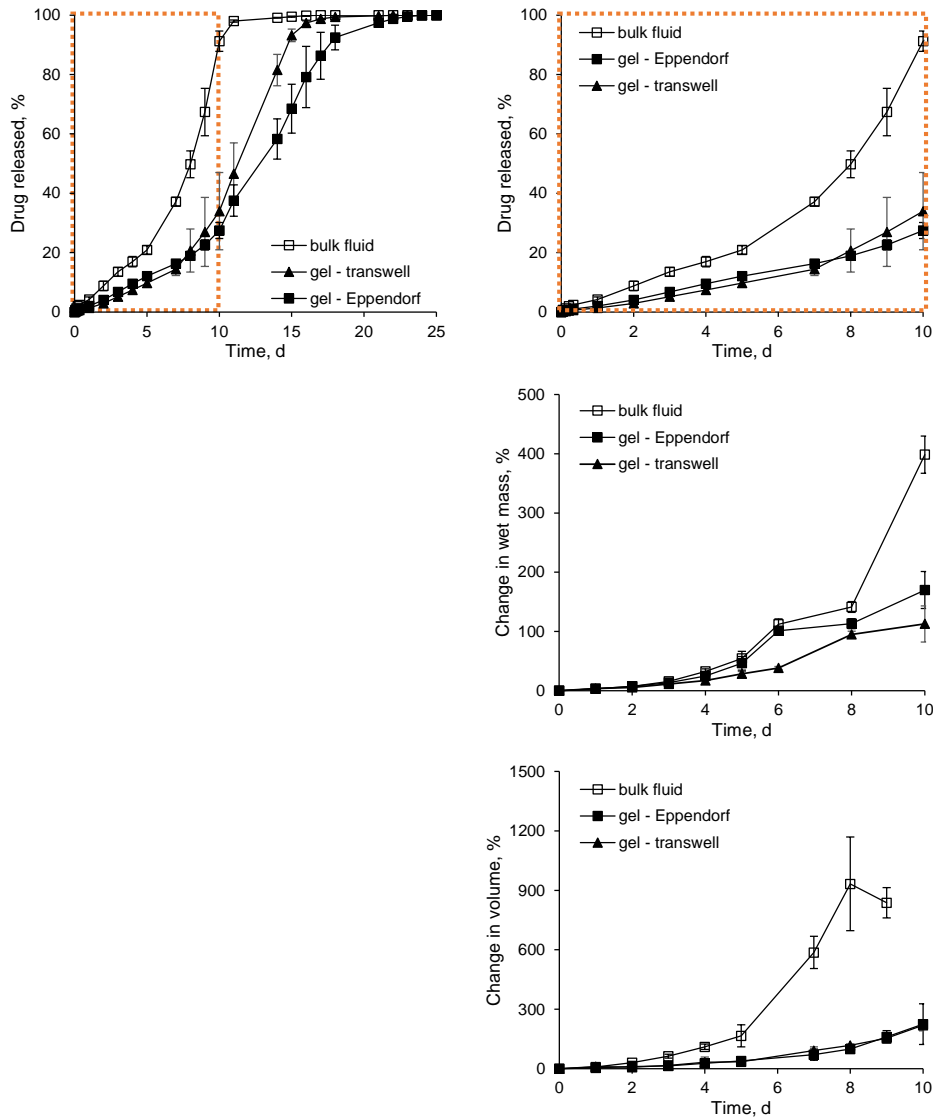


Figure II-2. *Ibuprofen release from and swelling of PLGA implants upon exposure to phosphate buffer pH 7.4, observed using 3 experimental set-ups: In bulk fluids in Eppendorf tubes, in agarose gels exposed to the release medium in Eppendorf tubes, and in agarose gels in transwell plates (the acceptor compartment containing the release medium). Please note the different scaling of the x-axes on the left versus the right hand side.*

Interestingly, all release profiles were “bi-phasic”: A zero order release phase (with an about constant release rate) was followed by a more rapid drug release phase, leading to complete drug exhaust. No noteworthy “burst release” was observed, irrespective of the experimental set-up. This can probably be explained by the fact that the implants were prepared by hot melt extrusion, leading to a non-porous surface, as also evidenced by SEM (e.g. pictures at the top on the left hand side of *Figure II-3*). Furthermore, in contrast to small PLGA microparticles, the release of minor *absolute* amounts of drug from surface-near regions of a “large” implant at

II. HOW HYDROGELS SURROUNDING PLGA IMPLANTS LIMIT SWELLING AND SLOW DOWN DRUG RELEASE

early time points is negligible from a *relative* point of view (the 100 % reference value being considerably higher).

The diagrams in the middle and at the bottom of *Figure II-2* show the dynamic changes in the wet mass and volume of the PLGA implants upon exposure to the release medium when using the 3 different set-ups. Clearly, all systems started to fundamentally swell after a “lag phase”. Importantly, as in the case of drug release, there was a clear impact of the presence of a hydrogel surrounding the PLGA implant: The onset of substantial system swelling was delayed by several days. The optical macroscopy pictures in *Figure II-4* illustrate this behavior: At the top, images of surfaces are shown, at the bottom images of cross-sections. The implants were exposed to the release medium for up to 10 d using the 3 different set-ups (as indicated). In all cases, system swelling was limited during the first few days, followed by the onset of substantial PLGA swelling. When looking at the 3 diagrams on the right hand side of *Figure II-2* (showing drug release as well as changes in the systems’ wet mass and volume during the first 10 d), it can be seen that the onset of important system swelling coincided with the onset of the final, rapid drug release phase in all cases. The observed ranking orders for the “lag time” for substantial system swelling and for the onset of the final rapid drug release phase were the same: “bulk fluid” < “gel -transwell” \approx “gel -Eppendorf” set-up.

The difference in the swelling kinetics of the implants upon exposure to a “bulk fluid” versus “gel” can probably be attributed to the sterical hindrance caused by the agarose matrix: Once the PLGA implants are in contact with the bulk fluid or gel, water penetrates into the system and the entire implant is rather rapidly wetted. Since the investigated PLGA is relatively hydrophobic, the amounts of water diffusing into the implants at early time points remain limited. But these “low” amounts of water are sufficient to initiate polymer degradation throughout the device (“bulk erosion”). Consequently, the macromolecules become shorter and less entangled with time. Also, since the newly created end groups (upon ester bond hydrolysis) are hydrophilic (-COOH and -OH), the polymer matrix becomes more and more hydrophilic. In addition, the concentration of water-soluble degradation products (short chain acids) is steadily increasing, generating a continuously increasing osmotic pressure inside the implant.

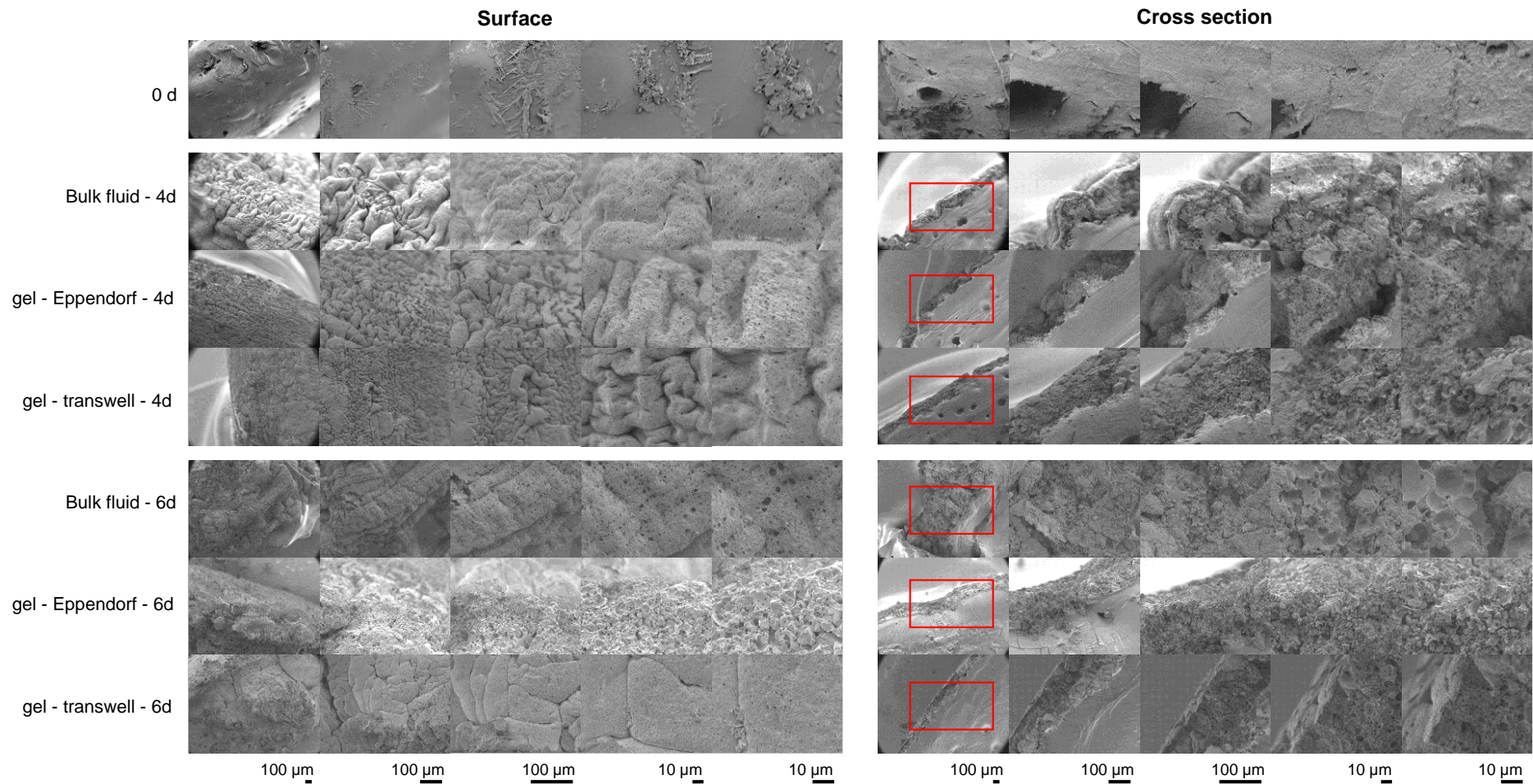


Figure II-3. SEM pictures of surfaces and cross sections of ibuprofen-loaded PLGA implants before and after exposure to phosphate buffer pH 7.4 using the 3 experimental set-ups. The type of set-up and exposure times are indicated on the left hand side. Please note that after exposure to the release medium the implants were freeze-dried prior to analysis. Thus, caution must be paid due to artefact creation.

II. HOW HYDROGELS SURROUNDING PLGA IMPLANTS LIMIT SWELLING AND SLOW DOWN DRUG RELEASE

At a certain time point, the mechanical stability of the initially dense polymeric system becomes insufficient (due to the decreasing degree of macromolecular entanglement) and substantial amounts of water penetrate into the device: driven by the generated osmotic pressure and hydrophilicity of the degrading implant. The presence of an agarose gel around the implant sterically hinders this phenomenon and delays the onset of substantial system swelling (*Figure II-2*, diagrams in the middle and at the bottom: filled versus open symbols). The considerable increase in the water content of the implant fundamentally changes the conditions for drug release: Initially, the ibuprofen was effectively trapped within a dense PLGA matrix. After this substantial device swelling, the drug is in contact with considerable amounts of water and surrounded by a highly swollen PLGA gel (as it can be seen in the pictures on the right hand side of *Figure II-4*). Under these conditions, drug release is very much facilitated. The scheme in *Figure II-5* schematically illustrates this hypothesized drug release mechanism (in a simplified manner). Due to the key importance of implant swelling for the control of drug release, its role might be considered as “orchestrating” (31). Please note that the dissolution of drug particles is probably not playing a role in the investigated implants, since at a practical loading of 6.6 %, the ibuprofen is likely completely dissolved in the PLGA matrix from the beginning (“monolithic solution”) (40).

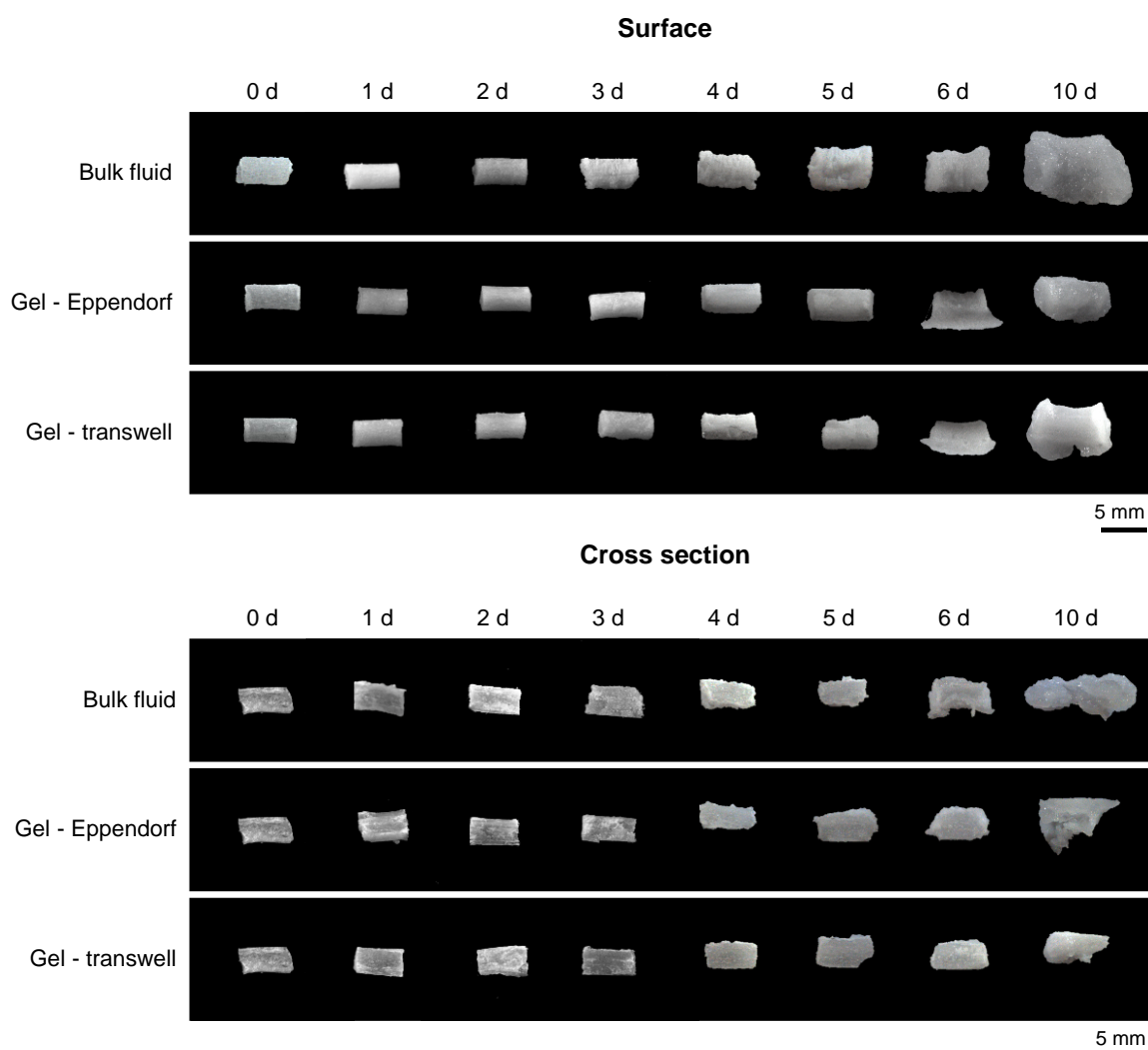


Figure II-4. Optical macroscopy pictures of surfaces and cross sections of ibuprofen-loaded PLGA implants before and after exposure to phosphate buffer pH 7.4 using 3 experimental set-ups: In bulk fluids in Eppendorf tubes, in agarose gels exposed to the release medium in Eppendorf tubes, and in agarose gels in transwell plates (the acceptor compartment containing the release medium). The exposure times are indicated at the top, the type of set-up is indicated on the left hand side

The above described hypotheses are in good agreement with SEM pictures of surfaces and cross sections of the implants obtained after different time periods using the 3 different set-ups. However, please note that great caution should be paid when drawing conclusions from these SEM images, because the implants had to be dried prior to analysis, creating artefacts. The pictures on the left hand side of *Figure II-3* show surfaces, those on the right hand side cross sections of implants exposed to the bulk fluid or gels for up to 6 d. As it can be seen, all implant surfaces became wrinkled and highly porous upon. These structures are clearly artefacts: During drug release, the polymer can be expected to be *highly* swollen in *surface-near* regions,

II. HOW HYDROGELS SURROUNDING PLGA IMPLANTS LIMIT SWELLING AND SLOW DOWN DRUG RELEASE

since the latter are in contact with high amounts of water (in contrast to regions deeper inside the implant). The presence of a highly swollen, surface-near matrix layer was also visible in the *optical* macroscopy pictures shown in *Figure II-4*, which were obtained without sample drying. The red rectangles in the SEM pictures on the right hand side of *Figure II-3* highlight the two zones which can be distinguished: A highly swollen surface-near layer and a “non swollen” layer located below. The thickness of the highly swollen surface-near zone increases with time. This growth is due to the fact that high amounts of water are present in the highly swollen outmost layer and are, thus, in contact with the PLGA in the layer right below. Please note that the scheme in *Figure II-5* does not reflect this phenomenon for reasons of simplicity.

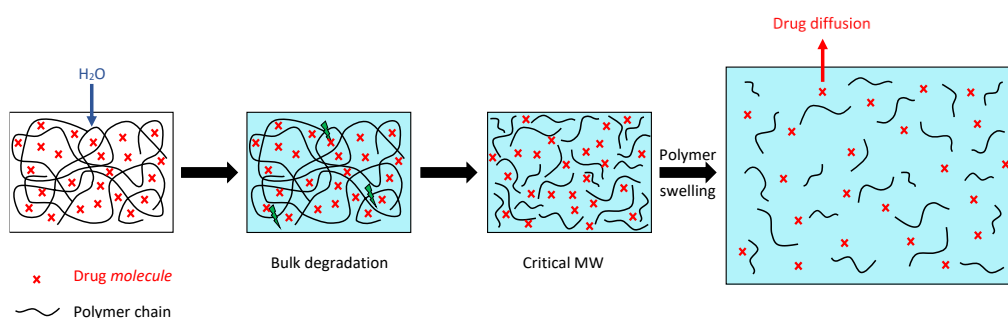


Figure II-5. Simplified schematic presentation of the mass transport mechanisms controlling ibuprofen release from the investigated PLGA implants. Initially, limited amounts of water diffuse into the system, leading to polyester degradation throughout the implants (“bulk erosion”). As soon as a critical polymer molecular weight is reached, substantial amounts of water penetrate into the device, facilitating subsequent drug release. Details are described in the text.

Interestingly, the SEM pictures of the cross sections shown in *Figure II-3* clearly evidence the impact of the presence of an agarose gel on implant swelling: As it can be seen, the highly swollen surface layer is much thicker in the “bulk fluid” set-up compared to the “gel – Eppendorf” and “gel – transwell” set-ups after 6 d.

II.4.3. Implant erosion and PLGA degradation

Figure II-6 shows the dynamic changes in the pH of the agitated bulk fluids in the 3 experimental set-ups (top) as well as the decrease of the dry mass and average polymer molecular weight of the PLGA upon implant exposure to the release media. The diagram on the right hand side at the top shows a zoom on the first 10 d. Importantly, the pH in the bulk fluids remained about constant (neutral) for up to 10 d in all cases. This corresponds to the entire release period of implants released in the “bulk fluid” set-up. Afterwards, a temporary

drop in the pH was observed, the importance of which decreased in the following rank order: “gel – transwell” > “gel – Eppendorf” > “bulk fluid” set-up. This drop can at least partially be attributed to the release of short chain, water-soluble acids (as degradation products of PLGA) into the bulk fluids: As discussed above, once the implants become sufficiently hydrophilic and mechanically instable, substantial system swelling sets on. This does not only fundamentally change the conditions for drug release, but also for the release of these water-soluble acids. Please note that this temporary drop in pH can also (in part) be attributed to the longer sampling interval (3 d “week-end gap”, compared to daily sampling during the week; at each sampling time point, the entire bulk fluid was renewed). Thus, the water-soluble acids accumulated during the longer sampling interval. However, as it can be seen, the following 3 d sampling gap at day 21 led to a much less important decrease in the pH of the bulk fluids.

It has to be pointed out that the pH values shown in *Figure II-6* were measured in the agitated *bulk fluids* in all set-ups. In the case of the “gel -Eppendorf” and “gel – transwell” set-ups, the implants were not in direct contact with this bulk fluid. This is why also potential dynamic changes in the pH within the *agarose gels* were monitored during drug release. Three pH indicators [phenol red (PR), bromothymol blue (BTB) and bromocresol green (BCG)] were added to the phosphate buffer pH 7.4, which was used for the preparation of the gels. On the left hand side of *Figure II-7*, the pH values are shown at which the indicators change their color. Implant samples were treated as for the in vitro drug release studies. After pre-determined exposure periods, optical macroscopy pictures were taken. The dotted red lines highlight the most informative images at each time point. In the case of the “gel – Eppendorf” set-up, the pH in the gel surrounding the implant remained above 6.6 during the first week, and then temporarily dropped: to pH 6.0-6.5 on day 10 and to pH 5.4-6.0 on day 14. It subsequently raised again. In the “gel – transwell” set-up a similar behavior was observed. These drops are consistent with the pH drops observed in the agitated bulk fluids used in these set-ups (which were discussed above). They can mainly be attributed to the release of short chain acids from the implants after the onset of substantial system swelling, and (in part) to the accumulation of the acids during the longer (3 d) sampling interval. Since the solubility of ibuprofen is pH-dependent, local acidic environments around the implant might limit drug solubility and, hence, slow down drug release. However, Kozac et al. (35) reported slower release from PLGA-based films and microparticles surrounded by agarose gel compared to agitated bulk fluid also for the free base lidocaine, which is more soluble at acidic pH.

II. HOW HYDROGELS SURROUNDING PLGA IMPLANTS LIMIT SWELLING AND SLOW DOWN DRUG RELEASE

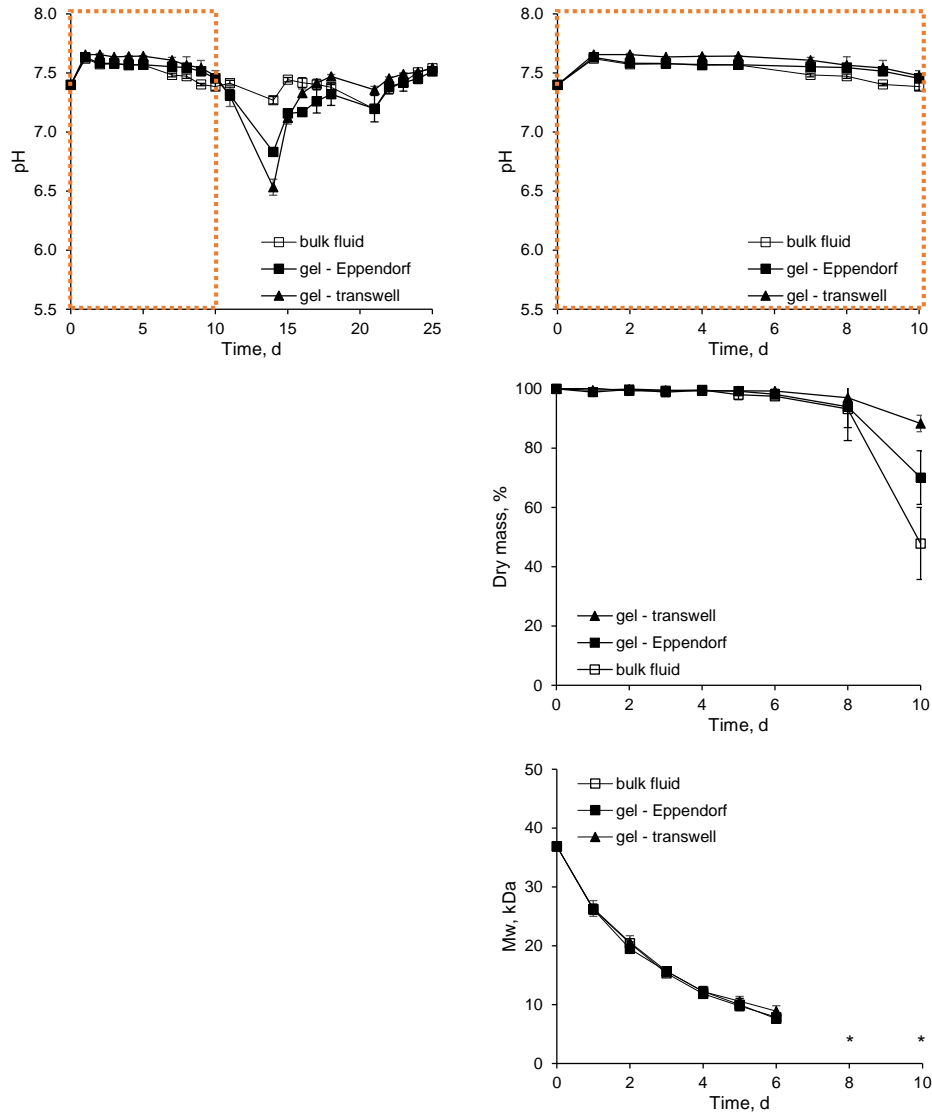


Figure II-6. Dynamic changes in the pH of the well agitated bulk fluids, dry mass (%) of the implants and PLGA polymer molecular weight (Mw) upon exposure of the implants to phosphate buffer pH 7.4 in the 3 experimental set-ups: In bulk fluids in Eppendorf tubes, in agarose gels exposed to the release medium in Eppendorf tubes, and in agarose gels in transwell plates (the acceptor compartment containing the release medium). Please note the different scaling of the x-axes on the left versus the right hand side. The Asterix indicates that the average polymer molecular weight (Mw) was below 5 kDa.

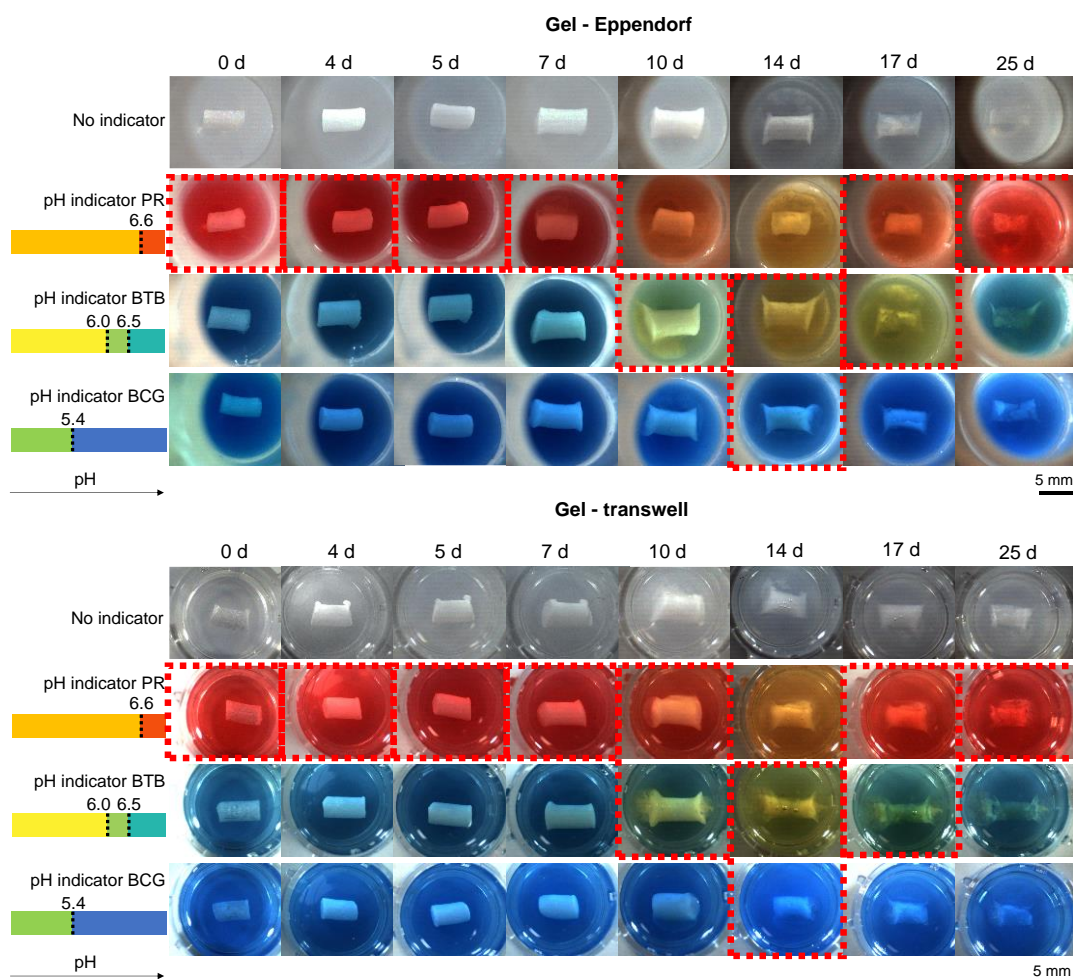


Figure II-7. Optical macroscopy pictures of ibuprofen-loaded PLGA implants embedded in agarose gels (“gel – Eppendorf” and “gel – transwell” set-ups) before and after exposure to phosphate buffer pH 7.4, optionally containing 0.0025 % phenol red (PR), bromothymol blue (BTB), or bromocresol green (BCG), as indicated

In addition to dynamic pH changes in the agitated bulk fluids and gels, also pH changes can occur *within* the PLGA-based implants during drug release. In an attempt to monitor such events, 4 different pH indicators were added to the bulk fluids and gels in the 3 experimental set-ups: phenol red (PR), bromothymol blue (BTB), bromocresol green (BCG) and bromophenol blue (BPB). The pH values at which they change colors are indicated on the left hand side of *Figure II-8*. The idea was that the pH indicators penetrate into the implants (together with the water) and optical macroscopy pictures of surfaces and cross sections of the devices would allow to map the pH within the systems at different time points. As it can be seen in *Figure II-8*, this strategy allowed to gain some insight in the case the “bulk fluid” set-up: After 10 d, sufficient amounts of the pH indicators penetrated into the implants to allow monitoring a pH value of 4.6-5.4 in regions close to the center of the implants, and pH values

II. HOW HYDROGELS SURROUNDING PLGA IMPLANTS LIMIT SWELLING AND SLOW DOWN DRUG RELEASE

in the range of 5.4-6.0 in the rest of the implants. This is interesting information, because PLGA ester hydrolysis is catalyzed by protons. However, in this case, drug release was already complete when using this set-up at this time point (*Figure II-2*). So, we prefer not to draw conclusions on the potential importance of autocatalytic effects based on these data. Due to the limited degrees of implant swelling at earlier time points, the concentrations of the pH indicators *within* the systems was too low to map the pH (*Figure II-8*). When using the gel set-ups, only the BTB indicator penetrated to a sufficient extent into the implants, indicating a pH below 6.0 for the “gel -Eppendorf” set-up (the implants were too fragile to be cut in the case of the “gel – transwell” set-up).

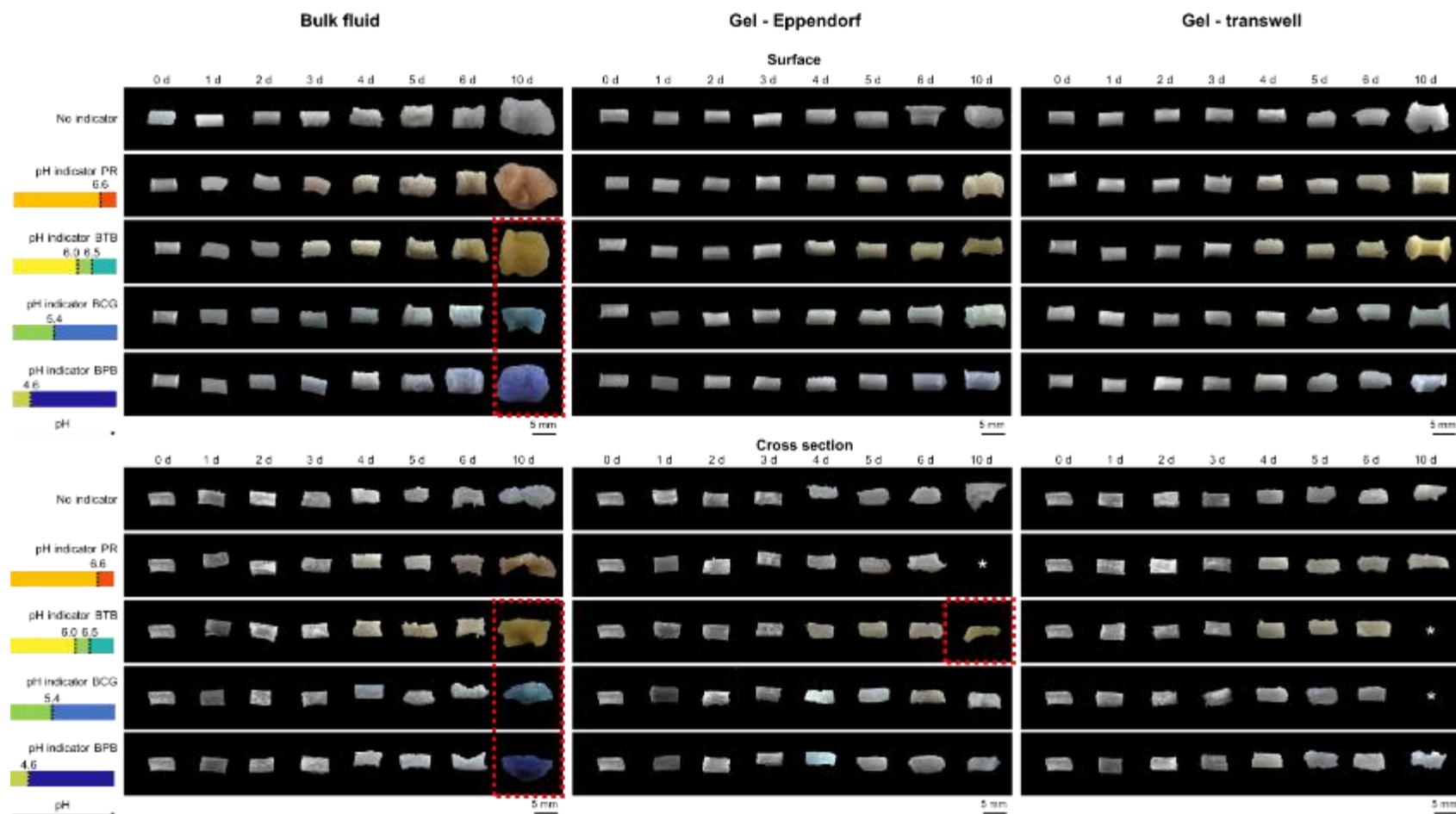


Figure II-8. Optical macroscopy pictures of surfaces and cross sections of ibuprofen-loaded PLGA implants before and after exposure to phosphate buffer pH 7.4 containing 0.0025 % phenol red (PR), bromothymol blue (BTB), bromocresol green (BCG) or bromophenol blue (BPB). Three experimental set-ups were used: Bulk fluids in Eppendorf tubes, agarose gels exposed to the release medium in Eppendorf tubes, and in agarose gels in transwell plates (the acceptor compartment containing the release medium). The type of set-up and exposure times are indicated at the top, the type of pH indicator is given on the left hand side. The Asterix indicates that the respective samples were too fragile to be cut.

II. HOW HYDROGELS SURROUNDING PLGA IMPLANTS LIMIT SWELLING AND SLOW DOWN DRUG RELEASE

As it can be seen in the middle of *Figure II-2*, the implants *dry mass* remained about constant during the first week, and then decreased, due to the release of water-soluble PLGA degradation products and drug. Importantly, the erosion rate was higher in the absence of an agarose gel. These observations are in good agreement with the hypothesized drug release mechanism: During the first few days, the PLGA network is still highly entangled and the small amounts of generated short chain acids and drug are poorly mobile, resulting in negligible dry mass loss. However, once substantial amounts of water are present in the system, drug and water-soluble degradation products are much more rapidly released. Since the presence of the agarose gel delays implant swelling, also the dry mass loss of the implants is delayed compared to the “bulk fluid” set-up.

The diagram at the bottom of *Figure II-2* shows that the *decrease in polymer molecular weight* of the PLGA is not significantly affected by the type of experimental set-up: In all cases, the length of the macromolecules exponentially decreased from the beginning, indicating pseudo-first order kinetics. After day 6, the values were too small to be reliably detected by the applied GPC method. These results suggest that the relatively rapid entire implant wetting and subsequent polyester bond cleavage during the first couple of days are not affected by the type of experimental set-up. This is consistent with the hypothesized drug release mechanism: The absence or presence of a hydrogel around the implant does not alter the rate at which the limited amounts of water diffuse into the system upon contact with phosphate buffer pH 7.4 to a noteworthy extent. Hence, also PLGA degradation throughout the polymer matrix is not affected during this initial phase.

Interestingly, the absence of a noteworthy effect of the type of experimental set-up on PLGA degradation during this early phase strengthens the hypothesis that implant *swelling* (and not PLGA *degradation*) orchestrates drug release: While the decrease in polymer molecular weight is very similar during the first 6 d in the 3 experimental set-ups (*Figure II-6* at the bottom), first indications for the hindrance of system swelling by the presence of an agarose gel are visible: as reflected by differences in the wet mass & volume changes (*Figure II-2*) as well as by optical microscopy pictures (*Figure II-4*). These differences in system swelling affect drug mobility and drug release as well as the mobility of the water-soluble PLGA degradation products and, thus, implant erosion (dry mass loss).

II.5. Conclusion

The presence of an agarose gel surrounding PLGA implants significantly hinders polymer swelling (sterically) and slows down drug release (due to delayed penetration of substantial amounts of water into the system). In vivo it can be expected that surrounding tissue has a similar mechanical effect. However, yet it is unknown how important the impact of mechanical stress caused by body movements (e.g., muscle contractions) for the fate of a degrading PLGA implant is. The results presented in this study can help developing more realistic in vitro drug release set-ups for parenteral drug delivery systems. They also strengthen the hypothesis that implant *swelling* plays an orchestrating role for the control of drug release from PLGA-based drug delivery systems.

II.6. Acknowledgements

This project has received funding from the Interreg 2 Seas programme 2014-2020 co-funded by the European Regional Development Fund under subsidy contract No 2S04-014 3DMed. The authors are very grateful for this support. They would also like to thank Mr. A. Fadel from the “Centre Commun de Microscopie” of the University of Lille (“Plateau technique de la Federation Chevreul CNRS FR 2638”) for his valuable technical help with the SEM pictures.

II.7. Authors statement

C. Bassand Investigation; Methodology; Validation; Conceptualization; Writing - Original Draft; Visualization

M. Lamatsch Investigation

J. Verin Investigation; Methodology, Validation

F. Siepmann Conceptualization; Methodology; Supervision; Resources; Writing - Review & Editing; Visualization; Project administration; Funding acquisition

J. Siepmann Conceptualization; Methodology; Supervision; Resources; Writing - Review & Editing; Visualization; Project administration; Funding acquisition

II. HOW HYDROGELS SURROUNDING PLGA IMPLANTS LIMIT SWELLING AND SLOW DOWN DRUG RELEASE

II.8. References

1. Park K, Skidmore S, Hadar J, Garner J, Park H, Otte A, et al. Injectable, long-acting PLGA formulations: Analyzing PLGA and understanding microparticle formation. *J Controlled Release*. 2019 Jun 28;304:125–34.
2. Sharifi F, Otte A, Yoon G, Park K. Continuous in-line homogenization process for scale-up production of naltrexone-loaded PLGA microparticles. *J Controlled Release*. 2020 Sep 10;325:347–58.
3. Shi N-Q, Zhou J, Walker J, Li L, Hong JKY, Olsen KF, et al. Microencapsulation of luteinizing hormone-releasing hormone agonist in poly (lactic-co-glycolic acid) microspheres by spray-drying. *J Controlled Release*. 2020 May 10;321:756–72.
4. Acharya G, Shin CS, Vedantham K, McDermott M, Rish T, Hansen K, et al. A study of drug release from homogeneous PLGA microstructures. *J Controlled Release*. 2010 Sep 1;146(2):201–6.
5. Fang Y, Zhang N, Li Q, Chen J, Xiong S, Pan W. Characterizing the release mechanism of donepezil-loaded PLGA microspheres in vitro and in vivo. *J Drug Deliv Sci Technol*. 2019 Jun 1;51:430–7.
6. Kempe S, Mäder K. In situ forming implants - an attractive formulation principle for parenteral depot formulations. *J Controlled Release*. 2012 Jul 20;161(2):668–79.
7. Anderson J, Shives M. Biodegradation and biocompatibility of PLA and PLGA microspheres. *Adv Drug Deliv Rev*. 1997 Oct 13;28(1):5–24.
8. Arrighi A, Marquette S, Peerboom C, Denis L, Goole J, Amighi K. Development of PLGA microparticles with high immunoglobulin G-loaded levels and sustained-release properties obtained by spray-drying a water-in-oil emulsion. *Int J Pharm*. 2019 Jul 20;566:291–8.
9. Parent M, Clarot I, Gibot S, Derive M, Maincent P, Leroy P, et al. One-week in vivo sustained release of a peptide formulated into in situ forming implants. *Int J Pharm*. 2017 Apr 15;521(1):357–60.
10. Ravivarapu HB, Burton K, DeLuca PP. Polymer and microsphere blending to alter the release of a peptide from PLGA microspheres. *Eur J Pharm Biopharm*. 2000 Sep 1;50(2):263–70.
11. Wischke C, Schwendeman SP. Principles of encapsulating hydrophobic drugs in PLA/PLGA microparticles. *Int J Pharm*. 2008 Dec 8;364(2):298–327.
12. Gèze A, Venier-Julienne MC, Mathieu D, Filmon R, Phan-Tan-Luu R, Benoit JP. Development of 5-iodo-2'-deoxyuridine milling process to reduce initial burst release from PLGA microparticles. *Int J Pharm*. 1999 Feb 15;178(2):257–68.
13. Ramazani F, Chen W, van Nostrum CF, Storm G, Kiessling F, Lammers T, et al. Strategies for encapsulation of small hydrophilic and amphiphilic drugs in PLGA microspheres: State-of-the-art and challenges. *Int J Pharm*. 2016 Feb 29;499(1):358–67.

14. Wan F, Yang M. Design of PLGA-based depot delivery systems for biopharmaceuticals prepared by spray drying. *Int J Pharm.* 2016 Feb 10;498(1):82–95.
15. Fredenberg S, Wahlgren M, Reslow M, Axelsson A. The mechanisms of drug release in poly(lactic-co-glycolic acid)-based drug delivery systems--a review. *Int J Pharm.* 2011 Aug 30;415(1–2):34–52.
16. Fredenberg S, Jönsson M, Laakso T, Wahlgren M, Reslow M, Axelsson A. Development of mass transport resistance in poly(lactide-co-glycolide) films and particles – A mechanistic study. *Int J Pharm.* 2011 May 16;409(1):194–202.
17. Göpferich A. Mechanisms of polymer degradation and erosion. *Biomaterials.* 1996 Jan;17(2):103–14.
18. Blasi P, Schoubben A, Giovagnoli S, Perioli L, Ricci M, Rossi C. Ketoprofen poly(lactide-co-glycolide) physical interaction. *AAPS PharmSciTech.* 2007 Jun;8(2):E78–85.
19. Blasi P, D’Souza SS, Selmin F, DeLuca PP. Plasticizing effect of water on poly(lactide-co-glycolide). *J Controlled Release.* 2005 Nov 2;108(1):1–9.
20. Brunner A, Mäder K, Göpferich A. pH and osmotic pressure inside biodegradable microspheres during erosion. *Pharm Res.* 1999 Jun;16(6):847–53.
21. Schädlich A, Kempe S, Mäder K. Non-invasive in vivo characterization of microclimate pH inside in situ forming PLGA implants using multispectral fluorescence imaging. *J Controlled Release.* 2014 Apr 10;179:52–62.
22. Fu K, Pack DW, Klibanov AM, Langer R. Visual Evidence of Acidic Environment Within Degrading Poly(lactic-co-glycolic acid) (PLGA) Microspheres. *Pharm Res.* 2000 Jan 1;17(1):100–6.
23. Siepmann J, Elkharraz K, Siepmann F, Klose D. How Autocatalysis Accelerates Drug Release from PLGA-Based Microparticles: A Quantitative Treatment. *Biomacromolecules.* 2005 Jul 1;6(4):2312–9.
24. Huang J, Mazzara JM, Schwendeman SP, Thouless MD. Self-healing of pores in PLGAs. *J Controlled Release.* 2015 May 28;206:20–9.
25. Gasmi H, Danede F, Siepmann J, Siepmann F. Does PLGA microparticle swelling control drug release? New insight based on single particle swelling studies. *J Controlled Release.* 2015 Sep 10;213:120–7.
26. Luan X, Bodmeier R. Modification of the tri-phasic drug release pattern of leuprolide acetate-loaded poly(lactide-co-glycolide) microparticles. *Eur J Pharm Biopharm Off J Arbeitsgemeinschaft Pharm Verfahrenstechnik EV.* 2006 Jun;63(2):205–14.
27. Mylonaki I, Allémann E, Delie F, Jordan O. Imaging the porous structure in the core of degrading PLGA microparticles: The effect of molecular weight. *J Controlled Release.* 2018 Sep 28;286:231–9.

II. HOW HYDROGELS SURROUNDING PLGA IMPLANTS LIMIT SWELLING AND SLOW DOWN DRUG RELEASE

28. Wang H, Zhang G, Sui H, Liu Y, Park K, Wang W. Comparative studies on the properties of glycyrrhetic acid-loaded PLGA microparticles prepared by emulsion and template methods. *Int J Pharm.* 2015 Dec 1;496(2):723–31.
29. Gasmi H, Willart J-F, Danede F, Hamoudi MC, Siepmann J, Siepmann F. Importance of PLGA microparticle swelling for the control of prilocaine release. *J Drug Deliv Sci Technol.* 2015 Dec 1;30:123–32.
30. Gasmi H, Siepmann F, Hamoudi MC, Danede F, Verin J, Willart J-F, et al. Towards a better understanding of the different release phases from PLGA microparticles: Dexamethasone-loaded systems. *Int J Pharm.* 2016 Nov 30;514(1):189–99.
31. Bode C, Kranz H, Fizez A, Siepmann F, Siepmann J. Often neglected: PLGA/PLA swelling orchestrates drug release: HME implants. *J Controlled Release.* 2019 Jul 28;306:97–107.
32. Kang J, Schwendeman SP. Pore Closing and Opening in Biodegradable Polymers and Their Effect on the Controlled Release of Proteins. *Mol Pharm.* 2007 Feb 1;4(1):104–18.
33. von Burkersroda F, Schedl L, Göpferich A. Why degradable polymers undergo surface erosion or bulk erosion. *Biomaterials.* 2002 Nov 1;23(21):4221–31.
34. Tamani F, Bassand C, Hamoudi MC, Danede F, Willart JF, Siepmann F, et al. Mechanistic explanation of the (up to) 3 release phases of PLGA microparticles: Diprophylline dispersions. *Int J Pharm.* 2019 Dec 1;572:118819.
35. Kožák J, Rabišková M, Lamprecht A. In-vitro drug release testing of parenteral formulations via an agarose gel envelope to closer mimic tissue firmness. *Int J Pharm.* 2021 Feb 1;594:120142.
36. Kozak J, Rabiskova M, Lamprecht A. Muscle Tissue as a Surrogate for In Vitro Drug Release Testing of Parenteral Depot Microspheres. *AAPS PharmSciTech.* 2021 Mar 29;22(3):119.
37. Allababidi S, Shah JC. Kinetics and Mechanism of Release from Glyceryl Monostearate-Based Implants: Evaluation of Release in a Gel Simulating in Vivo Implantation. *J Pharm Sci.* 1998 Jun 1;87(6):738–44.
38. Ye F, Larsen SW, Yaghmur A, Jensen H, Larsen C, Ostergaard J. Drug release into hydrogel-based subcutaneous surrogates studied by UV imaging. *J Pharm Biomed Anal.* 2012 Dec;71:27–34.
39. Jensen SS, Jensen H, Cornett C, Møller EH, Østergaard J. Real-time UV imaging identifies the role of pH in insulin dissolution behavior in hydrogel-based subcutaneous tissue surrogate. *Eur J Pharm Sci.* 2015 Mar 10;69:26–36.
40. Siepmann J, Siepmann F. Modeling of diffusion controlled drug delivery. *J Controlled Release.* 2012 Jul 20;161(2):351–62.

**III. HOT MELT EXTRUDED IBUPROFEN-
LOADED PLGA IMPLANTS: IMPORTANCE
OF HEAT EXPOSURE**

III. HOT MELT EXTRUDED IBUPROFEN-LOADED PLGA IMPLANTS: IMPORTANCE OF HEAT EXPOSURE

Research article – To be submitted in Journal of Drug Delivery Science and technology

Hot melt extruded ibuprofen-loaded PLGA implants: Importance of heat exposure

C. Bassand¹, L. Benabed¹, J. Verin¹, F. Danede², L.A. Lefol¹, J.F. Willart², F. Siepman¹,
J. Siepman¹

¹*Univ. Lille, Inserm, CHU Lille, U1008, F-59000 Lille, France*

²*Univ. Lille, USTL UMET UMR CNRS 8207, F-59650 Villeneuve d'Ascq, France*

III.1. Abstract

Hot melt extrusion offers an interesting potential for the manufacturing of poly(lactic-co-glycolic acid) (PLGA)-based implants. However, the heat treatment might substantially alter the polymer, drug and degree of drug-polymer mixing. The aim of this study was to better understand the impact of varying exposure to 105 °C from 3 to 15 min in the case of ibuprofen-loaded PLGA implants. In vitro drug release was measured in phosphate buffer pH 7.4, optical & scanning electron microscopy, DSC, GPC, X-ray diffraction and gravimetric analysis were used to monitor dynamic changes of the implants' morphology, dry & wet mass and average polymer molecular weight. Interestingly, increasing the heat exposure from 3 to 15 min led to a decrease in the amount of crystalline drug present in the system, resulting in a slight decrease in the initial burst release. The average PLGA molecular weight also slightly decreased during the heat treatment. In contrast, the relatively rapid penetration of water into the entire implants and subsequent polymer degradation throughout the devices was not affected to a noteworthy extent. Also the onset of substantial implant swelling after about 1 week and the subsequent onset of the final rapid drug release phase (accounting for about 80 % drug release) was not significantly altered. However, for different drugs and polymers changes in their physical state upon heat exposure during hot melt extrusion might have much more importance consequences for drug release, and the hot melt extrusion process might be much less robust.

Keywords: PLGA; implant; drug release mechanism; swelling; monolithic solution; solid dispersion

III. HOT MELT EXTRUDED IBUPROFEN-LODED PLGA IMPLANTS: IMPORTANCE OF HEAT EXPOSURE

III.2. Introduction

Poly(lactic-co-glycolic acid) (PLGA) is frequently used a matrix former for controlled drug delivery systems (1–5), because it is: (i) completely biodegradable (avoiding the removal of empty remnants upon drug exhaust), (ii) biocompatible (6), (iii) and offers the possibility to provide a considerable range of release periods, ranging from a few hours to several months (2,7,8). Different types of dosage forms can be produced, such as cylindrical implants (9–11), spherical microparticles (12–14) and thin films (2,5). A variety of manufacturing procedures can be applied to produce these systems, for instance solvent evaporation methods (10,15), direct compression (16,17), 3D printing (18,19), and hot melt extrusion (4,11,20,21).

The release mechanisms from PLGA-based drug delivery systems can be rather complex, because a variety of physic-chemical phenomena can be involved (12,22–25). This includes for example water penetration into the system, PLGA degradation via hydrolytic ester bond cleavage, physical water-polymer interactions (e.g., plasticizing effects) (26), drug particle dissolution, the diffusion of dissolved drug and water-soluble PLGA degradation products, the creation of local, acidic microenvironments leading to accelerated polymer degradation and drug release (“autocatalytic effects”) (27–31), polymer swelling (32–35), pore formation & closure (36–39), limited solubility effects, drug-polymer interactions (e.g., plasticizing effects) (40), as well as osmotic effects (41). The relative importance of these phenomena can strongly depend on the type of drug, type of polymer (e.g. average polymer molecular weight and type of end groups), composition of the system (8,42,43), and type of manufacturing procedure. The latter might fundamentally affect the resulting inner and outer system structure, in particular its porosity (44,45) and the physical state of the drug in the polymeric matrix (46,47). The drug might be dissolved in the PLGA (*molecularly* distributed throughout the polymer network), or dispersed in the form of crystalline or amorphous particles. The degree of possible drug-PLGA interactions obviously strongly depends on their physical states and degree of mixing. Thus, it is very interesting to characterize them and monitor potential changes during drug release.

Due to the frequently encountered complexity of the underlying mass transport mechanisms in PLGA-based dosage forms, it is often not fully understood how a specific device controls drug release. Consequently, unexpected tendencies might be observed when varying the systems’ composition or process parameters used during manufacturing. This can render system optimization and trouble shooting during production highly challenging. As an example: It can generally be expected that the increase in dosage form dimensions leads to a decrease in the resulting relative drug release rate, if diffusional mass transport plays a major role (because the

lengths of the diffusion pathways to be overcome increase) (48). However, it has been shown that in the case of initially non-porous, lidocaine-loaded PLGA-based microparticles a 7-fold increase in the systems' diameter did virtually not affect the relative drug release rate (49). This could be attributed to a compensating mechanism: an increase in the importance of autocatalytic effects in the system: the pH becomes more acidic *inside* larger microparticles, leading to higher drug mobility. In contrast, in *initially highly porous* lidocaine-loaded PLGA microparticles, the generated water-soluble acids can more rapidly be neutralized, resulting in decreasing drug release rates with increasing system size (50).

The aim of this study was to prepare ibuprofen-loaded PLGA implants by hot melt extrusion, varying the exposure time to 105 °C from 3 to 15 min, and to thoroughly characterize the systems before and during drug release in phosphate buffer pH 7.4. Optical & scanning electron microscopy were used to evaluate the inner and outer system structure. DSC and X-ray diffraction were applied to better understand the physical state of the drug. Gravimetric analysis was used to measure changes in the dry and wet mass of the systems, and GPC analysis to monitor the average PLGA molecular weight.

III. HOT MELT EXTRUDED IBUPROFEN-LOADED PLGA IMPLANTS: IMPORTANCE OF HEAT EXPOSURE

III.3. Materials and methods

III.3.1. Materials

Poly (D,L lactic-co-glycolic acid) (PLGA, 50:50 lactic acid: glycolic acid; Resomer RG 503H; Evonik, Darmstadt, Germany); ibuprofen (BASF, Ludwigshafen, Germany); agarose (genetic analysis grade) and tetrahydrofuran (HPLC grade) (Fisher Scientific, Illkirch, France); potassium dihydrogen orthophosphate and sodium hydroxide (Acros Organics, Geel, Belgium); acetonitrile (VWR, Fontenay-sous-Bois, France); sodium hydrogen phosphate (Na_2HPO_4 ; Panreac Quimica, Barcelona, Spain).

III.3.2. Implant preparation

PLGA was milled for 4 x 30 s in a grinder (Valentin, Seb, Ecully, France). Appropriate amounts of polymer and drug powders were blended for 5 min at 20 rpm in a Turbula T2C Shaker-Mixer (Willy A Bachofen, Basel, Switzerland). Three hundred mg mixture were filled into a 1 mL syringe (Henke Sass Wolf, Tuttlingen, Germany), followed by heating at 105°C for 3, 6, 9, 12 or 15 min in an oven (FP115, Binder, Tuttlingen, Germany) (*Figure III-1 A*). The molten blend was manually extruded using the syringe. The extrudate was cut with a hot scalpel into cylindrical implants of approximately 5 mm length.

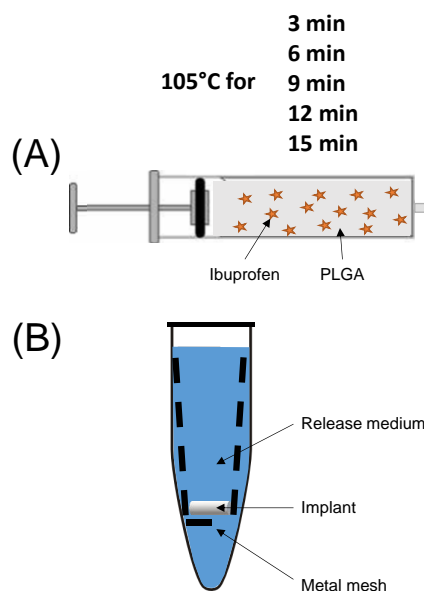


Figure III-1. Schematic presentations of the experimental set-ups used to: (A) prepare ibuprofen-loaded PLGA implants by hot melt extrusion, and (B) monitor drug release from the implants upon exposure to phosphate buffer pH 7.4 in well agitated Eppendorf tubes. Details are described in the text.

III.3.3. Practical drug loading

Implants were dissolved in 5 mL acetonitrile, followed by filtration (PVDF syringe filters, 0.45 μm ; Agilent Technologies, Santa Clara, USA) and drug content determination by HPLC-UV analysis using a Thermo Fisher Scientific Ultimate 3000 Series HPLC, equipped with an LPG 3400 SD/RS pump, an autosampler (WPS-3000 SL) and a UV-Vis detector (VWD-3400RS) (Thermo Fisher Scientific, Waltham, USA). A reversed-phase column C18 (Gemini 5 μm ; 110 A° ; 150 x 4.6 mm; Phenomenex, Le Pecq, France) was used. The mobile phase was a mixture of 30 mM Na_2HPO_4 pH 7.0: acetonitrile (60:40, v:v). The detection wavelength was 265 nm, and the flow rate 0.5 mL/min. Ten microliter samples were injected. All experiments were conducted in triplicate. Mean values \pm standard deviations are reported.

III.3.4. In vitro drug release

Implants were placed in 5 mL Eppendorf tubes (1 implant per tube), filled with 5 mL phosphate buffer pH 7.4 (USP 42). A metal mesh assured that the implants did not sink to the bottom of the tube (*Figure III-1 B*), potentially limiting the systems' surface area in direct contact with the release medium. The mesh size was 250 μm , allowing for convective flow and rapid exchange of medium inside and outside the metal "basket". The tubes were placed in a horizontal shaker (80 rpm, 37°C; GFL 3033; Gesellschaft fuer Labortechnik, Burgwedel, Germany). At predetermined time points, the entire bulk fluid was replaced by fresh release medium. The withdrawn samples were filtered (PVDF syringe filter, 0.45 μm ; Agilent) and analyzed for their ibuprofen contents by HPLC-UV as described in *section III.3.3*. In all cases, sink conditions were provided throughout the experiments. The latter were conducted in triplicate. Mean values \pm standard deviations are reported.

III.3.5. Implant swelling

Implants were treated as for the *in vitro* drug release studies (described in *section III.3.4*). At pre-determined time points, implant samples were withdrawn, and:

- (i) Pictures of the implants were taken with a SZN-6 trinocular stereo zoom microscope (Optika, Ponteranica, Italy), equipped with an optical camera (Optika Vision Lite 2.1 software). Unless otherwise indicated, the light came from the top. The lengths and diameters of the implants were determined using the ImageJ software (US National Institutes of Health). Dynamic changes in the systems' volume were calculated considering cylindrical geometry.

III. HOT MELT EXTRUDED IBUPROFEN-LOADED PLGA IMPLANTS: IMPORTANCE OF HEAT EXPOSURE

- (ii) Excess water was carefully removed using Kimtech precision wipes (Kimberly-Clark, Rouen, France) and weighed [*wet mass* (*t*)]. The *change in wet mass (%)* (*t*) was calculated as follows:

$$\text{change in wet mass } (\%) (t) = \frac{\text{wet mass } (t) - \text{mass } (t = 0)}{\text{mass } (t = 0)} \times 100 \%$$

where *mass* (*t* = 0) denotes the implant mass before exposure to the release medium.

All experiments were conducted in triplicate. Mean values +/- standard deviations are reported.

III.3.6. Implant erosion and PLGA degradation

Implants were treated as for the in vitro drug release studies (described in *section III.3.4*). At pre-determined time points, implant samples were withdrawn and freeze-dried (freezing at -45°C for 2 h 35 min, primary drying at -20 °C/0.940 mbar for 35 h 10 min, secondary drying at +20 °C/0.0050 mbar for 35 h; Christ Alpha 2-4 LSC+; Martin Christ, Osterode, Germany).

The *dry mass (%)* (*t*) was calculated as follows:

$$\text{dry mass } (\%) (t) = \frac{\text{dry mass } (t)}{\text{mass } (t = 0)} \times 100 \%$$

where *mass* (*t* = 0) denotes the implant mass before exposure to the release medium. All experiments were conducted in triplicate. Mean values +/- standard deviations are reported.

The average polymer molecular weight (M_w) of the PLGA was determined by gel permeation chromatography (GPC) as follows: Freeze-dried implant samples were dissolved in tetrahydrofuran (3 mg/mL). One hundred μL samples were injected into an Alliance GPC (refractometer detector: 2414 RI, separation module e2695, Empower GPC software; Waters, Milford, USA), equipped with a PLgel 5 μm MIXED-D column (kept at 35°C, 7.8 × 300 mm; Agilent). Tetrahydrofuran was the mobile phase (flow rate: 1 mL/min). Polystyrene standards with molecular weights between 1,480 and 70,950 Da (Polymer Laboratories, Varian, Les Ulis, France) were used to prepare the calibration curve. All experiments were conducted in triplicate. Mean values +/- standard deviations are reported.

III.3.7. Differential scanning calorimetry (DSC)

DSC thermograms were recorded using a DCS1 Star System (Mettler Toledo, Greifensee, Switzerland). Samples (approximately 5 mg in the case of raw materials & their physical blends, about 10 mg in the case of implants) were heated in closed aluminum pans as follows: from -

70 to 120 °C, cooling to -70 °C, re-heating to 120 °C (heating and cooling rates = 10 °C/min). The reported glass temperatures (T_gs) were determined from the 1st heating cycles in the case of the implants (the thermal history being of interest), and from the 2nd heating cycles in the case of the raw materials and their physical mixtures (the thermal history not being of interest). All experiments were conducted in triplicate. Mean values +/- standard deviations are reported.

III.3.8. X ray powder diffraction

X-ray powder diffraction patterns were recorded using a PANalytical X'Pert pro MPD powder diffractometer (PANalytical, Almelo, Netherlands), equipped with a Cu X-ray tube ($\lambda_{\text{CuK}\alpha} = 1.54 \text{ \AA}$) and the X'celerator detector. Samples were placed in a spinning flat sample holder. The measurements were performed in Bragg–Brentano θ - θ geometry. The diffractograms were recorded from 3 to 60° (2 θ) (0.0167 ° steps, 100 s/step).

III.3.9. Scanning electronic microscopy (SEM)

The internal and external morphology of the implants before and after exposure to the release medium was studied using a JEOL Field Emission Scanning Electron Microscope (JSM-7800F, Japan), equipped with the Aztec 3.3 software (Oxford Instruments, Oxford, England). Samples were fixed with a ribbon carbon double-sided adhesive and covered with a fine chrome layer. If indicated, the investigated implants had been exposed to the release medium before, as described for the in vitro release studies (please see *section III.3.4*). At predetermined time points, implant samples were withdrawn and freeze-dried (as described in *section III.3.6*). Cross sections were obtained by manual cutting with a scalpel, prior to freeze drying.

III. HOT MELT EXTRUDED IBUPROFEN-LOADED PLGA IMPLANTS: IMPORTANCE OF HEAT EXPOSURE

III.4. Results and discussion

Different types of ibuprofen-loaded, PLGA-based implants were prepared by hot melt extrusion using a syringe, as illustrated in Figure 1A. The drug and PLGA powders were blended and filled into a glass syringe, which was heated to 105 °C for 3, 6, 9, 12 or 15 min. The blends were manually extruded, and the extrudates were cut with a hot scalpel into cylindrical implants of approximately 5 mm length. The mean diameter was in the range of 2.5-2.8 mm in all cases (*Table III-1*). The practical drug loading varied between about 13 and 10 % (w/w). Partial ibuprofen loss might be explained by sublimation at 105 °C. The average polymer molecular weight decreased from about 21 to 18 kDa when prolonging the exposure time to 105 °C from 3 to 15 min (*Table III-1*). The Mw of the PLGA raw material was 23.1±1.1 kDa. This indicates that the polymer chains were partially cut upon heat exposure, which is consistent with reports in the literature (19,51).

Table III-1. Physical key properties of the investigated ibuprofen-loaded PLGA implants (T_g: glass transition temperature, Mw: average polymer molecular weight). The heating time applied during implant manufacturing is indicated in the top row. Mean values ± standard deviations are indicated (n = 3).

<i>Heating time</i>	<i>3 min</i>	<i>6 min</i>	<i>9 min</i>	<i>12 min</i>	<i>15 min</i>
Practical drug loading (%)	12.8 ± 0.6	11.2 ± 0.3	9.7 ± 1.0	10.9 ± 1.0	11.4 ± 1.0
Diameter (mm)	2.8 ± 0.1	2.5 ± 0.1	2.7 ± 0.1	2.6 ± 0.1	2.5 ± 0.1
T_g (°C)	33.9 ± 0.6	34.0 ± 0.3	34.3 ± 0.1	34.5 ± 0.4	33.3 ± 0.2
Mw (kDa)	21.2 ± 1.2	19.7 ± 0.8	18.9 ± 0.2	19.4 ± 0.8	18.4 ± 1.2

III.4.1. Implants before exposure to the release medium

Figure III-2. shows SEM pictures of surfaces and cross sections of the investigated ibuprofen-loaded PLGA implants before exposure to the release medium. The heating times applied during manufacturing are indicated on the left-hand side. As it can be seen, the internal and external structure was dominantly non-porous (some round shaped cavities might result from

ibuprofen sublimation during processing). Interestingly, evidence for the presence of crystalline drug particles could be seen in some of the cross sections, especially of implants prepared with shorter heating times (highlighted by the dotted red circles in *Figure III-2*).

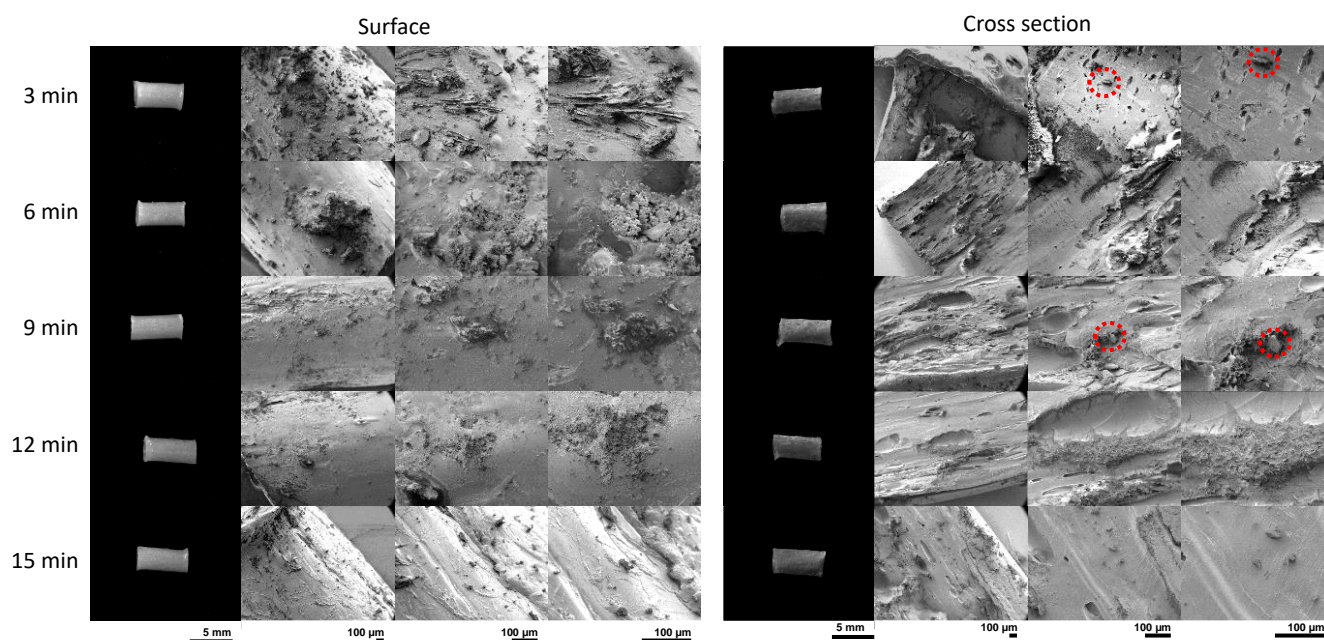


Figure III-2. Optical macroscopy pictures and SEM pictures of surfaces and cross sections of ibuprofen-loaded implants before exposure to release medium. The PLGA-ibuprofen blends were heated for 3 to 15 min during implant preparation (as indicated). Drug crystals are highlighted by dotted red circles.

To better understand the physical state of the drug in the hot melt extruded implants, DSC thermograms of the systems were recorded (*Figure III-3 A*), as well as of the raw materials (drug and polymer) for reasons of comparison (*Figure III-3 B*). Importantly, the ibuprofen powder as received showed a sharp melting peak at 79.7 ± 0.5 °C. This peak was also visible in the hot melt extruded implants, but its intensity substantially decreased with prolonged heat exposure during production. This suggests that the drug is initially present in the form of tiny crystals, which partially: (i) *dissolve* in the PLGA during processing (the temperature is raised to 105 °C, forming a “monolithic solution”), (ii) melt and re-solidify in the form of *amorphous* drug particles upon cooling (forming a “solid-in-solid dispersion”: amorphous-in-amorphous), and/or (iii) melt and re-solidify in the form of *crystalline* drug particles upon cooling (forming a “solid-in-solid dispersion”: crystalline-in-amorphous). To estimate the capacity of ibuprofen to *dissolve* in the investigated PLGA, the DSC thermograms of different drug-polymer blends were recorded, varying the ibuprofen content from 0 to 20 % (w/w). As it can be seen in

III. HOT MELT EXTRUDED IBUPROFEN-LOADED PLGA IMPLANTS: IMPORTANCE OF HEAT EXPOSURE

Figure 4, the glass transition temperature (T_g) of the blends decreased with increasing ibuprofen content up to about 10-15 % drug and then seems to level off. This indicates that ibuprofen acts as a plasticizer for PLGA and, under the conditions provided during the DSC measurements, at least about 10 % (w/w) drug can *dissolve* in the polymer. Interestingly, the T_g values of the implants prepared by hot melt extrusion was about constant in the investigated heating time range (varying between about 33-34 °C, *Table III-1*; please also see the DSC thermograms in *Figure III-3*). This suggests that already after 3 min heating, major parts of the ibuprofen are dissolved in the PLGA. This hypothesis is consistent with the amounts of crystalline ibuprofen determined in the PLGA implants when integrating the surfaces of the melting peaks observed during the DSC measurements (*Figure III-3*): The amounts of crystalline drug are relatively small in all cases. Thus, most of the ibuprofen is molecularly dispersed or in an amorphous form, representing about 10 % (w/w) of the total implant mass.

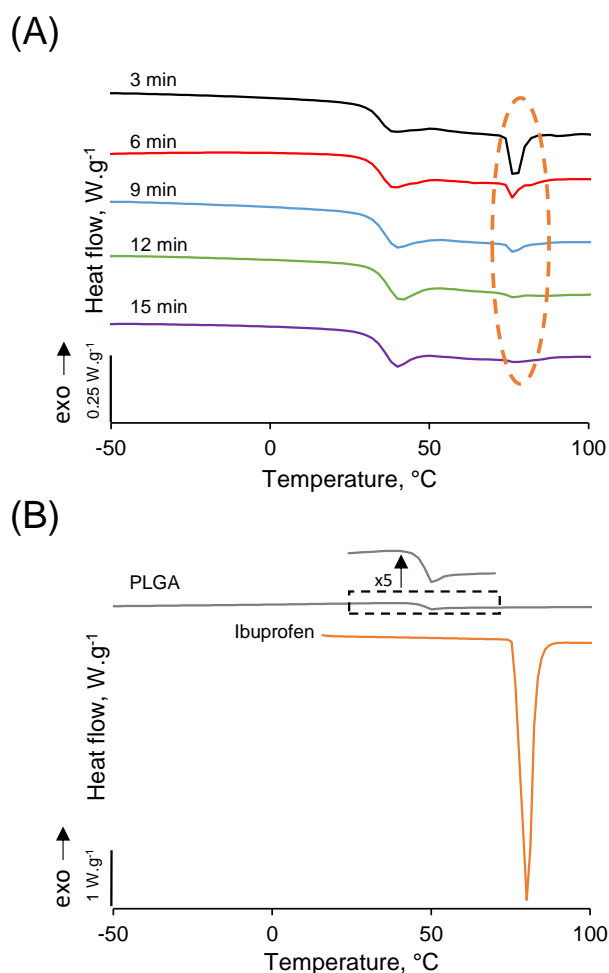


Figure III-3. DSC thermograms of the: (A) investigated ibuprofen-loaded PLGA implants (before exposure to the release medium), and (B) raw materials (PLGA & ibuprofen). During implant preparation, ibuprofen-PLGA blends were heated for 3 to 15 min (as indicated). The

dashed orange oval highlights ibuprofen melting events in the implants. Please note the different scaling of the y-axes in (A) and (B).

To further confirm the hypothesis of the presence of (some) crystalline ibuprofen in the PLGA implants, also X-ray diffraction patterns of the systems were recorded before exposure to the release medium. As it can be seen in *Figure III-4 A*, all implants exhibited sharp diffraction peaks as well as an underlying amorphous halo. The X-ray diffraction patterns of the raw materials are shown in *Figure III-4 B* for reasons of comparison. Clearly, the ibuprofen (as received) was crystalline, and the PLGA amorphous (confirming the DSC data discussed above). Importantly, the positions of the diffraction peaks observed with the drug-loaded implants corresponded well to the positions of the crystalline ibuprofen raw material. The dashed orange ovals in *Figure III-4 A* highlight some of these peaks.

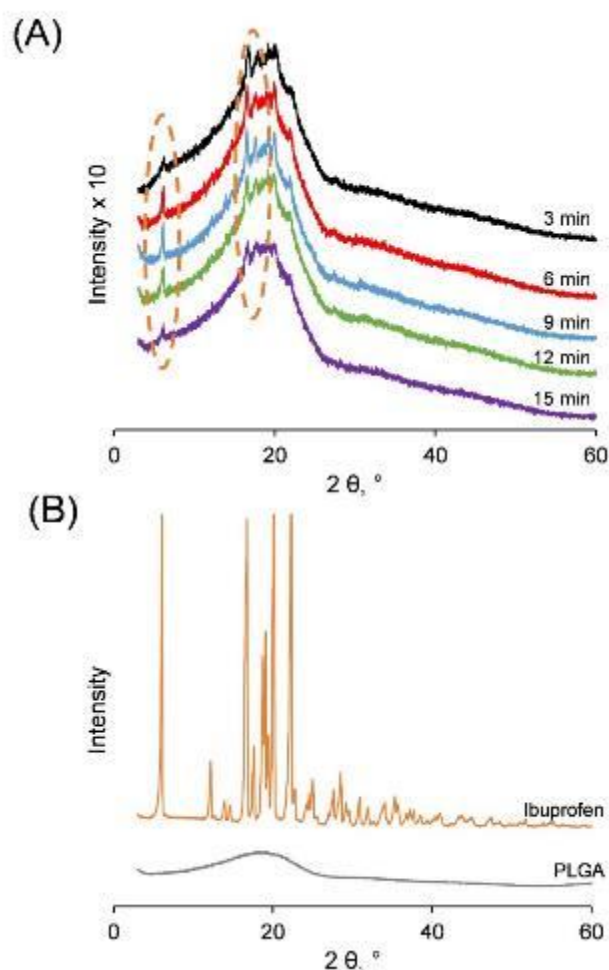


Figure III-4. X-ray diffraction patterns of the: (A) investigated ibuprofen-loaded PLGA implants, and (B) raw materials (PLGA & ibuprofen) (for reasons of comparison). During implant preparation, ibuprofen-PLGA blends were heated for 3 to 15 min (as indicated). The

III. HOT MELT EXTRUDED IBUPROFEN-LODED PLGA IMPLANTS: IMPORTANCE OF HEAT EXPOSURE

orange ovals highlight specific peaks. Please note the different scaling of the y-axes in (A) and (B).

In conclusion, based on the obtained SEM pictures of surfaces and cross sections, DSC thermograms and X-ray diffraction patterns of the implants, it can be hypothesized that major parts of the ibuprofen are *dissolved* in the PLGA matrix in the implants (are present in the form of *individual* drug molecules). And that a minor proportion is also present in the form of tiny drug crystals.

III.4.2. Implants after exposure to the release medium

The diagrams at the top of *Figure III-5* show the resulting ibuprofen release kinetics from the investigated implants upon exposure to phosphate buffer pH 7.4 in well agitated Eppendorf vials at 37 °C (the set-up is schematically shown in *Figure III-1 B*). The diagram on the right-hand side is a zoom on the first 10 d of drug release. The heating time applied during implant manufacturing is indicated in the legends. As it can be seen, tri-phasic drug release was observed in all cases: A (limited) initial rapid drug release phase (“burst release”) during the first few hours was followed by a zero-order release phase (with an about constant drug release rate), and a final, again more rapid drug release phase, leading to complete drug exhaust. The impact of the heating time (3 to 15 min) during implant preparation was only minor.

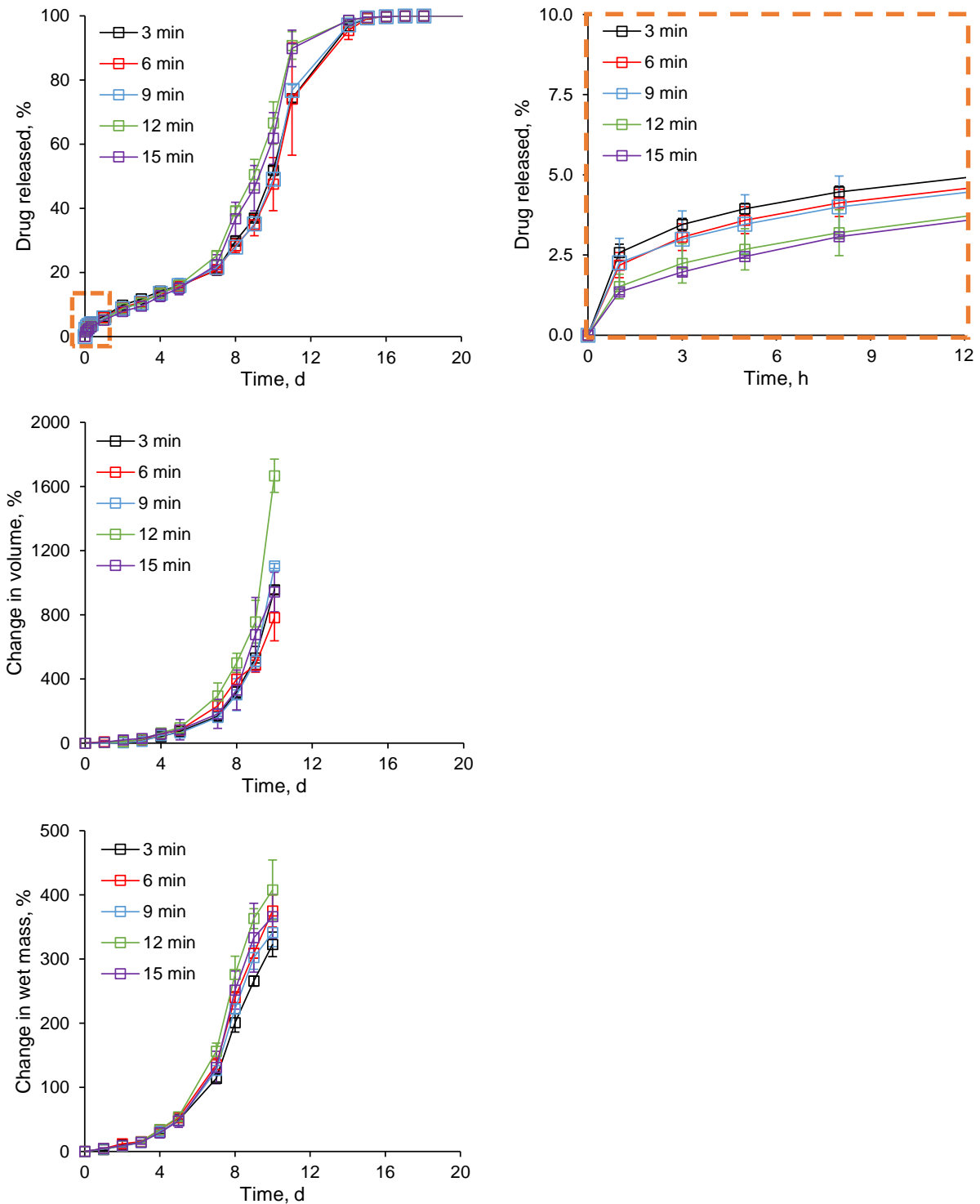


Figure III-5. *Ibuprofen release and swelling behavior of the investigated PLGA-based implants upon exposure to phosphate buffer pH 7.4. The diagram on the right-hand side at the top is a zoom on the first 10 h. The heating times of the ibuprofen-PLGA blends during implant preparation are indicated in the diagrams.*

III. HOT MELT EXTRUDED IBUPROFEN-LOADED PLGA IMPLANTS: IMPORTANCE OF HEAT EXPOSURE

The zoom on the right-hand side at the top shows that during the burst release phase the following ranking order was observed with respect to the release rate: 3 min > 6 min > 9 min > 12 min > 15 min. This can probably be explained by the fact that more drug crystals are present in the implants when prepared with shorter heating times (as discussed above). The initial burst release is likely due to drug with direct surface access once the system gets into contact with water. This includes tiny drug crystals located directly at the implants' surface, or very close to it and with access to surface pores. If such a drug crystal gets into contact with the release medium, it rapidly dissolves. In contrast, if the drug is *dissolved* in the polymer matrix, the probability that a drug molecule has direct surface access is lower (most of the molecules are separated from it, even if only by minor amounts of polymer).

The onset of the final rapid drug release phase from the investigated implants is observed after about 1 week exposure to the release medium (*Figure III-5*). This coincides with the onset of the penetration of substantial amounts of water into the systems, as illustrated in the diagrams in the middle and at the bottom of *Figure III-5*: showing the dynamic changes in the volume and wet mass of the implants upon contact with the release medium. This was true for all the investigated heating times. The optical macroscopy pictures shown in *Figure III-6* illustrate these considerable changes in implant size and morphology: During the first couple of days the system dimensions remain about constant. But after 1 week the implants substantially swell, irrespective of the heating time applied during manufacturing. The pictures on the right-hand side of *Figure III-6* were obtained with light coming from the bottom (for the other pictures the light came from the top). As it can be seen, after 10 d exposure to the release medium, some darker regions (= probably less swollen) are visible close to the center of the implants. *Figure III-7* shows SEM pictures of surfaces and cross sections of the implants prepared with 3 to 15 min heating time after 2, 6 and 8 d exposure to the release medium. Please note that the implants were freeze-dried prior to SEM analysis. Thus, the observed structures are in great part artefacts. The optical macroscopy pictures in *Figure III-6* indicate that upon contact with the aqueous bulk fluid the implant *surface* starts to swell (well before substantial swelling of the entire system sets on after about 1 week). This is consistent with the highly wizened and porous surface structure observed by SEM with all implants (*Figure III-7*): Upon drying during sample preparation, the highly swollen, thin surface layer of "PLGA gel" shrinks.

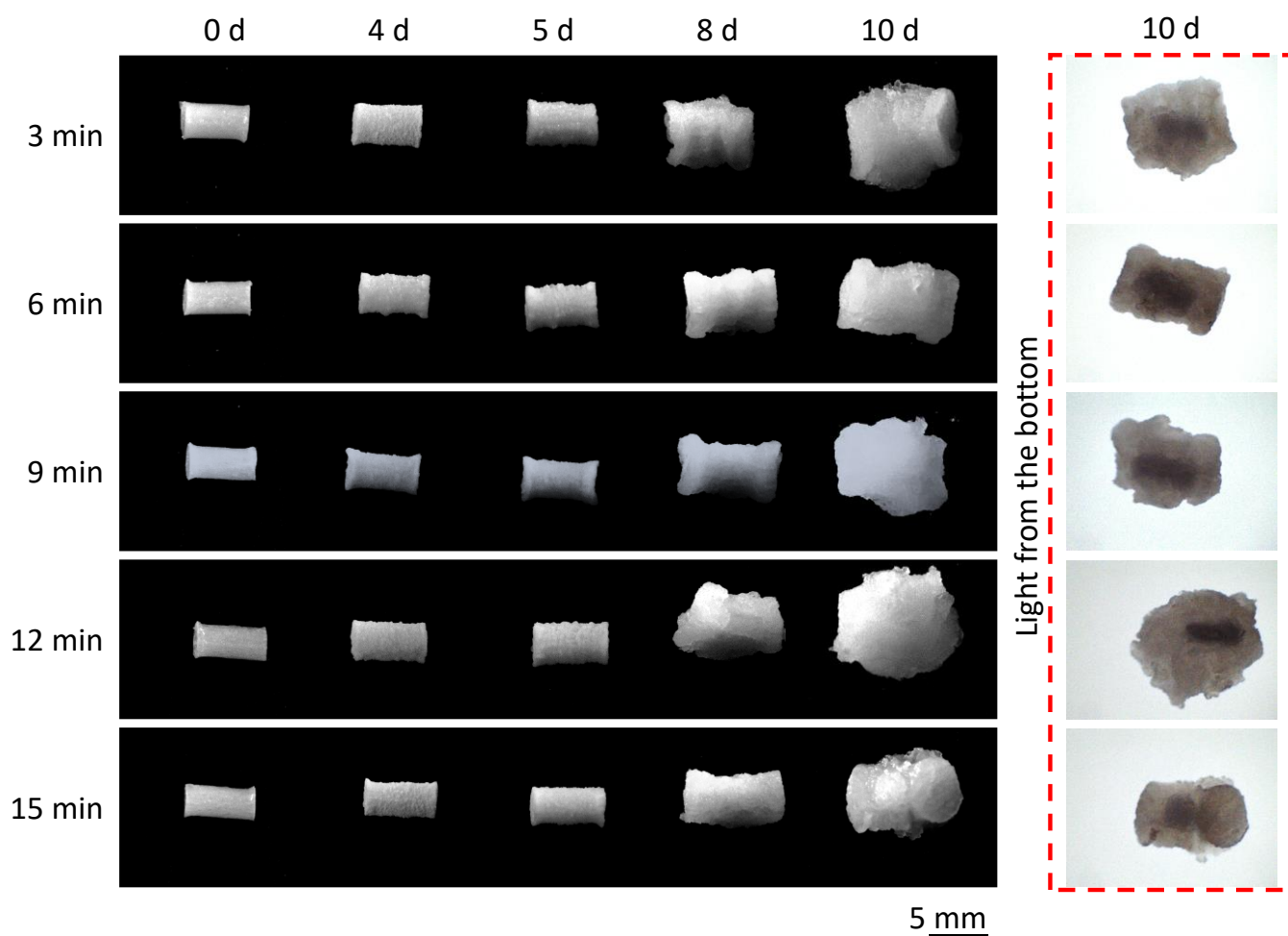


Figure III-6. Optical macroscopy pictures of the investigated ibuprofen-loaded PLGA implants upon exposure to phosphate buffer pH 7.4. At the top, the time periods of implant exposure to the release medium are shown. On the left-hand side, the heating times of the ibuprofen-PLGA blends during implant preparation are indicated. The pictures on the right-hand side were obtained with light coming from the bottom.

The SEM pictures on the right-hand side of *Figure III-7* show cross sections of the different implants after exposure to the release medium. The dotted red rectangles highlight zones in which swollen and “non-swollen” PLGA can be distinguished. With time the swollen zone becomes more and more important. However, it has to be pointed out that PLGA undergoes “*bulk erosion*”: The *entire* system is rather rapidly wetted upon exposure to an aqueous medium and polymer chain degradation takes place *throughout* the system (not only in highly swollen, surface-near zones). The average polymer molecular weight exponentially decreases right from the beginning, as shown in *Figure III-8 A*. This renders the polymeric system more and more hydrophilic: Upon hydrolytic cleavage of an ester bond, two new *hydrophilic* end groups are

III. HOT MELT EXTRUDED IBUPROFEN-LODED PLGA IMPLANTS: IMPORTANCE OF HEAT EXPOSURE

created: an -OH and a -COOH end group. In addition, the degree of polymer chain entanglement decreases (since the chains become shorter). Furthermore, generated water-soluble degradation products (short chain acids) accumulate, because they are poorly mobile in the wetted, but “non-swollen” polymer matrix. This generates a continuously increasing osmotic pressure in the system. At a certain time point, the PLGA matrix becomes sufficiently hydrophilic and mechanically instable and to allow for the penetration of substantial amounts of water into the system. Importantly, the conditions for the release of drug and water-soluble short chain acids, thus, fundamentally change: They become much more mobile in the highly swollen PLGA gel and can rather rapidly diffuse out: This leads to the onset of the final, again more rapid drug release phase (*Figure III-5*). The limited mobility in the wetted, but “non-swollen” PLGA matrix during the first week also explains why implant erosion does not set on before: As it can be seen in *Figure III-8 B*, the dry mass of the systems remains about constant, irrespective of the applied heating time.

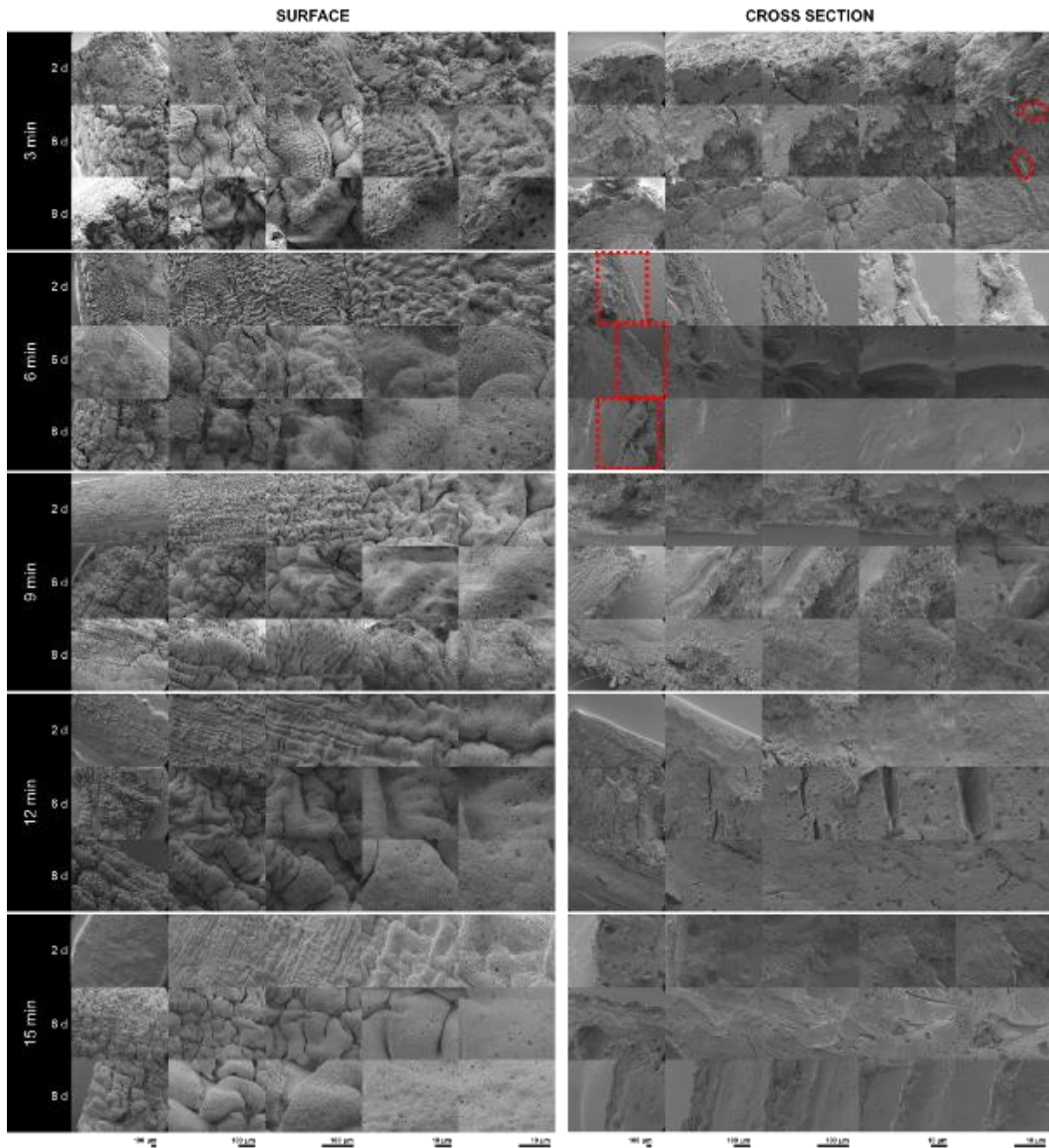


Figure III-7. SEM pictures (surfaces and cross sections) of the investigated ibuprofen-loaded PLGA implants after 2, 6 and 8 days exposure to phosphate buffer pH 7.4. The heating times (in min) of the ibuprofen-PLGA blends during implant preparation are indicated on the left-hand side. The dotted red circles highlight drug crystals, the dotted red rectangles surface-near regions including a highly swollen surface layer and the “not yet swollen” inner implant region.

III. HOT MELT EXTRUDED IBUPROFEN-LOADED PLGA IMPLANTS: IMPORTANCE OF HEAT EXPOSURE

Since the increase in heating time from 3 to 15 min during implant preparation does not impact the rate at which the limited amounts of water penetrate into the implants right upon contact with an aqueous medium, the subsequent polymer degradation is also not affected to a noteworthy extent (**Figure III-8 A**). Consequently, neither the onset of substantial polymer swelling (*Figure III-6* and *Figure III-7*), nor the onset of the final, rapid drug release phase (*Figure III-5*) are altered.

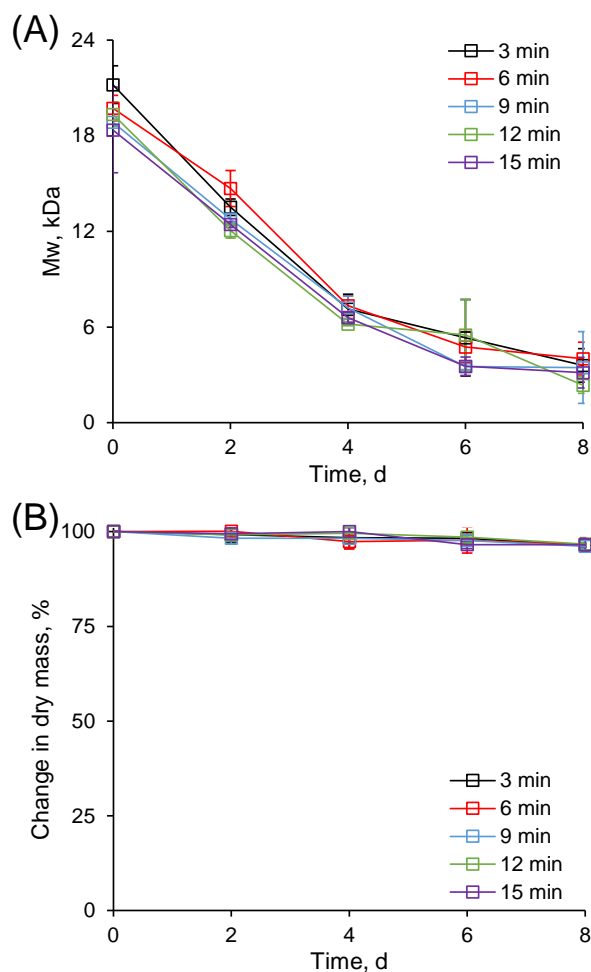


Figure III-8. Dynamic changes in the: (A) average polymer molecular weight (M_w) of the PLGA, and (B) dry mass of the investigated ibuprofen-loaded implants upon exposure of the systems to phosphate buffer pH 7.4. The heating times of the ibuprofen-PLGA blends during implant preparation are indicated in the diagrams.

III.5. Conclusions

Hot melt extrusion offers an interesting potential for the preparation of PLGA-based implants. However, the exposure to heat can decrease the average polymer molecular weight and alter the physical state of the drug in the polymeric matrix (and of course, thermally degrade heat sensitive drugs). The drug might be present in the form of individual molecules/ions distributed throughout the PLGA network (“dissolved”), or dispersed in the form of crystalline or amorphous tiny particles. It is worth to monitor the state of the drug and potential transformations during implant manufacturing. For instance, increasing exposure times to heat might increase the relative amount of drug, which is dissolved in the PLGA, altering the importance of the initial “burst release”. In the present study this phenomenon could be monitored, but its importance on drug release was limited. However, the impact for other drugs or other polymers might be much more pronounced and certain systems might be much less robust and “forgiving”.

III.6. Acknowledgments

This project has received funding from the Interreg 2 Seas programme 2014-2020 co-funded by the European Regional Development Fund under subsidy contract No 2S04-014 3DMed. The authors are very grateful for this support. They would also like to thank Mr. A. Fadel from the “Centre Commun de Microscopie” of the University of Lille (“Plateau technique de la Federation Chevreul CNRS FR 2638”) for his valuable technical help with the SEM pictures.

III.7. Author statement

C. Bassand Investigation; Methodology; Validation; Conceptualization; Writing - Original Draft; Visualization

L. Benabed Investigation

J. Verin Investigation; Methodology; Validation

F. Danede Investigation; Methodology; Validation

L.A. Lefol Investigation

J.F. Willart Methodology; Validation; Conceptualization; Writing - Review & Editing

F. Siepmann Conceptualization; Methodology; Supervision; Resources; Writing - Review & Editing; Visualization; Project administration; Funding acquisition

III. HOT MELT EXTRUDED IBUPROFEN-LODED PLGA IMPLANTS: IMPORTANCE OF HEAT EXPOSURE

J. Siepmann Conceptualization; Methodology; Supervision; Resources; Writing - Review & Editing; Visualization; Project administration; Funding acquisition

III.8. References

1. Brodbeck KJ, Pushpala S, McHugh AJ. Sustained Release of Human Growth Hormone from PLGA Solution Depots. *Pharm Res.* 1999 Dec 1;16(12):1825–9.
2. Dorta MJ, Santoveña A, Llabrés M, Fariña JB. Potential applications of PLGA film-implants in modulating in vitro drugs release. *Int J Pharm.* 2002 Nov 6;248(1):149–56.
3. Budhian A, Siegel SJ, Winey KI. Controlling the in vitro release profiles for a system of haloperidol-loaded PLGA nanoparticles. *Int J Pharm.* 2008 Jan 4;346(1):151–9.
4. Cossé A, König C, Lamprecht A, Wagner KG. Hot Melt Extrusion for Sustained Protein Release: Matrix Erosion and In Vitro Release of PLGA-Based Implants. *AAPS PharmSciTech.* 2017 Jan 1;18(1):15–26.
5. Abbasnezhad N, Zirak N, Shirinbayan M, Tcharkhtchi A, Bakir F. On the importance of physical and mechanical properties of PLGA films during drug release. *J Drug Deliv Sci Technol.* 2021 Jun 1;63:102446.
6. Anderson J, Shives M. Biodegradation and biocompatibility of PLA and PLGA microspheres. *Adv Drug Deliv Rev.* 1997 Oct 13;28(1):5–24.
7. Schreiner V, Detampel P, Jirkof P, Puchkov M, Huwyler J. Buprenorphine loaded PLGA microparticles: Characterization of a sustained-release formulation. *J Drug Deliv Sci Technol.* 2021 Jun 1;63:102558.
8. Ochi M, Wan B, Bao Q, Burgess DJ. Influence of PLGA molecular weight distribution on leuprolide release from microspheres. *Int J Pharm.* 2021 Apr 15;599:120450.
9. Ramchandani M, Robinson D. In vitro and in vivo release of ciprofloxacin from PLGA 50:50 implants. *J Controlled Release.* 1998 Jul 31;54(2):167–75.
10. Desai KGH, Mallery SR, Schwendeman SP. Effect of formulation parameters on 2-methoxyestradiol release from injectable cylindrical poly(dl-lactide-co-glycolide) implants. *Eur J Pharm Biopharm.* 2008 Sep 1;70(1):187–98.
11. Gosau M, Müller BW. Release of gentamicin sulphate from biodegradable PLGA-implants produced by hot melt extrusion. *Pharm - Int J Pharm Sci.* 2010 Jul 1;65(7):487–92.
12. Friess W, Schlapp M. Release mechanisms from gentamicin loaded poly(lactic-co-glycolic acid) (PLGA) microparticles. *J Pharm Sci.* 2002 Mar 1;91(3):845–55.
13. Regnier-Delplace C, Thillaye du Boullay O, Siepmann F, Martin-Vaca B, Degraeve N, Demonchaux P, et al. PLGA microparticles with zero-order release of the labile anti-Parkinson drug apomorphine. *Int J Pharm.* 2013 Feb 25;443(1):68–79.
14. Fang Y, Zhang N, Li Q, Chen J, Xiong S, Pan W. Characterizing the release mechanism of donepezil-loaded PLGA microspheres in vitro and in vivo. *J Drug Deliv Sci Technol.* 2019 Jun 1;51:430–7.

III. HOT MELT EXTRUDED IBUPROFEN-LODED PLGA IMPLANTS: IMPORTANCE OF HEAT EXPOSURE

15. Ospina-Villa JD, Gómez-Hoyos C, Zuluaga-Gallego R, Triana-Chávez O. Encapsulation of proteins from *Leishmania panamensis* into PLGA particles by a single emulsion-solvent evaporation method. *J Microbiol Methods*. 2019 Jul 1;162:1–7.
16. Hamoudi-Ben Yelles MC, Tran Tan V, Danede F, Willart JF, Siepmann J. PLGA implants: How Poloxamer/PEO addition slows down or accelerates polymer degradation and drug release. *J Controlled Release*. 2017 May 10;253:19–29.
17. Takahashi M, Onishi H, Machida Y. Development of implant tablet for a week-long sustained release. *J Controlled Release*. 2004 Nov 1;100(1):63–74.
18. Guo T, Holzberg TR, Lim CG, Gao F, Gargava A, Trachtenberg JE, et al. 3D printing PLGA: a quantitative examination of the effects of polymer composition and printing parameters on print resolution. *Biofabrication*. 2017 Apr;9(2):024101.
19. Feuerbach T, Callau-Mendoza S, Thommes M. Development of filaments for fused deposition modeling 3D printing with medical grade poly(lactic-co-glycolic acid) copolymers. *Pharm Dev Technol*. 2019 Apr 21;24(4):487–93.
20. Duque L, Körber M, Bodmeier R. Improving release completeness from PLGA-based implants for the acid-labile model protein ovalbumin. *Int J Pharm*. 2018 Mar 1;538(1):139–46.
21. Ghalanbor Z, Körber M, Bodmeier R. Protein release from poly(lactide-co-glycolide) implants prepared by hot-melt extrusion: Thioester formation as a reason for incomplete release. *Int J Pharm*. 2012 Nov 15;438(1):302–6.
22. Fredenberg S, Wahlgren M, Reslow M, Axelsson A. The mechanisms of drug release in poly(lactic-co-glycolic acid)-based drug delivery systems—A review. *Int J Pharm*. 2011 Aug 30;415(1):34–52.
23. Sun Y, Wang J, Zhang X, Zhang Z, Zheng Y, Chen D, et al. Synchronic release of two hormonal contraceptives for about one month from the PLGA microspheres: in vitro and in vivo studies. *J Control Release Off J Control Release Soc*. 2008 Aug 7;129(3):192–9.
24. Shah SS, Cha Y, Pitt CG. Poly (glycolic acid-co-dl-lactic acid): diffusion or degradation controlled drug delivery? *J Controlled Release*. 1992 Jan 1;18(3):261–70.
25. Hirota K, Doty AC, Ackermann R, Zhou J, Olsen KF, Feng MR, et al. Characterizing release mechanisms of leuprolide acetate-loaded PLGA microspheres for IVIVC development I: In vitro evaluation. *J Controlled Release*. 2016 Dec 28;244:302–13.
26. Blasi P, D'Souza SS, Selmin F, DeLuca PP. Plasticizing effect of water on poly(lactide-co-glycolide). *J Controlled Release*. 2005 Nov 2;108(1):1–9.
27. Göpferich A. Mechanisms of polymer degradation and erosion. *Biomaterials*. 1996 Jan 1;17(2):103–14.
28. Ding AG, Schwendeman SP. Determination of water-soluble acid distribution in poly(lactide-co-glycolide). *J Pharm Sci*. 2004 Feb 1;93(2):322–31.

29. Liu Y, Ghassemi AH, Hennink WE, Schwendeman SP. The microclimate pH in poly(D,L-lactide-co-hydroxymethyl glycolide) microspheres during biodegradation. *Biomaterials*. 2012 Oct 1;33(30):7584–93.
30. Antheunis H, van der Meer J-C, de Geus M, Heise A, Koning CE. Autocatalytic Equation Describing the Change in Molecular Weight during Hydrolytic Degradation of Aliphatic Polyesters. *Biomacromolecules*. 2010 Apr 12;11(4):1118–24.
31. Schädlich A, Kempe S, Mäder K. Non-invasive in vivo characterization of microclimate pH inside in situ forming PLGA implants using multispectral fluorescence imaging. *J Controlled Release*. 2014 Apr 10;179:52–62.
32. Gasmi H, Willart J-F, Danede F, Hamoudi MC, Siepmann J, Siepmann F. Importance of PLGA microparticle swelling for the control of prilocaine release. *J Drug Deliv Sci Technol*. 2015 Dec 1;30:123–32.
33. Tamani F, Bassand C, Hamoudi MC, Danede F, Willart JF, Siepmann F, et al. Mechanistic explanation of the (up to) 3 release phases of PLGA microparticles: Diprophylline dispersions. *Int J Pharm*. 2019 Dec 15;572:118819.
34. Bode C, Kranz H, Fizez A, Siepmann F, Siepmann J. Often neglected: PLGA/PLA swelling orchestrates drug release: HME implants. *J Controlled Release*. 2019 Jul 28;306:97–107.
35. Kožák J, Rabišková M, Lamprecht A. In-vitro drug release testing of parenteral formulations via an agarose gel envelope to closer mimic tissue firmness. *Int J Pharm*. 2021 Feb 1;594:120142.
36. Kim HK, Chung HJ, Park TG. Biodegradable polymeric microspheres with ‘open/closed’ pores for sustained release of human growth hormone. *J Control Release Off J Control Release Soc*. 2006 May 15;112(2):167–74.
37. Kang J, Schwendeman SP. Pore closing and opening in biodegradable polymers and their effect on the controlled release of proteins. *Mol Pharm*. 2007 Feb;4(1):104–18.
38. Huang J, Mazzara JM, Schwendeman SP, Thouless MD. Self-healing of pores in PLGAs. *J Controlled Release*. 2015 May 28;206:20–9.
39. Wang T, Xue P, Wang A, Yin M, Han J, Tang S, et al. Pore change during degradation of octreotide acetate-loaded PLGA microspheres: The effect of polymer blends. *Eur J Pharm Sci*. 2019 Oct 1;138:104990.
40. Blasi P, Schoubben A, Giovagnoli S, Perioli L, Ricci M, Rossi C. Ketoprofen poly(lactide-co-glycolide) physical interaction. *AAPS PharmSciTech*. 2007 Jun;8(2):E78–85.
41. Jonnalagadda S, Robinson DH. A bioresorbable, polylactide reservoir for diffusional and osmotically controlled drug delivery. *AAPS PharmSciTech*. 2000 Dec 1;1(4):26–34.
42. Siegel SJ, Kahn JB, Metzger K, Winey KI, Werner K, Dan N. Effect of drug type on the degradation rate of PLGA matrices. *Eur J Pharm Biopharm*. 2006 Nov 1;64(3):287–93.

III. HOT MELT EXTRUDED IBUPROFEN-LODED PLGA IMPLANTS: IMPORTANCE OF HEAT EXPOSURE

43. Kohno M, Andhariya JV, Wan B, Bao Q, Rothstein S, Hezel M, et al. The effect of PLGA molecular weight differences on risperidone release from microspheres. *Int J Pharm.* 2020 May 30;582:119339.
44. Meeus J, Scurr DJ, Appeltans B, Amssoms K, Annaert P, Davies MC, et al. Influence of formulation composition and process on the characteristics and in vitro release from PLGA-based sustained release injectables. *Eur J Pharm Biopharm.* 2015 Feb 1;90:22–9.
45. Andhariya JV, Shen J, Wang Y, Choi S, Burgess DJ. Effect of minor manufacturing changes on stability of compositionally equivalent PLGA microspheres. *Int J Pharm.* 2019 Jul 20;566:532–40.
46. Zlomke C, Barth M, Mäder K. Polymer degradation induced drug precipitation in PLGA implants – Why less is sometimes more. *Eur J Pharm Biopharm.* 2019 Jun 1;139:142–52.
47. Nieto K, Mallery SR, Schwendeman SP. Microencapsulation of amorphous solid dispersions of fenretinide enhances drug solubility and release from PLGA in vitro and in vivo. *Int J Pharm.* 2020 Aug 30;586:119475.
48. Siepmann J, Siepmann F. Modeling of diffusion controlled drug delivery. *J Controlled Release.* 2012 Jul 20;161(2):351–62.
49. Siepmann J, Elkharraz K, Siepmann F, Klose D. How autocatalysis accelerates drug release from PLGA-based microparticles: a quantitative treatment. *Biomacromolecules.* 2005 Aug;6(4):2312–9.
50. Klose D, Siepmann F, Elkharraz K, Krenzlin S, Siepmann J. How porosity and size affect the drug release mechanisms from PLGA-based microparticles. *Int J Pharm.* 2006 May 18;314(2):198–206.
51. Houchin ML, Topp EM. Physical properties of PLGA films during polymer degradation. *J Appl Polym Sci.* 2009;114(5):2848–54.

**IV. PLGA IMPLANTS FOR CONTROLLED
DRUG RELEASE: IMPACT OF THE
DIAMETER**

IV. PLGA IMPLANTS FOR CONTROLLED DRUG RELEASE: IMPACT OF THE DIAMETER

Research article – To be submitted European Journal of Pharmaceutics and Biopharmaceutics

PLGA implants for controlled drug release: Impact of the diameter

C. Bassand, J. Freitag, L. Benabed, J. Verin, F. Siepman, J. Siepman

Univ. Lille, Inserm, CHU Lille, U1008, F-59000 Lille, France

IV.1. Abstract

The aim of this study was to better understand the importance of the diameter of poly(lactic-co-glycolic acid) (PLGA)-based implants on system performance, in particular the control drug release. Different types of ibuprofen-loaded implants were prepared by hot melt extrusion using a Leistritz Nano 16 twin-screw extruder. Drug release was measured in well agitated phosphate buffer pH 7.4 bulk fluid and in agarose gels in Eppendorf tubes and transwell plates. Dynamic changes in the implants' dry & wet mass, volume, polymer molecular weight, inner & outer morphology were monitored using optical macroscopy, gravimetric analysis and scanning electron microscopy. The physical states of the drug and polymer were determined by DSC and pH changes in the release medium investigated. Irrespective of the type of experimental set-up, the resulting absolute and relative drug release rates decreased with increasing implant diameter (0.7 to 2.8 mm). Bi-phasic drug release was observed in all cases from the monolithic solutions (the ibuprofen being completely dissolved in the polymer matrices): A zero order release phase was followed by a final, rapid drug release phase (accounting for 80-90 % drug). The decrease in the relative drug release rate with increasing system diameter can be explained by the increase in the diffusion pathway lengths to be overcome. Furthermore, the observed delay in the onset of the final rapid drug release phase with increasing implant diameter could be explained by the higher mechanical stability of the devices, delaying the onset of substantial entire system swelling after a lag phase of about 5 to 10 d. Interestingly, no signs for the occurrence of important autocatalytic effects were observed in this study, despite the considerable system dimensions.

Keywords: PLGA implant; ibuprofen; swelling; drug release mechanism; monolithic solution

IV.2. Introduction

Poly(lactic-co-glycolic acid) (PLGA) is frequently used as polymeric matrix former to control drug release from implants and microparticles (1–3). Several PLGA-based, injectable/implantable drug products are available on the market since decades. The reason for the success of this polymer include: (i) its good biocompatibility " (4–6), (ii) complete biodegradability into lactic acid and glycolic acid, and (iii) the possibility to provide desired drug release rates during flexible time periods, ranging from a few hours to several months (7,8).

Different manufacturing techniques can be used to prepare PLGA-based dosage forms, for example: emulsification – solvent evaporation methods (9,10), compression (11), 3D printing (12) and hot melt extrusion (13–15). The type of manufacturing method and selected process parameters can significantly affect the resulting inner and outer structure of the dosage forms and, hence, the resulting drug release kinetics (16,17). Also, the composition of the devices can have a crucial effect, such as the drug loading, type of drug (e.g., its hydrophilicity) (18), type of PLGA (e.g., average polymer molecular weight, type of end groups) (19,20), and potential addition of further excipients (2,21,22). In this study, hot melt extrusion was chosen, since this technique offers an interesting potential for the preparation of homogeneous drug-polymer blends (14,22,23). However, care must be taken not to thermally degrade the polymer, nor the drug.

The mass transport mechanisms controlling drug release from a PLGA-based dosage form can be complex (24,25). Upon contact with aqueous media (e.g. living tissue or phosphate buffer in vitro), water penetrates into the dosage form. This process is generally relatively rapid, assuring that the entire device is wetted and hydrolytic polymer chain cleavage occurs throughout the system ("bulk erosion") (26,27). However, initially, the PLGA is rather hydrophobic and the amounts of water inside the system are limited. Importantly, once an ester bond is hydrolyzed, a new -OH and a new -COOH end group is generated. Consequently, the polymeric matrix becomes more and more hydrophilic with time. In addition, the degree of polymer chain entanglement decreases and the matrix becomes mechanically less stable. Furthermore, the water-soluble degradation products create a steadily increasing osmotic pressure in the system. This can result in substantial system swelling (28–31). The presence of pores as well as pore closure (32–34), drug dissolution and diffusion (24,35), the creation of local acidic microenvironments and subsequent autocatalytic effects (36,37), as well as drug – polymer and water – polymer interactions (38–40) can also play a major role. The relative importance of

these phenomena might strongly depend on the type of system, e.g. geometry, size, composition and manufacturing method. Often, it is not fully understood which are the dominant mass transport steps, resulting in sometimes surprising effects of formulation and processing parameters. Hence, the optimization of this type of advanced drug delivery systems might be highly cumbersome, requiring cost-intensive and time-consuming series of trial-and-error experiments.

One of the key properties of a controlled drug delivery system, which can often relatively easily be varied and which might offer the possibility to adjust desired drug release profiles is the system size (41–44): This is for example the case, if diffusion plays an important role: Varying the system size means varying the length of the diffusion pathways and, thus, the resulting release rate. However, in the case of initially non-porous PLGA-based microparticles loaded with small amounts of lidocaine, an increase in system size by a factor of 7 did hardly alter drug release (45). This could be explained by the increasing importance of autocatalytic effects inside the microparticles: Not only the diffusion pathways for the drug, but also for the generated short chain acids increases with increasing system size. In this case, this led to more pronounced drops in the micro pH inside the microparticles and, thus, accelerated polymer degradation (hydrolytic ester bond cleavage being catalyzed by protons) and increased drug mobility: Larger microparticle became much more porous inside than smaller microparticles. In contrast, these effects were much less pronounced in microparticles based on the same polymer and drug, but being highly porous from the beginning (46). In these cases, acids and bases were more mobile and pH drops less pronounced.

The aim of this study was to better understand the importance of the diameter of PLGA-based implants prepared by hot melt extrusion on ibuprofen release. Differently sized implants were exposed to phosphate buffer pH 7.4 in 3 experimental set-ups: in well agitated bulk fluid, in agarose gels exposed to phosphate buffer in Eppendorf tubes and in agarose gels exposed to phosphate buffer in transwell plates. The gels were intended to mimic living tissue more realistically than bulk fluids. Optical microscopy, gravimetric analysis, DSC, GPC, scanning electron microscopy, and pH measurements were used to monitor the implants' key properties before and after exposure to the release medium.

IV.3. Materials and methods

IV.3.1. Materials

Poly (D,L lactic-co-glycolic acid) (PLGA, 50:50 lactic acid: glycolic acid; Resomer RG 503H; Evonik, Darmstadt, Germany); ibuprofen (BASF, Ludwigshafen, Germany); agarose (genetic analysis grade) and tetrahydrofuran (HPLC grade) (Fisher Scientific, Illkirch, France); potassium dihydrogen orthophosphate and sodium hydroxide (Acros Organics, Geel, Belgium); acetonitrile (VWR, Fontenay-sous-Bois, France); sodium hydrogen phosphate (Na_2HPO_4 ; Panreac Quimica, Barcelona, Spain).

IV.3.2. Implant preparation

PLGA was milled for 4 x 30 s in a grinder (Valentin, Seb, Ecully, France). Appropriate amounts of polymer and drug powders were blended for 5 min with a mortar and a pestle, followed by extrusion using a Nano 16 twin-screw extruder (screw diameter = 16 mm, die diameter = 0.5, 1, 2 or 3 mm, length/diameter ratio = 26.25, gravitational feeder) (Leistritz, Nuremberg, Germany). The process temperatures were kept constant at 80 - 75 - 70 - 65 °C (die - zone 3 - zone 2 - zone 1). The screw speed was set at 50 rpm, the screw configuration is illustrated in Figure S1. After cooling, the hot melt extrudates were manually cut into cylinders of 5 mm length.

IV.3.3. Optical macroscopy

Pictures of implants before exposure to the release medium were taken using a SZN-6 trinocular stereo zoom microscope (Optika, Ponteranica, Italy), equipped with an optical camera (Optika Vision Lite 2.1 software). The lengths and diameters of the implants were determined using the ImageJ software (US National Institutes of Health, Bethesda, Maryland, USA).

IV.3.4. Practical drug loading

Implants were dissolved in 5 mL acetonitrile, followed filtration (PVDF syringe filters, 0.45 μm ; Agilent Technologies, Santa Clara, USA) and drug content determination by HPLC-UV analysis using a Thermo Fisher Scientific Ultimate 3000 Series HPLC, equipped with a LPG 3400 SD/RS pump, an auto sampler (WPS-3000 SL) and a UV-Vis detector (VWD-3400RS) (Thermo Fisher Scientific, Waltham, USA). A reversed phase column C18 (Gemini 5 μm ; 110 Å; 150 x 4.6 mm; Phenomenex, Le Pecq, France) was used. The mobile phase was a mixture of 30 mM Na_2HPO_4 pH 7.0: acetonitrile (60:40, v:v). The detection wavelength was 225 nm, and the flow rate 0.5 mL/min. Ten microliter samples were injected.

IV.3.5. Differential scanning calorimetry (DSC)

DSC thermograms of the raw materials (PLGA and ibuprofen) and implants were recorded using a DCS1 Star System (Mettler Toledo, Greifensee, Switzerland). Approximately 5 mg raw material samples and around 10 mg implant samples were heated in perforated aluminum pans as follows: from -70 to 120 °C, cooling to -70 °C, re-heating to 120 °C (heating/cooling rate = 10 °C/min). The reported glass temperatures (T_gs) were determined from the 1st heating cycles in the case of implants (the thermal history being of interest), and from the 2nd heating cycle in the case of the raw material (the thermal history not being of interest). All experiments were conducted in triplicate. Mean values +/- standard deviations are reported.

IV.3.6. In vitro drug release

Three experimental set-ups were used to measure ibuprofen release from the PLGA implants:

IV.3.6.1. In well agitated bulk fluids

Implants were placed in 5 mL Eppendorf tubes (1 implant per tube), filled with 5 mL phosphate buffer pH 7.4 USP 42 (*Figure IV-1 A*). Metal baskets avoided that the implants sank to the bottom of the tubes (resulting in potentially limited contact with the bulk fluid). The mesh size (250 µm) was sufficient to allow for convective flow and rapid medium exchange “inside – outside” the basket. The tubes were placed in a horizontal shaker (80 rpm, 37°C; GFL 3033; Gesellschaft fuer Labortechnik, Burgwedel, Germany). At predetermined time points, the entire bulk fluid was replaced by fresh release medium. The withdrawn samples were filtered (PVDF syringe filter, 0.45 µm; Agilent, Santa Clara, California, USA) and analyzed for their ibuprofen contents by HPLC-UV, as described in *section IV.3.4*.

IV.3.6.2. In agarose gels in Eppendorf tubes

Implants were embedded into agarose gels in 5 mL Eppendorf tubes, as illustrated in *Figure IV-1 B* (1 implant per tube). An agarose dispersion (0.5% w:v) in phosphate buffer pH 7.4 (USP 42) was heated to 100 °C under magnetic stirring (250 rpm) until a clear solution was obtained. The latter was cooled to 47°C and continuously stirred (to prevent gelation). 0.5 mL of the solution was placed into the bottom of an Eppendorf tube and cooled in a refrigerator for 5 min to allow for gelation. An implant was carefully placed on top of the gel, and covered with second layer of 0.5 mL agarose solution (47 °C), followed by cooling in a refrigerator for 5 min. Four mL phosphate buffer pH 7.4 USP 42 were added on top of the gel, and the tubes were placed in a horizontal shaker (80 rpm, 37°C; GFL 3033). At predetermined time points, the

IV. PLGA IMPLANTS FOR CONTROLLED DRUG RELEASE: IMPACT OF THE DIAMETER

entire bulk fluid was replaced by fresh release medium. The withdrawn samples were treated as for the drug release measurements in well agitated bulk fluids.

IV.3.6.3. In agarose gels in transwell plates

Implants were embedded in agarose gels in transwell plates (1 implant per insert, membranes: 1.13 cm², 11 μm, 0.4 μm pore size; Nunc, Roskilde, Denmark), as illustrated in *Figure IV-1 C*. The agarose gels were prepared as described above, and the implants included accordingly (placed between 2 “layers” of 0.5 mL gel). The well plates were filled with 4 mL phosphate buffer pH 7.4, covered with lids and Parafilm to minimize evaporation, and placed in a horizontal shaker (80 rpm, 37°C; GFL 3033). At predetermined time points, the entire bulk fluid was replaced by fresh (pre-heated) release medium. The withdrawn samples were treated as for the drug release measurements in well agitated bulk fluids.

In all cases, sink conditions were provided throughout the experiments in the well-agitated bulk fluids. Furthermore, the pH of the bulk fluids was measured at pre-determined time points using a pH meter (InoLab pH Level 1; WTW, Weilheim, Germany). All experiments were conducted in triplicate. Mean values +/- standard deviations are reported.

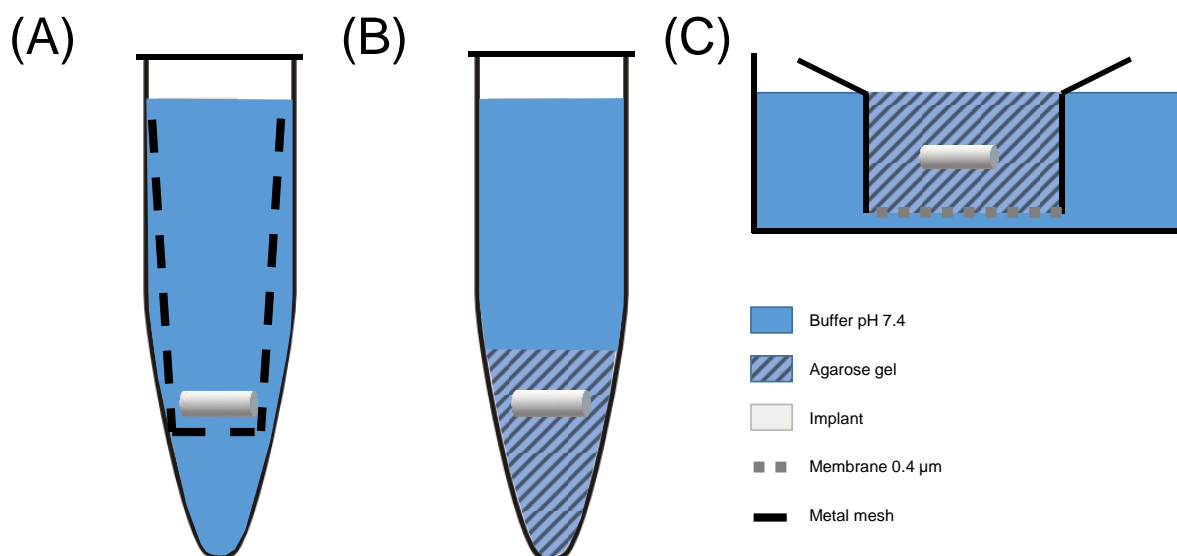


Figure IV-1. Schematic presentations of the experimental set-ups used to monitor drug release from the PLGA-based implants: (A) In well-agitated release medium in Eppendorf tubes (with metal baskets), (B) In agarose gels in Eppendorf tubes, the gels being exposed to well-agitated release medium, (C) In agarose gels in transwell plates, the receptor compartment containing well-agitated release medium. In all cases, sink conditions were provided throughout the experiments in the well-agitated bulk fluids. Details are described in the text.

IV.3.7. Implant swelling

Implants were treated as for the in vitro drug release studies described above. At pre-determined time points:

- (i) Pictures of the implants were taken with a SZN-6 trinocular stereo zoom microscope (Optika), equipped with an optical camera (Optika Vision Lite 2.1 software). The lengths and diameters of the implants were determined using the ImageJ software (US National Institutes of Health). Dynamic changes in the systems' volume were calculated considering cylindrical geometry.
- (ii) Implant samples were withdrawn and excess water was carefully removed using Kimtech precision wipes (Kimberly-Clark, Rouen, France) and weighed [*wet mass (t)*]. The *change in wet mass (%) (t)* was calculated as follows:

$$\text{change in wet mass } (\%)(t) = \frac{\text{wet mass } (t) - \text{mass } (t = 0)}{\text{mass } (t = 0)} \times 100 \%$$

where *mass (t = 0)* denotes the implant mass before exposure to the release medium.

All experiments were conducted in triplicate. Mean values +/- standard deviations are reported.

IV.3.8. Implant erosion and PLGA degradation

Implants were treated as for the in vitro drug release studies described above. At pre-determined time points, implant samples were withdrawn and freeze-dried (freezing at -45°C for 2 h 35 min, primary drying at -20 °C/0.940 mbar for 35 h 10 min and secondary drying at +20 °C/0.0050 mbar for 35 h; Christ Alpha 2-4 LSC+; Martin Christ, Osterode, Germany).

The *dry mass (%) (t)* was calculated as follows:

$$\text{dry mass } (\%)(t) = \frac{\text{dry mass } (t)}{\text{mass } (t = 0)} \times 100 \%$$

where *mass (t = 0)* denotes the implant's mass before exposure to the release medium. All experiments were conducted in triplicate. Mean values +/- standard deviations are reported.

The average polymer molecular weight (Mw) of the PLGA was determined by gel permeation chromatography (GPC) as follows: Freeze-dried implant samples were dissolved in tetrahydrofuran (at a concentration of 3 mg/mL). One hundred μL samples were injected into an Alliance GPC (refractometer detector: 2414 RI, separation module e2695, Empower GPC

IV. PLGA IMPLANTS FOR CONTROLLED DRUG RELEASE: IMPACT OF THE DIAMETER

software; Waters, Milford, USA), equipped with a PLgel 5 μm MIXED-D column (kept at 35°C, 7.8 \times 300 mm; Agilent). Tetrahydrofuran was the mobile phase (flow rate: 1 mL/min). Polystyrene standards with molecular weights between 1,480 and 70,950 Da (Polymer Laboratories, Varian, Les Ulis, France) were used to prepare the calibration curve. All experiments were conducted in triplicate. Mean values +/- standard deviations are reported.

IV.3.9. Scanning electronic microscopy (SEM)

The internal and external morphology of the implants before and after exposure to the release medium was studied using a JEOL Field Emission Scanning Electron Microscope (JSM-7800F, Japan), equipped with the Aztec 3.3 software (Oxford Instruments, Oxfordshire, England). Samples were fixed with a ribbon carbon double-sided adhesive and covered with a fine chrome layer. In the case of implants which had been exposed to the release medium, the systems were treated as for the in vitro release studies described in *section IV.3.6*. At predetermined time points, implant samples were withdrawn, optionally cut (for cross sections) using a scalpel and freeze-dried (as described in *section IV.3.8*).

IV.4. Results and discussion

The aim of this study was to better understand the importance of the diameter of PLGA implants on system performance upon exposure to phosphate buffer pH 7.4 using different experimental set-ups, in particular in the light of the resulting drug release kinetics. Cylindrical ibuprofen-loaded implants were prepared by hot melt extrusion using a Leistritz Nano 16 twin-screw extruder, equipped with differently sized dies.

IV.4.1. Implants before exposure to the release medium

Figure IV-2 shows optical macroscopy pictures of the implants prepared with dies with a diameter of 0.5, 1, 2 or 3 mm (as indicated). As it can be seen, they have a homogeneous appearance and smooth surface. The diameters of the implants are indicated in Table 1, ranging from 0.7 to 2.8 mm. The practical drug loading was about 12 % and rather homogeneous in all samples. The polymer molecular weight was about 24-26 kDa, which is slightly higher compared to implants of similar composition prepared by hot melt extrusion using a syringe and heating to 105 °C for 3 to 15 min (47). This difference can probably be explained by the lower temperatures applied in this study during processing (80 - 75 - 70 - 65 °C: die - zone 3 - zone 2 - zone 1). PLGA is partially cut into shorter chains at elevated temperatures. This also explains the slightly higher glass transition temperatures of the implants prepared in this study (around 35-37 °C) compared to the implants of similar composition prepared at via a heat treatment at 105 °C for 3 to 15 min in a syringe (about 33-34 °C) (47).

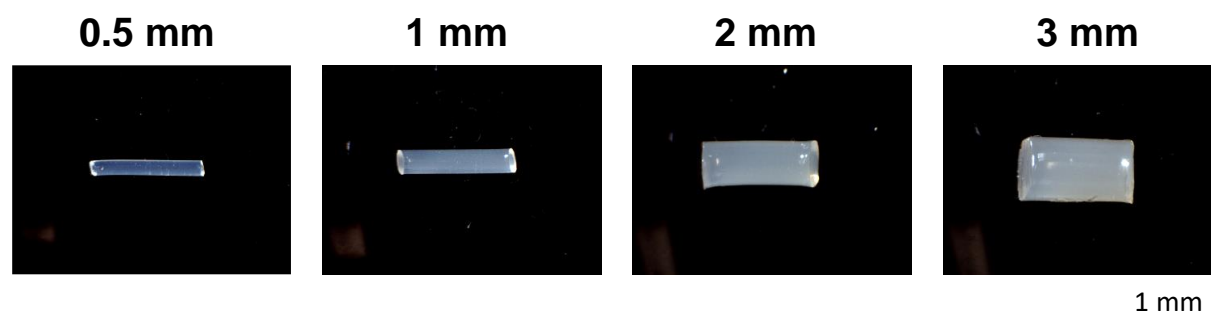


Figure IV-2. Optical macroscopy pictures of implants before exposure to release medium. The diameter of the die used for hot melt extrusion is indicated at the top.

Importantly, there were no signs of the presence of *crystalline* drug in the implants prepared using the Nano 16 twin-screw extruder: neither in the DSC thermograms (Figure IV-3), nor in the SEM pictures of surfaces and cross sections (Figure IV-4). This is in contrast to implants of similar composition prepared at 105 °C in a syringe, which contained also some crystalline

IV. PLGA IMPLANTS FOR CONTROLLED DRUG RELEASE: IMPACT OF THE DIAMETER

ibuprofen (in addition to *dissolved* drug) (47). The much more effective mixing of the drug-polymer blend in the Nano 16 twin-screw extruder during processing (compared to the heated syringe) can likely explain this difference: Convective flow and shear forces facilitate drug dissolution into the PLGA matrix. *Figure IV-3A* shows the DSC thermograms of the investigated implants, differing in their diameter. For reasons of comparison, also the thermograms of the PLGA and ibuprofen raw materials were recorded (*Figure IV-3A and B*). Clearly, the PLGA was amorphous, while the ibuprofen raw material showed a sharp melting peak at 79.7 ± 0.5 °C. Importantly, no sign for ibuprofen melting was visible in any implant, only one single glass transition temperature (T_g) could be detected in the investigated temperature range: at about 35-37 °C. The T_g of the PLGA raw material was about 47.0 °C. Thus, ibuprofen acts as a plasticizer for this polymer.

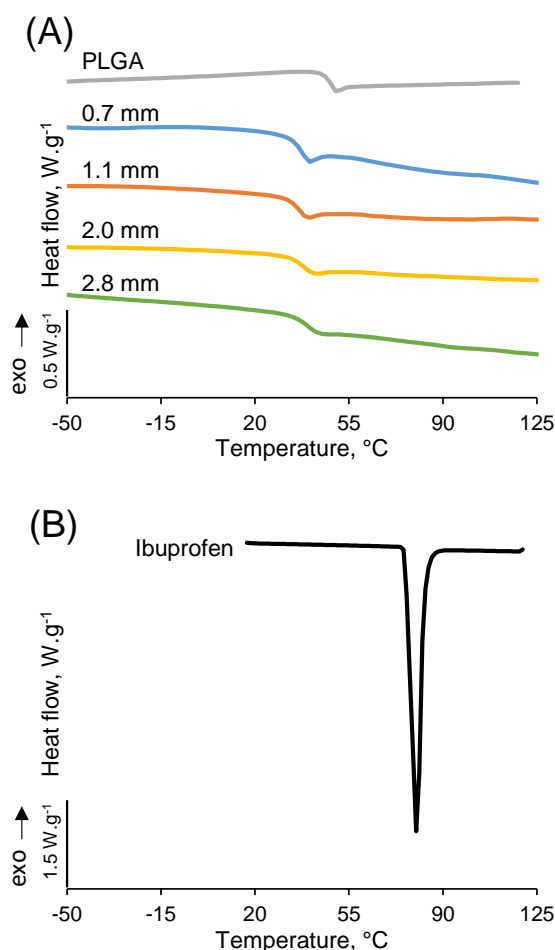


Figure IV-3. DSC thermograms of: (A) PLGA raw material and the investigated ibuprofen-loaded implants (the diameter of the implants are indicated on the left hand-side), and (B) ibuprofen raw material.

Figure IV-4 show SEM pictures of surfaces and cross sections of the differently sized implants before exposure to the release medium. The system diameters are indicated on the left hand-side. As it can be seen, all surfaces and cross sections were smooth and essentially non-porous. Some tiny cavities were visible, which might be attributable to ibuprofen sublimation during processing. As it has previously been demonstrated (47), the ibuprofen can be expected to be essentially dissolved (*molecularly* dispersed) in the polymeric matrix at these drug loadings (47).

IV. PLGA IMPLANTS FOR CONTROLLED DRUG RELEASE: IMPACT OF THE DIAMETER

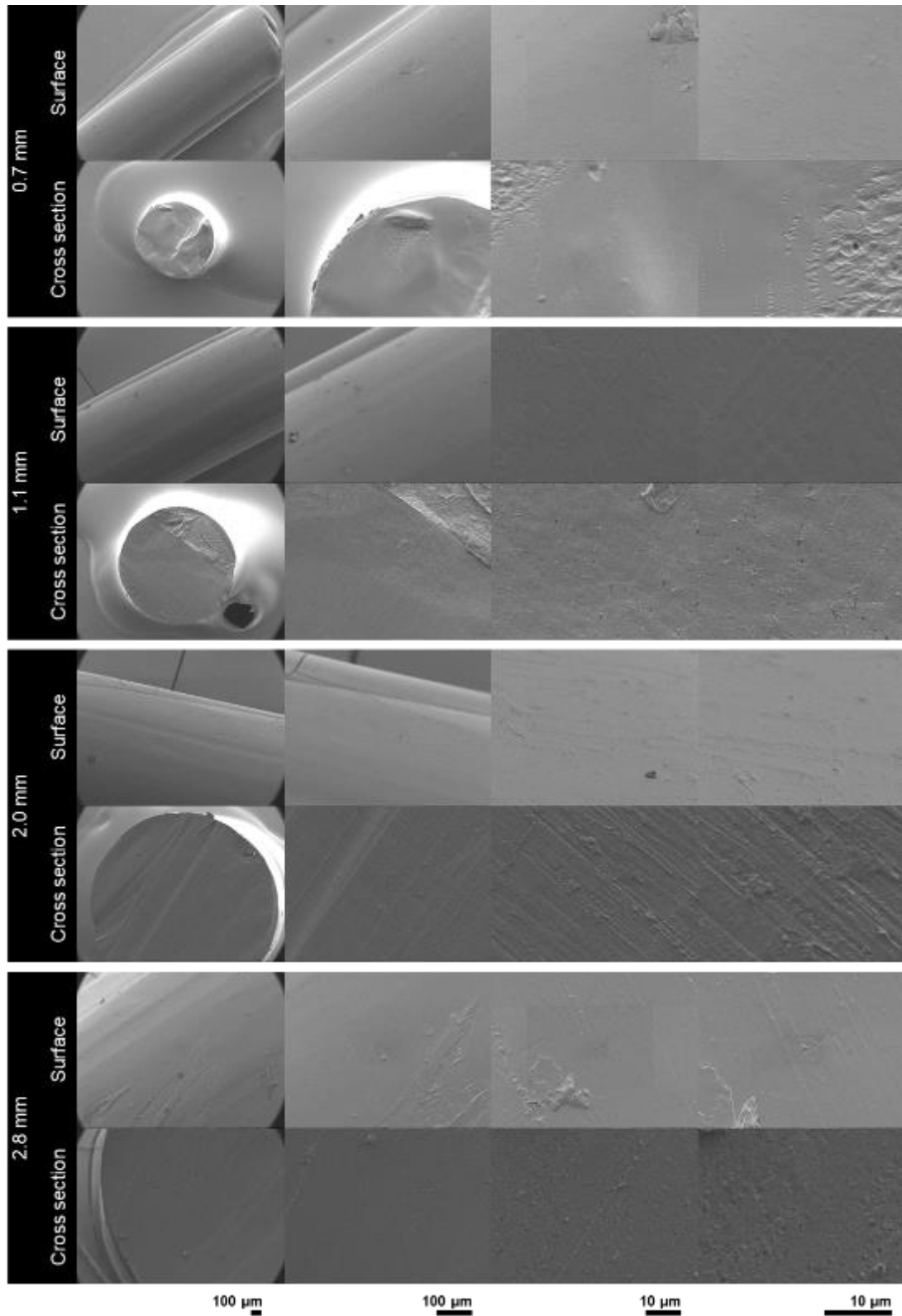


Figure IV-4. Scanning electron microscopy pictures of surfaces and cross sections of implants before exposure to release medium. The diameters of the implants are indicated on the left hand-side.

IV.4.2. Implants after exposure to the release medium

The schemes in *Figure IV-1* shows the 3 experimental set-ups, which were used to monitor drug release from the investigated PLGA implants in this study: (i) Samples were exposed to well agitated phosphate buffer pH 7.4 in Eppendorf tubes (metal baskets with 250 μm meshes assuring that the systems did not sink to the bottom of the tubes). (ii) Implants were embedded into agarose gels, which were placed into Eppendorf tubes and exposed to well agitated phosphate buffer pH 7.4. (iii) Implants were embedded into agarose gels, which were placed into the donor compartments of transwell plates, the acceptor compartments containing well agitated phosphate buffer pH 7.4. The agarose gels were intended to better mimic the conditions upon subcutaneous administration. The top row in *Figure IV-5* shows the *relative* drug release rates from the differently sized PLGA implants observed in the 3 set-ups. Clearly, in all cases, an increase in the implant diameter led to slower relative ibuprofen release. But please note that the opposite trend was observed when looking at the respective *absolute* drug release rates (bottom row in *Figure IV-5*). Normalizing the absolute ibuprofen release to the available surface area leads to about similar release rates at the beginning. This is sound, because the drug and polymer are the same, and the composition as well as the inner and outer system structures are very similar (*Table IV-1*, *Figure IV-2*, *Figure IV-4*). However, the systems differ substantially in their *total absolute* drug loadings and length of the diffusion pathways to be overcome by the drug. This is why the smaller implants were much more rapidly depleted of ibuprofen compared to the larger implants (e.g. bottom row in *Figure IV-5*).

Table IV-1. Key properties of the investigated ibuprofen-loaded PLGA implants (*T_g*: glass transition temperature, *M_w*: average polymer molecular weight). Mean values \pm standard deviations are indicated ($n = 3$).

Implant	Diameter, die			
	0.5 mm	1 mm	2 mm	3 mm
Diameter (mm)	0.66 \pm 0.02	1.08 \pm 0.02	1.98 \pm 0.03	2.79 \pm 0.19
Weight (mg)	2.53 \pm 0.10	6.84 \pm 0.21	23.58 \pm 1.11	46.22 \pm 6.83
Practical loading (%)	12.1 \pm 0.1	12.5 \pm 0.1	12.3 \pm 0.1	12.0 \pm 0.1
T _g (°C)	35.6 \pm 0.2	35.2 \pm 0.2	36.2 \pm 0.1	36.9 \pm 0.3
M _w (kDa)	23.9 \pm 0.3	24.5 \pm 0.3	25.7 \pm 0.1	24.6 \pm 0.4

IV. PLGA IMPLANTS FOR CONTROLLED DRUG RELEASE: IMPACT OF THE DIAMETER

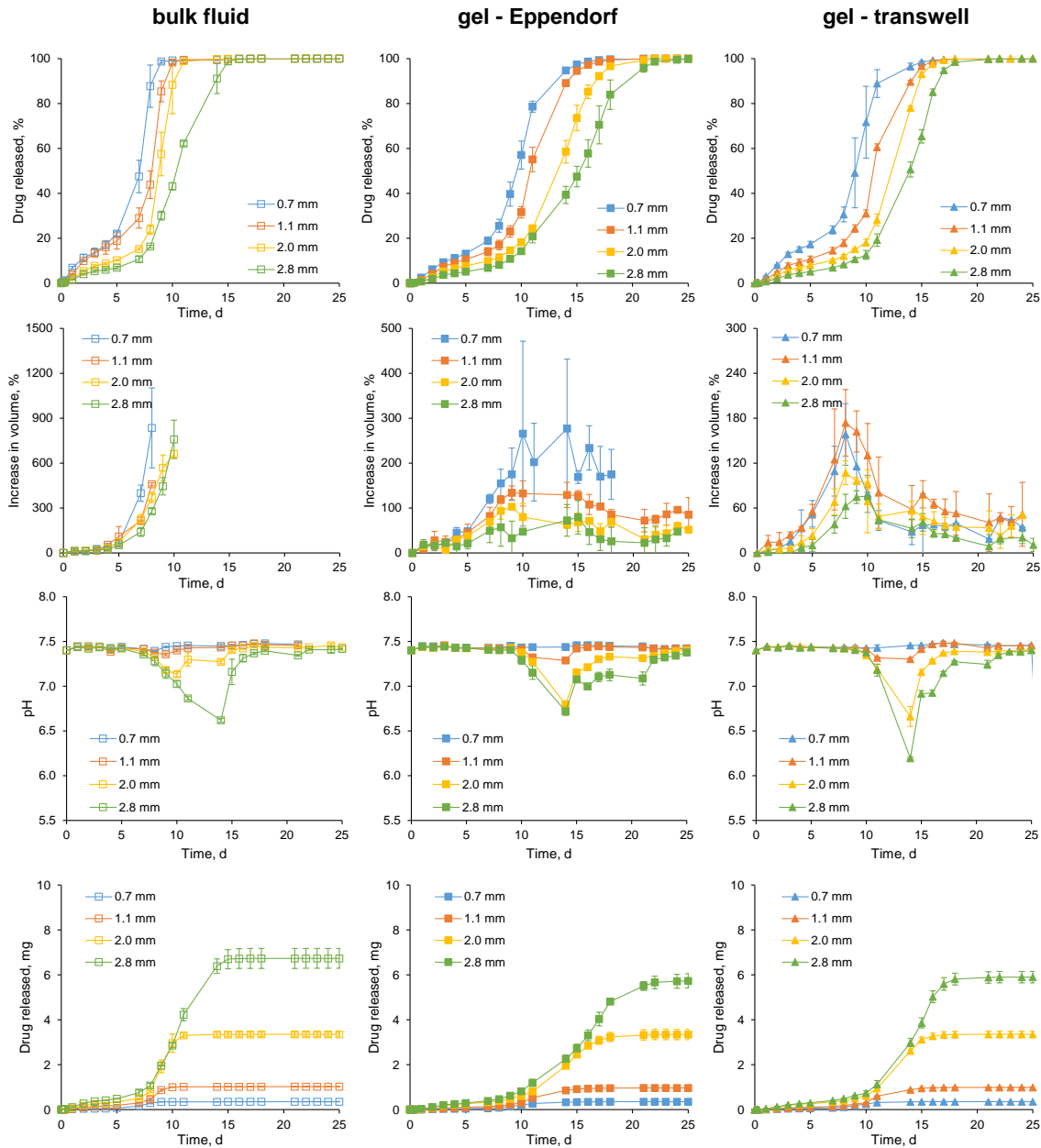


Figure IV-5. Implant behavior of the ibuprofen-loaded PLGA implants upon exposure to phosphate buffer pH 7.4 using the 3 experimental set-ups: Relative (%) and absolute (mg) ibuprofen release kinetics (top and bottom), dynamic changes in the implant volume and pH of the well agitated bulk fluids (middle rows). The implant diameters are indicated in the diagrams.

As it can be seen in *Figure IV-5*, the observed drug release kinetics were bi-phasic in all cases, irrespective of the implants' diameter and experimental set-up: An about zero order drug release rate (with an about constant release rate) was followed by a final rapid drug release phase (accounting for approximately 80-90 % of the total drug). An initial burst phase was (if present at all) not of noteworthy importance. This is in good agreement with the hypothesis that the

initial (limited) burst release (about 3-5 % in the first 12 h) from implants of similar composition, but in which the drug was partially present in the form of crystalline particles, can mainly be attributed to the presence of pure drug particles with direct surface access (47).

Interestingly, all implants did not substantially swell during the first few days after exposure to the release medium, but substantial system swelling set on after a certain lag time : The diagrams in the 2nd row in *Figure IV-5* illustrate the dynamic changes in the implants' volume as a function of time, *Figure IV-6* shows optical macroscopy pictures of implants studied in the different set-ups at pre-determined time points (please note that if exposed to well agitated bulk fluids, the samples became too fragile to be withdrawn from the medium after 8 or 10 d to take pictures). The diagrams in the 2nd row in *Figure IV-7* illustrate the dynamic changes in the implants' wet mass (the top row in this figure shows a zoom on drug release during the first 10 d). Comparing the 2 top 2 rows in *Figure IV-2* and the 2 top rows in *Figure IV-7*, it becomes obvious that the lag-times for substantial implant swelling and the onset of the final rapid drug release phase coincided in all cases, irrespective of the implants' size and experimental set-up. Furthermore, this onset was delayed to later time points when embedding the implants in agarose gels and when increasing the implants' diameter.

IV. PLGA IMPLANTS FOR CONTROLLED DRUG RELEASE: IMPACT OF THE DIAMETER

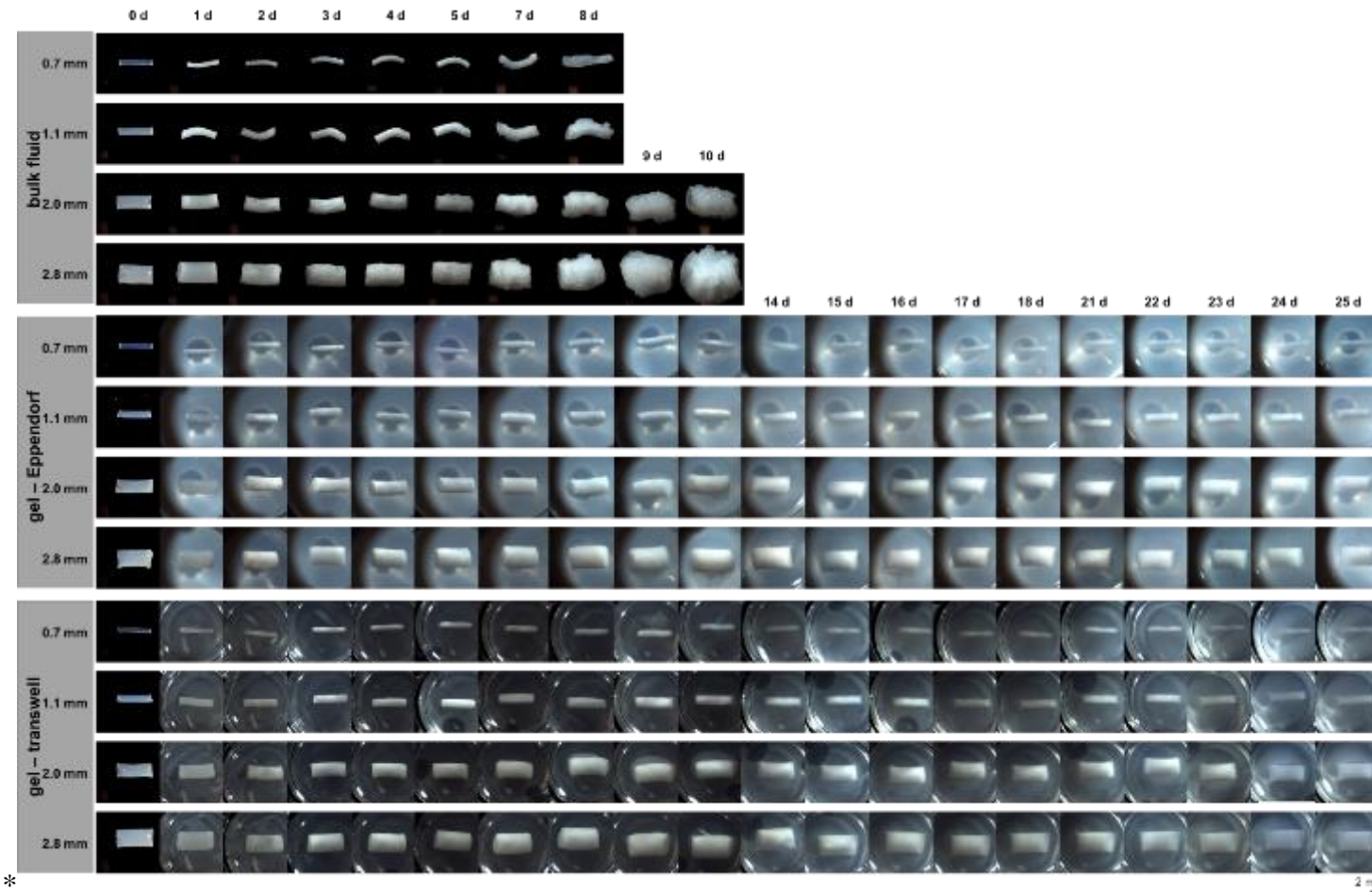


Figure IV-6. Optical macroscopy pictures ibuprofen-loaded PLGA implants upon exposure to phosphate buffer pH 7.4 in the 3 experimental set-ups: In bulk fluids in Eppendorf tubes, in agarose gels exposed to the release medium in Eppendorf tubes, and in agarose gels in transwell plates containing the release medium in the acceptor compartment. In the case of the bulk fluids, the implants became too fragile after 8 or 10 d to allow sample withdrawal for imaging.

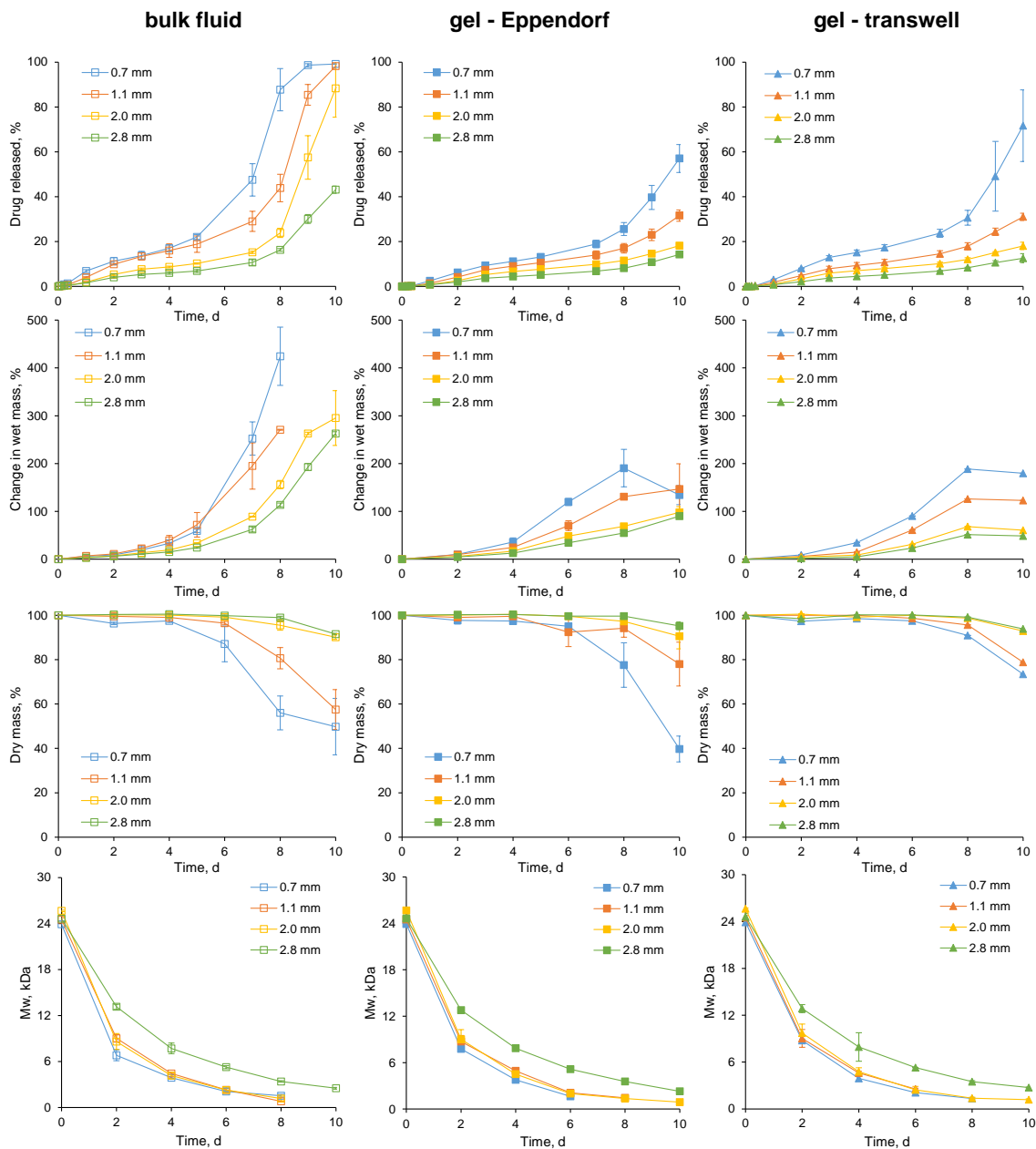


Figure IV-7. Zoom on the first 10 d of implant exposure to phosphate buffer pH 7.4 using the 3 experimental set-ups: Relative drug release, dynamic changes in the wet mass & dry mass of the systems and in the average polymer molecular weight of the PLGA. The implant diameters are indicated in the diagrams.

These phenomena can probably be explained as follows: Upon contact with aqueous media, limited amounts of water penetrate into the implants, which become rapidly *entirely* wetted. Thus, hydrolytic polymer chain cleavage occurs *throughout* the systems and starts from the beginning (“bulk erosion”). This is also consistent with the observed decrease in the average polymer molecular weight measured by GPC (bottom row in *Figure IV-7*). However, most of the PLGA matrix remains dense (PLGA being hydrophobic, limiting the amounts of water

IV. PLGA IMPLANTS FOR CONTROLLED DRUG RELEASE: IMPACT OF THE DIAMETER

within the systems) and the ibuprofen molecules are effectively entrapped. Only surface-near regions undergo substantial swelling: *Figure IV-8* shows SEM pictures of surfaces and cross sections of the investigated PLGA implants after 2, 4 and 8 d exposure to the release media. Please note that the samples had to be dried before SEM analysis, thus, artefacts have been created. The highly wizened structure which can be seen on all surfaces result from the drying of highly swollen PLGA surface layers. Since the surface polymer is in contact with very high amounts of water from the beginning, ester bond cleavage is particularly rapid in these zones. Upon cleavage of an ester bond, a new hydrophilic -OH and a new hydrophilic -CCOH group are generated. This renders the degrading polymer more and more water-loving. In addition, the mechanical stability of the 3-dimensional polymer network decreases (since the macromolecules become shorter and less entangled, *Figure IV-7* bottom row). In addition, water-soluble short chain acids accumulate and create a continuously increasing osmotic pressure. This leads to substantial PLGA swelling once the polymer is sufficiently hydrophilic and mechanically instable. Importantly, this phenomenon is initially limited to surface-near regions, as it can be seen in the cross sections in *Figure IV-8*. With time these highly swollen PLGA surface layer increases in thickness. Importantly, the mobility of ibuprofen molecules located in these regions fundamentally changes: They can be expected to be poorly mobile in the dense, non-swollen PLGA, but to be much more mobile in a highly swollen PLGA gel: The distances between the macromolecules has considerably increased and the polymer chains themselves are much more mobile. This can be expected to result in relatively rapid drug release from highly swollen PLGA zones. Since the rate at which the thickness of the highly swollen surface layer increases can be expected to be about constant (the conditions for the swelling of “deeper” polymer layers do not change over time), also the resulting drug release rate can be expected to be about constant. This is in good agreement with the observed zero order release phases (*Figure IV-5*, top row).

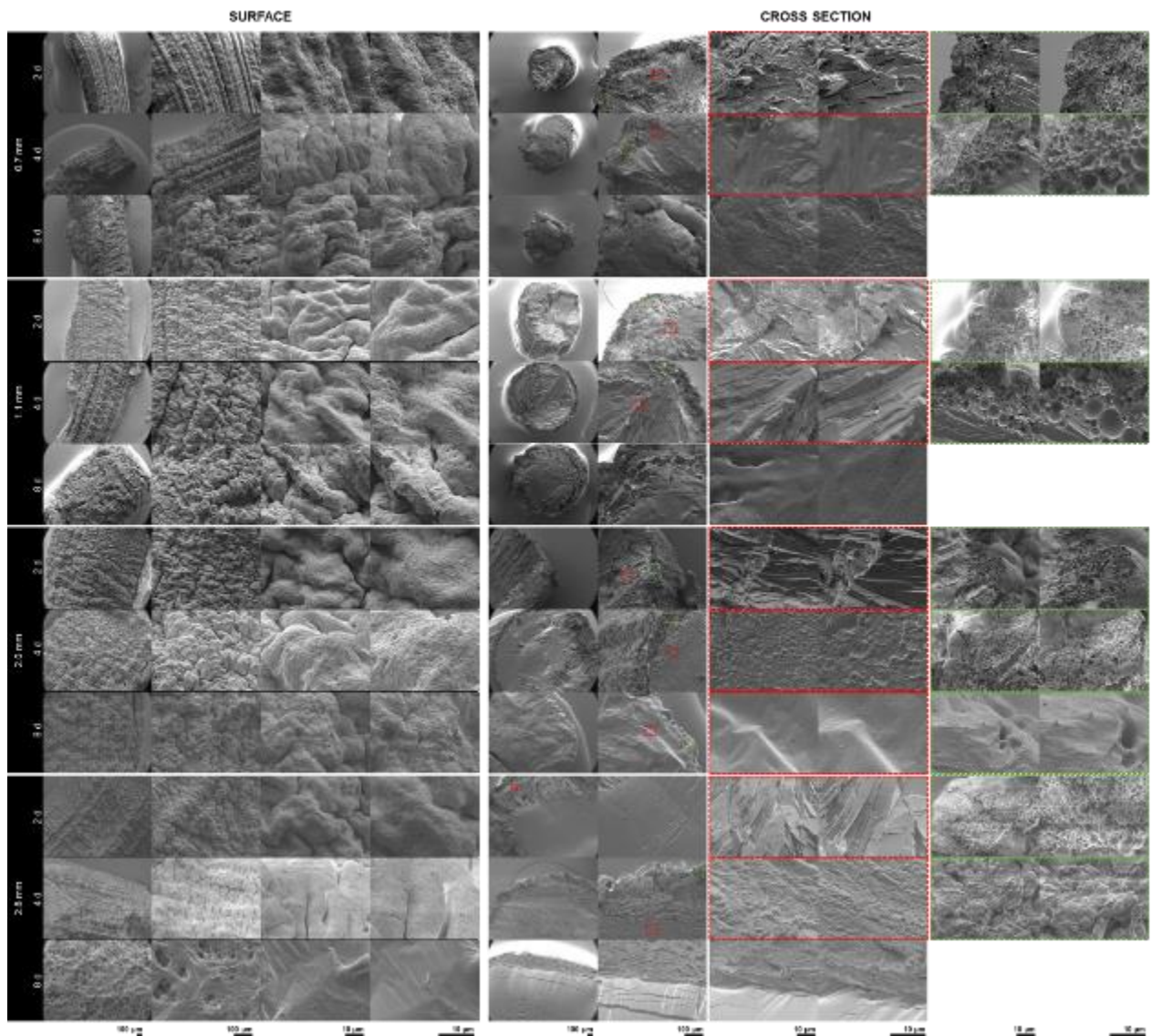


Figure IV-8. SEM pictures of surfaces and cross sections of ibuprofen-loaded PLGA implants after exposure for 2, 4 or 8 d to phosphate buffer pH 7.4 (as indicated on the left hand-side). Please note that the implants were freeze-dried prior to analysis, creating artefacts. The implant diameters are also indicated in the diagrams.

This *local*, surface-near PLGA swelling has to be distinguished from the observed substantial entire system swelling occurring after about 5-10 d: Due to the fact that the entire implants are rather rapidly wetted upon contact with the release medium, polymer chain degradation occurs *throughout* the systems (even if at a lower rate compared to the outmost surface layers). Hence, after a certain lag time, the entire implant is sufficiently hydrophilic and mechanically instable and exhibits an osmotic pressure, which attracts *substantial* amounts of water into the *entire* device. This is the onset of fundamental entire system swelling. The consequences for ibuprofen release are the same: It becomes much more mobile in the highly swollen PLGA gel. Looking

IV. PLGA IMPLANTS FOR CONTROLLED DRUG RELEASE: IMPACT OF THE DIAMETER

at the optical macroscopic pictures at later time points in Figure 6, this can also be “visualized”. For example, the mobility of an ibuprofen molecule in the dense PLGA matrix in an implant with an initial diameter of 3 mm exposed to a well agitated bulk fluid can be expected to be limited. However, after 1 week, the implant has tremendously swollen and ibuprofen can much more easily be released. But not only the mobility of the drug molecules/ions fundamentally increases: also the water-soluble degradation products of the PLGA can more easily diffuse out of the systems. This causes a drop in the pH of the respective bulk fluid (3rd row in Figure 5). Please note that the importance of the observed pH drop can in part also be attributed to the longer (3 d week end) sampling period, resulting in short chain accumulation in the bulk fluid. As it can be seen, the drop in pH is more pronounced with larger implants, which can be explained by the higher amounts of PLGA in these systems and, thus, higher amounts of degradation products. The facilitated release of drug and short chain acids in the highly swollen PLGA matrices also leads to the onset of implant erosion, as illustrated in the 3rd row in *Figure IV-7*. Before, the dry mass loss is limited, because the polymer matrix is dense and poorly permeable.

When looking at the blue, orange, yellow and green curves in the top row of *Figure IV-5*, it becomes obvious that the onset of the final rapid drug release phase is delayed with increasing implant diameter, irrespective of the experimental set-up. This can be explained by the delayed onset of substantial system swelling (increase in volume in *Figure IV-5*, optical macroscopy pictures in *Figure IV-6*, increase in wet mass in *Figure IV-7*, SEM pictures in *Figure IV-8*): Larger matrices can be expected to be mechanically more stable than smaller ones, the mass of the investigated implants varying by a factor of about 20 (*Table IV-1*). Interestingly, no signs for the occurrence of important autocatalytic effects were observed in this study, despite the considerable system dimensions. This might eventually be explained by the relatively rapidly occurring substantial *entire* system swelling, which sets on after only about 5 to 10 d (*Figure IV-5-8*). Once the PLGA is highly swollen, generated water-soluble acids can rather rapidly diffuse out and be neutralized, and bases from the release medium can diffuse into the system.

Comparing the implant swelling kinetics in the 3 experimental set-ups in *Figure IV-5* (increase in volume), *Figure IV-6* (optical macroscopy), *Figure IV-7* (increase in wet mass) and *Figure IV-8* (SEM pictures), it can be seen that the presence of the agarose gel surrounding the implants delays substantial device swelling. This is probably due to the steric hindrance by the gels. As a consequence, also the onset of the final rapid drug release phase is delayed in the gel

set-ups (*Figure IV-5*, top row), as well as the onset of implant erosion (*Figure IV-7*, 3rd row) and of the drop in the pH of the bulk fluid (*Figure IV-5*, 3rd row).

IV.5. Conclusions

The variation of the diameter of a PLGA implant is an effective tool to adjust desired absolute and relative release kinetics. In the case of hot melt extruded ibuprofen-loaded implants, bi-phasic release patterns were observed: A zero order release phase was followed by a rapid, final drug release phase (accounting for 80-90 % drug). The decrease in the *relative* drug release rate with increasing system diameter can be attributed to the longer diffusion pathways to be overcome. The onset of the final rapid drug release phase was delayed, because the larger polymer matrices are mechanically more stable, retarding the onset of substantial entire implant swelling, which facilitates drug release.

IV.6. Acknowledgments

This project has received funding from the Interreg 2 Seas programme 2014-2020 co-funded by the European Regional Development Fund under subsidy contract No 2S04-014 3DMed. The Authors would also like to thank Mr. A. Fadel from the “Centre Commun de Microscopie” of the University of Lille (“Plateau technique de la Federation Chevreul CNRS FR 2638”) for his valuable technical help with the SEM pictures.

IV.7. Authors statement

C. Bassand	Investigation; Methodology; Validation; Conceptualization; Writing - Original Draft; Visualization
J. Freitag	Investigation
L. Benabed	Investigation
J. Verin	Investigation; Methodology, Validation
F. Siepmann	Conceptualization; Methodology; Supervision; Resources; Writing - Review & Editing; Visualization; Project administration; Funding acquisition
J. Siepmann	Conceptualization; Methodology; Supervision; Resources; Writing - Review & Editing; Visualization; Project administration; Funding acquisition

IV. PLGA IMPLANTS FOR CONTROLLED DRUG RELEASE: IMPACT OF THE DIAMETER

IV.8. References

1. Shah NH, Railkar AS, Chen FC, Tarantino R, Kumar S, Murjani M, et al. A biodegradable injectable implant for delivering micro and macromolecules using poly (lactic-co-glycolic) acid (PLGA) copolymers. *J Controlled Release*. 1993 Nov 1;27(2):139–47.
2. Schliecker G, Schmidt C, Fuchs S, Ehinger A, Sandow J, Kissel T. In vitro and in vivo correlation of busarelin release from biodegradable implants using statistical moment analysis. *J Control Release Off J Control Release Soc*. 2004 Jan 8;94(1):25–37.
3. Kraus VB, Conaghan PG, Aazami HA, Mehra P, Kivitz AJ, Lufkin J, et al. Synovial and systemic pharmacokinetics (PK) of triamcinolone acetonide (TA) following intra-articular (IA) injection of an extended-release microsphere-based formulation (FX006) or standard crystalline suspension in patients with knee osteoarthritis (OA). *Osteoarthritis Cartilage*. 2018 Jan;26(1):34–42.
4. Nair LS, Laurencin CT. Biodegradable polymers as biomaterials. *Prog Polym Sci*. 2007 Aug 1;32(8):762–98.
5. Grund S, Bauer M, Fischer D. Polymers in Drug Delivery—State of the Art and Future Trends. *Adv Eng Mater*. 2011;13(3):B61–87.
6. Anderson JM, Shive MS. Biodegradation and biocompatibility of PLA and PLGA microspheres. *Adv Drug Deliv Rev*. 2012 Dec 1;64:72–82.
7. Schreiner V, Detampel P, Jirkof P, Puchkov M, Huwyler J. Buprenorphine loaded PLGA microparticles: Characterization of a sustained-release formulation. *J Drug Deliv Sci Technol*. 2021 Jun 1;63:102558.
8. Dorta MJ, Santoveña A, Llabrés M, Fariña JB. Potential applications of PLGA film-implants in modulating in vitro drugs release. *Int J Pharm*. 2002 Nov 6;248(1):149–56.
9. Schwach G, Oudry N, Delhomme S, Lück M, Lindner H, Gurny R. Biodegradable microparticles for sustained release of a new GnRH antagonist – part I: screening commercial PLGA and formulation technologies. *Eur J Pharm Biopharm*. 2003 Nov 1;56(3):327–36.
10. Présumey J, Salzano G, Courties G, Shires M, Ponchel F, Jorgensen C, et al. PLGA microspheres encapsulating siRNA anti-TNF α : Efficient RNAi-mediated treatment of arthritic joints. *Eur J Pharm Biopharm*. 2012 Nov 1;82(3):457–64.
11. Takahashi M, Onishi H, Machida Y. Development of implant tablet for a week-long sustained release. *J Controlled Release*. 2004 Nov 5;100(1):63–74.
12. Guo T, Lim CG, Noshin M, Ringel JP, Fisher JP. 3D printing bioactive PLGA scaffolds using DMSO as a removable solvent. *Bioprinting*. 2018 Jun 1;10:e00038.
13. McConville C, Tawari P, Wang W. Hot melt extruded and injection moulded disulfiram-loaded PLGA millirods for the treatment of glioblastoma multiforme via stereotactic injection. *Int J Pharm*. 2015 Oct 15;494(1):73–82.

14. Duque L, Körber M, Bodmeier R. Improving release completeness from PLGA-based implants for the acid-labile model protein ovalbumin. *Int J Pharm.* 2018 Mar 1;538(1):139–46.
15. Goel M, Leung D, Famili A, Chang D, Nayak P, Al-Sayah M. Accelerated in vitro release testing method for a long-acting peptide-PLGA formulation. *Eur J Pharm Biopharm.* 2021 Aug 1;165:185–92.
16. Andhariya JV, Jog R, Shen J, Choi S, Wang Y, Zou Y, et al. Development of Level A in vitro-in vivo correlations for peptide loaded PLGA microspheres. *J Control Release Off J Control Release Soc.* 2019 Aug 28;308:1–13.
17. Vay K, Scheler S, Frieß W. Application of Hansen solubility parameters for understanding and prediction of drug distribution in microspheres. *Int J Pharm.* 2011 Sep 15;416(1):202–9.
18. Grizic D, Lamprecht A. Predictability of drug encapsulation and release from propylene carbonate/PLGA microparticles. *Int J Pharm.* 2020 Aug 30;586:119601.
19. Zolnik BS, Burgess DJ. Evaluation of in vivo–in vitro release of dexamethasone from PLGA microspheres. *J Controlled Release.* 2008 Apr 21;127(2):137–45.
20. Xiao P, Qi P, Chen J, Song Z, Wang Y, He H, et al. The effect of polymer blends on initial release regulation and in vitro-in vivo relationship of peptides loaded PLGA-Hydrogel Microspheres. *Int J Pharm.* 2020 Dec 15;591:119964.
21. Thalhauser S, Peterhoff D, Wagner R, Breunig M. Silica particles incorporated into PLGA-based in situ-forming implants exploit the dual advantage of sustained release and particulate delivery. *Eur J Pharm Biopharm.* 2020 Nov 1;156:1–10.
22. Lehner E, Gündel D, Liebau A, Plontke S, Mäder K. Intracochlear PLGA based implants for dexamethasone release: Challenges and solutions. *Int J Pharm X.* 2019 Dec 1;1:100015.
23. Breitenbach J. Melt extrusion: from process to drug delivery technology. *Eur J Pharm Biopharm.* 2002 Sep 1;54(2):107–17.
24. Shah SS, Cha Y, Pitt CG. Poly (glycolic acid-co-dl-lactic acid): diffusion or degradation controlled drug delivery? *J Controlled Release.* 1992 Jan 1;18(3):261–70.
25. Fredenberg S, Wahlgren M, Reslow M, Axelsson A. The mechanisms of drug release in poly(lactic-co-glycolic acid)-based drug delivery systems—A review. *Int J Pharm.* 2011 Aug 30;415(1):34–52.
26. Göpferich A. Mechanisms of polymer degradation and erosion. *Biomaterials.* 1996 Jan 1;17(2):103–14.
27. Burkersroda F von, Schedl L, Göpferich A. Why degradable polymers undergo surface erosion or bulk erosion. *Biomaterials.* 2002 Nov 1;23(21):4221–31.

IV. PLGA IMPLANTS FOR CONTROLLED DRUG RELEASE: IMPACT OF THE DIAMETER

28. Gasmi H, Danede F, Siepmann J, Siepmann F. Does PLGA microparticle swelling control drug release? New insight based on single particle swelling studies. *J Controlled Release*. 2015 Sep 10;213:120–7.
29. Tamani F, Bassand C, Hamoudi MC, Danede F, Willart JF, Siepmann F, et al. Mechanistic explanation of the (up to) 3 release phases of PLGA microparticles: Diprophylline dispersions. *Int J Pharm*. 2019 Dec 15;572:118819.
30. Bode C, Kranz H, Fizez A, Siepmann F, Siepmann J. Often neglected: PLGA/PLA swelling orchestrates drug release: HME implants. *J Control Release Off J Control Release Soc*. 2019 Jul 28;306:97–107.
31. Gu B, Sun X, Papadimitrakopoulos F, Burgess DJ. Seeing is believing, PLGA microsphere degradation revealed in PLGA microsphere/PVA hydrogel composites. *J Controlled Release*. 2016 Apr 28;228:170–8.
32. Kim HK, Chung HJ, Park TG. Biodegradable polymeric microspheres with “open/closed” pores for sustained release of human growth hormone. *J Controlled Release*. 2006 May 15;112(2):167–74.
33. Wang T, Xue P, Wang A, Yin M, Han J, Tang S, et al. Pore change during degradation of octreotide acetate-loaded PLGA microspheres: The effect of polymer blends. *Eur J Pharm Sci*. 2019 Oct 1;138:104990.
34. Tipnis NP, Shen J, Jackson D, Leblanc D, Burgess DJ. Flow-through cell-based in vitro release method for triamcinolone acetonide poly (lactic-co-glycolic) acid microspheres. *Int J Pharm*. 2020 Apr 15;579:119130.
35. Zolnik BS, Leary PE, Burgess DJ. Elevated temperature accelerated release testing of PLGA microspheres. *J Control Release Off J Control Release Soc*. 2006 May 30;112(3):293–300.
36. Ding AG, Shenderova A, Schwendeman SP. Prediction of Microclimate pH in Poly(lactic-co-glycolic Acid) Films. *J Am Chem Soc*. 2006 Apr 1;128(16):5384–90.
37. Antheunis H, van der Meer J-C, de Geus M, Heise A, Koning CE. Autocatalytic Equation Describing the Change in Molecular Weight during Hydrolytic Degradation of Aliphatic Polyesters. *Biomacromolecules*. 2010 Apr 12;11(4):1118–24.
38. Blasi P, D’Souza SS, Selmin F, DeLuca PP. Plasticizing effect of water on poly(lactide-co-glycolide). *J Controlled Release*. 2005 Nov 2;108(1):1–9.
39. Blasi P, Schoubben A, Giovagnoli S, Perioli L, Ricci M, Rossi C. Ketoprofen poly(lactide-co-glycolide) physical interaction. *AAPS PharmSciTech*. 2007 Jun;8(2):E78–85.
40. Zlomke C, Barth M, Mäder K. Polymer degradation induced drug precipitation in PLGA implants – Why less is sometimes more. *Eur J Pharm Biopharm*. 2019 Jun 1;139:142–52.
41. Dunne M, Corrigan OI, Ramtoola Z. Influence of particle size and dissolution conditions on the degradation properties of polylactide-co-glycolide particles. *Biomaterials*. 2000 Aug 1;21(16):1659–68.

42. Siepmann J, Faisant N, Akiki J, Richard J, Benoit JP. Effect of the size of biodegradable microparticles on drug release: experiment and theory. *J Control Release Off J Control Release Soc.* 2004 Apr 16;96(1):123–34.
43. Chen W, Palazzo A, Hennink WE, Kok RJ. Effect of Particle Size on Drug Loading and Release Kinetics of Gefitinib-Loaded PLGA Microspheres. *Mol Pharm.* 2017 Feb 6;14(2):459–67.
44. Lin X, Yang H, Su L, Yang Z, Tang X. Effect of size on the in vitro/in vivo drug release and degradation of exenatide-loaded PLGA microspheres. *J Drug Deliv Sci Technol.* 2018 Jun 1;45:346–56.
45. Siepmann J, Elkharraz K, Siepmann F, Klose D. How autocatalysis accelerates drug release from PLGA-based microparticles: a quantitative treatment. *Biomacromolecules.* 2005 Aug;6(4):2312–9.
46. Klose D, Siepmann F, Elkharraz K, Krenzlin S, Siepmann J. How porosity and size affect the drug release mechanisms from PLGA-based microparticles. *Int J Pharm.* 2006 May 18;314(2):198–206.
47. Bassand C, Benabed L, Verin J, Danede F, Willart J-F, Siepmann F, et al. Hot melt extruded ibuprofen-loaded PLGA implants: Importance of heat exposure. *Journal of Drug Delivery Science and Technology* - Submitted. 2021;

**V. HOW BULK FLUID RENEWAL CAN
AFFECT DRUG RELEASE FROM PLGA
IMPLANTS**

V. HOW BULK FLUID RENEWAL CAN AFFECT DRUG RELEASE FROM PLGA IMPLANTS

Research article – To be submitted in AAPS PharmSci Tech

How bulk fluid renewal can affect drug release from PLGA implants

C. Bassand, L. Benabed, J. Freitag, J. Verin, F. Siepman, J. Siepman

Univ. Lille, Inserm, CHU Lille, U1008, F-59000 Lille, France

V.1. Abstract

The aim of this study was to better understand the potential impact of partial and complete renewal of the bulk fluid during drug release measurements from poly (lactic-co-glycolic acid) (PLGA)-based implants. A “standard experimental set-up”, in which the implants were directly exposed to well agitated phosphate buffer pH 7.4 was used, as well as set-ups, in which the implants were embedded within agarose hydrogels (mimicking living tissue). The gels were exposed to well agitated phosphate buffer pH 7.4. Ibuprofen-loaded implants were prepared by hot melt extrusion. The systems were thoroughly characterized before and during drug release by optical and scanning electron microscopy, gravimetric analysis, pH and solubility measurements as well as gel permeation chromatography. The bulk fluid was either completely or partially replaced by fresh medium at each sampling time point. Interestingly, the agarose set-ups did not show any impact of the bulk fluid sampling volume on the observed drug release patterns, whereas complete fluid renewal in the “standard set-up” led to accelerated drug release. This could be explained by the considerable fragility of the implants once substantial polymer swelling set on, transforming them into PLGA gels: Complete fluid renewal caused partial disintegration and damage of the highly swollen systems, decreasing the lengths of the diffusion pathways for the drug. The mechanical stress is very much reduced at low sampling volumes, or if the implants are embedded within agarose gels. Thus, great care must be taken when defining the conditions for in vitro drug release measurements from PLGA-based implants: Once substantial system swelling sets on, the devices become highly fragile.

Keywords: PLGA; implant; controlled drug delivery; experimental set-up; ibuprofen

V. HOW BULK FLUID RENEWAL CAN AFFECT DRUG RELEASE FROM PLGA IMPLANTS

V.2. Introduction

Poly (D,L lactic-co-glycolic acid) (PLGA)-based implants offer an interesting potential for parenteral controlled drug delivery (1–3). This is because: (i) PLGA is biocompatible and completely biodegradable (avoiding the need to remove empty remnants after drug exhaust) (1,2,4). (ii) Drug release can be controlled during periods ranging from a few days up to several months (5). (iii) A variety of manufacturing processes can be applied for their preparation, including for example hot melt extrusion (6), compression (7) and 3D printing (8).

The underlying mass transport mechanisms controlling drug release from PLGA implants can be very complex (5,9,10). The following are examples for phenomena which can be involved. Their relative importance can very much depend on the composition and structure of the implant (and, hence the manufacturing procedure), as well as on the experimental conditions chosen for the *in vitro* release measurements: Upon implantation, water penetrates into the implants. Generally, the entire system is rapidly wetted. However, the amounts of water at this stage are often limited, because the commonly used PLGA grades are rather hydrophobic and the polymeric matrix is dense. The presence of the water initiates ester bond cleavage throughout the device (“bulk erosion”) (11). In addition, the drug can dissolve in the water and becomes mobile (although often only to a limited extent, since the amounts of water in the system are still low). Consequently, the dissolved drug molecules/ions diffuse out into the surrounding environment, due to concentration gradients (9,12). Depending on the system size and initial inner structure, the pH might *locally* significantly drop (13–15). This is because ester bond cleavage generates shorter chain acids, which might accumulate, especially at the center of the implant: The diffusion of these acids out of the device takes time (as well as the diffusion of bases from the environment into the system), and the rate at which the acids are generated can be higher than the rate at which they are neutralized (16). Since ester bond hydrolysis is catalyzed by protons, this can lead to autocatalytic effects (10,15,16). Consequently, polymer degradation can be accelerated and the drug release rate increases. Furthermore, limited drug solubility effects within the PLGA implants as well as within the surrounding bulk fluid might play a major role (17,18). Also, drug diffusion through water-filled pores might be of importance. If the pores exist from the beginning, this might cause a high initial drug release rate. The pores might then be closed by (limited) PLGA swelling, terminating the related burst release phase (19,20).

One of the key reasons for the potential complexity of the drug release mechanisms from PLGA-based implants is polymer degradation, which has multiple consequences over time:

(i) The macromolecular network becomes more and more hydrophilic, since the cleavage of each ester bond generates two new hydrophilic end groups: an -OH and a -COOH group. (ii) The mechanical stability of the polymeric matrix decreases, since the macromolecular chain length decreases, resulting in less intense polymer entanglement. (iii) Water-soluble degradation products accumulate (being poorly mobile in the initially dense polymeric system, similar to the drug), creating a steadily increasing hydrostatic pressure in the implant. Thus, the implants become more and more water-loving with time, get less resistant to dimensional changes and more and more actively attract water. Consequently, at a certain time point, substantial implant swelling sets on (21–24). Increases in system wet mass up to 1000 % have been reported (21,25). This tremendous device swelling fundamentally changes the conditions for drug release: The polymer network becomes much less dense, the dissolved drug molecules/ions become much more mobile. Hence, the final, rapid drug release phase sets on (9,26,27).

Unfortunately, yet no compendial method has been described for the measurement of drug release from parenteral controlled drug delivery systems. So, great care must be taken when comparing drug release kinetics obtained under different conditions. Frequently, the implants are directly exposed to a well agitated bulk fluid, such as phosphate buffer pH 7.4 (28–30). At pre-determined time points, samples are withdrawn from the release medium and often replaced by fresh bulk fluid. It is well known that the sampling frequency and volume likely affect the observed drug release patterns, if limited drug solubility effects in the bulk fluid are of importance. Also, since PLGA degradation is catalyzed by protons, temporary drops in the pH of the bulk fluid can lead to accelerated polymer chain cleavage and faster drug release (10,15,31). However, little is yet known about potential further impacts of the sampling schedule on drug release.

To more realistically mimic the conditions experienced by the dosage forms upon implantation into human tissue, hydrogels have been proposed (32–34). The idea is to minimize convective mass transport (as in well agitated bulk fluids) and place the system in a semi-solid environment. It has recently been shown that the presence of such a hydrogel can limit substantial implant swelling and, thus, slow down drug release (35). The group of Ostergaard published some very interesting reports on how drug transport in a surrounding hydrogel can be monitored using UV analysis from a controlled release implant (36–38). This type of results can be very helpful to better understand which phenomena are decisive for drug transport into the environment surrounding the implant.

V. HOW BULK FLUID RENEWAL CAN AFFECT DRUG RELEASE FROM PLGA IMPLANTS

The aim of this study was to better understand how sensitive the experimentally measured drug release profiles from PLGA-based implants might be on the renewal of the release medium. Ibuprofen-loaded PLGA implants were prepared by hot melt extrusion. Three experimental set-ups were used: The implants were either directly exposed to well agitated phosphate buffer pH 7.4, or embedded within agarose gels, which were exposed to phosphate buffer in Eppendorf tubes or transwell plates (35). The systems were thoroughly characterized before and during drug release by optical and scanning electron microscopy, gravimetric analysis, pH and solubility measurements as well as gel permeation chromatography, to explain the observed results.

V.3. Materials and methods

V.3.1. Materials

Poly (D,L lactic-co-glycolic acid) (PLGA, 50:50 lactic acid: glycolic acid; Resomer RG 503H; Evonik, Darmstadt, Germany); ibuprofen (BASF, Ludwigshafen, Germany); agarose (genetic analysis grade; Fisher Scientific, Janssen Pharmaceutical, Geel, Belgium); potassium dihydrogen orthophosphate and sodium hydroxide (Acros Organics, Geel, Belgium); tetrahydrofuran (HPLC grade) (Fisher Scientific, Illkirch, France); acetonitrile (VWR, Fontenay-sous-Bois, France); sodium hydrogen phosphate (Na_2HPO_4 ; Panreac Quimica, Barcelona, Spain); lactic acid solution 85% (Sigma Aldrich, Saint-Louis, Missouri, USA); Sodium hydroxide solution 10% (Sigma Aldrich, Saint-Louis, Missouri, USA).

V.3.2. Implant preparation

Appropriate amounts of polymer [milled for 4 x 30 s with a grinder (Valentin, Seb, Ecully, France)] and drug powders were blended for 5 min at 20 rpm in a Turbula T2C Shaker-Mixer (Willy A Bachofen, Basel, Switzerland). Three hundred mg of the mixture were filled into a 1 mL syringe (Henke Sass Wolf, Tuttlingen, Germany), followed by heating to 105°C for 15 min in an oven (FP115, Binder, Tuttlingen, Germany). The molten blend was manually extruded using the syringe. The extrudate was cut with a hot scalpel into cylindrical implants of approximately 5 mm length.

V.3.3. Optical macroscopy and implant dimensions

Pictures of implants before exposure to the release medium were taken using a SZN-6 trinocular stereo zoom microscope (Optika, Ponteranica, Italy), equipped with an optical camera (Optika Vision Lite 2.1 software). The lengths and diameters of the implants were determined using the ImageJ software (US National Institutes of Health, Bethesda, Maryland, USA).

V.3.4. Practical drug loading

Implants were dissolved in 5 mL acetonitrile, followed by filtration (PVDF syringe filters, 0.45 μm ; Agilent Technologies, Santa Clara, USA) and drug content determination by HPLC-UV analysis using a Thermo Fisher Scientific Ultimate 3000 Series HPLC. The latter was equipped with an LPG 3400 SD/RS pump, an autosampler (WPS-3000 SL) and a UV-Vis detector (VWD-3400RS) (Thermo Fisher Scientific, Waltham, USA). A reversed-phase column C18 (Gemini 5 μm ; 110 Å; 150 x 4.6 mm; Phenomenex, Le Pecq, France) was used. The mobile

V. HOW BULK FLUID RENEWAL CAN AFFECT DRUG RELEASE FROM PLGA IMPLANTS

phase was a mixture of 30 mM Na₂HPO₄ pH 7.0: acetonitrile (60:40, v:v). The detection wavelength was 264 nm, and the flow rate 0.5 mL/min. Ten microliter samples were injected.

V.3.5. Drug solubility measurements

Excess amounts of ibuprofen were exposed to 20 mL phosphate buffer pH 7.4 USP 42 in glass flasks, which were horizontally shaken (80 rpm) at 37°C in an incubator (GFL 3033; Gesellschaft fuer Labortechnik, Burgwedel, Germany). Optionally, the pH was adjusted using aqueous solutions of 10 N lactic acid or 0.05 N NaOH (final pH values are reported). At pre-determined time points, samples were withdrawn, immediately filtered (PVDF syringe filter, 0.45 µm; Agilent, Santa Clara, USA) and diluted. The drug contents of the samples were determined by HPLC-UV, as described above. Samples were withdrawn until equilibrium was reached. Each experiment was conducted in triplicate, mean values +/- standard deviations are reported.

V.3.6. In vitro drug release

Three experimental set-ups were used to measure ibuprofen release from the PLGA implants:

V.3.6.1. In well-agitated bulk fluids

Implants were placed in 5 mL Eppendorf tubes (1 implant per tube), filled with 5 mL phosphate buffer pH 7.4 USP 42 (*Figure V-1A*). Metal baskets avoided that the implants sank to the bottom of the tubes (resulting in potentially limited contact with the bulk fluid). The mesh size (250 µm) was sufficient to allow for convective flow and rapid medium exchange “inside – outside” the basket. The tubes were placed in a horizontal shaker (80 rpm, 37°C; GFL 3033; Gesellschaft fuer Labortechnik, Burgwedel, Germany). At predetermined time points, the entire bulk fluid (5 mL), or 3 mL or 1 mL of the bulk fluid was replaced by fresh release medium. The withdrawn samples were filtered (PVDF syringe filter, 0.45 µm; Agilent) and analyzed for their ibuprofen contents by HPLC-UV, as described above.

V.3.6.2. In agarose gels in Eppendorf tubes

Implants were embedded into agarose gels in 5 mL Eppendorf tubes, as illustrated in *Figure V-1B* (1 implant per tube). An agarose dispersion (0.5% w:v) in phosphate buffer pH 7.4 (USP 42) was heated to 100 °C under magnetic stirring (250 rpm) until a clear solution was obtained. The latter was cooled to 47°C and continuously stirred (to prevent gelation). 0.5 mL of the solution was placed into the bottom of an Eppendorf tube and cooled in a refrigerator for 5 min to allow for gelation. An implant was carefully placed on top of the gel, and covered with

second layer of 0.5 mL agarose solution (47 °C), followed by cooling in a refrigerator for 5 min. Four mL phosphate buffer pH 7.4 USP 42 were added on top of the gel, and the tubes were placed in a horizontal shaker (80 rpm, 37°C; GFL 3033). At predetermined time points, the entire bulk fluid, or 3 mL or 1 mL of the bulk fluid was replaced by fresh release medium. The withdrawn samples were treated as for the drug release measurements in well agitated bulk fluids.

V.3.6.3. In agarose gels in transwell pates

Implants were embedded in agarose gels in transwell plates (1 implant per insert, membranes: 1.13 cm², 11 µm, 0.4 µm pore size; Nunc, Roskilde, Denmark), as illustrated in *Figure V-1C*. The agarose gels were prepared as described above, and the implants included accordingly (placed between 2 “layers” of 0.5 mL gel). The well plates were filled with 4 mL phosphate buffer pH 7.4, covered with lids and Parafilm to minimize evaporation, and placed in a horizontal shaker (80 rpm, 37°C; GFL 3033). At predetermined time points, the entire bulk fluid, or 3 mL or 1 mL of the bulk fluid was replaced by fresh (pre-heated) release medium. The withdrawn samples were treated as for the drug release measurements in well agitated bulk fluids.

In all cases, sink conditions were provided in the agitated bulk fluids. All experiments were conducted in triplicate. Mean values +/- standard deviations are reported.

Furthermore, the pH of the bulk fluids was measured at pre-determined time points using a pH meter (InoLab pH Level 1; WTW, Weilheim, Germany). Mean values +/- standard deviations are reported.

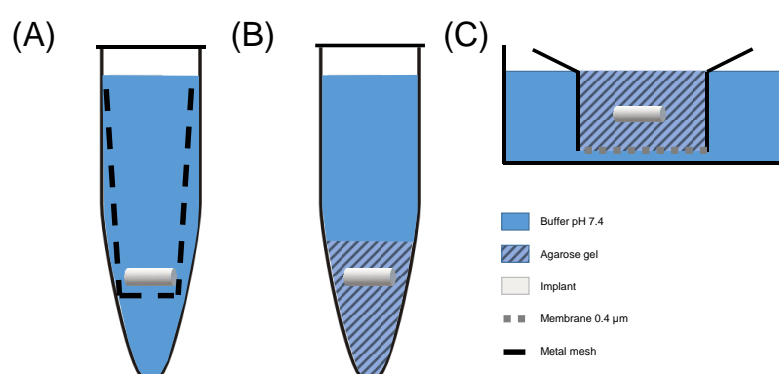


Figure V-1. Schematic presentations of the experimental set-ups used to monitor drug release from the PLGA-based implants: (A) In well-agitated release medium in Eppendorf tubes, (B) In agarose gels in Eppendorf tubes, the gels being exposed to well-agitated release medium,

V. HOW BULK FLUID RENEWAL CAN AFFECT DRUG RELEASE FROM PLGA IMPLANTS

(C) In agarose gels in transwell plates, the receptor compartment containing well-agitated release medium. Details are given in the text.

V.3.7. Implant swelling

Implants were treated as for the in vitro drug release studies described above. At pre-determined time points:

(i) Pictures of the implants were taken with a SZN-6 trinocular stereo zoom microscope (Optika), equipped with an optical camera (Optika Vision Lite 2.1 software). The lengths and diameters of the implants were determined using the ImageJ software (US National Institutes of Health). Dynamic changes in the systems' volume were calculated considering cylindrical geometry.

(ii) Implant samples were withdrawn and excess water was carefully removed using Kimtech precision wipes (Kimberly-Clark, Rouen, France) and weighed [*wet mass (t)*]. The *change in wet mass (%) (t)* was calculated as follows:

$$\text{change in wet mass } (\%)(t) = \frac{\text{wet mass } (t) - \text{mass } (t = 0)}{\text{mass } (t = 0)} \times 100 \%$$

where *mass (t = 0)* denotes the implant mass before exposure to the release medium.

All experiments were conducted in triplicate. Mean values +/- standard deviations are reported.

V.3.8. Implant erosion and PLGA degradation

Implants were treated as for the in vitro drug release studies described above. At pre-determined time points, implant samples were withdrawn and freeze-dried (freezing at -45°C for 2 h 35 min, primary drying at -20 °C/0.940 mbar for 35 h 10 min and secondary drying at +20 °C/0.0050 mbar for 35 h; Christ Alpha 2-4 LSC+; Martin Christ, Osterode, Germany).

The *dry mass (%) (t)* was calculated as follows:

$$\text{dry mass } (\%)(t) = \frac{\text{dry mass } (t)}{\text{mass } (t = 0)} \times 100 \%$$

where *mass (t = 0)* denotes the implant's mass before exposure to the release medium. All experiments were conducted in triplicate. Mean values +/- standard deviations are reported.

The average polymer molecular weight (Mw) of the PLGA was determined by gel permeation chromatography (GPC) as follows: Freeze-dried implant samples were dissolved in tetrahydrofuran (at a concentration of 3 mg/mL). One hundred µL samples were injected into

an Alliance GPC (refractometer detector: 2414 RI, separation module e2695, Empower GPC software; Waters, Milford, USA), equipped with a PLgel 5 μ m MIXED-D column (kept at 35°C, 7.8 \times 300 mm; Agilent). Tetrahydrofuran was the mobile phase (flow rate: 1 mL/min). Polystyrene standards with molecular weights between 1,480 and 70,950 Da (Polymer Laboratories, Varian, Les Ulis, France) were used to prepare the calibration curve. All experiments were conducted in triplicate. Mean values \pm standard deviations are reported.

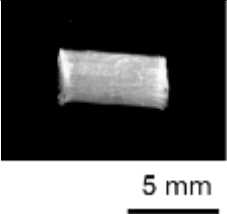
V.3.9. Scanning electronic microscopy (SEM)

The internal and external morphology of the implants before and after exposure to the release medium was studied using a JEOL Field Emission Scanning Electron Microscope (JSM-7800F, Japan), equipped with the Aztec 3.3 software (Oxford Instruments, Oxfordshire, UK). Samples were fixed with a ribbon carbon double-sided adhesive and covered with a fine chrome (Cr) layer. In the case of implants which had been exposed to the release medium before observation, the systems were treated as described for the *in vitro* release studies described above. At predetermined time points, implant samples were withdrawn, optionally cut with a scalpel and freeze-dried (as described in *section V.3.8 Implant erosion and PLGA degradation*).

V.4. Results and discussion

During in vitro drug release measurements from PLGA implants, often parts of the release medium are withdrawn at pre-determined time points and replaced with fresh medium. This procedure might affect the dosage form and alter the release rate. The aim of this study was to investigate the potential importance of the replaced bulk fluid volume, using the 3 experimental set-ups illustrated in *Figure V-1*. The bulk fluid (phosphate buffer pH 7.4) was either in direct contact with the implants, or in contact with a hydrogel in which the implants were embedded. The bulk fluid was entirely replaced (100 %), to a major extent (60-75 %), or to a minor extent (20-25 %). Ibuprofen-loaded implants were prepared by hot melt extrusion. The drug loading was about 8 %, the implants were cylindrical in shape (5.7 mm length, 2.7 mm diameter) and had a homogeneous appearance (optical macroscopy picture in *Table V-1*).

Table V-1. Key properties of the investigated ibuprofen-loaded PLGA implants before exposure to the release medium (*T_g*: glass transition temperature, *T_m*: melting temperature). Mean values \pm standard deviations are indicated ($n=3$).

Practical drug loading (%)	Weight (mg)	Length (mm)	Diameter (mm)	Macroscopic picture
8.0 \pm 0.9	30.9 \pm 3.5	5.7 \pm 0.3	2.7 \pm 0.2	

V.4.1. In vitro drug release and implant swelling

The diagrams at the top of *Figure V-2* show the observed ibuprofen release kinetics from the PLGA implants. The experiments were conducted in triplicate, mean values \pm standard deviations are reported. In each case, a single implant was:

- (i) directly exposed to 5 mL phosphate buffer pH 7.4 in an Eppendorf tube (*Figure V-1A*). The latter was horizontally shaken at 80 rpm at 37 °C. A metal basket avoided that the implant could sink to the bottom of the tube. Its mesh size (250 μ m) was sufficiently large to allow for convective flow and rapid medium exchange between the fluid inside and the outside of the basket.

- (ii) embedded within an agarose gel (1 mL), which was exposed to 4 mL phosphate buffer pH 7.4 in an Eppendorf tube (Figure V-1B). The latter was horizontally shaken at 80 rpm at 37 °C.
- (iii) embedded within an agarose gel (1 mL), located in the donor compartment of a transwell plate (Figure V-1C). The acceptor compartment was filled with 4 mL phosphate buffer pH 7.4. The transwell plate was horizontally shaken at 80 rpm at 37 °C.

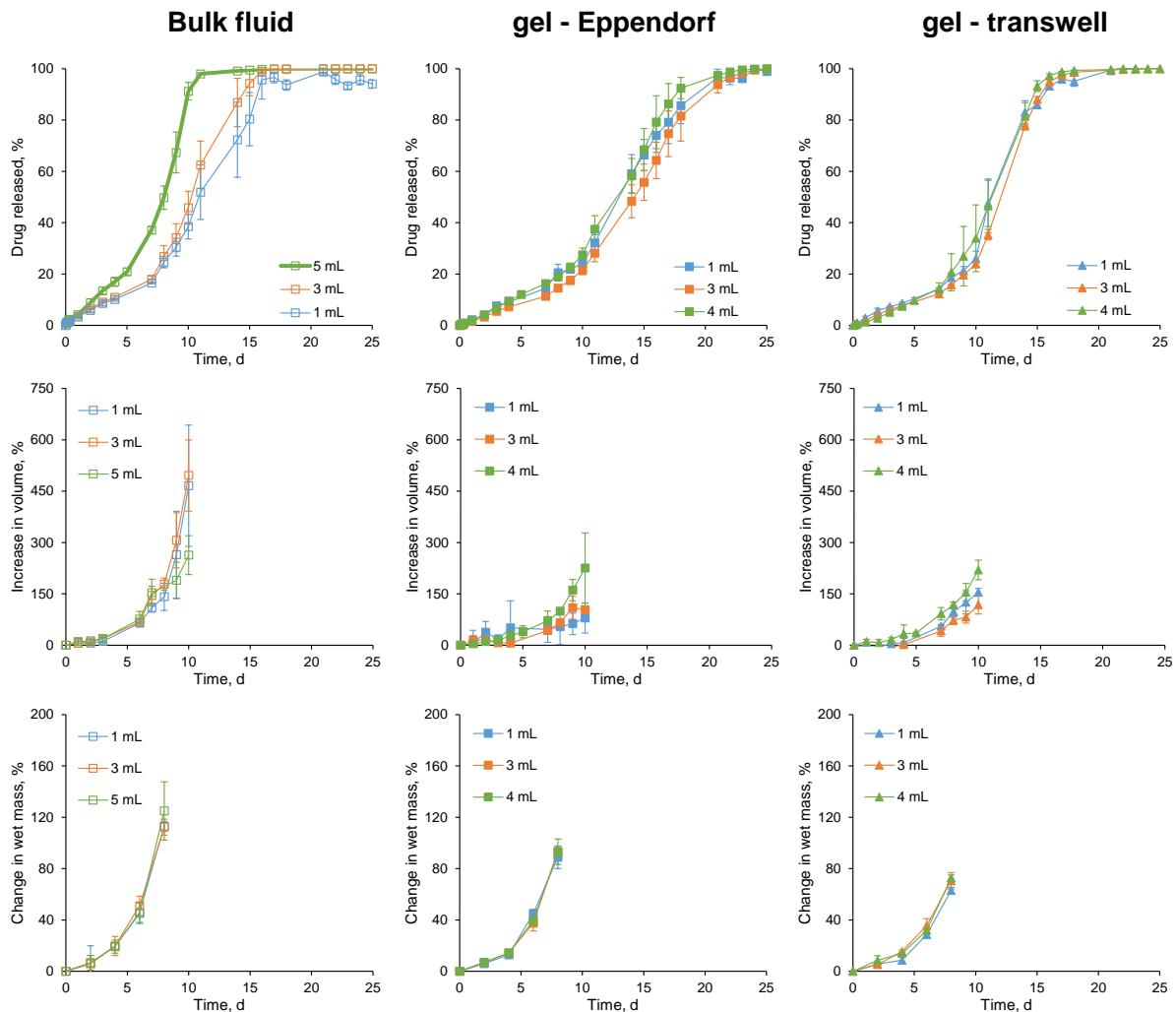


Figure V-2. Drug release, increase in volume and change in wet mass of ibuprofen-loaded PLGA implants upon exposure to phosphate buffer pH 7.4 using the 3 experimental set-ups. The implants were placed in well agitated bulk fluids in Eppendorf tubes, in agarose gels exposed to well agitated bulk fluid in Eppendorf tubes, or in agarose gels in transwell plates (the receptor compartment containing well-agitated bulk fluid). At pre-determined time points, the entire bulk fluid, or 1 or 3 mL thereof, was renewed (as indicated).

V. HOW BULK FLUID RENEWAL CAN AFFECT DRUG RELEASE FROM PLGA IMPLANTS

The bulk fluids were completely renewed at each sampling time point (4 or 5 mL), or only 3 or 1 mL of it (green, orange and blue curves). As it can be seen, the volume of the renewed bulk fluid did not have a noteworthy impact on drug release from the implants embedded within an agarose gel. In contrast, in the case of direct exposure to the phosphate buffer (standard set-up), ibuprofen release was faster when the entire release medium was renewed, compared to only partial replacement (*Figure V-2*, diagram at the top on the left-hand side). To better understand the reasons for this set-up dependent sensitivity, the implants were thoroughly characterized, monitoring the dynamic changes in the systems' dimensions, dry and wet mass, PLGA polymer molecular weight, inner & outer morphology as well as pH of the bulk fluids.

Furthermore, as it can be seen in the top row of *Figure V-2*, ibuprofen release was bi-phasic in all cases: irrespective of the type of experimental set-up and renewed bulk fluid volume. No noteworthy burst release was observed in any case. A zero-order release phase (with an about constant drug release rate) started from the beginning. After about 7-10 d, the final rapid release phase began (accounting for about 80 % drug release), leading to complete ibuprofen exhaust. The onset of this final rapid release phase coincided with the onset of substantial implant swelling, as it can be seen in the diagrams in the middle and at the bottom of *Figure V-2*. It has previously been suggested that initially only limited amounts of water are able to penetrate into PLGA-based drug delivery systems, so that drug mobility remains limited (21). Nevertheless, the entire dosage forms are rather rapidly wetted (by small amounts of water), initiating PLGA degradation throughout the system ("bulk erosion"). Upon hydrolytic cleavage of an ester bond of a PLGA chain, 2 shorter chains are created 2 new hydrophilic end groups: an -OH and a -COOH end group. Thus, with time the polymeric system becomes more and more hydrophilic. In addition, the PLGA chains get shorter and, hence, less entangled. Furthermore, water-soluble degradation products create a steadily increasing hydrostatic pressure inside the implant. At a certain time point, these changes result in the penetration of considerable amounts of water into the system, e.g. the volume of the investigated PLGA implants increased by about 500 % after 10 d upon direct exposure to phosphate buffer pH 7.4 (*Figure V-2*, diagram on the left hand side in the middle row). This dramatically changes the conditions for drug release: Ibuprofen is much more mobile in a highly swollen PLGA gel compared to the initially "dry" and dense polymer matrix. Consequently, the drug release rate increases.

It has previously been shown that the presence of a hydrogel surrounding a PLGA implant of similar composition substantially limits implant swelling, resulting in slower drug release (35). This tendency has been confirmed in this study: As it can be seen in the diagrams middle and

at the bottom of *Figure V-2*, system swelling was less pronounced, if the implants were embedded in a gel. The optical macroscopy pictures in *Figure V-3* illustrate these phenomena: The implants underwent substantial swelling after about 7-10 d. This process was particularly pronounced upon direct exposure to the bulk fluid (compared to the agarose gel set-ups).

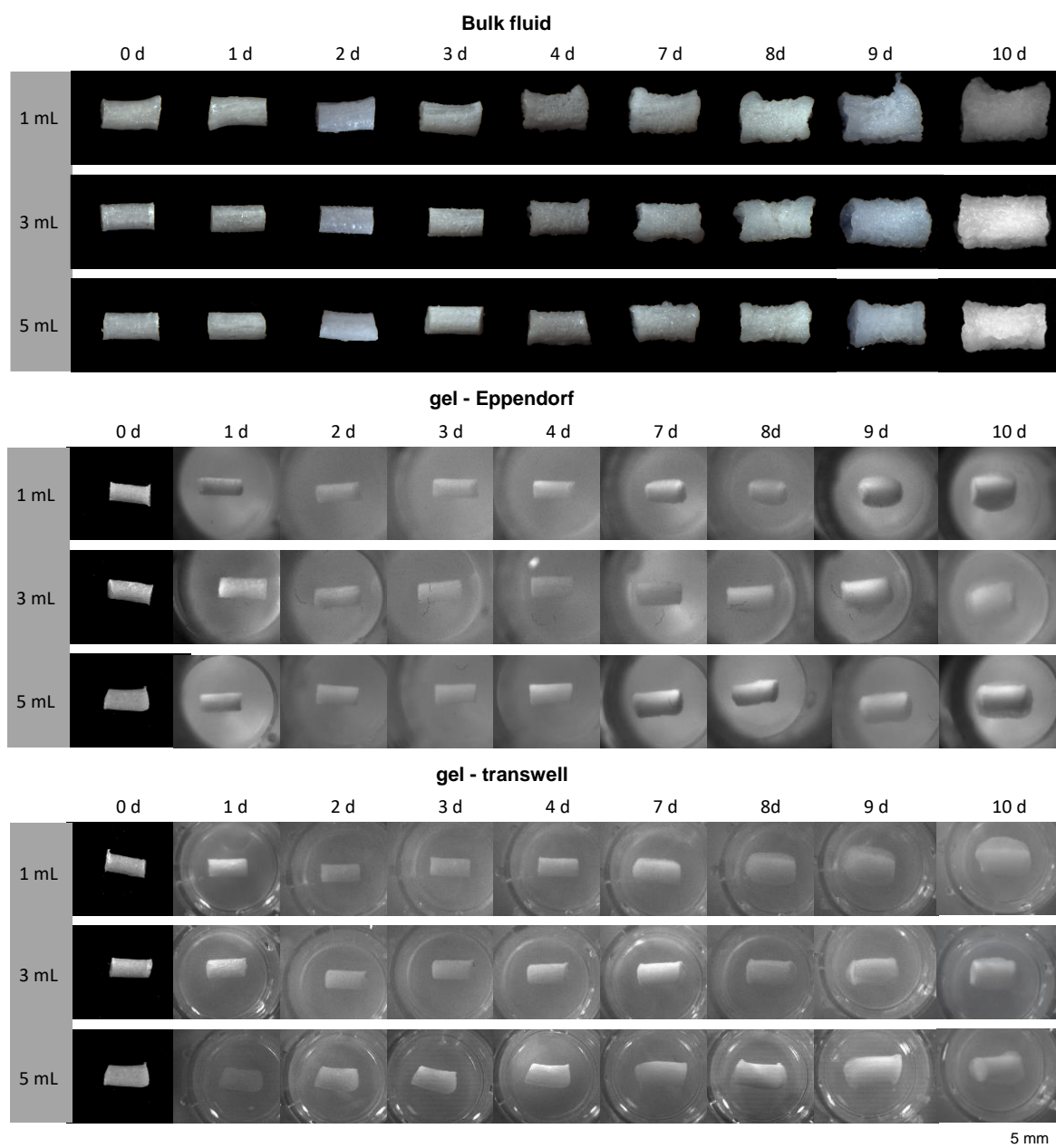


Figure V-3. Optical macroscopy pictures of ibuprofen-loaded PLGA implants after different exposure times to phosphate buffer pH 7.4 using the 3 experimental set-ups. The implants were placed in well agitated bulk fluids in Eppendorf tubes, in agarose gels exposed to well agitated bulk fluid in Eppendorf tubes, or in agarose gels in transwell plates (the receptor compartment containing well-agitated bulk fluid). At pre-determined time points, the entire bulk fluid, or 1 or 3 mL thereof, was renewed (as indicated).

V. HOW BULK FLUID RENEWAL CAN AFFECT DRUG RELEASE FROM PLGA IMPLANTS

The SEM pictures at the top of *Figure V-4* show surfaces and cross-sections of ibuprofen-loaded implants before exposure to the release medium. As it can be seen, the surface was smooth and non-porous (due to the manufacturing process), which can in part explain the absence of any noteworthy burst release. The other SEM pictures in *Figure V-4* show implants which had been directly exposed to the release medium, or embedded within agarose gels for 8 d. Please note that the samples had been freeze-dried before analysis, so artefacts have been created. The pictures of surfaces show highly porous and “folded” structures. These likely result from the drying of highly swollen PLGA gels (35,39,40). The cross-sections indicate that in addition to these highly swollen surface-near regions, much less swollen regions exist, irrespective of the type of set-up at this time point. Please note that the pictures were not systematically taken at similar positions. Importantly, there was no sign for a significant impact of the volume of the replaced bulk fluid on the dynamic changes of the inner and outer implant morphology.

To better understand the sensitivity of drug release on the sampling volume in the case of direct exposure to the release medium and insensitivity in the case of implants which were embedded into agarose gels, also the dynamic changes in the PLGA polymer molecular weight, implants' dry mass and pH of the bulk fluid were studied.

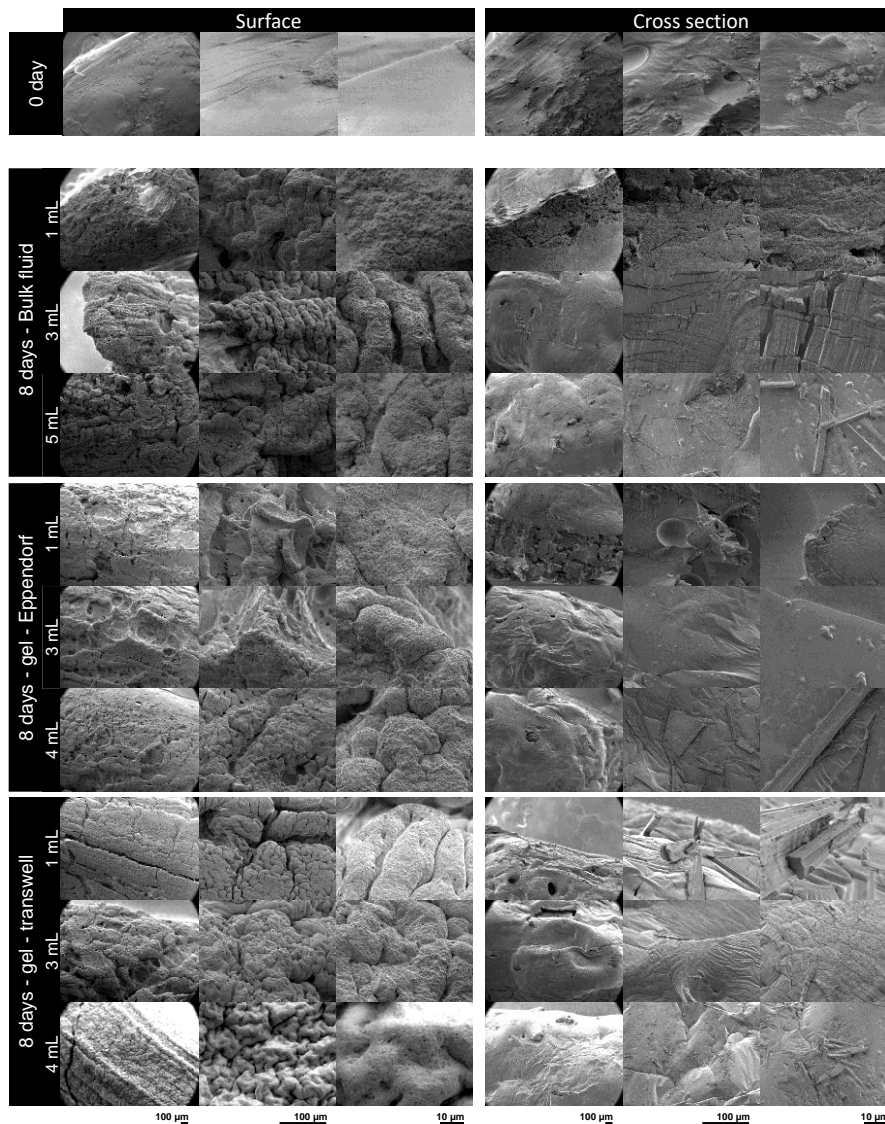


Figure V-4. SEM pictures of surfaces and cross-sections of ibuprofen-loaded PLGA implants before and after 8 days exposure to phosphate buffer pH 7.4 using the 3 experimental set-ups. The implants were placed in well agitated bulk fluids in Eppendorf tubes, in agarose gels exposed to well agitated bulk fluid in Eppendorf tubes, or in agarose gels in transwell plates (the receptor compartment containing well-agitated bulk fluid). At pre-determined time points, the entire bulk fluid, or 1 or 3 mL thereof, was renewed (as indicated). Please note that after exposure to the release medium, the implants were freeze-dried prior to analysis. Thus, caution must be paid due to artefact creation.

V.4.2. PLGA degradation and implant erosion

The diagrams at the top of *Figure V-5* show the pH of the bulk fluids the implants or agarose gels were exposed to, as a function of the exposure time (*Figure V-1*). Green, orange and blue curves indicate complete and partial bulk fluid renewal. As it can be seen, the pH remained about constant during the first 7-10 d, and then temporarily dropped. This can be explained by

V. HOW BULK FLUID RENEWAL CAN AFFECT DRUG RELEASE FROM PLGA IMPLANTS

the release of short chain acids into the bulk fluids. As for the drug, the mobility of these water-soluble compounds fundamentally increases once substantial system swelling sets on. The fact that the temporary pH drop is less pronounced in the case of lower bulk fluid volume renewals can be explained by the lower amounts of withdrawn acids and added bases. Since ibuprofen exhibits strongly pH dependent solubility (*Figure V-6*), it might be that pronounced drops in the pH of the release medium lead to non-sink conditions and, thus, slower drug release. However, in this study, sink conditions were provided in all bulk fluids in all set-ups during the entire observation periods.

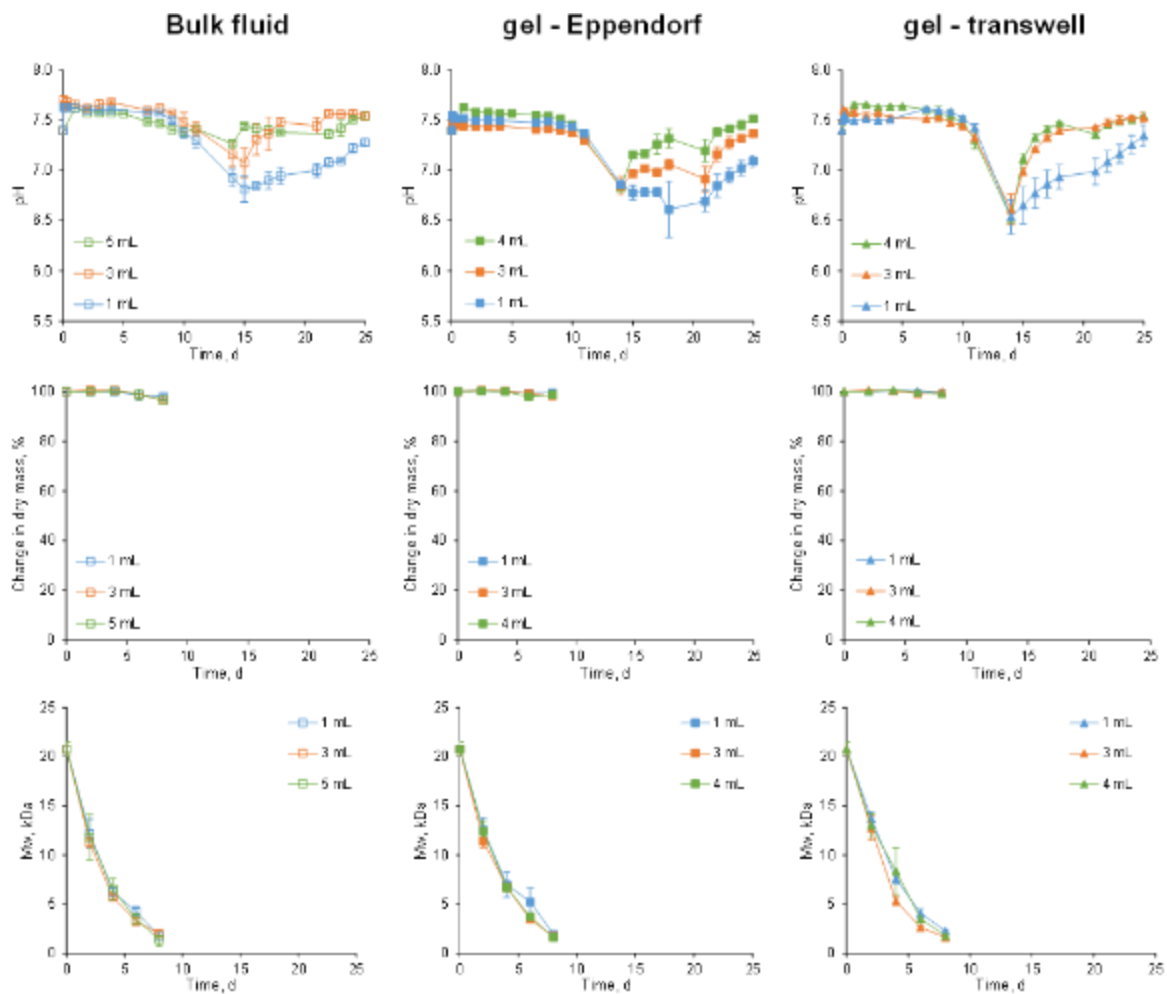


Figure V-5. Dynamic changes in the pH of the well agitated bulk fluid, in the implants' dry mass and PLGA polymer molecular weight (M_w) upon exposure of ibuprofen-loaded implants to phosphate buffer pH 7.4 using the 3 experimental set-ups. The implants were placed in well agitated bulk fluids in Eppendorf tubes, in agarose gels exposed to well agitated bulk fluid in Eppendorf tubes, or in agarose gels in transwell plates (the receptor compartment containing well-agitated bulk fluid). At pre-determined time points, the entire bulk fluid, or 1 or 3 mL thereof, was renewed (as indicated).

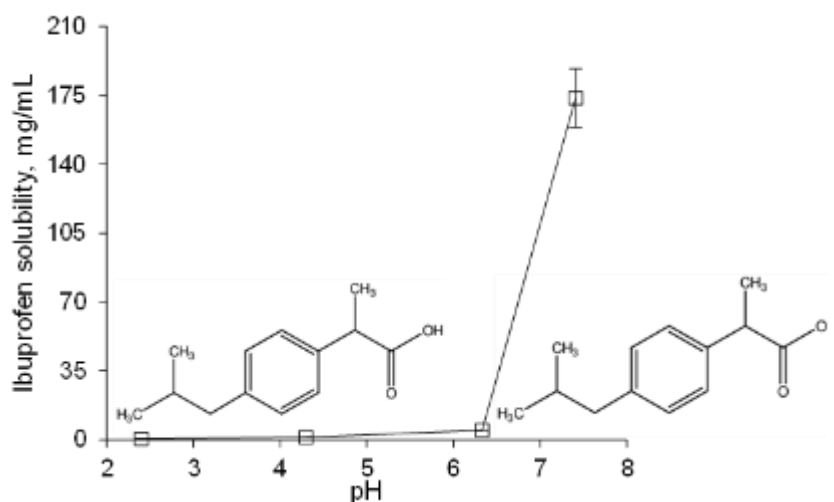


Figure V-6. Dependence of the solubility of ibuprofen as a function of the pH at 37 °C. Phosphate buffer pH 7.4 USP 42 served as bulk fluid. Its pH was adjusted using of 10 N lactic acid or 0.05 N NaOH (final pH values are reported).

Importantly, the sampling volume did not affect the dynamic changes in the implants' dry mass and PLGA polymer molecular weight during the first 8 d upon direct exposure to phosphate buffer pH 7.4 or agarose gels (*Figure V-5*, diagrams in the middle and at the bottom). However, the implants became very fragile with time: The highly swollen implants were difficult to handle. During bulk fluid removal, the systems were rather well protected when embedded in an agarose gel and the risk of accidental damage during sampling was limited. In contrast, in the case of implants which were directly exposed to the phosphate buffer in Eppendorf tubes, the bulk fluid removal became more and more delicate with time: Especially, if the entire release medium was to be replaced. This accelerated implant disintegration (visual observation) and was the reason why most of the measurements had to be stopped after 8 d. The partial disintegration of the highly swollen PLGA gel led to a decrease in the length of the diffusion pathways to be overcome by the drug to be released. Consequently, ibuprofen release was accelerated. In contrast, the agarose gel effectively protected the implants. In addition, the presence of the agarose gels slowed down implant swelling (*Figure V-2*, diagrams in the middle and bottom rows). So, the observed sensitivity of drug release from the investigated PLGA implants to the sampling volume in the case of direct exposure to the release medium can likely be attributed to the mechanical stress experienced by the systems during complete bulk fluid renewal.

V.5. Conclusions

Great caution has to be paid when defining the conditions for in vitro drug release measurements from PLGA implants: The systems become highly fragile once substantial polymer swelling sets on. The renewal of important parts of the release medium can cause partial damage of the highly fragile polymeric systems, accelerating device disintegration and decreasing the length of the diffusion pathways for the drug to be overcome. Embedding implants into agarose gels and limiting the sampling volume can limit these effects. In any case, it must not be forgotten that, once substantial system swelling sets on, the devices become highly fragile.

V.6. Acknowledgments

This project has received funding from the Interreg 2 Seas programme 2014-2020 co-funded by the European Regional Development Fund under subsidy contract No 2S04-014 3DMed. The authors are very grateful for this support. They would also like to thank Mr. A. Fadel from the “Centre Commun de Microscopie” of the University of Lille (“Plateau technique de la Federation Chevreul CNRS FR 2638”) for his valuable technical help with the SEM pictures.

V.7. Author statement

C. Bassand	Investigation; Methodology; Validation; Conceptualization; Writing - Original Draft; Visualization
L. Benabed	Investigation
J. Freitag	Investigation
J. Verin	Investigation; Methodology, Validation
F. Siepman	Conceptualization; Methodology; Supervision; Resources; Writing - Review & Editing; Visualization; Project administration; Funding acquisition
J. Siepman	Conceptualization; Methodology; Supervision; Resources; Writing - Review & Editing; Visualization; Project administration; Funding acquisition

V.8. References

1. Shah NH, Railkar AS, Chen FC, Tarantino R, Kumar S, Murjani M, et al. A biodegradable injectable implant for delivering micro and macromolecules using poly (lactic-co-glycolic) acid (PLGA) copolymers. *J Controlled Release*. 1993 Nov 1;27(2):139–47.
2. Nair LS, Laurencin CT. Biodegradable polymers as biomaterials. *Prog Polym Sci*. 2007 Aug 1;32(8):762–98.
3. Grund S, Bauer M, Fischer D. Polymers in Drug Delivery—State of the Art and Future Trends. *Adv Eng Mater*. 2011;13(3):B61–87.
4. Dorta MJ, Santoveña A, Llabrés M, Fariña JB. Potential applications of PLGA film-implants in modulating in vitro drugs release. *Int J Pharm*. 2002 Nov 6;248(1):149–56.
5. Ochi M, Wan B, Bao Q, Burgess DJ. Influence of PLGA molecular weight distribution on leuprolide release from microspheres. *Int J Pharm*. 2021 Apr 15;599:120450.
6. McConville C, Tawari P, Wang W. Hot melt extruded and injection moulded disulfiram-loaded PLGA millirods for the treatment of glioblastoma multiforme via stereotactic injection. *Int J Pharm*. 2015 Oct 15;494(1):73–82.
7. Hamoudi-Ben Yelles MC, Tran Tan V, Danede F, Willart JF, Siepmann J. PLGA implants: How Poloxamer/PEO addition slows down or accelerates polymer degradation and drug release. *J Control Release Off J Control Release Soc*. 2017 May 10;253:19–29.
8. Guo T, Lim CG, Noshin M, Ringel JP, Fisher JP. 3D printing bioactive PLGA scaffolds using DMSO as a removable solvent. *Bioprinting*. 2018 Jun 1;10:e00038.
9. Fredenberg S, Wahlgren M, Reslow M, Axelsson A. The mechanisms of drug release in poly(lactic-co-glycolic acid)-based drug delivery systems—A review. *Int J Pharm*. 2011 Aug 30;415(1):34–52.
10. Siepmann J, Elkharraz K, Siepmann F, Klose D. How autocatalysis accelerates drug release from PLGA-based microparticles: a quantitative treatment. *Biomacromolecules*. 2005 Aug;6(4):2312–9.
11. Burkersroda F von, Schedl L, Göpferich A. Why degradable polymers undergo surface erosion or bulk erosion. *Biomaterials*. 2002 Nov 1;23(21):4221–31.
12. Siepmann J, Siepmann F. Sink conditions do not guarantee the absence of saturation effects. *Int J Pharm*. 2020 Mar 15;577:119009.
13. Ding AG, Shenderova A, Schwendeman SP. Prediction of Microclimate pH in Poly(lactic-co-glycolic Acid) Films. *J Am Chem Soc*. 2006 Apr 1;128(16):5384–90.
14. Chen W, Palazzo A, Hennink WE, Kok RJ. Effect of Particle Size on Drug Loading and Release Kinetics of Gefitinib-Loaded PLGA Microspheres. *Mol Pharm*. 2017 Feb 6;14(2):459–67.

V. HOW BULK FLUID RENEWAL CAN AFFECT DRUG RELEASE FROM PLGA IMPLANTS

15. Ford Versypt AN, Pack DW, Braatz RD. Mathematical modeling of drug delivery from autocatalytically degradable PLGA microspheres--a review. *J Control Release Off J Control Release Soc.* 2013 Jan 10;165(1):29–37.
16. Antheunis H, van der Meer J-C, de Geus M, Heise A, Koning CE. Autocatalytic Equation Describing the Change in Molecular Weight during Hydrolytic Degradation of Aliphatic Polyesters. *Biomacromolecules.* 2010 Apr 12;11(4):1118–24.
17. Hu Z, Liu Y, Yuan W, Wu F, Su J, Jin T. Effect of bases with different solubility on the release behavior of risperidone loaded PLGA microspheres. *Colloids Surf B Biointerfaces.* 2011 Aug 1;86(1):206–11.
18. Faisant N, Akiki J, Siepmann F, Benoit JP, Siepmann J. Effects of the type of release medium on drug release from PLGA-based microparticles: Experiment and theory. *Int J Pharm.* 2006 May 18;314(2):189–97.
19. Huang J, Mazzara JM, Schwendeman SP, Thouless MD. Self-healing of pores in PLGAs. *J Controlled Release.* 2015 May 28;206:20–9.
20. Kim HK, Chung HJ, Park TG. Biodegradable polymeric microspheres with “open/closed” pores for sustained release of human growth hormone. *J Controlled Release.* 2006 May 15;112(2):167–74.
21. Bode C, Kranz H, Fizez A, Siepmann F, Siepmann J. Often neglected: PLGA/PLA swelling orchestrates drug release: HME implants. *J Controlled Release.* 2019 Jul 28;306:97–107.
22. Tamani F, Bassand C, Hamoudi MC, Danede F, Willart JF, Siepmann F, et al. Mechanistic explanation of the (up to) 3 release phases of PLGA microparticles: Diprophylline dispersions. *Int J Pharm.* 2019 Dec 15;572:118819.
23. Gasmi H, Danede F, Siepmann J, Siepmann F. Does PLGA microparticle swelling control drug release? New insight based on single particle swelling studies. *J Controlled Release.* 2015 Sep 10;213:120–7.
24. Gu B, Sun X, Papadimitrakopoulos F, Burgess DJ. Seeing is believing, PLGA microsphere degradation revealed in PLGA microsphere/PVA hydrogel composites. *J Controlled Release.* 2016 Apr 28;228:170–8.
25. Bode C, Kranz H, Siepmann F, Siepmann J. Coloring of PLGA implants to better understand the underlying drug release mechanisms. *Int J Pharm.* 2019 Oct 5;569:118563.
26. Brunner A, Mäder K, Göpferich A. pH and osmotic pressure inside biodegradable microspheres during erosion. *Pharm Res.* 1999 Jun;16(6):847–53.
27. Matsumoto A, Matsukawa Y, Suzuki T, Yoshino H. Drug release characteristics of multi-reservoir type microspheres with poly(dl-lactide-co-glycolide) and poly(dl-lactide). *J Control Release Off J Control Release Soc.* 2005 Aug 18;106(1–2):172–80.
28. Ghalanbor Z, Körber M, Bodmeier R. Interdependency of protein-release completeness and polymer degradation in PLGA-based implants. *Eur J Pharm Biopharm.* 2013 Nov 1;85(3, Part A):624–30.

29. Gosau M, Müller BW. Release of gentamicin sulphate from biodegradable PLGA-implants produced by hot melt extrusion. *Pharm.* 2010 Jul;65(7):487–92.
30. Li L, Li C, Zhou J. Effective sustained release of 5-FU-loaded PLGA implant for improving therapeutic index of 5-FU in colon tumor. *Int J Pharm.* 2018 Oct 25;550(1):380–7.
31. Blasi P, Schoubben A, Giovagnoli S, Perioli L, Ricci M, Rossi C. Ketoprofen poly(lactide-co-glycolide) physical interaction. *AAPS PharmSciTech.* 2007 Jun;8(2):E78–85.
32. Kožák J, Rabišková M, Lamprecht A. In-vitro drug release testing of parenteral formulations via an agarose gel envelope to closer mimic tissue firmness. *Int J Pharm.* 2021 Feb 1;594:120142.
33. Klose D, Azaroual N, Siepmann F, Vermeersch G, Siepmann J. Towards More Realistic In Vitro Release Measurement Techniques for Biodegradable Microparticles. *Pharm Res.* 2008 Oct 29;26(3):691.
34. Leung DH, Kapoor Y, Alleyne C, Walsh E, Leithead A, Habulihaz B, et al. Development of a Convenient In Vitro Gel Diffusion Model for Predicting the In Vivo Performance of Subcutaneous Parenteral Formulations of Large and Small Molecules. *AAPS PharmSciTech.* 2017 Aug;18(6):2203–13.
35. Bassand C, Verin J, Lamatsch M, Siepmann F, Siepmann J. How hydrogels surrounding PLGA implants limit swelling and slow down drug release. *Journal of Controlled Release - Submitted.* 2021;
36. Østergaard J. UV imaging in pharmaceutical analysis. *J Pharm Biomed Anal.* 2018 Jan 5;147:140–8.
37. Jensen SS, Jensen H, Goodall DM, Østergaard J. Performance characteristics of UV imaging instrumentation for diffusion, dissolution and release testing studies. *J Pharm Biomed Anal.* 2016 Nov 30;131:113–23.
38. Sun Y, Jensen H, Petersen NJ, Larsen SW, Østergaard J. Phase separation of in situ forming poly (lactide-co-glycolide acid) implants investigated using a hydrogel-based subcutaneous tissue surrogate and UV-vis imaging. *J Pharm Biomed Anal.* 2017 Oct 25;145:682–91.
39. Bassand C, Benabed L, Verin J, Danede F, Willart J-F, Siepmann F, et al. Hot melt extruded ibuprofen-loaded PLGA implants: Importance of heat exposure. *Journal of Drug Delivery Science and Technology - Submitted.* 2021;
40. Bassand C, Freitag J, Benabed L, Verin J, Siepmann F, Siepmann J. PLGA implants for controlled drug release: Impact of the diameter. *European Journal of Pharmaceutics and Biopharmaceutics - Submitted.* 2021;

**VI. 3D PRINTING OF IBUPROFEN LOADED
CONTROLLED RELEASE IMPLANTS
WITH PLGA – PROOF OF CONCEPT AND
IMPACT FILLING PATTERN ON DRUG
RELEASE**

VI. 3D PRINTING OF IBUPROFEN LOADED CONTROLLED RELEASE IMPLANTS WITH PLGA – PROOF OF CONCEPT AND IMPACT FILLING PATTERN

Research article – To be reviewed by the co-authors

3D printing of ibuprofen loaded controlled release implants with PLGA – Proof of concept and impact filling pattern on drug release

C. Bassand¹, L. Benabed¹, S. Charlon², M. Nagalakshmaiah², C. Samuel², F. Siepmann¹,
J. Soulestin², J. Siepmann¹

¹*Univ. Lille, Inserm, CHU Lille, U1008, F-59000 Lille, France*

²*IMT Lille Douai, Dept Polymers & Composites Technol & Mech Engn, F-59500 Douai, France*

VI.1. Abstract

This study aimed to determine the impact of heating treatment by fused filament fabrication (FFF) on poly (lactic-co-glycolic acid) (PLGA) properties and to investigate the impact of filling pattern on in vitro drug release from printed ibuprofen loaded PLGA implants. To do so, the interaction between the PLGA and Ibuprofen was investigated by differential scanning calorimetry and thermogravimetric analysis. The viscoelastic properties of the melt polymer and Ibuprofen PLGA mixture were investigated by rheology temperature sweep experiments. Ibuprofen-loaded PLGA filaments were produced by hot-melt extrusion (HME) using a Leistritz Nano 16 twin-screw extruder coupled with a laser sensor Tolerance Puller Noztek[®]. Those filaments were used to investigate the impact of temperature applied by 3D printing, via fused filament fabrication (FFF) with a Volumic[®] printer, on PLGA molecular weight and ibuprofen content. PLGA ibuprofen mixture was suitable for 3D printing, as their viscoelastic properties allow to (i) obtain ibuprofen loaded filaments by HME, (ii) 3D printing with temperature from 115°C to 150°C without any substantial loss of PLGA molecular weight or ibuprofen content (iii) obtain ibuprofen loaded implants with three different internal structures. The *in vitro* performance of the different 3D printed implants was investigated after exposure to phosphate buffer pH 7.4 37°C 80 RPM. Absolute and relative drug release, increase in wet mass, pH in the release medium, and morphology of those implants after exposure to the release medium were investigated. The obtained ibuprofen-loaded 3D printed PLGA implants allow to maintain the release of ibuprofen for up to 9 days, with a monophasic release pattern.

Keywords: PLGA, 3D printing, melt rheology, infill pattern, fused deposition modeling, drug release

VI. 3D PRINTING OF IBUPROFEN LOADED CONTROLLED RELEASE IMPLANTS WITH PLGA – PROOF OF CONCEPT AND IMPACT FILLING PATTERN

VI.2. Introduction

Three-dimension printing technologies are additives manufacturing technics, able to produce various 3D products (1). The final object is formed either by deposition, binding, or polymerization of materials in successive layers (1,2). There is a different way to classify 3D printing technologies, the most common one counts seven different ones depending on how the object is produced: photopolymerization, powder bed fusion, material jetting, direct energy deposition, binder jetting, selective deposition lamination, and material extrusion (1,2). Among them, five have been used in the pharmaceuticals fields either on research or in FDA approved products such as SPRITAM (2,3): photopolymerization (4–7), powder bed fusion (8–12), material extrusion (13–18), material jetting (19,20), binder jetting (21,22).

3D printing technologies have demonstrated high flexibility in the preparation of dosage forms such as: combining different drug substances (17), personalized devices (18), reaching complex patterns (23)... Conventional pharmaceutical technologies allow modulating the release pattern, by playing on the size of classical shape devices (24–27) or the choice of the appropriate carrier (28–30). With the right choice of polymer and technology, it might be possible to precisely modulate drug release by taking advantage of the precision of 3D printing technologies to modulate the internal structure, reaching complex geometries (31), etc...

The applicability of 3D printing technologies on controlled drug delivery has been widely studied for oral dosage forms (13,16,17). Compared to oral delivery while only a few studies focus on PLGA based 3D printed controlled drug delivery devices (32–35) for parenteral delivery. Yet PLGA is widely used as a matrix former for controlled drug release, with conventional pharmaceutical technologies/ microparticles (28,29,36), implants (30,37), in situ forming implants (38–40). Due to its biocompatibility and complete biodegradability, it is widely used in different FDA-approved products (29). Drug release kinetics from such devices is mainly influenced by the type of drug, polymer grade, size of the device (24,25,28). The use of 3D printing technologies with PLGA could bring a new opportunity to modulate drug release kinetics.

Fused filament fabrication (FFF) is based on the fused deposition modeling developed and patented by L. Crump and S. Scott in 1989 (41,42). These technologies use a continuous filament of thermoplastic material as the base material. The filament is fed by a spool, via a heated, mobile printer extrusion head, often referred to as an extruder. The molten material is expelled from the extrusion nozzle and deposited first on a 3D printing platform, which can be

heated to ensure good adhesion. Once the first layer is complete, the extruder and the platform move away simultaneously and the second layer can then be directly deposited on the part being manufactured (43). thermoplastic behavior of PLGA makes it a good candidate for 3D printing with FFF.

The printability of drug-polymer mixture by extrusion-based technologies can be investigated via the rheological properties of these systems (44). Investigation of the melt rheology properties can contribute to the understanding of the properties of the material that are meaningful for extrusion, injection modeling, and 3D printing (45). Proper melt rheology studies could help to understand and overcome some issues with the sometimes encountered, lack of drug-polymer miscibility, high processing temperature, and poor printability (31).

This study aimed to determine the impact of ibuprofen on viscoelastic properties of PLGA, and the impact of heating treatment by FFF on PLGA molecular weight and drug content. Moreover, ibuprofen-loaded PLGA filaments were prepared by hot-melt extrusion and used to feed a Volumic FFF 3D printer. Thus, implants with different internal structures were produced and exposed to phosphate buffer pH 7.4. Optical macroscopy, gravimetric analysis, DSC, GPC, scanning electron microscopy, and pH measurements were used to monitor the implants' key properties before and after exposure to the release medium.

VI. 3D PRINTING OF IBUPROFEN LOADED CONTROLLED RELEASE IMPLANTS WITH PLGA – PROOF OF CONCEPT AND IMPACT FILLING PATTERN

VI.3. Materials and methods

VI.3.1. Materials

Poly (D,L lactic-co-glycolic acid) (PLGA, 50:50 lactic acid: glycolic acid; Resomer RG 503H; Evonik, Darmstadt; Germany); ibuprofen (BASF, Ludwigshafen, Germany); agarose (genetic analysis grade), tetrahydrofuran (HPLC grade) (Fisher Scientific, Illkirch, France); acetonitrile (VWR, Fontenoy-sous-Bois, France); sodium hydrogen phosphate (Na_2HPO_4 , Panreac Quimica, Barcelona, Spain).

VI.3.2. Differential scanning calorimetry (DSC)

DSC thermograms of the raw materials (PLGA and ibuprofen), their physical mixture (from 5:95 to 20:80; ibuprofen:PLGA), ibuprofen loaded PLGA filaments, and 3D printed implants were recorded using a DCS1 Star System (Mettler Toledo, Greifensee, Switzerland). Approximately 5 mg material were heated in pierced aluminum pans as follows: from -70 to 120 °C, cooling to -70 °C, re-heating to 120 °C (heating/cooling rate = 10 °C/min. The reported glass temperatures (T_g s) were determined from the 2nd heating cycle for the raw materials and the physical mixture. The melting point and the thermograms of the ibuprofen-loaded and 3D printed implant were determined from 1st heating cycle (thermal historic is of interest). All experiments were conducted in triplicate. Mean values +/- standard deviations are reported.

VI.3.3. Thermogravimetric analysis (TGA)

The thermal stability of PLGA, ibuprofen, and their physical mixture (from 5:95 to 20:80; ibuprofen:PLGA), was measured using a (GA 2 system (GF, Mettler Toledo, Greifensee, Switzerland). The mass loss upon heating was obtained for 20-30 mg of samples at 10 °C / min in the temperature range 25 to 750 °C.

VI.3.4. Disc preparation

Appropriate amounts of polymer (milled for 4 x 30 s with a Seb Valentin grinder) and drug were mixed for 5 min at 20 rpm in a Turbula Shaker-Mixer (Sausheim, France). The blends were then mixed with a mortar and a pestle for 2 min. The obtained mixture was filled in aluminium pans (ref 0452155, Grosseron, Couëron, France) of 43 mm diameter, before heating with a MR Hei-Tec hot plate (442-1358, Avantor, Radnor, Pennsylvania, USA) under vacuum to allow moisture evaporation required for rheological studies as described in *Figure 1*, and *Table VI-1*. Pictures of the disc were taken using a SZN-6 trinocular stereo zoom microscope (Optika, Ponteranica, Italy), equipped with an optical camera (Optika Vision Lite 2.1 software).

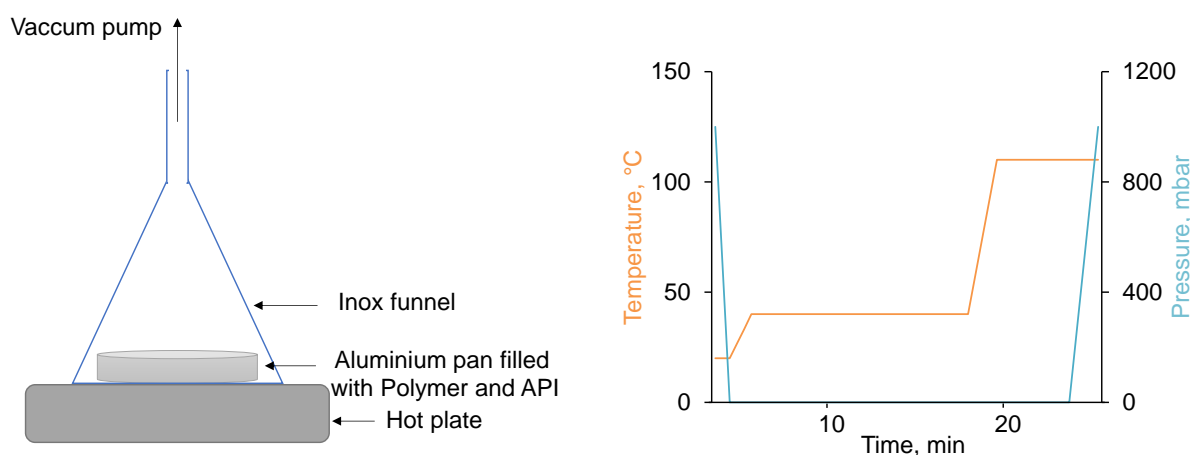


Figure VI-1. Schematic representation of the method used to prepare the polymer discs for melt rheology studies.

Table VI-1. Preparation method of polymer discs for melt rheology studies.

Temperature (°C)	Time (min)	Vaccum
Heating from 20 to 40	1 : 07	
40	15 : 00	
Heating from 40 to 110	1 : 37	Yes
110	5 : 00	
110	2 : 00	No

VI.3.5. Melt rheology

The rheological studies were carried out using an Anton Paar rheometer (MCR 72; Anton Paar®, Les Ulis, France). The temperature sweep experiment was performed in the linear domain, at an oscillation frequency of 10 Hz, a strain of 1%, a gap of 0.800 mm, and using a plane-plane module with a diameter of 25 mm. Data were recorded and analyzed using RheoCompass software. Complex viscosity, storage (G'), and loss (G'') modulus were determined.

VI.3.6. Hot-melt extrusion

The PLGA was milled (4 x 30 s) with a grinder (Valentin, Seb, Ecully, France). Appropriate amounts of polymer and ibuprofen were mixed and then pre-melted in a crystallizer on a film



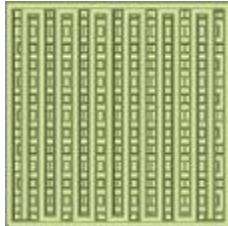
VI. 3D PRINTING OF IBUPROFEN LOADED CONTROLLED RELEASE IMPLANTS WITH PLGA – PROOF OF CONCEPT AND IMPACT FILLING PATTERN

applicator hot plate (110 °C, 6 min, Erichsen, Rueil-Malmaison, France), followed by extrusion using a Nano 16 twin-screw extruder (screw diameter = 16 mm, length/diameter ratio = 26.25, feeder flow regulator set at a speed between 5 and 8 cc/min; Leistritz, Nuremberg, Germany), equipped with a 4 mm diameter die. The process temperatures were kept constant at 70 - 75 - 70 - 65 °C (die - zone 3 - zone 2 - zone 1). The screw speed was set at 50 rpm. The diameter of the filament obtained at the exit of the extruder was controlled by a laser sensor (target diameter between 1.60 and 1.80 mm, Tolerance Puller Noztek, Shoreham-by-Sea, United Kingdom).

VI.3.7. 3D printing test

The filaments obtained were used to feed the Volumic® 30 Stream Ultra printer (Volumic, Nice, France). Parallelepiped-shaped implants with dimensions of 2 mm x 2 mm x 0.5 mm were printed with printing temperatures ranging from 115 °C to 150 °C. Parallelepiped-shaped implants with dimensions of 10 mm x 10 mm x 2.5 mm and different filling patterns were printed according to the parameters described in *Table VI-2*.

Table VI-2. Printing parameters used to obtain the ibuprofen loaded PLGA-implant.

	Hexagonal	Cross	Zigzag
Filling pattern			
Number of contour layers	1		
Number of lower and upper layers	1		
Filling density (%)	30		
Nozzle diameter (mm)	0.25		
Layer thickness (mm)	0.25		
Printing temperature (°C)	1 st layer: 125 Next layers: 115		
Printing speed (mm/s)	50		
Bed temperature (°C)	30		
Ventilation (%)	10		
Retraction speed (mm/s)	40		

VI.3.8. Practical drug loading

Pieces of filaments and 3D printed object were dissolved in 5 mL acetonitrile, followed by filtering (PVDF syringe filters, 0.45 μm ; Agilent Technologies, Santa Clara, USA) and drug content determination by HPLC-UV analysis using a Thermo Fisher Scientific Ultimate 3000 Series HPLC, equipped with a LPG 3400 SD/RS pump, an autosampler (WPS-3000 SL) and a UV-Vis detector (VWD-3400RS) (Thermo Fisher Scientific, Waltham, USA). A reversed-phase column C18 (Gemini 5 μm ; 110 Å ; 150 x 4.6 mm; Phenomenex, Le Pecq, France) was used. The mobile phase was a mixture of 30 mM Na_2HPO_4 pH 7.0: acetonitrile (60:40, v:v). The detection wavelength was 225 nm, and the flow rate was 0.5 mL/min. Ten microliter samples were injected. Each experiment was conducted in triplicate. Mean values \pm standard deviations are reported.

VI.3.9. Gel permeation chromatography (GPC)

The average polymer molecular weight (M_w) of the PLGA was determined by gel permeation chromatography (GPC) as follows: raw materials, samples were dissolved in tetrahydrofuran (3 mg/mL). Fifty μL samples were injected into an Alliance GPC (refractometer detector: 2414 RI, separation module e2695, Empower GPC software; Waters, Milford, USA), equipped with a PLgel 5 μm MIXED-D column (kept at 35°C, 7.8 x 300 mm; Agilent). Tetrahydrofuran was the mobile phase (flow rate: 1 mL/min). Polystyrene standards with molecular weights between 1,480 and 70,950 Da (Polymer Laboratories, Varian, Les Ulis, France) were used to prepare the calibration curve. All experiments were conducted in triplicate. Mean values \pm standard deviations are reported.

VI.3.10. In vitro drug release

Implants were placed in 50 mL tubes (352070 Corning-Falcon, New York, U.S; 1 implant per tube), filled with 50 mL phosphate buffer pH 7.4 USP 42. The tubes were placed in a horizontal shaker (80 rpm, 37°C; GFL 3033; Gesellschaft fuer Labortechnik, Burgwedel, Germany). At predetermined time points, the entire bulk fluid was replaced by fresh release medium. The withdrawn samples were filtered (PVDF syringe filter, 0.45 μm ; Agilent, Santa Clara, California, USA) and analyzed for their ibuprofen contents by HPLC-UV, as described in *section VI.3.8*.

In all cases, at pre-determined time points, pictures were taken as described in *section VI.3.4*. and the pH of the release medium was measured using a pH meter (InoLab pH Level 1; WTW, Weilheim, Germany). Also, in all cases, sink conditions were provided throughout the

VI. 3D PRINTING OF IBUPROFEN LOADED CONTROLLED RELEASE IMPLANTS WITH PLGA – PROOF OF CONCEPT AND IMPACT FILLING PATTERN

experiments in all agitated bulk fluids. All experiments were conducted in triplicate. Mean values +/- standard deviations are reported.

VI.3.11. Implant swelling

Implants were treated as for the *in vitro* drug release measurements. At pre-determined time points: implant samples were withdrawn and excess water was carefully removed using Kimtech precision wipes (Kimberly-Clark, Rouen, France). The implants were weighed [*wet mass (t)*], and the *change in wet mass (%) (t)* was calculated as follows:

$$\text{change in wet mass } (\%)(t) = \frac{\text{wet mass } (t) - \text{mass } (t = 0)}{\text{mass } (t = 0)} \times 100 \%$$

where *mass (t = 0)* denotes the implant mass before exposure to the release medium.

All experiments were conducted in triplicate. Mean values +/- standard deviations are reported.

VI.4. Results and discussion

This study aimed to better understand the impact of the heating treatment of PLGA ibuprofen mixture on the viscoelastic properties, molecular weight of the polymer, and drug content. Thus, the use of PLGA and ibuprofen as feed materials for 3D printing by FFF was investigated. The impact of the internal structure of 3D printing ibuprofen-loaded PLGA implants on system performance upon exposure to phosphate buffer pH 7.4 was investigated, in particular in light of the resulting drug release kinetics.

VI.4.1. Raw materials characterization

To assess the impact of the percentage of ibuprofen on the thermal behavior of the mixture, the thermograms of the raw materials, and the various ratios of PLGA and ibuprofen, PLGA Tg variation over ibuprofen content, as well as the loss of mass obtained by thermogravimetry are presented in *Figure VI-2*.

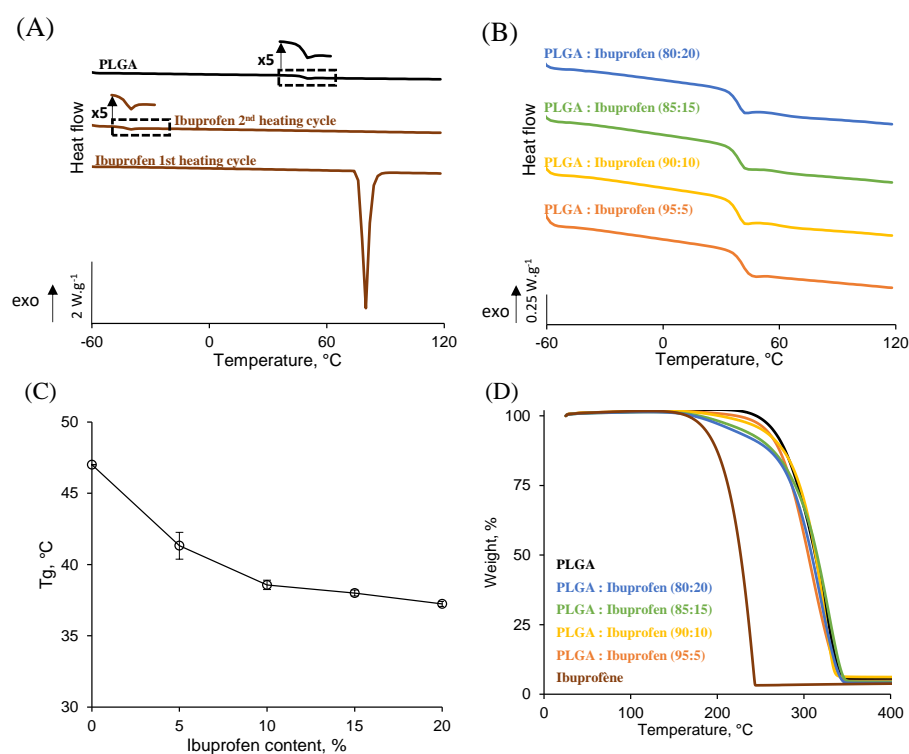


Figure VI-2. Thermograms of (A) the raw materials, (B) their physical mixture, (C) impact of the ibuprofen content on PLGA glass transition temperature measured by differential scanning calorimetry, and (D) PLGA, ibuprofen, and PLGA/ibuprofen physical mixture loss of mass upon heating, obtained by thermogravimetric analysis.

The presence of a melting point of ibuprofen during the first heating cycle confirms its crystalline state. During the second heating cycle, the absence of this melting point in favor of

VI. 3D PRINTING OF IBUPROFEN LOADED CONTROLLED RELEASE IMPLANTS WITH PLGA – PROOF OF CONCEPT AND IMPACT FILLING PATTERN

a glass transition temperature could be observed. The thermograms obtained during the second DSC heating of the physical mixtures of PLGA and ibuprofen, each show a single glass transition and the absence of a melting event. There is therefore complete amorphization of ibuprofen, as well as it is in the polymer matrix. Interestingly, a decrease of PLGA glass transition temperature with ibuprofen content is observed, indicating its plasticizing effect, which has been reported before (39,46). It could be taken as an advantage for lowering the 3D printing temperature of PLGA. However, for a mixture containing 20% of ibuprofen, it has been noticed, that a non-homogeneous amorphous mixture is in place, with the presence of two glass transition temperatures, indicating that this could be the limit of solubility of ibuprofen in PLGA. Regarding these results, it has been decided to continue the study with a special focus on ibuprofen content corresponding to 15%.

The TGA results (*Figure VI-2D*) show that the mass loss of ibuprofen begins at approximately 160 ° C. This is probably due to its evaporation rather than its degradation, as it has been reported to have a boiling point of 157 ° C, and its degradation to be in a range between 180 ° C and 300 ° C (47). On the other hand, if the mass loss of PLGA begins at temperatures around 250 ° C, this does not give any indication of the state of degradation (shortening of polymer chains) of PLGA at lower temperatures. The degradation being linked to a scission of the bonds of the polymer chains influences the molar mass but not necessarily the total mass. For 3D printing, the factors limiting the maximum printing temperature appear to be the evaporation temperature of ibuprofen and the state of degradation of the PLGA chains.

VI.4.2. Melt rheology studies

Pure PLGA discs and 15% ibuprofen-loaded PLGA discs have been investigated for melt rheology study. It is important to note that the setup used to obtain the polymer discs, allows manufacturing discs without any air bubbles. The process used (*Figure VI-1*), allows moisture evaporation (by heating under vacuum at a temperature below the T_g of the polymer), before melting the polymer. When studying rheological behavior, it is of great importance that the material is exempt from any air bubbles and moisture (45). Importantly, the experiments have been conducted in the linear range of both investigated materials (data not shown).

Figure VI-3 shows the complex viscosity of the pure PLGA and ibuprofen PLGA mixture over-temperature, and their viscoelastic behavior. The plasticizing effect of ibuprofen on PLGA observed in *Figure VI-2C*, is also confirmed with the melt rheology experiments. For the same temperatures, the addition of ibuprofen leads to a drop of the complex viscosity and storage and

loss modulus (*Figure VI-3B*). Ibuprofen by inserting itself between the macromolecular chains and by reducing polymer-polymer interactions in favor of polymer-plasticizer interactions facilitate the polymer chains mobility. The plasticizing effect of ibuprofen induced by hydrogen bridges has been described in the literature on certain polymers such as Eudragit® RS 30D (48,49) or ethyl cellulose (50), but also PLGA Resomer 502H and 503H (39,46). By increasing the temperature, the polymer chains increase, as well as the free volume around the polymer chains. Thus, leading to easier molecular mobility and then decreases viscosity (51). Moreover, for PLGA and PLGA ibuprofen mixture, the investigation is made in a range of temperatures above the T_g value, and in each case, the mixture behaves like a solution with a loss modulus G'' value higher than storage modulus G' .

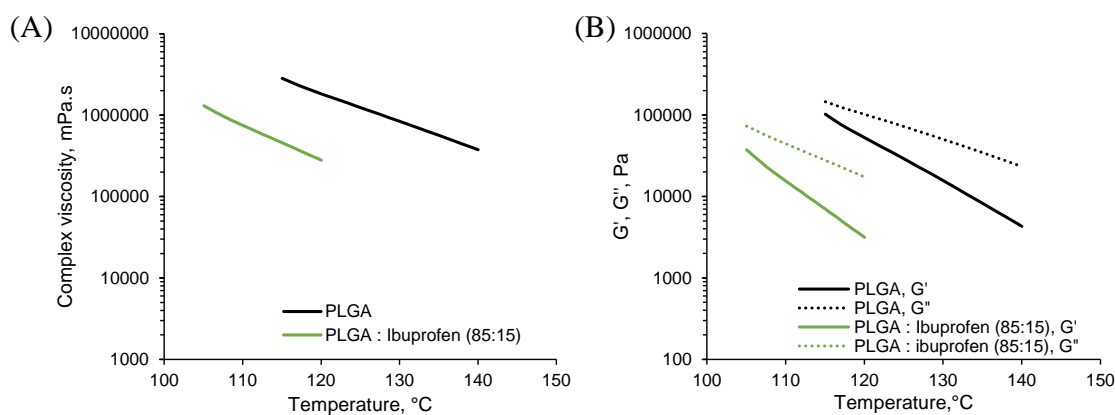


Figure VI-3. Effect of temperature on (A) PLGA and PLGA: ibuprofen (85:15) complex viscosity and (B) storage G' and loss G'' modulus.

VI.4.3. Preliminary printing test

PLGA filament loaded with 15% theoretic ibuprofen content has been produced by hot-melt extrusion. Practical drug loading of the filament was $11.4 \pm 0.9 \%$, and the obtain diameter was 1.63 ± 0.10 mm, the molecular weight of the polymer was 21.3 ± 1.3 kDa and its T_g of 33.7 ± 0.6 °C. Please note that the differences observed in the T_g of the filament (± 33 °C for $\pm 11\%$ of ibuprofen) compared to the value of the physical mixture (± 38 °C for 10% of ibuprofen) is because the analysis was done in the first heating cycle for the filament and second heating cycle for the physical mixtures. These filaments have been used as feedstock materials for 3D printing, with extrusion at a temperature ranging from 115 to 150°C.

The impact of the heating treatment of those filaments on the Mw of the PLGA and ibuprofen content was investigated and illustrated in *Figure VI-4*. Both molecular weight of PLGA and ibuprofen content are not significantly impacted by 3D printing at a temperature ranging from

VI. 3D PRINTING OF IBUPROFEN LOADED CONTROLLED RELEASE IMPLANTS WITH PLGA – PROOF OF CONCEPT AND IMPACT FILLING PATTERN

115°C to 150°C. This might be because the filament is heated for a very short period, leading to a non-significant impact on those parameters. However, as a precautionary measure, it has been chosen to continue the study, by printing the implant at 115°C, which was the lowest temperature allowing the extrusion of the filament, except for the first layer which was printed at 125°C to improve first layer adherence (*Table VI-2*).

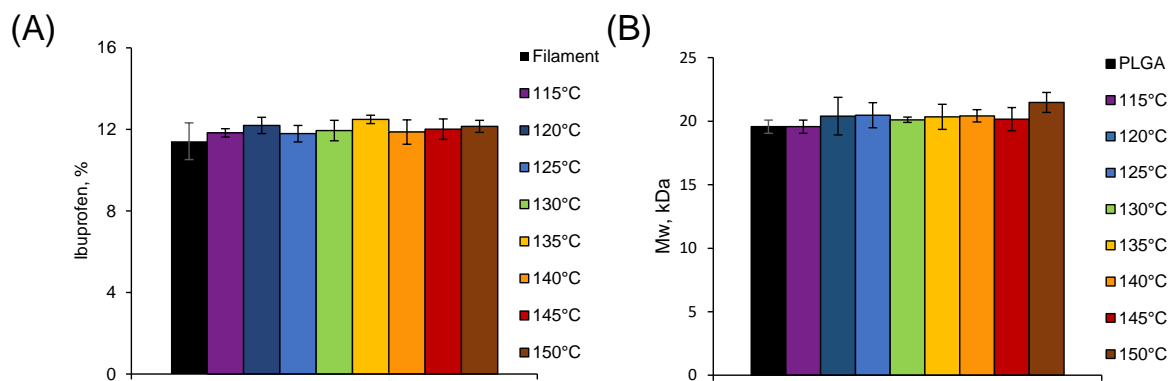


Figure VI-4. Effect of printing temperature on (A) ibuprofen content and (B) PLGA molecular weight.

Implants with different internal structures have been successfully printed using the printing parameters described in *Table VI-2*. *Figure VI-5* shows macroscopic pictures of those implants at different magnifications and their main physicochemical characteristics have been summarized in *Table VI-3*. Compared with the value of the filaments, 3D printing does not significantly impact the polymer molecular weight, Tg nor drug loading. The photos were taken by optical microscope allow to see each fill pattern by transparency. In all cases, the visual appearance of the implant is correct. However, it should be noted that the space inside and/or between the fill patterns makes printing of the last layer particularly difficult. Having no support, the latter can sag in places and the adhesion between lines might be reduced. The three different implants have similar characteristics (drug loading, PLGA molecular weight, height, thickness), except for the weight of the zigzag-filled implants which is slightly lower than the two others due to the difference in internal filling pattern.

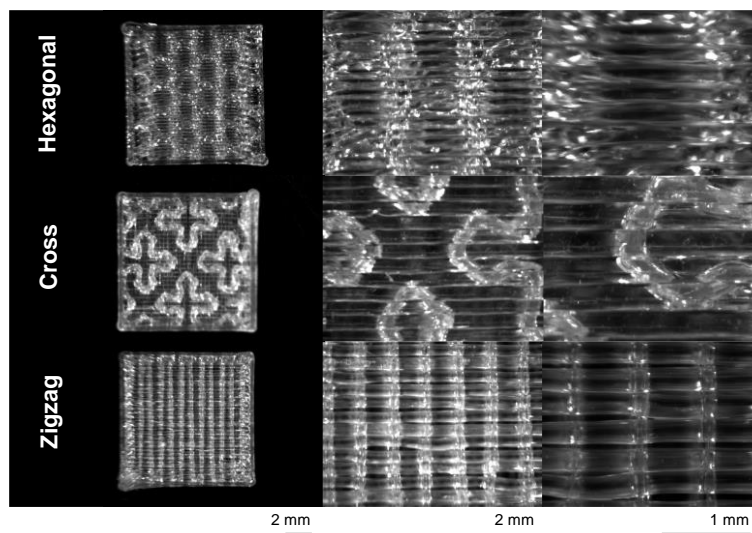


Figure VI-5. Optical macroscopic pictures of the surface of ibuprofen PLGA-implants printed with the three different filling patterns.

Table VI-3. Key properties of the ibuprofen loaded PLGA-implants. (*T_g*: glass transition temperature, *M_w*: molecular weight). Mean values \pm standard deviations are indicated (*Weight, Length, Width, Practical drug loading* $n=6$, *Thickness, T_g, M_w* $n=3$).

	Hexagonal	Cross	Zigzag
Weight (mg)	138.1 \pm 13.5	136.5 \pm 7.1	127.9 \pm 5.9
Length – width (mm)	10.1 \pm 0.1	10.0 \pm 0.1	10.0 \pm 0.1
Thickness (mm)			
Practical drug loading (%)	10.3 \pm 0.6	10.7 \pm 0.5	10.5 \pm 0.3
T_g (°C)	35.7 \pm 0.2	35.8 \pm 0.4	35.8 \pm 0.1
M_w (kDa)	21.7 \pm 0.3	21.5 \pm 0.6	21.7 \pm 0.2

Figure VI-6 shows the DSC thermograms of the different implants and the filament used to print these implants. In every case, the ibuprofen is completely solubilized in the polymer matrix, indicating that the second heating treatment applied to the 3D printer does not seem to affect the interactions between ibuprofen and PLGA.

VI. 3D PRINTING OF IBUPROFEN LOADED CONTROLLED RELEASE IMPLANTS WITH PLGA – PROOF OF CONCEPT AND IMPACT FILLING PATTERN

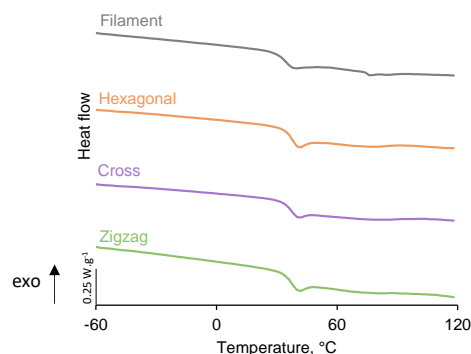


Figure VI-6. Thermograms of the ibuprofen loaded PLGA filaments, and the ibuprofen loaded PLGA 3D printed implants.

VI.4.4. In vitro drug release performance

The in vitro drug release performance of the printed implants upon exposure to phosphate buffer pH 7.4 at 37°C 80 RPM has been investigated. The two top row figures in *Figure VI-7* show the *relative* and *absolute* ibuprofen release rates from the differently filled 3D printed PLGA implants. Clearly, in all cases drug release patterns were similar. In all cases, a monophasic release pattern was observed, with a complete release reach after 9 days of exposure to the release medium. Interestingly, pH in the release medium remain constant during all the in vitro drug release experiments, and no significant differences were observed depending on the filling pattern of the different (*Figure VI-7 C*). *Figure VI-7 D* and *Figure VI-8* illustrate the water uptake and the deformation of the implants upon exposure to the release medium. An important water uptake occurs directly after exposure to the release medium (*Figure VI-7 D*) leading to the swelling of the implant (*Figure VI-8*).

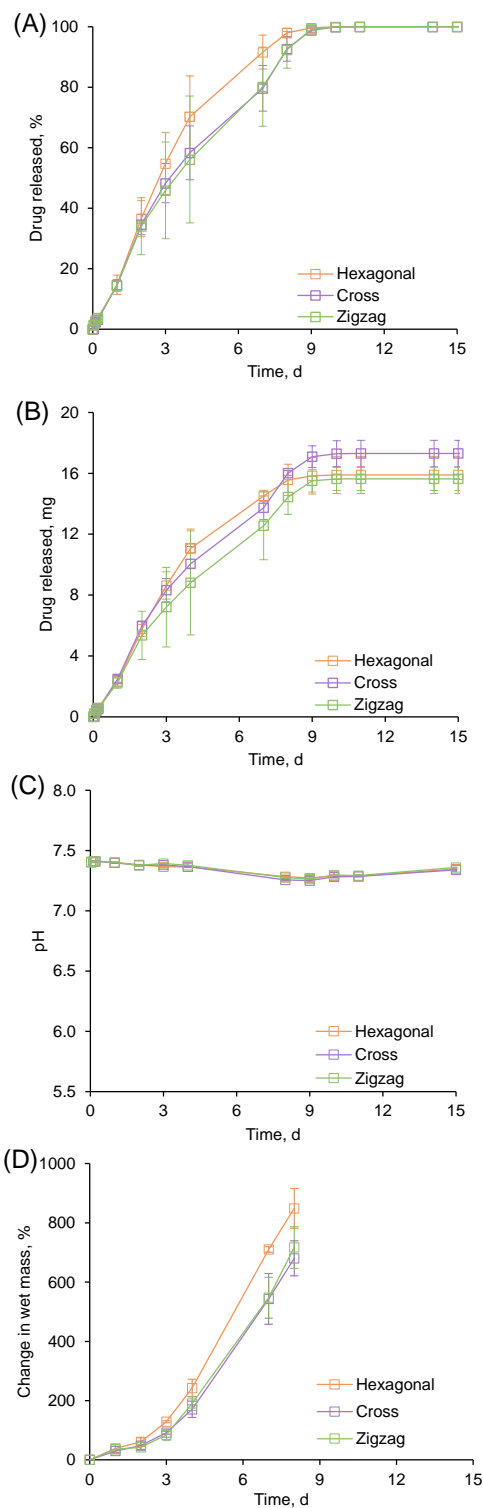


Figure VI-7. (A) Relative (%) and (B) absolute (mg) ibuprofen release from 3D printed PLGA implants, (C) pH changes of the release medium upon exposure to phosphate buffer pH 7.4, and (D) increase in wet mass (%) of the implants after exposure to the release medium.

VI. 3D PRINTING OF IBUPROFEN LOADED CONTROLLED RELEASE IMPLANTS WITH PLGA – PROOF OF CONCEPT AND IMPACT FILLING PATTERN

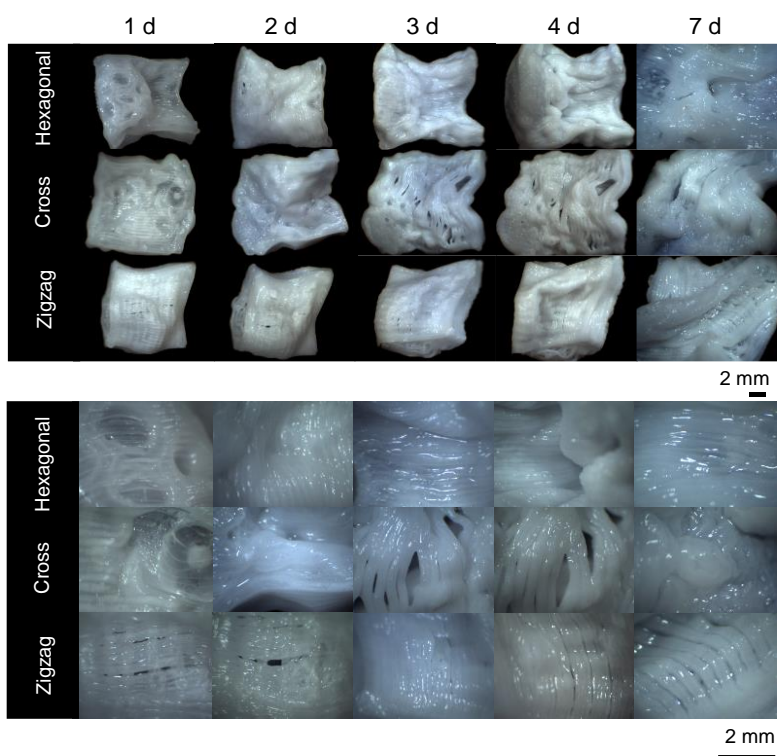


Figure VI-8. Optical macroscopy pictures ibuprofen-loaded PLGA implants upon exposure to phosphate buffer pH 7.4 37°C 80 RPM.

However, as illustrated in *Figure VI-8*, directly after exposure to the release medium, implants are completely unshaped, due to their T_g that is below the temperature of the release medium, leading to the mobility of the polymeric chains, and deformation of the implants. This might explain why release rates are the same whatever the filling pattern. In a recent study, Zhang *et al* demonstrated that ibuprofen release rates from polycaprolactone implants with filling patterns with different angles were similar (52).

VI.5. Conclusion

3D printing by FFF is an interesting tool for the manufacturing of PLGA based control drug delivery devices. The polymer demonstrated viscoelastic properties compatible with the 3D printing technologies. The use of hot-melt extrusion made possible the manufacturing of Ibuprofen-loaded PLGA filament with diameters allowing 3D printing by FFF. Moreover, those filaments were printable without any substantial loss of molecular weight of the polymer nor ibuprofen up to 150°C. 3D printing of implants containing ibuprofen, with three different internal structures was achievable. This leading to the obtention of implants allowing to maintain the release of ibuprofen for up to 9 days, with a monophasic release pattern.

VI.6. Acknowledgments

This project has received funding from the Interreg 2 Seas programme 2014-2020 co-funded by the European Regional Development Fund under subsidy contract No 2S04-014 3DMed. The authors are very grateful for this support.

VI.7. Author statement

C. Bassand	Investigation; Methodology; Validation; Conceptualization; Writing - Original Draft; Visualization
L. Benabed	Investigation; Methodology; Validation
S. Charlon	Writing - Review & Editing; Visualization; Project administration
M. Nagalakshmaiah	Investigation
C. Samuel	Writing - Review & Editing; Visualization; Project administration
F. Siepmann	Conceptualization; Methodology; Supervision; Resources; Writing - Review & Editing; Visualization; Project administration; Funding acquisition
J. Soulestin	Conceptualization; Methodology; Supervision; Resources; Writing - Review & Editing; Visualization; Project administration; Funding acquisition
J. Siepmann	Conceptualization; Methodology; Supervision; Resources; Writing - Review & Editing; Visualization; Project administration; Funding acquisition

VI. 3D PRINTING OF IBUPROFEN LOADED CONTROLLED RELEASE IMPLANTS WITH PLGA – PROOF OF CONCEPT AND IMPACT FILLING PATTERN

VI.8. References

1. Pravin S, Sudhir A. Integration of 3D printing with dosage forms: A new perspective for modern healthcare. *Biomed Pharmacother Biomedecine Pharmacother*. 2018 Nov;107:146–54.
2. Lim SH, Kathuria H, Tan JJY, Kang L. 3D printed drug delivery and testing systems - a passing fad or the future? *Adv Drug Deliv Rev*. 2018 May 18;
3. Spritam--a new formulation of levetiracetam for epilepsy. *Med Lett Drugs Ther*. 2016 Jun 20;58(1497):78–9.
4. Shin D, Hyun J. Silk fibroin microneedles fabricated by digital light processing 3D printing. *J Ind Eng Chem*. 2021 Mar 25;95:126–33.
5. Martinez PR, Goyanes A, Basit AW, Gaisford S. Fabrication of drug-loaded hydrogels with stereolithographic 3D printing. *Int J Pharm*. 2017 Oct 30;532(1):313–7.
6. Karakurt I, Aydoğdu A, Çıkrıkçı S, Orozco J, Lin L. Stereolithography (SLA) 3D printing of ascorbic acid loaded hydrogels: A controlled release study. *Int J Pharm*. 2020 Jun 30;584:119428.
7. Bloomquist CJ, Mecham MB, Paradzinsky MD, Januszewicz R, Warner SB, Luft JC, et al. Controlling release from 3D printed medical devices using CLIP and drug-loaded liquid resins. *J Controlled Release*. 2018 May 28;278:9–23.
8. Awad A, Fina F, Goyanes A, Gaisford S, Basit AW. Advances in powder bed fusion 3D printing in drug delivery and healthcare. *Adv Drug Deliv Rev*. 2021 Jul 1;174:406–24.
9. Fina F, Goyanes A, Gaisford S, Basit AW. Selective laser sintering (SLS) 3D printing of medicines. *Int J Pharm*. 2017 Aug 30;529(1):285–93.
10. Hassanin H, Finet L, Cox SC, Jamshidi P, Grover LM, Shepherd DET, et al. Tailoring selective laser melting process for titanium drug-delivering implants with releasing micro-channels. *Addit Manuf*. 2018 Mar 1;20:144–55.
11. Bezuidenhout MB, Booysen E, van Staden AD, Uheida EH, Hugo PA, Oosthuizen GA, et al. Selective Laser Melting of Integrated Ti6Al4V ELI Permeable Walls for Controlled Drug Delivery of Vancomycin. *ACS Biomater Sci Eng*. 2018 Dec 10;4(12):4412–24.
12. Vaithilingam J, Kilsby S, Goodridge RD, Christie SDR, Edmondson S, Hague RJM. Functionalisation of Ti6Al4V components fabricated using selective laser melting with a bioactive compound. *Mater Sci Eng C*. 2015 Jan 1;46:52–61.
13. Goyanes A, Robles Martinez P, Buanz A, Basit AW, Gaisford S. Effect of geometry on drug release from 3D printed tablets. *Int J Pharm*. 2015 Oct 30;494(2):657–63.
14. Goyanes A, Allahham N, Trenfield SJ, Stoyanov E, Gaisford S, Basit AW. Direct powder extrusion 3D printing: Fabrication of drug products using a novel single-step process. *Int J Pharm*. 2019 Aug 15;567:118471.

15. Welsh NR, Malcolm RK, Devlin B, Boyd P. Dapivirine-releasing vaginal rings produced by plastic freeforming additive manufacturing. *Int J Pharm.* 2019 Dec 15;572:118725.
16. Khaled SA, Burley JC, Alexander MR, Roberts CJ. Desktop 3D printing of controlled release pharmaceutical bilayer tablets. *Int J Pharm.* 2014 Jan 30;461(1):105–11.
17. Khaled SA, Burley JC, Alexander MR, Yang J, Roberts CJ. 3D printing of tablets containing multiple drugs with defined release profiles. *Int J Pharm.* 2015 Oct 30;494(2):643–50.
18. Muwaffak Z, Goyanes A, Clark V, Basit AW, Hilton ST, Gaisford S. Patient-specific 3D scanned and 3D printed antimicrobial polycaprolactone wound dressings. *Int J Pharm.* 2017 Jul 15;527(1):161–70.
19. Grottkau BE, Hui Z, Pang Y. A Novel 3D Bioprinter Using Direct-Volumetric Drop-On-Demand Technology for Fabricating Micro-Tissues and Drug-Delivery. *Int J Mol Sci.* 2020 Jan;21(10):3482.
20. Clark EA, Alexander MR, Irvine DJ, Roberts CJ, Wallace MJ, Sharpe S, et al. 3D printing of tablets using inkjet with UV photoinitiation. *Int J Pharm.* 2017 Aug 30;529(1–2):523–30.
21. Jacob J, COYLE N, West TG, Monkhouse DC, Surprenant HL, Jain NB. Rapid disperse dosage form containing levetiracetam [Internet]. WO2014144512A1, 2014 [cited 2021 Jul 8]. Available from: <https://patents.google.com/patent/WO2014144512A1/en>
22. Yu D-G, Branford-White C, Ma Z-H, Zhu L-M, Li X-Y, Yang X-L. Novel drug delivery devices for providing linear release profiles fabricated by 3DP. *Int J Pharm.* 2009 Mar 31;370(1–2):160–6.
23. Maroni A, Melocchi A, Parietti F, Foppoli A, Zema L, Gazzaniga A. 3D printed multi-compartment capsular devices for two-pulse oral drug delivery. *J Controlled Release.* 2017 Dec 1;268:10–8.
24. Chen W, Palazzo A, Hennink WE, Kok RJ. Effect of Particle Size on Drug Loading and Release Kinetics of Gefitinib-Loaded PLGA Microspheres. *Mol Pharm.* 2017 Feb 6;14(2):459–67.
25. Klose D, Siepmann F, Elkharraz K, Krenzlin S, Siepmann J. How porosity and size affect the drug release mechanisms from PLGA-based microparticles. *Int J Pharm.* 2006 May 18;314(2):198–206.
26. Tamani F. Towards a better understanding of the drug release mechanisms in PLGA microparticles [Internet] [These de doctorat]. Lille; 2019 [cited 2021 Jul 12]. Available from: <http://www.theses.fr/fr/2019LILUS048>
27. Bassand C, Freitag J, Benabed L, Verin J, Siepmann F, Siepmann J. PLGA implants for controlled drug release: Impact of the diameter. *European Journal of Pharmaceutics and Biopharmaceutics* - Submitted. 2021;

VI. 3D PRINTING OF IBUPROFEN LOADED CONTROLLED RELEASE IMPLANTS WITH PLGA – PROOF OF CONCEPT AND IMPACT FILLING PATTERN

28. Kohno M, Andhariya JV, Wan B, Bao Q, Rothstein S, Hezel M, et al. The effect of PLGA molecular weight differences on risperidone release from microspheres. *Int J Pharm.* 2020 May 30;582:119339.
29. Ochi M, Wan B, Bao Q, Burgess DJ. Influence of PLGA molecular weight distribution on leuprolide release from microspheres. *Int J Pharm.* 2021 Apr 15;599:120450.
30. Bode C, Kranz H, Fizez A, Siepmann F, Siepmann J. Often neglected: PLGA/PLA swelling orchestrates drug release: HME implants. *J Controlled Release.* 2019 Jul 28;306:97–107.
31. Patel SK, Khoder M, Peak M, Alhnan MA. Controlling drug release with additive manufacturing-based solutions. *Adv Drug Deliv Rev.* 2021 Jul 1;174:369–86.
32. Lai Y, Li Y, Cao H, Long J, Wang X, Li L, et al. Osteogenic magnesium incorporated into PLGA/TCP porous scaffold by 3D printing for repairing challenging bone defect. *Biomaterials.* 2019 Mar 1;197:207–19.
33. Kwon B-J, Seon GM, Lee MH, Koo M-A, Kim MS, Kim D, et al. Locally delivered ethyl-2,5-dihydroxybenzoate using 3D printed bone implant for promotion of bone regeneration in a osteoporotic animal model. *Eur Cell Mater.* 2018 12;35:1–12.
34. Lin S, Cui L, Chen G, Huang J, Yang Y, Zou K, et al. PLGA/ β -TCP composite scaffold incorporating salvianolic acid B promotes bone fusion by angiogenesis and osteogenesis in a rat spinal fusion model. *Biomaterials.* 2019 Mar 1;196:109–21.
35. Jakus AE, Geisendorfer NR, Lewis PL, Shah RN. 3D-printing porosity: A new approach to creating elevated porosity materials and structures. *Acta Biomater.* 2018 May 1;72:94–109.
36. Allison SD. Analysis of initial burst in PLGA microparticles. *Expert Opin Drug Deliv.* 2008 Jun;5(6):615–28.
37. Ghalanbor Z, Körber M, Bodmeier R. Interdependency of protein-release completeness and polymer degradation in PLGA-based implants. *Eur J Pharm Biopharm.* 2013 Nov 1;85(3, Part A):624–30.
38. Bode C, Kranz H, Siepmann F, Siepmann J. In-situ forming PLGA implants for intraocular dexamethasone delivery. *Int J Pharm.* 2018 Sep 5;548(1):337–48.
39. Lizambard M, Menu T, Fossart M, Bassand C, Agossa K, Huck O, et al. In-situ forming implants for the treatment of periodontal diseases: Simultaneous controlled release of an antiseptic and an anti-inflammatory drug. *Int J Pharm.* 2019 Dec 15;572:118833.
40. Schädlich A, Kempe S, Mäder K. Non-invasive in vivo characterization of microclimate pH inside in situ forming PLGA implants using multispectral fluorescence imaging. *J Control Release Off J Control Release Soc.* 2014 Apr 10;179:52–62.
41. Su A, Al'Aref SJ. Chapter 1 - History of 3D Printing. In: Al'Aref SJ, Mosadegh B, Dunham S, Min JK, editors. *3D Printing Applications in Cardiovascular Medicine* [Internet]. Boston: Academic Press; 2018 [cited 2021 Jul 1]. p. 1–10. Available from: <https://www.sciencedirect.com/science/article/pii/B9780128039175000018>

42. Crump SS. Modeling apparatus for three-dimensional objects [Internet]. US5340433A, 1994 [cited 2021 Jul 1]. Available from: <https://patents.google.com/patent/US5340433/en>
43. Stavropoulos P, Foteinopoulos P. Modelling of additive manufacturing processes: a review and classification. *Manuf Rev*. 2018;5:2.
44. Aho J, Boetker JP, Baldursdottir S, Rantanen J. Rheology as a tool for evaluation of melt processability of innovative dosage forms. *Int J Pharm*. 2015 Oct 30;494(2):623–42.
45. Treffer D, Troiss A, Khinast J. A novel tool to standardize rheology testing of molten polymers for pharmaceutical applications. *Int J Pharm*. 2015 Nov 10;495(1):474–81.
46. Bassand C, Benabed L, Verin J, Danede F, Willart J-F, Siepmann F, et al. Hot melt extruded ibuprofen-loaded PLGA implants: Importance of heat exposure. *Journal of Drug Delivery Science and Technology* - Submitted. 2021;
47. Tita B, Fulas A, Stefanescu M, Marian E, Tița D. Kinetic Study of Decomposition of Ibuprofen under Isothermal Conditions. *Rev Chim -Buchar- Orig Ed-*. 2011 Feb 1;62:216–21.
48. Wu C, McGinity JW. Influence of ibuprofen as a solid-state plasticizer in eudragit® RS 30 D on the physicochemical properties of coated beads. *AAPS PharmSciTech*. 2001 Dec;2(4):35–43.
49. Wu C, McGinity JW. Non-traditional plasticization of polymeric films. *Int J Pharm*. 1999 Jan 15;177(1):15–27.
50. De Brabander C, Van Den Mooter G, Vervaet C, Remon JP. Characterization of ibuprofen as a nontraditional plasticizer of ethyl cellulose. *J Pharm Sci*. 2002 Jul;91(7):1678–85.
51. Ferry JD. *Viscoelastic Properties of Polymers*. John Wiley & Sons; 1980. 676 p.
52. Zhang B, Gleadall A, Belton P, McDonagh T, Bibb R, Qi S. New insights into the effects of porosity, pore length, pore shape and pore alignment on drug release from extrusionbased additive manufactured pharmaceuticals. *Addit Manuf*. 2021 Oct 1;46:102196.

**VII. PLGA BASED 3D PRINTED IMPLANT –
IMPACT OF THE 3D PRINTED
TECHNOLOGY ON DRUG RELEASE**

VII. PLGA BASED 3D PRINTED IMPLANTS – IMPACT OF THE 3D PRINTED TECHNOLOGY ON DRUG RELEASE

Research article - To be reviewed by the co-authors

PLGA based 3D printed implants – the impact of the 3D printed technology on drug release

C. Bassand¹, L. Benabed¹, S. Charlon², J. Verin¹, J. Freitag¹, F. Siepmann¹, J. Soulestin², J. Siepmann¹

¹*Univ. Lille, Inserm, CHU Lille, U1008, F-59000 Lille, France*

²*IMT Lille Douai, Dept Polymers & Composites Technol & Mech Engn, F-59500 Douai, France*

VII.1. Abstract

Three-dimension (3D) printing has many advantages, such as the flexibility of dosages or the possibility of creating complex structures. However, the choice of printing technology and settings can greatly influence product performance. The objective of this research was, first of all, to study and compare the impact of two printing processes on the physicochemical properties of poly (lactic-co-glycolic) acid (PLGA) and the in vitro performance of ibuprofen loaded-implants obtained. To do so, two sets of implants were printed using Droplet Deposition Modeling (DDM) with the Arburg Freeformer[®] technology and Fused Filament Fabrication (FFF) with a Volumic[®] printer. The obtained implants were characterized regarding morphology (optical macroscopy and scanning electronic microscopy), solid-state (differential scanning calorimetry), drug loading, and molecular weight of the polymer. The implants in vitro performance was assessed after exposure to phosphate buffer pH 7.4, 37°C, 80 RPM. Absolute and relative in vitro drug release, the evolution of the pH in the release medium, increase in wet mass, and morphologically changed upon exposure to release medium were evaluated. The degradation behavior of PLGA upon exposure to release medium (loss of dry mass, and molecular weight of the polymer) with the two types of implants obtained was also investigated. The implants printed by DDM have a three-phase in vitro release profile with a “burst” effect, then a slower release phase, and finally a final rapid release phase due to the significant swelling of the PLGA. While the FFF-printed implants exhibit a two-phase in vitro release profile.

Keywords: PLGA, 3D printing, fused filament fabrication, droplet deposition modeling, in vitro drug release.

VII.2. Introduction

Additive manufacturing, also known as three-dimension (3D) printing technologies allow to manufacture of objects either by deposition, binding, or polymerization of successive materials layers (1,2). Different classification of the 3D printing technologies has been reported, one of them classify those technologies depending on the object production: photopolymerization, powder bed fusion, material jetting, direct energy deposition, binder jetting, selective deposition lamination, and material extrusion (1,2). Lately, the use of 3D printing in the pharmaceutical field reached its highest point with the FDA approval of SPRITAM the first FDA-approved 3D printed drug product (1,3). This drug product is printed by binder jetting (4,5), and four other 3D printing technologies have been investigated for use in pharmaceuticals: photopolymerization (6–9), powder bed fusion (10–14), material extrusion (15–20), and material jetting (21,22).

The advantages of 3D printing technologies for the controlled release of oral dosage forms have been extensively investigated in the past few years (15,21,23). However, only a few studies focus on parenteral 3D printed devices, especially poly (lactic-co-glycolic) acid (PLGA) based devices (24–29). Even so, PLGA is a well-known and used polymer in controlled drug delivery systems obtained with conventional pharmaceutical technologies (30–32). Thanks to its great biocompatible and biodegradable properties (33–37), this polyester is widely studied (38–40) and present in numerous FDA-approved drug products, such as microparticles, implants, or *in situ* forming implants (41). Modulating either the polymer grade, the type of devices, its porosity, or its size could lead to different drug release kinetics (42–44). The manufacturing process as well influences the release rate (45–47).

The emerging 3D printing technologies provide new expediency to precisely control drug release from PLGA based devices. Thanks to its high flexibility, the 3D printing technologies allow the manufacturing of a wild range of dosage forms: a combination of several drug substances (19), patient-specific devices (20), complex release patterns (48)... By combining the adapted polymer and the appropriate technology precisely modulating drug release should be possible. The preciseness of 3D printing technologies is a crucial advantage when it comes to controlling the internal structure of the device, reaching complex geometries (23), etc... Due to its thermoplastic properties, PLGA seems to be a good candidate for 3D printing by extrusion-based technologies (49).

The material extrusion-based 3D printing technologies can be divided into two parts: (i) extrusion of low melting point past or gel and (ii) extrusion of high melting point thermoplastic

polymer (1). In both cases, it consists of dispensing molten or semi-solid material through the orifice of a nozzle, deposited layers by layers to obtain a 3D object (50). Nowadays, these printing technologies are considered the simplest and are the most widely used. Concerning the high melting point thermoplastic polymers, several technologies have been reported such as Fused Deposition Modeling (FDM) also known as Fused Filament Fabrication (FFF), Direct Powder Extrusion (DPE), and Droplet Deposition Modeling (DDM) (1,15–17,50–53). FFF-based technologies have been investigated lately for 3D printing of PLGA based devices by Carlier *et al* (28,29). In the meantime, DDM technology has been used for producing vaginal rings for control drug delivery of Dapivirine by Welsh *et al* (17).

The study aimed to evaluate the impact of DDM and FFF, two material extrusion-based 3D printing technologies, on ibuprofen-loaded PLGA implants physicochemical characteristics and *in vitro* drug release performance. To do so, ibuprofen-loaded PLGA implants were 3D printed using either the DDM Arburg Freeformer® technology or the FFF Volumic® technology. Thus, both implants' physicochemical characteristics were investigated before and after exposure to phosphate buffer pH 7.4. The impact of the 3D printing technology on the practical drug loading, polymer molecular weight, morphology by optical macroscopy, and scanning electronic microscopy was investigated. The impact of the difference observed on the *in vitro* drug release after exposure to phosphate buffer pH 7.4 was also investigated.

VII.3. Materials and methods

VII.3.1. Materials

Poly (D,L lactic-co-glycolic acid) (PLGA, 50:50 lactic acid: glycolic acid; Resomer RG 503H; Evonik, Darmstadt; Germany); ibuprofen (BASF, Ludwigshafen, Germany); agarose (genetic analysis grade), tetrahydrofuran (HPLC grade) (Fisher Scientific, Illkirch, France); potassium dihydrogen orthophosphate and sodium hydroxide (Acros Organics, Geel, Belgium); acetonitrile (VWR, Fontenoy-sous-Bois, France); sodium hydrogen phosphate (Na_2HPO_4 , Panreac Quimica, Barcelona, Spain).

VII.3.2. Implants preparation

VII.3.2.1. Droplet deposition modeling, Arburg Freeformer®

PLGA was milled (4 x 30 s) with a grinder (Valentin, Seb, Ecully, France). Appropriate amounts of polymer and drug powders were blended for 5 min with a mortar and a pestle, followed by extrusion using a Nano 16 twin-screw extruder (screw diameter = 16 mm, length/diameter ratio = 26.25, gravitational feeder; Leistritz, Nuremberg, Germany), equipped with a 2 mm diameter die. The process temperatures were kept constant at 80 - 75 - 70 - 65 °C (die - zone 3 - zone 2 - zone 1). After cooling, the hot melt extrudates were manually cut into pellets of 5 mm length.

The pellets obtained by hot extrusion were fed into the feeder of the Arburg Freeformer® printer (Freeformer, Arburg, Germany). Parallelepiped-shaped implants with dimensions of 10 mm x 10 mm x 2.5 mm were printed using a 250 µm nozzle according to the parameters described in *Table VII-1*.

Table VII-1. Printing parameters used to obtain the ibuprofen-loaded PLGA-implants.

Used technology	Droplet deposition modeling (DDM)	Fused filament fabrication (FFF)
Number of contouring layers		0
Number of lower and upper layer		0
Filling pattern		ZigZag
Filling density (%)		30
Nozzle diameter (mm)		0.25
Layer thickness (mm)		0.25
Printing temperature (°C)	zone 1 : 120 zone 2 : 110 zone 3 : 110	First layer: 125 Otherwise: 115
Printing speed (mm/s)	40	50
Température du plateau (°C)	25	30
Ventilation (%)	Not applicable	10
Speed of retraction (mm/s)	Not applicable	40

VII.3.2.2. Fused deposition modeling, Volumic®

The PLGA was milled (4 x 30 s) with a grinder (Valentin, Seb, Ecully, France). Appropriate amounts of polymer and ibuprofen were mixed and then pre-melted in a crystallizer on a film applicator hot plate (110 ° C, 6 min, Erichsen, Rueil-Malmaison, France), then extruded as described in section 2.2.1. Except that: (i) a 4 mm die was used, (ii) the die temperature was set at 70 ° C, (iii) and a feeder flow regulator was used at a speed between 5 and 8 cc/min. The diameter of the filament obtained at the exit of the extruder was controlled by a laser sensor

VII. PLGA BASED 3D PRINTED IMPLANTS – IMPACT OF THE 3D PRINTED TECHNOLOGY ON DRUG RELEASE

(target diameter between 1.60 and 1.80 mm, Tolerance Puller Noztek, Shoreham-by-Sea, United Kingdom).

The filaments obtained were used to feed the Volumic[®] 30 Stream Ultra printer (Volumic, Nice, France). Parallelepiped-shaped implants with dimensions of 10 mm x 10 mm x 2.5 mm were printed according to the parameters described in *Table VII-1*. *Figure VII-1* show a schematic illustration of the two-printing technology investigated here.

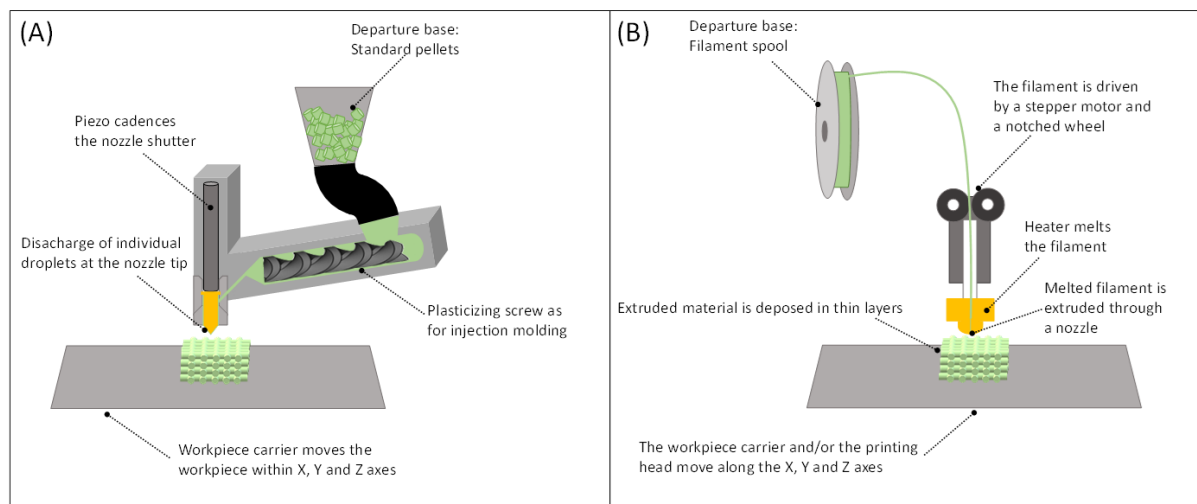


Figure VII-1. Schematic representation of (A) droplet deposition modeling by Arburg[®] Freeformer, and (B) fused filament fabrication by Volumic[®].

VII.3.3. Optical microscopy

Pictures of the implants before exposure to the release medium were taken using a SZN-6 trinocular stereo zoom microscope (Optika, Ponteranica, Italy), equipped with an optical camera (Optika Vison Lite 2.1 software). The lengths/width and implants pore size were determined using the ImageJ software (US National Institutes of Health, Bethesda, Maryland, USA).

VII.3.4. Practical drug loading

Pellets and pieces of 3D printed implants were dissolved in 5 mL acetonitrile, followed by filtering (PVDF syringe filters, 0.45 μm ; Agilent Technologies, Santa Clara, USA) and drug content determination by HPLC-UV analysis using a Thermo Fisher Scientific Ultimate 3000 Series HPLC, equipped with an LPG 3400 SD/RS pump, an autosampler (WPS-3000 SL) and a UV-Vis detector (VWD-3400RS) (Thermo Fisher Scientific, Waltham, USA). A reversed-phase column C18 (Gemini 5 μm ; 110 Å ; 150 x 4.6 mm; Phenomenex, Le Pecq, France) was used. The mobile phase was a mixture of 30 mM Na_2HPO_4 pH 7.0: acetonitrile (60:40, v:v).

The detection wavelength was 225 nm, and the flow rate was 0.5 mL/min. Ten microliter samples were injected.

VII.3.5. Differential scanning calorimetry (DSC)

DSC thermograms of the raw materials (PLGA and ibuprofen), pellets, filament, and 3D printed implants were recorded using a DCS1 Star System (Mettler Toledo, Greifensee, Switzerland). Approximately 5 mg raw material, pellets, and 3D printed implants, were heated in pierced aluminum pans as follows: from -70 to 120 °C, cooling to -70 °C, re-heating to 120 °C (heating/cooling rate = 10 °C/min. The reported glass temperatures (T_{gs}) were determined from the 1st heating cycles in the case of the pellets, filaments, and 3D printed implants (the thermal history being of interest), and from the 2nd heating cycle in the case of the raw material (the thermal history not being of interest). All experiments were conducted in triplicate. Mean values +/- standard deviations are reported.

VII.3.6. Gel permeation chromatography (GPC)

The average polymer molecular weight (M_w) of the PLGA was determined by gel permeation chromatography (GPC) as follows: raw materials, samples were dissolved in tetrahydrofuran (3 mg/mL). Fifty µL samples were injected into an Alliance GPC (refractometer detector: 2414 RI, separation module e2695, Empower GPC software; Waters, Milford, USA), equipped with a PLgel 5 µm MIXED-D column (kept at 35°C, 7.8 × 300 mm; Agilent). Tetrahydrofuran was the mobile phase (flow rate: 1 mL/min). Polystyrene standards with molecular weights between 1,480 and 70,950 Da (Polymer Laboratories, Varian, Les Ulis, France) were used to prepare the calibration curve. All experiments were conducted in triplicate. Mean values +/- standard deviations are reported.

VII.3.7. In vitro drug release

Implants were placed in 50 mL tubes (352070 Corning-Falcon, New York, U.S; 1 implant per tube), filled with 50 mL phosphate buffer pH 7.4 USP 42. The tubes were placed in a horizontal shaker (80 rpm, 37°C; GFL 3033; Gesellschaft fuer Labortechnik, Burgwedel, Germany). At predetermined time points, the entire bulk fluid was replaced by fresh release medium. The withdrawn samples were filtered (PVDF syringe filter, 0.45 µm; Agilent, Santa Clara, California, USA) and analyzed for their ibuprofen contents by HPLC-UV, as described in *section VII.3.4*.

VII. PLGA BASED 3D PRINTED IMPLANTS – IMPACT OF THE 3D PRINTED TECHNOLOGY ON DRUG RELEASE

In all cases, at pre-determined time points, pictures were taken as described in *section VII.3.3*. and the pH of the release medium was measured using a pH meter (InoLab pH Level 1; WTW, Weilheim, Germany). Also, in all cases, sink conditions were provided throughout the experiments in all agitated bulk fluids. All experiments were conducted in triplicate. Mean values +/- standard deviations are reported.

VII.3.8. Implants swelling

Implants were treated as for the *in vitro* drug release measurements. At pre-determined time points: implants samples were withdrawn and excess water was carefully removed using Kimtech precision wipes (Kimberly-Clark, Rouen, France). The implants were weighed [*wet mass (t)*], and the *change in wet mass (%) (t)* was calculated as follows:

$$\text{change in wet mass } (\%)(t) = \frac{\text{wet mass } (t) - \text{mass } (t = 0)}{\text{mass } (t = 0)} \times 100 \%$$

where *mass (t = 0)* denotes the mass of the implant before exposure to the release medium. All experiments were conducted in triplicate. Mean values +/- standard deviations are reported.

VII.3.9. Implants erosion and PLGA degradation

Implants samples were treated as for the *in vitro* drug release studies described above. At pre-determined time points, implants samples were withdrawn and freeze-dried (freezing at -45°C for 2 h 35 min, primary drying at -20 °C/0.940 mbar for 35 h 10 min, secondary drying at +20 °C/0.0050 mbar for 35 h; Christ Alpha 2-4 LSC+; Martin Christ, Osterode, Germany).

The *dry mass (%) (t)* was calculated as follows:

$$\text{dry mass } (\%)(t) = \frac{\text{dry mass } (t)}{\text{mass } (t = 0)} \times 100 \%$$

where *mass (t = 0)* denotes the mass of the implant before exposure to the release medium. All experiments were conducted in triplicate. Mean values +/- standard deviations are reported.

The average polymer molecular weight (Mw) of the PLGA was determined by gel permeation chromatography (GPC) as described in *section VII.3.6*. All experiments were conducted in triplicate. Mean values +/- standard deviations are reported.

VII.3.10. . Scanning electronic microscopy (SEM)

The internal and external morphology of the implants before and after exposure to the release medium was studied using a JEOL Field Emission Scanning Electron Microscope (JSM-7800F, Japan), equipped with the Aztec 3.3 software (Oxford Instruments, Oxfordshire, England). Samples were fixed with a ribbon carbon double-sided adhesive and covered with a fine chrome layer. In the case of implants that had been exposed to the release medium, the systems were treated as described for the in vitro release studies as described in *section VII.3.7*. At predetermined time points, implant samples were withdrawn, optionally cut (for cross-sections) using a scalpel, and freeze-dried (as described in *section VII.3.9*).

VII.4. Results and discussion

VII.4.1. Characterization of the implants before exposure to the release medium

As previously described (*Table VII-1*) two types of similar implants were produced using DDM and FFF technologies. The morphology of the implants was observed by optical macroscopy and illustrated in *Figure VII-2* and their physicochemical characteristics in *Table VII-2*. The photos obtained by MO (*Figure VII-2A*) show the difference in the appearance of the printed lines. Interestingly the lines printed by DDM are more tortuous than those printed by FFF. As the droplets are deposited one after the other with a high outlet pressure by DDM (400-500 bar) ref. Thus, might lead to the collapse of the printed line by gravity while by printing by FFF, a relatively rigid filament is deposited continuously, leading to implant with different morphology as illustrated in *Figure VII-2B*. As a consequence of this, the weight of the corresponding implant is also higher for those obtained by DDM compared to those obtained by FFF (

Table VII-2).

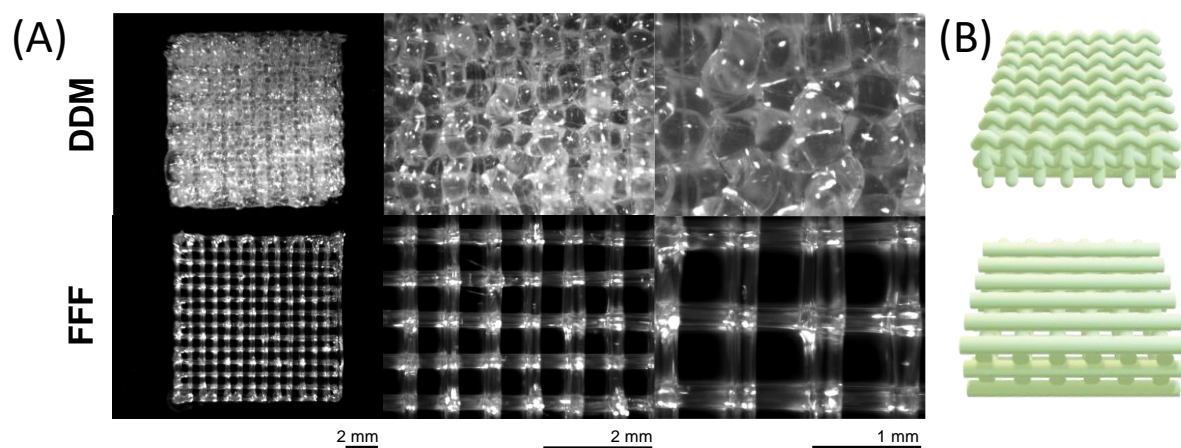


Figure VII-2. (A) Optical macroscopic pictures of the surface of ibuprofen PLGA-implants obtained either with DDM with the Arburg Freeformer® technology, or FFF with the Volumic® printer, before exposure to the release medium and (B) schematic representation of the deposited lines of PLGA-ibuprofen loaded implants obtained either with DDM with the Arburg Freeformer® technology, or FFF with the Volumic® printer.

VII. PLGA BASED 3D PRINTED IMPLANTS – IMPACT OF THE 3D PRINTED TECHNOLOGY ON DRUG RELEASE

Table VII-2. Key properties of the obtained ibuprofen-loaded PLGA-implants. (*T_g*: glass transition temperature, *M_w*: molecular weight). Mean values ± standard deviations are indicated (Weight, Length, Width, Implants pore size *n*=36, Practical drug loading *n*=6, Thickness, *T_g*, *M_w* *n*=3).

Used technology	Droplet deposition modeling	Fused filament fabrication
	(DDM)	(FFF)
Weight (mg)	212.1 ± 8.4	89.7 ± 8.7
Length – width (mm)	10.4 ± 0.2	10.0 ± 0.1
Thickness (mm)	2.45 ± 0.04	2.50 ± 0.02
Implants pore size (mm)	0.5 ± 0.1	0.5 ± 0.2
Practical drug loading (%)	13.8 ± 0.1	11.8 ± 0.2
T_g (°C)	34.6 ± 0.1	35.4 ± 0.3
M_w (kDa)	15.8 ± 0.3	19.6 ± 0.5

Photos taken by SEM (*Figure VII-3*) confirmed this observation, as the difference in the deposited line can be seen. Both types of implants show a slight surface roughness and small cross-sectional pores (enlighten in dotted red line). Those pores are more numerous inside the polymer matrix of DDM implants. These small pores are described in the literature as being the consequence of a high pressure exceeding 400 bar at the nozzle of the Arburg® Freeformer printer which would induce the evaporation of either ibuprofen molecules, even at lower temperatures than its boiling point, or residual water contained in the raw materials (17).

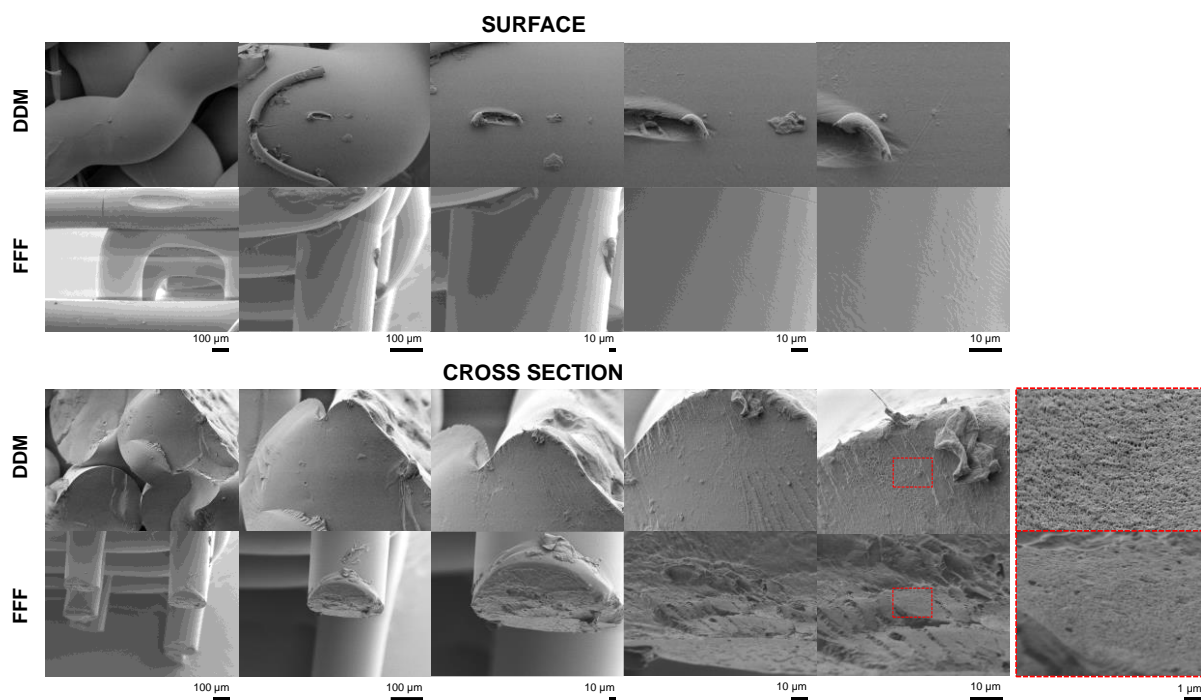


Figure VII-3. Scanning electronic microscopic pictures of the surface and cross-section of ibuprofen PLGA-implants obtained either with DDM with the Arburg Freeformer® technology, or FFF with the Volumic® printer, before exposure to the release medium.

Figure VII-4 diagrams illustrate the variety of molecular weight of the PLGA and ibuprofen content of the different feedstock materials (pellets, and filaments) and the implants obtained either by DDM or FFF.

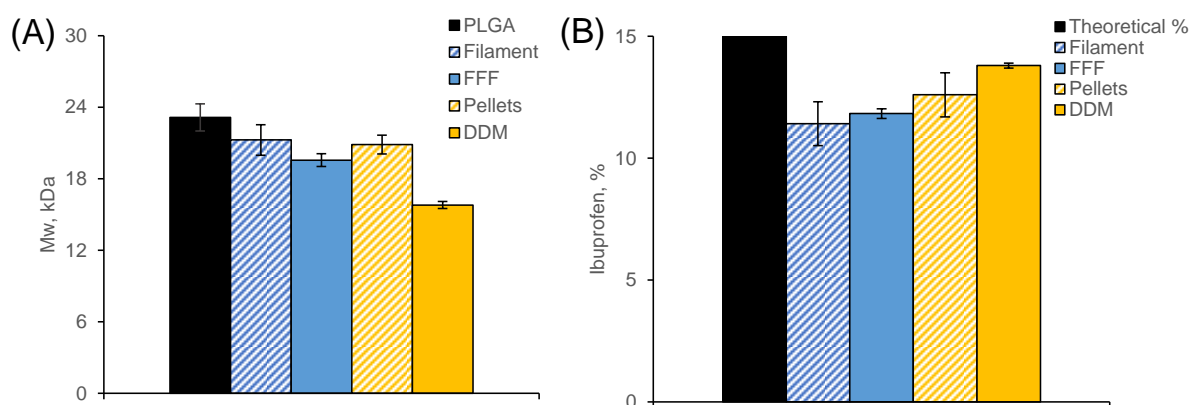


Figure VII-4. Impact of the 3D printing technology used on (A) PLGA molecular weight and (B) the ibuprofen content.

The differences observed between the feedstock materials (filament and pellets), can be explained by the differences during the production by HME. Indeed, the production of pellets

VII. PLGA BASED 3D PRINTED IMPLANTS – IMPACT OF THE 3D PRINTED TECHNOLOGY ON DRUG RELEASE

does not require having a homogeneous diameter at the outlet, since the extruded material is then cut. To obtain a filament that can be used in 3D printing, the output diameter must be finely controlled by a laser sensor placed at the output of the extruder. To operate under optimal conditions, this requires that the material comes out of the extruder at a high speed, and at the lowest temperature, so this implies the following differences during the production of pellets and filaments:

- (i) Pellets: extrusion using the "gravitational" mode of the extruder, where the powder mixture, contained in a funnel, flows by gravity to the extrusion screw, and an outlet temperature of 80°C
- (ii) Filament: extrusion using the "feeder" mode, where the powder is pushed by a piston at the level of the extruder screws at a controlled speed, and an outlet temperature of 70 ° C.

Those differences imply a shorter residence time in the extruder for the filament (the residence time being reduced by the force applied by the feeder, which pushes the molten material). This, coupled with an outlet temperature below the melting point of ibuprofen, therefore induces the presence of greater ibuprofen crystalline residues in the filaments than in the pellets (*Figure VII-5*). However, it is interesting to note that this difference is found to be smoothed out after printing. Indeed, the heating undergone by the filament during printing seems to have been sufficient to amorphized the small crystalline amount of ibuprofen that remained in the filament (54).

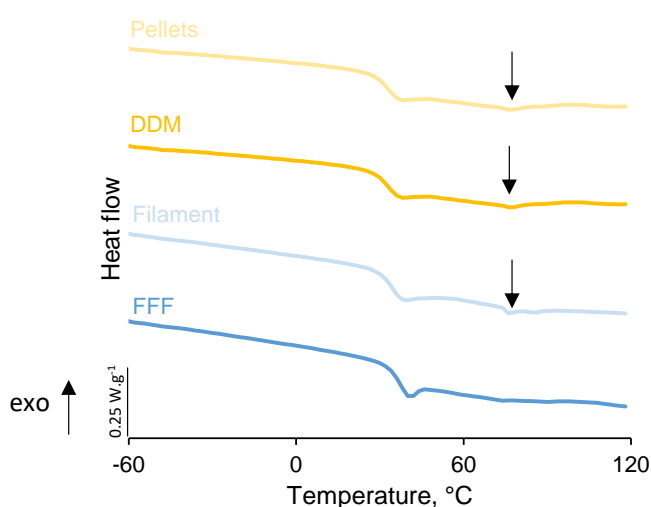


Figure VII-5. Impact of the 3D printing technology used on the thermograms of the obtained PLGA-ibuprofen loaded implants and intermediate products (pellets and filaments).

On the other hand, the use of the "feeder" mode used for the production of the filament requires pretreating the mixture by heating it (otherwise the grain size is too fine, and clogs the "feeder"). This pretreatment has the consequence of increasing the losses of Ibuprofen (*Figure VII-4B*). For the filament obtained by hot extrusion, it should also be noted that its diameter is smaller and less homogeneous (1.63 ± 0.10 mm) than the recommendations of the printer manufacturer (1.75 ± 0.05 mm). Regarding implants obtained with the two 3D printing techniques, the ibuprofen content of FFF implants is significantly lower and more variable than that of DDM-zigzag implants (*Figure VII-4B*). Indeed, DDM technology makes it possible to print an implant from a statistical mixture of pellets, this promotes homogeneity, unlike the FFF technology which uses a short portion of the filament.

Despite greater mechanical stress for the production of the filament than the pellets (the force applied to the molten polymer is the combination of the rotation of the screws, and the force applied by the material supplied by the "feeder") the PLGA molecular weight in the filament and pellets are equivalent (*Figure VII-4A*). In contrast, FFF implants have a higher PLGA molecular weight compared to implants obtained by FFF technology. This is a consequence of the considerable mechanical stress associated with the Arburg® Freeformer printer screw (79).

VII.4.2. Characterization of the implants after exposure to the release medium

The impact of 3D printing technology from previously produced and characterized implants on the relative and absolute in vitro release kinetics of ibuprofen and pH changes in the release medium have been illustrated in *Figure VII-6*.

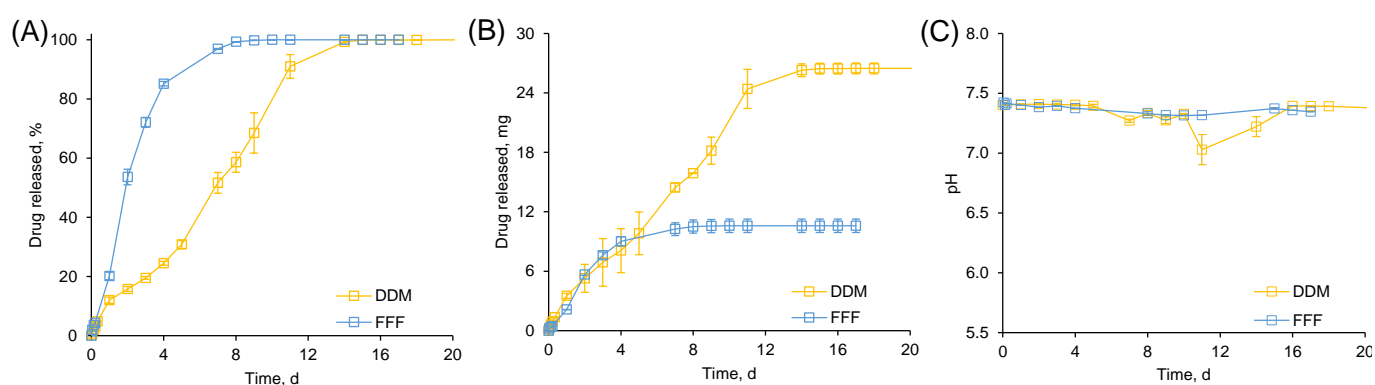


Figure VII-6. (A) Relative (%) and (B) absolute (mg) ibuprofen release from PLGA implants, and (C) pH changes upon exposure to phosphate buffer pH 7.4, 37°C, 80 RPM.

The relative (*Figure VII-6A*) and absolute (*Figure VII-6B*) release kinetics of the implants obtained with the two different technologies are significantly different. *Figure VII-6C* shows

VII. PLGA BASED 3D PRINTED IMPLANTS – IMPACT OF THE 3D PRINTED TECHNOLOGY ON DRUG RELEASE

that the pH drops sharply after 10 days of exposure of the implants obtained by DDM to the release medium, before returning to its initial value on day 16. This drop coincides with the end of the third phase during which there is a rapid release of ibuprofen which is an acidic molecule ($pK_a = 5.3$) and during which PLGA is hydrolyzed and degraded into acidic components (lactic and glycolic acid). Ibuprofen and the degradation products of PLGA are then released into the medium in large quantities and lower the pH. However, this drop in pH is not observed with implants obtained by FFF. This may be since those implants are lighter than the ones obtained by DDM, the degradation products and ibuprofen released is not in sufficient quantity to lead to a comparable drop of pH.

Figure VII-7 diagrams show the dynamical changes of the two types of implant upon exposure to the release medium. It was observed that the water uptake of implants obtained by FFF is slightly higher than that of implants obtained by DDM (*Figure VII-7A*). The impact of this water uptake on the change in the morphology of the implants is also visible in the photos (*Figure VII-8*). Implants obtained by DDM show triphasic release pattern (*Figure VII-6A and B*) with:

- (i) The first phase which takes place during the first day describes a so-called “burst” effect. This is a rapid increase in release due to diffusion of ibuprofen to the surface of implants and due to diffusion of ibuprofen through pores filled with water (55,56).
- (ii) When the pores formed by the release of the ibuprofen during the “burst” close due to the mobility of the polymer chains, the second phase of slow diffusion of ibuprofen through the polymer matrix begins (from day 2 to day 4) (57,58).
- (iii) The third rapid release phase (from day 4) is correlated with the significant swelling of the PLGA which begins at the same time (*Figure VII-7A*), thus letting enough space for ibuprofen to diffuse freely (59)

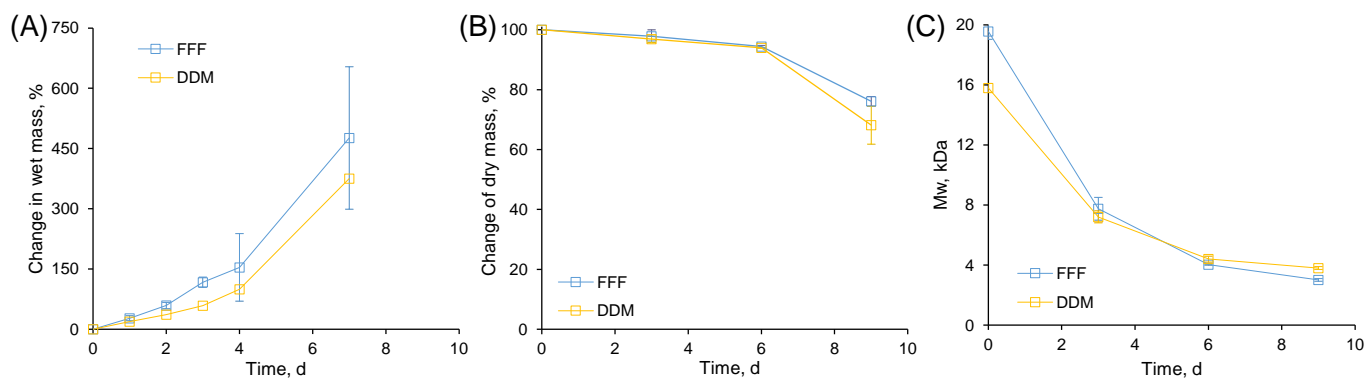


Figure VII-7. (A) Change in wet mass (%), (B) dry mass (%), and (C) molecular weight (M_w) of ibuprofen-loaded PLGA implants upon exposure to phosphate buffer pH 7.4 37°C 80 RPM.

Concerning implants obtained by FFF show a biphasic release pattern (**Figure 6 A and B**) with:

- (i) The first phase of release (from day 1 to day 4) shows the same “burst” effect as the implants obtained by DDM but over a longer period.
- (ii) The second phase of slower release begins on day 4 until the complete release of the ibuprofen is achieved.

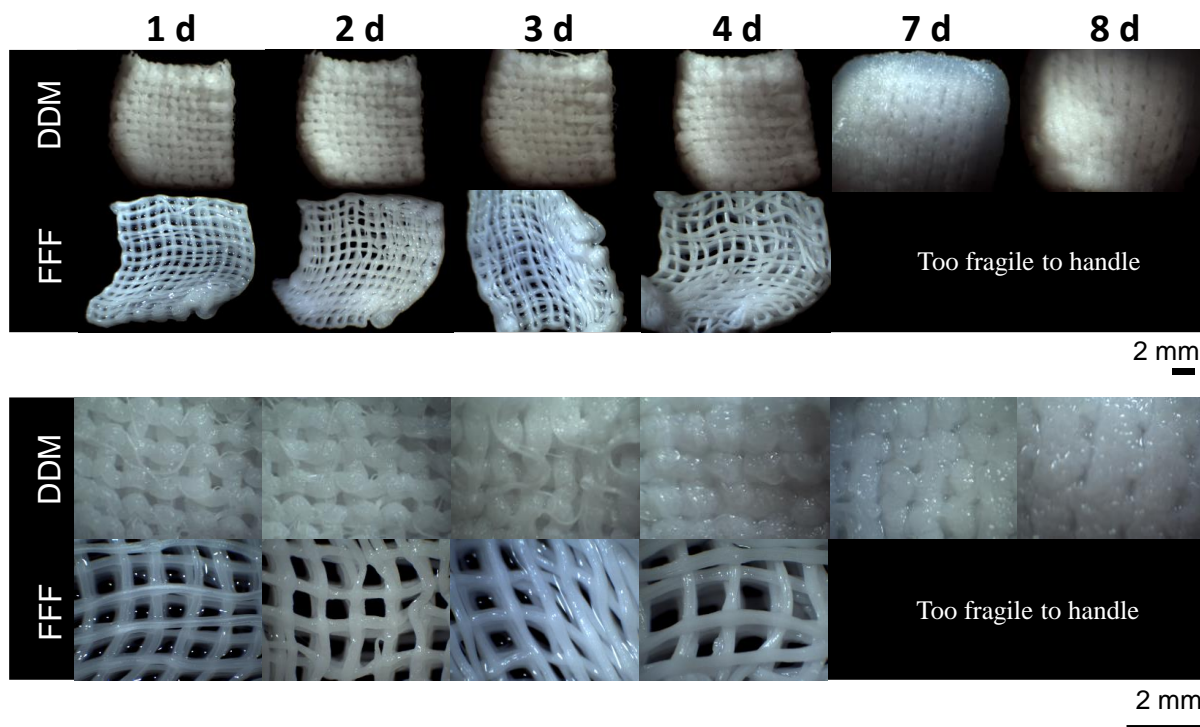


Figure VII-8. Optical macroscopy pictures ibuprofen-loaded PLGA implants upon exposure to phosphate buffer pH 7.4, 37°C, 80 RPM.

VII. PLGA BASED 3D PRINTED IMPLANTS – IMPACT OF THE 3D PRINTED TECHNOLOGY ON DRUG RELEASE

On the other hand, the absolute release kinetics (*Figure VII-6B*) of both types of implants are superposed until the complete release of ibuprofen contained in the implant obtained by FFF is reached. This suggests that the implants obtained by FFF released most of the ibuprofen before the onset of the swelling of the PLGA (*Figure VII-7A*), the absence of lag phase and 3rd rapid release phase is also due to shorter diffusion pathway due to the difference in the shape of the implants (*Figure VII-8*). For both types of implants, the loss of dry mass and the molecular weight of the polymer over time are very similar (*Figure VII-7B and C*). The polymer erosion profile is typical of bulk erosion (60). Until day 6, the first degradation products remain in the matrix, decrease the micro-surrounding pH, and cause, by an autocatalytic effect, the accelerated degradation of PLGA (61).

Figure VII-9 shows SEM pictures of the surface and cross-section of the implants after 3 days of exposure to the release medium. In both cases, exposure to the release medium leads to porous and unshaped structures. For implants produced by FFF the event after 3 days exposure to a release medium at a temperature higher than the T_g of the implant (

Table VII-2) the polymer filament deposited by the printer remains visible and the structure intact.

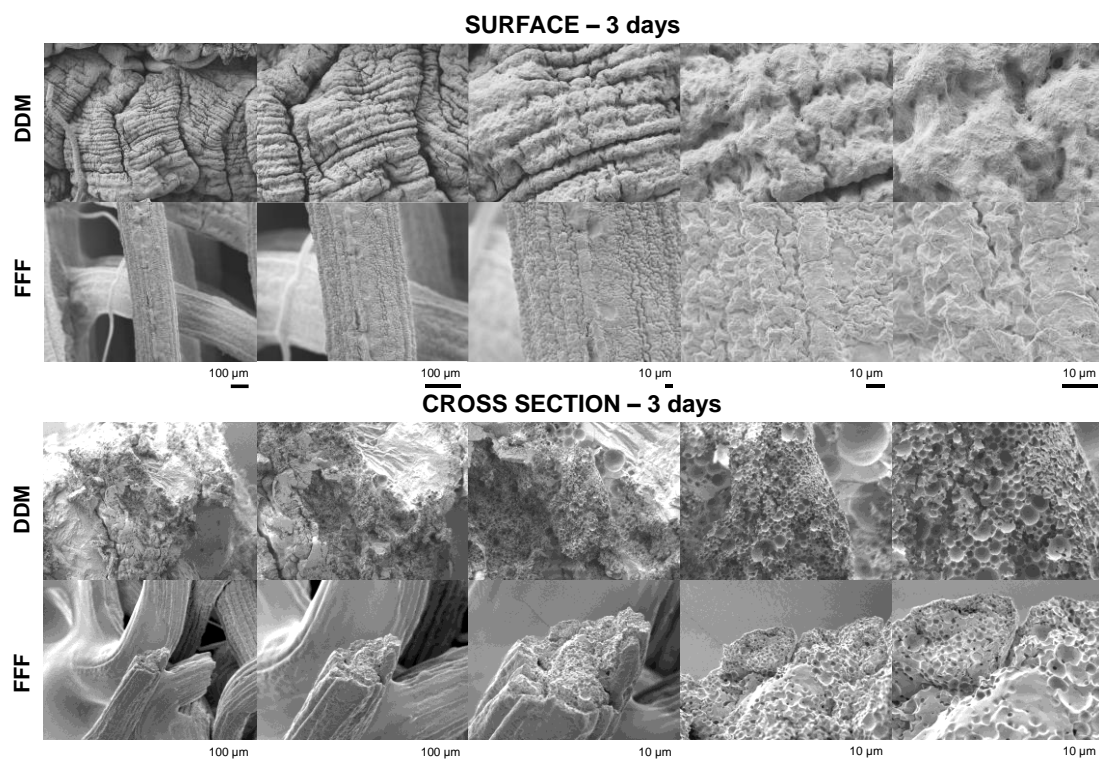


Figure VII-9. SEM pictures of surfaces and cross-sections of ibuprofen-loaded PLGA implants after exposure to phosphate buffer pH 7.4, 37°C, 80 RPM. Please note that after exposure to the release medium the implants were freeze-dried before analysis. Thus, caution must be paid due to artefact creation.

VII.5. Conclusion

3D printing has many advantages, such as the flexibility of dosages or the possibility of creating complex structures. However, the choice of printing technology and settings can greatly influence product performance. The objective of this research was, to study and compare the impact of two printing processes on the physicochemical properties of PLGA and the in vitro performance of the implants obtained. For this, two sets of implants were printed using DDM and FFF technology. Both technologies appear to have advantages and disadvantages regarding the production of 3D printing PLGA based control drug delivery devices. DDM technology allows to easily obtain homogeneous drug-loaded implants as the printing is done from a statistical mixture of pellets. Another advantage of this technology is that it allows avoiding the challenging development needed with FFF for the obtention of filament homogeneous in diameter. However, this technology exposes the polymer and the drug substance to high

VII. PLGA BASED 3D PRINTED IMPLANTS – IMPACT OF THE 3D PRINTED TECHNOLOGY ON DRUG RELEASE

mechanical stress compared to FFF technology. The implants printed by DDM have a three-phase in vitro release profile with a “burst” effect, then a slower release phase, and finally a final rapid release phase due to the significant swelling of the PLGA. FFF-printed implants exhibit a two-phase in vitro release profile. This difference is mainly due to the difference in structure obtained, leading to heavier implants by DDM, and to a longer diffusion pathway for the drug substance.

VII.6. Acknowledgments

This project has received funding from the Interreg 2 Seas programme 2014-2020 co-funded by the European Regional Development Fund under subsidy contract No 2S04-014 3DMed. The authors are very grateful for this support. They would also like to thank Mr. A. Fadel from the “Centre Commun de Microscopie” of the University of Lille (“Plateau technique de la Federation Chevreul CNRS FR 2638”) for his valuable technical help with the SEM pictures.

VII.7. Author statement

C. Bassand	Investigation; Methodology; Validation; Conceptualization; Writing - Original Draft; Visualization
L. Benabed	Investigation; Methodology; Validation
S. Charlon	Investigation, Visualization; Project administration
J. Verin	Investigation; Methodology; Validation
J. Freitag	Investigation
F. Siepmann	Conceptualization; Methodology; Supervision; Resources; Writing - Review & Editing; Visualization; Project administration; Funding acquisition
J. Soulestin	Conceptualization; Methodology; Supervision; Resources; Writing - Review & Editing; Visualization; Project administration; Funding acquisition
J. Siepmann	Conceptualization; Methodology; Supervision; Resources; Writing - Review & Editing; Visualization; Project administration; Funding acquisition

VII.8. References

1. Lim SH, Kathuria H, Tan JJY, Kang L. 3D printed drug delivery and testing systems - a passing fad or the future? *Adv Drug Deliv Rev.* 2018 May 18;
2. Pravin S, Sudhir A. Integration of 3D printing with dosage forms: A new perspective for modern healthcare. *Biomed Pharmacother Biomedecine Pharmacother.* 2018 Nov;107:146–54.
3. Spritam--a new formulation of levetiracetam for epilepsy. *Med Lett Drugs Ther.* 2016 Jun 20;58(1497):78–9.
4. Jacob J, COYLE N, West TG, Monkhouse DC, Surprenant HL, Jain NB. Rapid disperse dosage form containing levetiracetam [Internet]. WO2014144512A1, 2014 [cited 2021 Jul 8]. Available from: <https://patents.google.com/patent/WO2014144512A1/en>
5. Yu D-G, Branford-White C, Ma Z-H, Zhu L-M, Li X-Y, Yang X-L. Novel drug delivery devices for providing linear release profiles fabricated by 3DP. *Int J Pharm.* 2009 Mar 31;370(1–2):160–6.
6. Shin D, Hyun J. Silk fibroin microneedles fabricated by digital light processing 3D printing. *J Ind Eng Chem.* 2021 Mar 25;95:126–33.
7. Martinez PR, Goyanes A, Basit AW, Gaisford S. Fabrication of drug-loaded hydrogels with stereolithographic 3D printing. *Int J Pharm.* 2017 Oct 30;532(1):313–7.
8. Karakurt I, Aydoğdu A, Çıkrıkçı S, Orozco J, Lin L. Stereolithography (SLA) 3D printing of ascorbic acid loaded hydrogels: A controlled release study. *Int J Pharm.* 2020 Jun 30;584:119428.
9. Bloomquist CJ, Mecham MB, Paradzinsky MD, Januszewicz R, Warner SB, Luft JC, et al. Controlling release from 3D printed medical devices using CLIP and drug-loaded liquid resins. *J Controlled Release.* 2018 May 28;278:9–23.
10. Awad A, Fina F, Goyanes A, Gaisford S, Basit AW. Advances in powder bed fusion 3D printing in drug delivery and healthcare. *Adv Drug Deliv Rev.* 2021 Jul 1;174:406–24.
11. Fina F, Goyanes A, Gaisford S, Basit AW. Selective laser sintering (SLS) 3D printing of medicines. *Int J Pharm.* 2017 Aug 30;529(1):285–93.
12. Hassanin H, Finet L, Cox SC, Jamshidi P, Grover LM, Shepherd DET, et al. Tailoring selective laser melting process for titanium drug-delivering implants with releasing micro-channels. *Addit Manuf.* 2018 Mar 1;20:144–55.
13. Bezuidenhout MB, Booyesen E, van Staden AD, Uheida EH, Hugo PA, Oosthuizen GA, et al. Selective Laser Melting of Integrated Ti6Al4V ELI Permeable Walls for Controlled Drug Delivery of Vancomycin. *ACS Biomater Sci Eng.* 2018 Dec 10;4(12):4412–24.
14. Vaithilingam J, Kilsby S, Goodridge RD, Christie SDR, Edmondson S, Hague RJM. Functionalisation of Ti6Al4V components fabricated using selective laser melting with a bioactive compound. *Mater Sci Eng C.* 2015 Jan 1;46:52–61.

VII. PLGA BASED 3D PRINTED IMPLANTS – IMPACT OF THE 3D PRINTED TECHNOLOGY ON DRUG RELEASE

15. Goyanes A, Robles Martinez P, Buanz A, Basit AW, Gaisford S. Effect of geometry on drug release from 3D printed tablets. *Int J Pharm.* 2015 Oct 30;494(2):657–63.
16. Goyanes A, Allahham N, Trenfield SJ, Stoyanov E, Gaisford S, Basit AW. Direct powder extrusion 3D printing: Fabrication of drug products using a novel single-step process. *Int J Pharm.* 2019 Aug 15;567:118471.
17. Welsh NR, Malcolm RK, Devlin B, Boyd P. Dapivirine-releasing vaginal rings produced by plastic freeforming additive manufacturing. *Int J Pharm.* 2019 Dec 15;572:118725.
18. Khaled SA, Burley JC, Alexander MR, Roberts CJ. Desktop 3D printing of controlled release pharmaceutical bilayer tablets. *Int J Pharm.* 2014 Jan 30;461(1):105–11.
19. Khaled SA, Burley JC, Alexander MR, Yang J, Roberts CJ. 3D printing of tablets containing multiple drugs with defined release profiles. *Int J Pharm.* 2015 Oct 30;494(2):643–50.
20. Muwaffak Z, Goyanes A, Clark V, Basit AW, Hilton ST, Gaisford S. Patient-specific 3D scanned and 3D printed antimicrobial polycaprolactone wound dressings. *Int J Pharm.* 2017 Jul 15;527(1):161–70.
21. Grottkau BE, Hui Z, Pang Y. A Novel 3D Bioprinter Using Direct-Volumetric Drop-On-Demand Technology for Fabricating Micro-Tissues and Drug-Delivery. *Int J Mol Sci.* 2020 Jan;21(10):3482.
22. Clark EA, Alexander MR, Irvine DJ, Roberts CJ, Wallace MJ, Sharpe S, et al. 3D printing of tablets using inkjet with UV photoinitiation. *Int J Pharm.* 2017 Aug 30;529(1–2):523–30.
23. Patel SK, Khoder M, Peak M, Alhnan MA. Controlling drug release with additive manufacturing-based solutions. *Adv Drug Deliv Rev.* 2021 Jul 1;174:369–86.
24. Lai Y, Li Y, Cao H, Long J, Wang X, Li L, et al. Osteogenic magnesium incorporated into PLGA/TCP porous scaffold by 3D printing for repairing challenging bone defect. *Biomaterials.* 2019 Mar 1;197:207–19.
25. Kwon B-J, Seon GM, Lee MH, Koo M-A, Kim MS, Kim D, et al. Locally delivered ethyl-2,5-dihydroxybenzoate using 3D printed bone implant for promotion of bone regeneration in a osteoporotic animal model. *Eur Cell Mater.* 2018 12;35:1–12.
26. Lin S, Cui L, Chen G, Huang J, Yang Y, Zou K, et al. PLGA/ β -TCP composite scaffold incorporating salvianolic acid B promotes bone fusion by angiogenesis and osteogenesis in a rat spinal fusion model. *Biomaterials.* 2019 Mar 1;196:109–21.
27. Jakus AE, Geisendorfer NR, Lewis PL, Shah RN. 3D-printing porosity: A new approach to creating elevated porosity materials and structures. *Acta Biomater.* 2018 May 1;72:94–109.
28. Carlier E, Marquette S, Peerboom C, Denis L, Benali S, Raquez J-M, et al. Investigation of the parameters used in fused deposition modeling of poly(lactic acid) to optimize 3D printing sessions. *Int J Pharm.* 2019 Jun 30;565:367–77.

29. Carlier E, Marquette S, Peerboom C, Amighi K, Goole J. Development of mAb-loaded 3D-printed (FDM) implantable devices based on PLGA. *Int J Pharm.* 2021 Mar 15;597:120337.
30. Park K, Skidmore S, Hadar J, Garner J, Park H, Otte A, et al. Injectable, long-acting PLGA formulations: Analyzing PLGA and understanding microparticle formation. *J Controlled Release.* 2019 Jun 28;304:125–34.
31. Sharifi F, Otte A, Yoon G, Park K. Continuous in-line homogenization process for scale-up production of naltrexone-loaded PLGA microparticles. *J Controlled Release.* 2020 Sep 10;325:347–58.
32. Shi N-Q, Zhou J, Walker J, Li L, Hong JKY, Olsen KF, et al. Microencapsulation of luteinizing hormone-releasing hormone agonist in poly (lactic-co-glycolic acid) microspheres by spray-drying. *J Controlled Release.* 2020 May 10;321:756–72.
33. Anderson J, Shives M. Biodegradation and biocompatibility of PLA and PLGA microspheres. *Adv Drug Deliv Rev.* 1997 Oct 13;28(1):5–24.
34. Arrighi A, Marquette S, Peerboom C, Denis L, Goole J, Amighi K. Development of PLGA microparticles with high immunoglobulin G-loaded levels and sustained-release properties obtained by spray-drying a water-in-oil emulsion. *Int J Pharm.* 2019 Jul 20;566:291–8.
35. Parent M, Clarot I, Gibot S, Derive M, Maincent P, Leroy P, et al. One-week in vivo sustained release of a peptide formulated into in situ forming implants. *Int J Pharm.* 2017 Apr 15;521(1):357–60.
36. Ravivarapu HB, Burton K, DeLuca PP. Polymer and microsphere blending to alter the release of a peptide from PLGA microspheres. *Eur J Pharm Biopharm.* 2000 Sep 1;50(2):263–70.
37. Wischke C, Schwendeman SP. Principles of encapsulating hydrophobic drugs in PLA/PLGA microparticles. *Int J Pharm.* 2008 Dec 8;364(2):298–327.
38. Acharya G, Shin CS, Vedantham K, McDermott M, Rish T, Hansen K, et al. A study of drug release from homogeneous PLGA microstructures. *J Controlled Release.* 2010 Sep 1;146(2):201–6.
39. Fang Y, Zhang N, Li Q, Chen J, Xiong S, Pan W. Characterizing the release mechanism of donepezil-loaded PLGA microspheres in vitro and in vivo. *J Drug Deliv Sci Technol.* 2019 Jun 1;51:430–7.
40. Kempe S, Mäder K. In situ forming implants - an attractive formulation principle for parenteral depot formulations. *J Controlled Release.* 2012 Jul 20;161(2):668–79.
41. Ochi M, Wan B, Bao Q, Burgess DJ. Influence of PLGA molecular weight distribution on leuprolide release from microspheres. *Int J Pharm.* 2021 Apr 15;599:120450.
42. Chen W, Palazzo A, Hennink WE, Kok RJ. Effect of Particle Size on Drug Loading and Release Kinetics of Gefitinib-Loaded PLGA Microspheres. *Mol Pharm.* 2017 Feb 6;14(2):459–67.

VII. PLGA BASED 3D PRINTED IMPLANTS – IMPACT OF THE 3D PRINTED TECHNOLOGY ON DRUG RELEASE

43. Klose D, Siepmann F, Elkharraz K, Krenzlin S, Siepmann J. How porosity and size affect the drug release mechanisms from PLGA-based microparticles. *Int J Pharm.* 2006 May 18;314(2):198–206.
44. Kohno M, Andhariya JV, Wan B, Bao Q, Rothstein S, Hezel M, et al. The effect of PLGA molecular weight differences on risperidone release from microspheres. *Int J Pharm.* 2020 May 30;582:119339.
45. Gèze A, Venier-Julienne MC, Mathieu D, Filmon R, Phan-Tan-Luu R, Benoit JP. Development of 5-iodo-2'-deoxyuridine milling process to reduce initial burst release from PLGA microparticles. *Int J Pharm.* 1999 Feb 15;178(2):257–68.
46. Ramazani F, Chen W, van Nostrum CF, Storm G, Kiessling F, Lammers T, et al. Strategies for encapsulation of small hydrophilic and amphiphilic drugs in PLGA microspheres: State-of-the-art and challenges. *Int J Pharm.* 2016 Feb 29;499(1):358–67.
47. Wan F, Yang M. Design of PLGA-based depot delivery systems for biopharmaceuticals prepared by spray drying. *Int J Pharm.* 2016 Feb 10;498(1):82–95.
48. Maroni A, Melocchi A, Parietti F, Foppoli A, Zema L, Gazzaniga A. 3D printed multi-compartment capsular devices for two-pulse oral drug delivery. *J Controlled Release.* 2017 Dec 1;268:10–8.
49. Feuerbach T, Callau-Mendoza S, Thommes M. Development of filaments for fused deposition modeling 3D printing with medical grade poly(lactic-co-glycolic acid) copolymers. *Pharm Dev Technol.* 2019 Apr 21;24(4):487–93.
50. Madla CM, Trenfield SJ, Goyanes A, Gaisford S, Basit AW. 3D Printing Technologies, Implementation and Regulation: An Overview. In: Basit AW, Gaisford S, editors. *3D Printing of Pharmaceuticals* [Internet]. Cham: Springer International Publishing; 2018 [cited 2021 Jul 6]. p. 21–40. (AAPS Advances in the Pharmaceutical Sciences Series). Available from: https://doi.org/10.1007/978-3-319-90755-0_2
51. Stavropoulos P, Foteinopoulos P. Modelling of additive manufacturing processes: a review and classification. *Manuf Rev.* 2018;5:2.
52. Guessasma S, Nouri H, Roger F. Microstructural and Mechanical Implications of Microscaled Assembly in Droplet-based Multi-Material Additive Manufacturing. *Polymers.* 2017 Aug 18;9(8):372.
53. Gradwohl M, Chai F, Payen J, Guerreschi P, Marchetti P, Blanchemain N. Effects of Two Melt Extrusion Based Additive Manufacturing Technologies and Common Sterilization Methods on the Properties of a Medical Grade PLGA Copolymer. *Polymers.* 2021 Jan;13(4):572.
54. Censi R, Gigliobianco MR, Casadidio C, Di Martino P. Hot Melt Extrusion: Highlighting Physicochemical Factors to Be Investigated While Designing and Optimizing a Hot Melt Extrusion Process. *Pharmaceutics.* 2018 Jul 11;10(3):E89.
55. Wang J, Wang BM, Schwendeman SP. Characterization of the initial burst release of a model peptide from poly(D,L-lactide-co-glycolide) microspheres. *J Control Release Off J Control Release Soc.* 2002 Aug 21;82(2–3):289–307.

56. Huang X, Brazel CS. On the importance and mechanisms of burst release in matrix-controlled drug delivery systems. *J Control Release Off J Control Release Soc.* 2001 Jun 15;73(2–3):121–36.
57. Gasmi H, Siepmann F, Hamoudi MC, Danede F, Verin J, Willart J-F, et al. Towards a better understanding of the different release phases from PLGA microparticles: Dexamethasone-loaded systems. *Int J Pharm.* 2016 Nov 30;514(1):189–99.
58. Huang J, Mazzara JM, Schwendeman SP, Thouless MD. Self-healing of pores in PLGAs. *J Controlled Release.* 2015 May 28;206:20–9.
59. Bode C, Kranz H, Fizez A, Siepmann F, Siepmann J. Often neglected: PLGA/PLA swelling orchestrates drug release: HME implants. *J Controlled Release.* 2019 Jul 28;306:97–107.
60. Grund S, Bauer M, Fischer D. Polymers in Drug Delivery—State of the Art and Future Trends. *Adv Eng Mater.* 2011;13(3):B61–87.
61. Antheunis H, van der Meer J-C, de Geus M, Heise A, Koning CE. Autocatalytic equation describing the change in molecular weight during hydrolytic degradation of aliphatic polyesters. *Biomacromolecules.* 2010 Apr 12;11(4):1118–24.

VII. PLGA BASED 3D PRINTED IMPLANTS – IMPACT OF THE 3D PRINTED TECHNOLOGY ON DRUG RELEASE

**VIII. PLGA BASED 3D PRINTED IMPLANTS
– IMPACT OF FILLING DENSITY ON
DRUG RELEASE**

VIII. PLGA BASED 3D PRINTED IMPLANTS – IMPACT OF FILLING DENSITY ON DRUG RELEASE

PLGA based 3D printed implant – impact of filling density on drug release

C. Bassand¹, L. Benabed¹, J. Verin¹, J. Freitag¹, S. Charlon², F. Siepmann¹, J. Soulestin², J. Siepmann¹

¹*Univ. Lille, Inserm, CHU Lille, U1008, F-59000 Lille, France*

²*IMT Lille Douai, Dept Polymers & Composites Technol & Mech Engn, F-59500 Douai, France*

VIII.1. Abstract

Among the several advantages of the three-dimension (3D) printing technologies, the ability to precisely modulate the filling density of the printed devices is particularly interesting. This study aimed to study the impact of filling density on ibuprofen-loaded poly (lactic-co-glycolic) acid (PLGA) implant printed with the “Arburg Plastic Freeforming[®]” droplet deposition modeling technology. To do so implants with filling densities of 10% and 100% were printed, and characterized regarding morphology (optical macroscopy and scanning electronic microscopy), solid-state (differential scanning calorimetry), drug loading, and molecular weight of the polymer. The in vitro performances resulting from those implants were investigated after exposure to phosphate buffer pH 7.4, at 37°C 80 RPM. Absolute (%) and relative (mg) in vitro ibuprofen release kinetic, increase in wet mass, and morphological changes upon exposure to release medium were evaluated. The degradation behavior of PLGA upon exposure to the phosphate buffer (loss of dry mass, and molecular weight of the polymer) depending on the filling density of the implant was also investigated. The obtained implants exhibit a triphasic release pattern: with a slight burst effect after 1 day from 5 to 10% of ibuprofen released respectively for the 100% and 10% filling density implants. This is followed by a lag phase up to day 5 or 9 respectively for the 10% and 100% filling density implants. The decrease in the *relative* drug release rate with increasing implant filling can be attributed to the longer diffusion pathways to be overcome.

Keywords: PLGA, 3D printing, Droplet deposition modeling, Filling density, in vitro drug release.

VIII. PLGA BASED 3D PRINTED IMPLANTS – IMPACT OF FILLING DENSITY ON
DRUG RELEASE

VIII.2. Introduction

During the past years, (3D) printing technologies revolutionized the pharmaceutical field. Objects are built by deposition, binding, or polymerization of successive materials layers (1,2). The desired object can be printed by: photopolymerization, powder bed fusion, material jetting, direct energy deposition, binder jetting, selective deposition lamination, and material extrusion (1,2). Lately, the FDA approved SPRITAM, the first 3D printed dosage to obtain such an approval (1,3). The SPRITAM drug product is by binder jetting (4,5), allowing to reach an extremely high porosity and fast oral dispersing product. Besides binder jetting, four 3D printing technologies have been used for pharmaceutical applications: photopolymerization (6–9), powder bed fusion (10–14), material extrusion (15–20), and material jetting (21,22).

In the past few years, oral controlled release dosage forms obtained by 3D printing have been widely studied (15,21,23–25). Lately, an emerging interest is reached on 3D printed dosage forms intended for parenteral administration with polyester matrix (26–28), and especially poly (lactic-co-glycolic) acid (PLGA) based devices (29–34). PLGA is a usually used polymer in controlled drug delivery systems for parenteral administration (35–37). Its excellent biocompatible and biodegradable properties allow avoiding the removal of the device after the treatment (38–42). Those properties conducted to an intense interest in this polyester (43–45) and led to his use in numerous FDA-approved drug products, such as microparticles, implants, or *in situ* forming implants for decades (46,47). From such a polymer, the drug release kinetics can be tailored either by using different polymer grades, devices, porosity, or size (48–51). The manufacturing process as well influences the release rate (52–54).

The emerging 3D printing technologies provide new horizons to precisely control drug release from PLGA based devices. PLGA thermoplastic properties make it a good choice for use with extrusion-based 3D printing technologies (55). Modeling (FDM) also known as Fused Filament Fabrication (FFF), Direct Powder Extrusion (DPE), and Droplet Deposition Modeling (DDM) are extrusion-based 3D printed technologies and are nowadays the most widely used (15–17,56–58). The “Arburg Plastic Freeforming[®]” technology is a thermoplastic DDM technology, capable to process a wide range of granulated polymer feedstocks commonly used in injection molding processes (17,58). For example, Welsh *et al* studied the possibility to modulate Dapivirine, release from polyurethane matrix for vaginal delivery (17). They investigate the impact of the filling density on drug release kinetic from vaginal rings, highlighting that by decreasing the filling density, the Dapirivine release rate increases.

VIII. PLGA BASED 3D PRINTED IMPLANTS – IMPACT OF FILLING DENSITY ON DRUG RELEASE

The study aimed to evaluate the impact of filling density of ibuprofen-loaded PLGA implants obtained by DDM on implants' physicochemical characteristics and *in vitro* drug release performance. To do so, ibuprofen-loaded PLGA implants with 10% and 100% filling density were printed using the DDM Arburg Freeformer® technology. Thus, both implants' physicochemical characteristics were investigated before and after exposure to phosphate buffer pH 7.4. The impact of the filling density on the practical drug loading, polymer molecular weight, morphology by optical macroscopy, and scanning electronic microscopy was investigated. The impact of the difference observed on the *in vitro* drug release after exposure to phosphate buffer pH 7.4, and erosion of PLGA was also investigated.

VIII.3. Materials and methods

VIII.3.1. Materials

Poly (D,L lactic-co-glycolic acid) (PLGA, 50:50 lactic acid: glycolic acid; Resomer RG 503H; Evonik, Darmstadt; Germany); ibuprofen (BASF, Ludwigshafen, Germany); agarose (genetic analysis grade), tetrahydrofuran (HPLC grade) (Fisher Scientific, Illkirch, France); potassium dihydrogen orthophosphate and sodium hydroxide (Acros Organics, Geel, Belgium); acetonitrile (VWR, Fontenoy-sous-Bois, France); sodium hydrogen phosphate (Na_2HPO_4 , Panreac Quimica, Barcelona, Spain).

VIII.3.2. Pellets preparation

PLGA was milled (4 x 30 s) with a grinder (Valentin, Seb, Ecully, France). Appropriate amounts of polymer and drug powders were blended for 5 min with a mortar and a pestle, followed by extrusion using a Nano 16 twin-screw extruder (screw diameter = 16 mm, length/diameter ratio = 26.25, gravitational feeder; Leistritz, Nuremberg, Germany), equipped with a 2 mm diameter die. The process temperatures were kept constant at 80 - 75 - 70 - 65 °C (die - zone 3 - zone 2 - zone 1). The screw speed was set at 50 rpm. After cooling, the hot melt extrudates were manually cut into pellets of 5 mm length.

VIII.3.3. 3D printing of the implant

Parallelepipeds (10 mm, 10 mm, 2.5 mm) with different filling densities (10 %, and 100 %) were printed using the Arburg Plastic Freeforming ® technology (Arburg GmbH, Loßburg, Allemagne) illustrated in *Figure VIII-1*. The pellets obtained by hot melt extrusion were fed into the Freeformer ®. The manufacturing parameters were set depending on the filling density as indicated in *Table VIII-1*.

Table VIII-1. Printing parameters used to obtain the ibuprofen loaded PLGA-implants of different density.

Filling density	10 %	100 %
Nozzle diameter (µm)		250
Printing speed (mm/s)		40
Layer thickness (mm)	0.18	0.33
T° 1 st zone (°C)		120
T° 2 nd zone (°C)		110
T° 3 rd zone (°C)		110
T° Printing chamber (°C)		25

VIII. PLGA BASED 3D PRINTED IMPLANTS – IMPACT OF FILLING DENSITY ON DRUG RELEASE

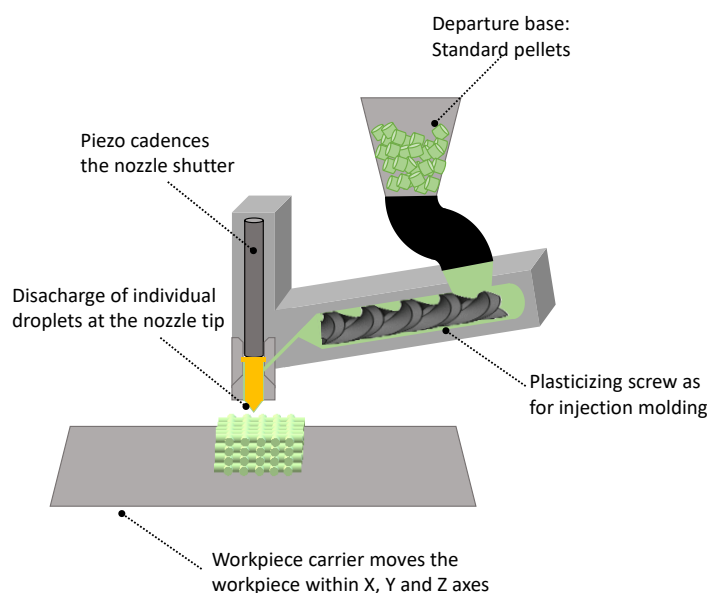


Figure VIII-1. Schematic presentation of the Arburg Freeformer® technology.

VIII.3.4. Optical microscopy

Pictures of the implant before exposure to the release medium were taken using a SZN-6 trinocular stereo zoom microscope (Optika, Ponteranica, Italy), equipped with an optical camera (Optika Vison Lite 2.1 software). The lengths and implant pore size were determined using the ImageJ software (US National Institutes of Health, Bethesda, Maryland, USA).

VIII.3.5. Practical drug loading

Pellets and pieces of the 3D printed implant were dissolved in 5 mL acetonitrile, followed by filtering (PVDF syringe filters, 0.45 μm ; Agilent Technologies, Santa Clara, USA) and drug content determination by HPLC-UV analysis using a Thermo Fisher Scientific Ultimate 3000 Series HPLC, equipped with an LPG 3400 SD/RS pump, an autosampler (WPS-3000 SL) and a UV-Vis detector (VWD-3400RS) (Thermo Fisher Scientific, Waltham, USA). A reversed-phase column C18 (Gemini 5 μm ; 110 A° ; 150 x 4.6 mm; Phenomenex, Le Pecq, France) was used. The mobile phase was a mixture of 30 mM Na_2HPO_4 pH 7.0: acetonitrile (60:40, v:v). The detection wavelength was 225 nm, and the flow rate was 0.5 mL/min. Ten microliter samples were injected.

VIII.3.6. Differential scanning calorimetry (DSC)

DSC thermograms of the raw materials (PLGA and ibuprofen), pellets and 3D printed implant were recorded using a DCS1 Star System (Mettler Toledo, Greifensee, Switzerland). Approximately 5 mg raw material, pellets, and 3D printed implant, were heated in pierced

aluminum pans as follows: from -70 to 120 °C, cooling to -70 °C, re-heating to 120 °C (heating/cooling rate = 10 °C/min. The reported glass temperatures (T_gs) were determined from the 1st heating cycles in the case of the pellets and 3D printed implant (the thermal history being of interest), and from the 2nd heating cycle in the case of the raw material (the thermal history not being of interest). All experiments were conducted in triplicate. Mean values +/- standard deviations are reported.

VIII.3.7. Gel permeation chromatography (GPC)

The average polymer molecular weight (M_w) of the PLGA was determined by gel permeation chromatography (GPC) as follows: raw materials, samples were dissolved in tetrahydrofuran (3 mg/mL). Fifty µL samples were injected into an Alliance GPC (refractometer detector: 2414 RI, separation module e2695, Empower GPC software; Waters, Milford, USA), equipped with a PLgel 5 µm MIXED-D column (kept at 35°C, 7.8 × 300 mm; Agilent). Tetrahydrofuran was the mobile phase (flow rate: 1 mL/min). Polystyrene standards with molecular weights between 1,480 and 70,950 Da (Polymer Laboratories, Varian, Les Ulis, France) were used to prepare the calibration curve. All experiments were conducted in triplicate. Mean values +/- standard deviations are reported.

VIII.3.8. In vitro drug release

Implants were placed in 50 mL tubes (352070 Corning-Falcon, New York, U.S.; 1 implant per tube), filled with 50 mL phosphate buffer pH 7.4 USP 42. The tubes were placed in a horizontal shaker (80 rpm, 37°C; GFL 3033; Gesellschaft fuer Labortechnik, Burgwedel, Germany). At predetermined time points, the entire bulk fluid was replaced by fresh release medium. The withdrawn samples were filtered (PVDF syringe filter, 0.45 µm; Agilent, Santa Clara, California, USA) and analyzed for their ibuprofen contents by HPLC-UV, as described in *section VIII.3.5*.

In all cases, at pre-determined time points, pictures were taken as described in *section VIII.3.4*. Also, in all cases, sink conditions were provided throughout the experiments in all agitated bulk fluids. All experiments were conducted in triplicate. Mean values +/- standard deviations are reported.

VIII.3.9. Implant swelling

Implants were treated as for the *in vitro* drug release measurements. At pre-determined time points: implant samples were withdrawn and excess water was carefully removed using

VIII. PLGA BASED 3D PRINTED IMPLANTS – IMPACT OF FILLING DENSITY ON DRUG RELEASE

Kimtech precision wipes (Kimberly-Clark, Rouen, France). The implants were weighed [*wet mass (t)*], and the *change in wet mass (%) (t)* was calculated as follows:

$$\text{change in wet mass } (\%)(t) = \frac{\text{wet mass } (t) - \text{mass } (t = 0)}{\text{mass } (t = 0)} \times 100 \%$$

where *mass (t = 0)* denotes the implant mass before exposure to the release medium.

All experiments were conducted in triplicate. Mean values +/- standard deviations are reported.

VIII.3.10. Implant erosion and PLGA degradation

Implant samples were treated as for the in vitro drug release studies described above. At pre-determined time points, implant samples were withdrawn and freeze-dried (freezing at -45°C for 2 h 35 min, primary drying at -20 °C/0.940 mbar for 35 h 10 min, secondary drying at +20 °C/0.0050 mbar for 35 h; Christ Alpha 2-4 LSC+; Martin Christ, Osterode, Germany).

The *dry mass (%) (t)* was calculated as follows:

$$\text{dry mass } (\%)(t) = \frac{\text{dry mass } (t)}{\text{mass } (t = 0)} \times 100 \%$$

where *mass (t = 0)* denotes the implant mass before exposure to the release medium. All experiments were conducted in triplicate. Mean values +/- standard deviations are reported.

The average polymer molecular weight (Mw) of the PLGA was determined by gel permeation chromatography (GPC) as described in *section VIII.3.8*. All experiments were conducted in triplicate. Mean values +/- standard deviations are reported.

VIII.3.11. . Scanning electronic microscopy (SEM)

The internal and external morphology of the implant before and after exposure to the release medium was studied using a JEOL Field Emission Scanning Electron Microscope (JSM-7800F, Japan), equipped with the Aztec 3.3 software (Oxford Instruments, Oxfordshire, England). Samples were fixed with a ribbon carbon double-sided adhesive and covered with a fine chrome layer. In the case of implants that had been exposed to the release medium, the systems were treated as described for the in vitro release studies as described in *section VIII.3.7*. At predetermined time points, implant samples were withdrawn, optionally cut (for cross-sections) using a scalpel, and freeze-dried (as described in *section VIII.3.10*).

VIII.4. Results and discussion

VIII.4.1. Characterization of the implants before exposure to the release medium

This study aimed to produce ibuprofen-loaded PLGA implants by 3D printing with different filling densities to investigate the impact of the filling density on the in vitro performance. *Figure VIII-2* show macroscopic pictures of the implants obtained by 3D printing (*Table VIII-1*). Please note that different layers thickness had to be defined depending on the filling density of the implant, to limit the polymer collapsing for the implants with low filling density. The implants pores size created by the different filling density, are highlighted in green dotted line in *Figure VIII-2* and their size (measured in diagonal) are summarized in *Table VIII-2*. Apart from that and the weight of the implants, they exhibit similar properties regarding their, length, width, thickness, practical drug loading, glass transition temperature, and molecular weight of the polymer (*Table VIII-2*).

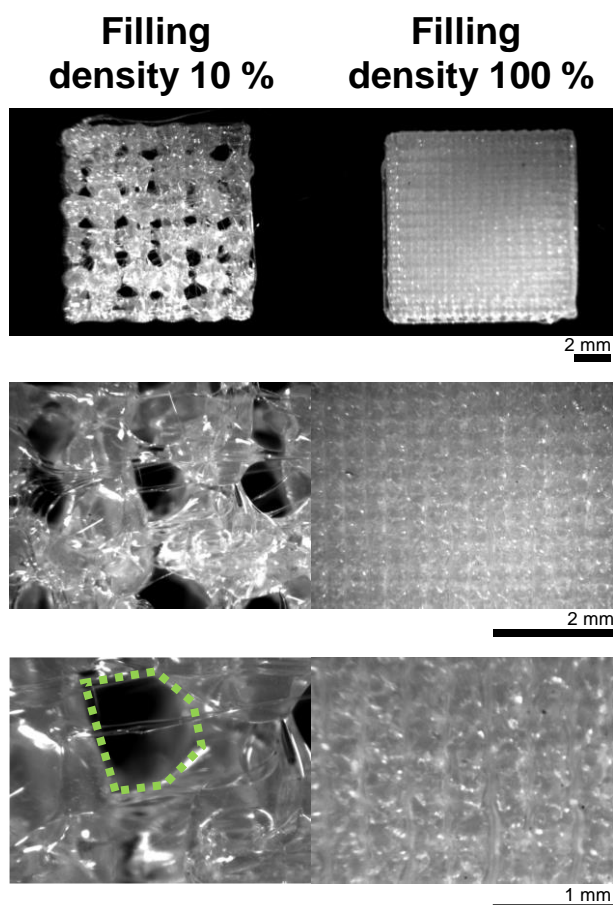


Figure VIII-2. Optical macroscopic pictures of the surface of ibuprofen PLGA-implant obtained with the Arburg Freeformer® technology, with a filling density of either 10 %, or 100 % before exposure to the release medium.

VIII. PLGA BASED 3D PRINTED IMPLANTS – IMPACT OF FILLING DENSITY ON DRUG RELEASE

Table VIII-2. Key properties of the obtained ibuprofen loaded PLGA-implants. (Tg: glass transition temperature, Mw: molecular weight). Mean values \pm standard deviations are indicated (Weight, Length, Width, Implant pore size $n=36$, Practical drug loading $n=6$, Tg, Mw $n=3$).

Filling density	10 %	100 %
Weight (mg)	206.5 \pm 5.9	304.7 \pm 11.1
Length – width (mm)	10.4 \pm 0.4	10.0 \pm 0.1
Implants pore size (mm)	1.1 \pm 0.2	-
Practical drug loading (%)	13.6 \pm 0.2	13.4 \pm 0.1
Tg ($^{\circ}$ C)	33.7 \pm 0.3	34.0 \pm 0.8
Mw (kDa)	16.7 \pm 0.5	15.0 \pm 2.0

As previously reported (17) DDM induces high mechanical stress, leading to a decrease in PLGA molecular weight (from 27.7 kDa before printing to 16.7 kDa, and 15.0 kDa respectively for the implants printed with 10% and 100 % filling density) (*Figure VIII-3*). A previous study reported that such a degradation of PLGA was not observed, even at a higher temperature, with fused filament fabrication confirming that the degradation observed here is mainly due to the high pressure during the process (± 400 bars).

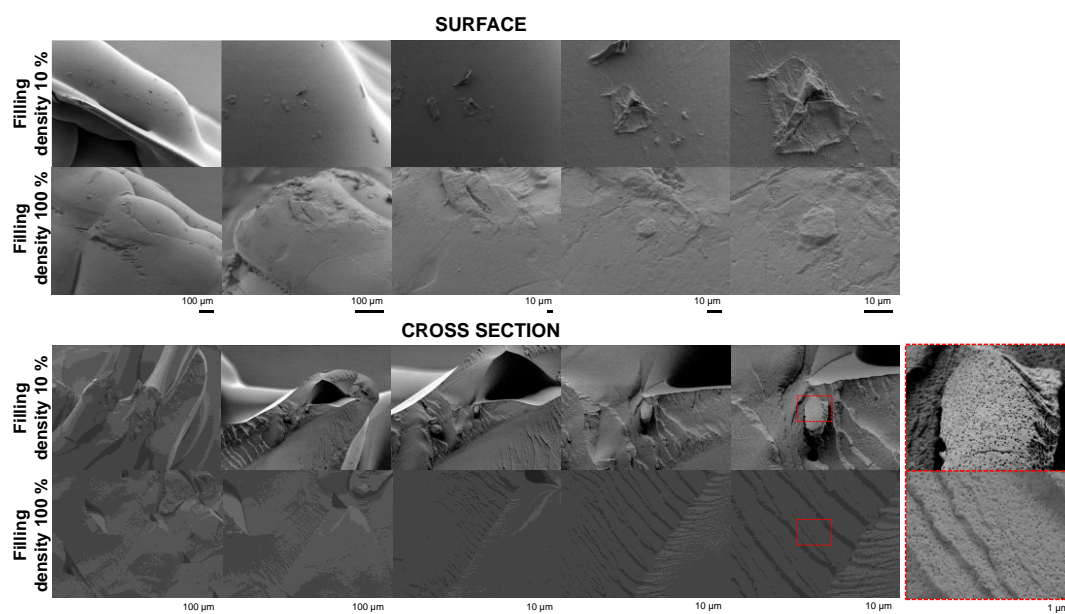


Figure VIII-3. Scanning electronical microscopic pictures of the surface and cross section of ibuprofen PLGA-implant obtained with the Arburg Freeformer® technology, with a filling density of either 10 %, or 100 % before exposure to the release medium.

Moreover, this mechanical stress and high pressure also have consequences on the internal structure observed by scanning electronic microscopy (*Figure VIII-4*). Thus, leading to pores formation (highlighted in red dotted line) due to high mechanical stress upon printing which would induce the evaporation of either ibuprofen molecules, even at lower temperatures than its boiling point, or residual water contained in the raw materials (17).

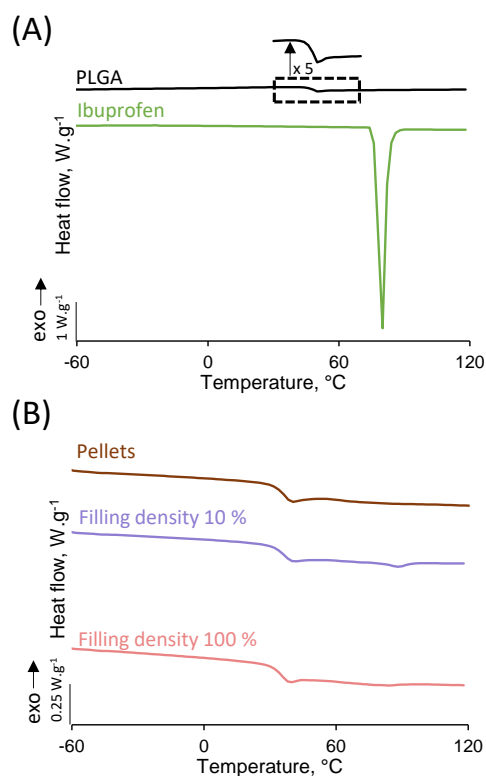


Figure VIII-4. DSC thermograms of: (A) the raw materials (PLGA & ibuprofen), and (B) pellets and ibuprofen loaded PLGA implant obtained with Arburg freeformer ® technology.

As illustrated in *Figure VIII-5*, ibuprofen was fully amorphized in the PLGA matrix, as well in the feedstock materials (pellets) and the 3D printed implants. Leading to a polymer matrix without any crystals at the surface nor in the cross-section (*Figure VIII-4*), and thermograms exempt of any melting point of ibuprofen (*Figure VIII-4*). This solubilization of the ibuprofen in the polymer matrix combined with the ibuprofen plasticizing effect (59,60), decreases the PLGA glass transition from 47°C for the raw material to about 34°C in the 3D printed implant (*Table VIII-2*). Please note that this decrease might not be entirely due to the ibuprofen effect, but also to the PLGA molecular weight decrease after printing.

VIII. PLGA BASED 3D PRINTED IMPLANTS – IMPACT OF FILLING DENSITY ON DRUG RELEASE

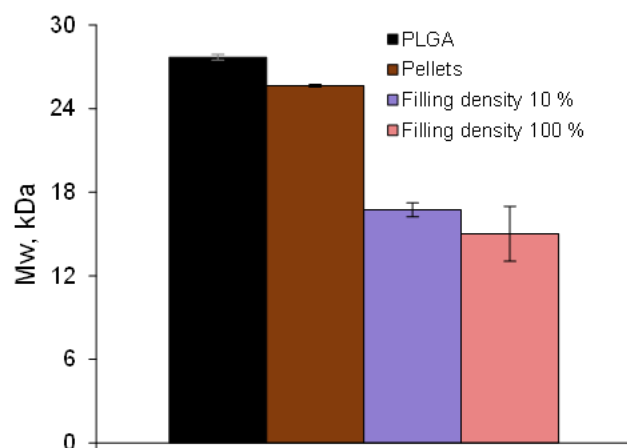


Figure VIII-5. PLGA polymer molecular weight as: raw material, hot-melt extruded pellets and 3D printed ibuprofen loaded PLGA implant.

VIII.4.2. Characterization of the implant after exposure to the release medium

The in vitro performance of the implants with different filling densities obtained by 3D printing upon exposure to phosphate buffer pH 7.4, 37°C, 80 RPM was investigated. The aim was to better understand how initial surface area impacts drug release from ibuprofen-loaded PLGA implants obtained by 3D printing. *Figure VIII-6A and B* diagrams exhibit the relative (%) and absolute (mg) ibuprofen release from the implants previously obtained. Despite the molecular weight decrease observed after 3D printing, the obtained implants demonstrate the ability to sustained ibuprofen release up to 15 days (*Figure VIII-6A and B*).

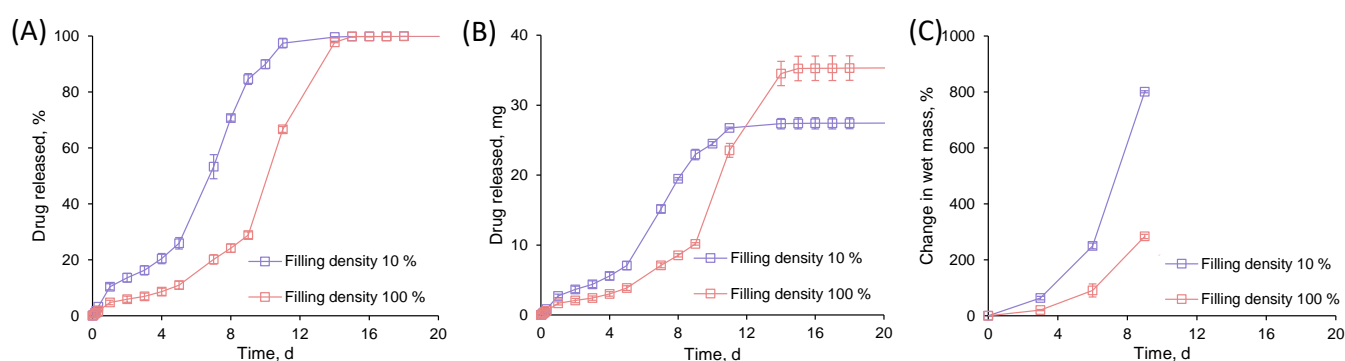


Figure VIII-6. (A) Relative (%), (B) absolute (mg) ibuprofen release for the 3D printed PLGA implants, and (C) increase in wet mass, upon exposure to phosphate buffer pH 7.4.

All the implants exhibit a triphasic release pattern, with different behavior (*Figure VIII-6A and B*). Regarding ibuprofen release, 10% filling density implants and 100% filling density implants have different behavior, with the 100% filling density implants exhibiting a lower burst (about

10% of ibuprofen released during the burst for the 10% filling density and about 5% of ibuprofen released during the burst for the 100% filling density implants), and longer lag phase (up to day 5 for the 10% filling density implants, and up to day 10 for the 100% filling density implants). This relative decrease in release rate by increasing the filling density of polyester-based 3D printed implants is consistent with the reported results recently discussed by Zhang *et al* (26). This could be explained like that:

- (i) For the 10% filling density implant: during the first days (from day 1 to day 2) of exposure to the release medium, a high surface of the implants is in contact with water (due to the created porosity with the 3D printing filling density), leading to water penetration in the polymer matrix and diffusion of the dissolved molecule of ibuprofen close to the surface of the printed line. Once the ibuprofen close to the surface is released, then the length of the diffusion pathway for ibuprofen in the center of the polymer matrix starts to increase, slowing down the release leading to the lag phase. Then starting from day 5, the PLGA reaches a critical molecular weight leading to a more hydrophilic matrix and significant water uptake and swelling of the whole system (*Figure VIII-6C and Figure VIII-7*). Thus, letting enough space for the remaining ibuprofen entrapped to quickly release, leading to the third release phase (*Figure VIII-6A and B*).
- (ii) For the 100% filling density implants: during the first day of exposure to the release medium (from day 1 to day 2) a lower surface of the implants is in contact with water (as not such a porosity as for the 10% filling density implant is created by 3D printing as shown in *Figure VIII-2 and Figure VIII-3*), leading to a lower *relative* amount (%) of ibuprofen close to the surface released during burst (*Figure VIII-6A*). However, as the 100% filling density implants exhibit a higher weight, this leads to the same total amount (mg) of ibuprofen released than the 10% filling density implants (*Figure VIII-6B*). Then the diffusion pathway becomes even longer than for the 10% filling density implants, as only the parallelepiped faces are in direct

VIII. PLGA BASED 3D PRINTED IMPLANTS – IMPACT OF FILLING DENSITY ON DRUG RELEASE

contact with the release medium. Thus, a lag phase with a slower release rate and a longer period is reached, as water penetrated more sluggishly compared to the lower filling density implants (*Figure VIII-6V*). Then after 7 days of exposure to the release medium, they start to significantly swell (*Figure VIII-7*), leading to initiation of the third phase which is then even accelerated at day 10.

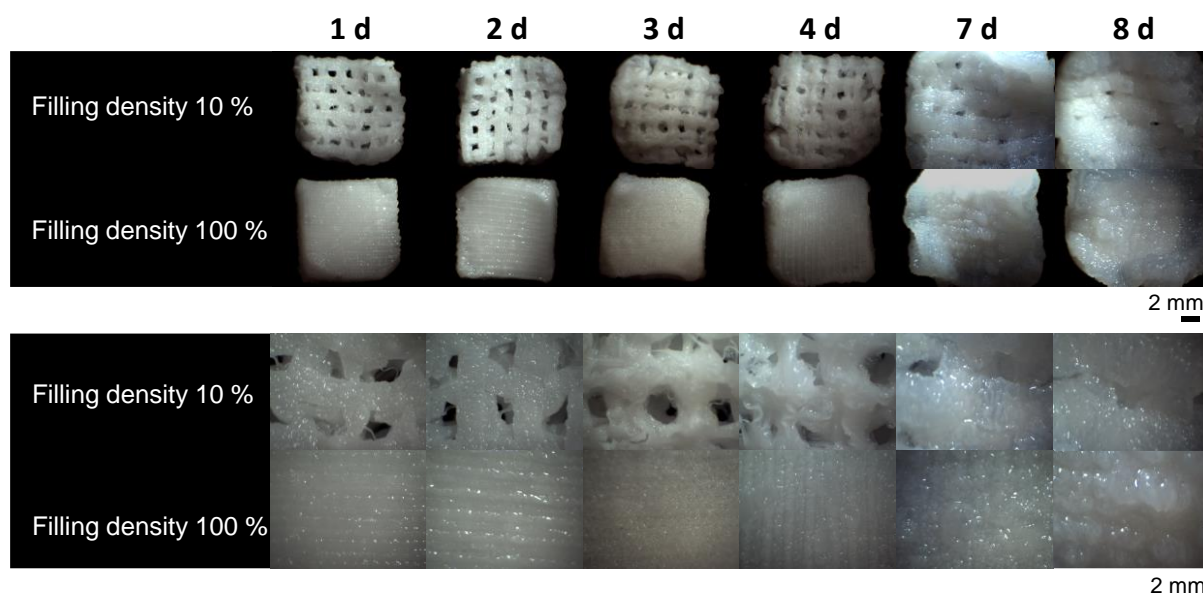


Figure VIII-7. Optical macroscopy pictures of surfaces of ibuprofen loaded PLGA implant after exposure to phosphate buffer pH 7.4.

The diagrams shown in *Figure VIII-8* illustrate the erosion of the implants upon exposure to the phosphate buffer pH 7.4, 37°C, 80 RPM. The loss of dry mass of the polymer is significantly different for the two types of implants (*Figure VIII-8A*), with a higher loss of mass for the implants with the lowest filling density. Their higher surface area leads to a higher probability of losing portions of the degraded polymer. Despite this difference in the loss of dry mass, the molecular weight of the PLGA decreases following the same kinetic whatever the implant filling density (*Figure VIII-8B*).

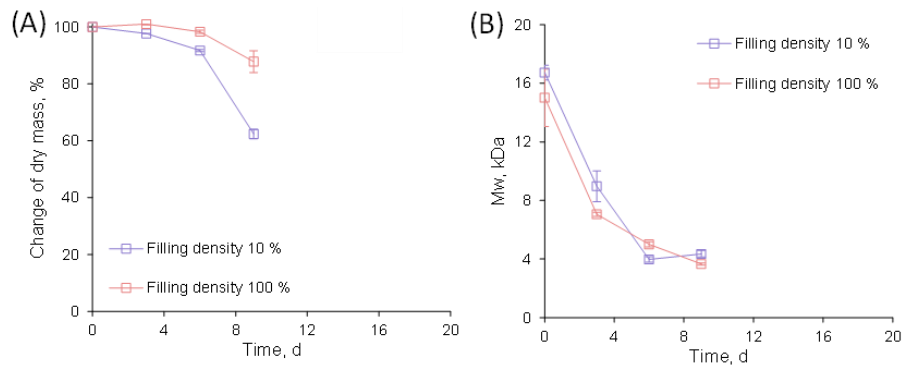


Figure VIII-8. Dynamic changes in the (A) dry mass (%) of the implant and (B) PLGA polymer molecular weight (M_w) upon exposure of the implant to phosphate buffer pH 7.4.

Figure VIII-9 shows SEM pictures of the surface and cross-section of the implants after 3 days of exposure to the release medium. Unfortunately, implants with a 10% filling density were too fragile to cut and obtain a cross-section for SEM pictures. However, for the 100% filling density implants cross-section, it can be seen that there are two different phases, with a thin layer of porous and swelled PLGA close to the surface of the implants (Figure VIII-9). Regarding the surface of the implants after 3 days of exposure to the release medium, whatever the filling density, the surface is unshaped, due to the hydration of the surface of the polymer.

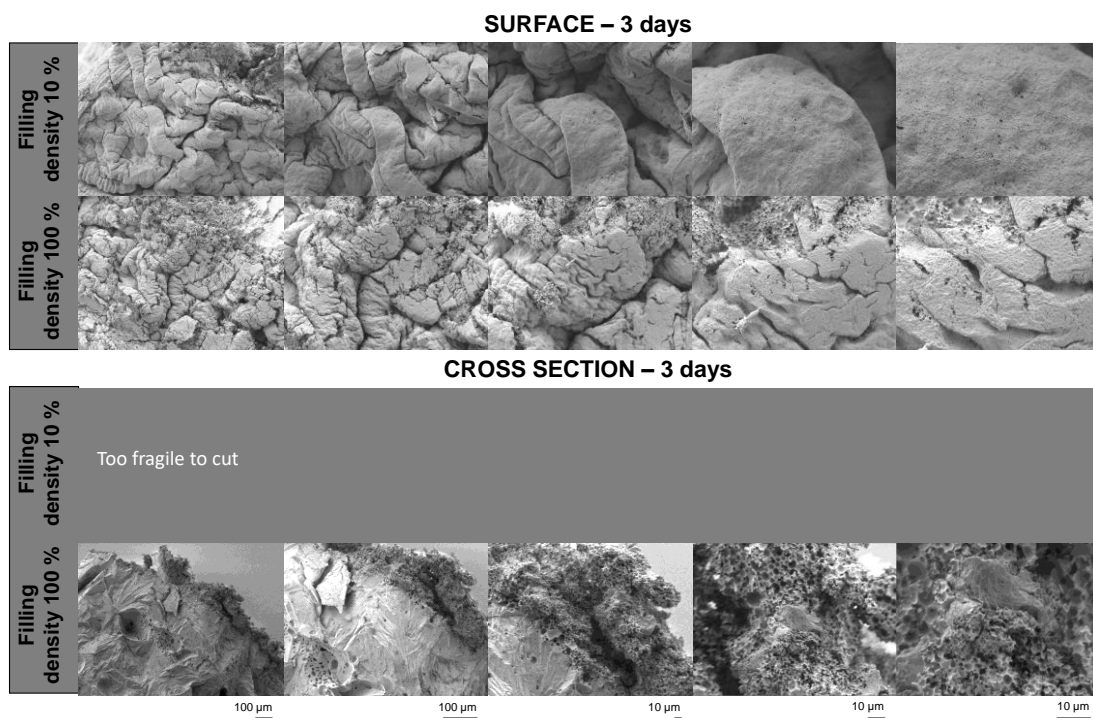


Figure VIII-9. SEM pictures of surfaces and cross-sections of ibuprofen loaded PLGA implant after 3 days exposure to phosphate buffer pH 7.4. Please note that after exposure to the release medium the implants were freeze-dried prior to analysis. Thus, caution must be paid due to artefact creation.

VIII.5. Conclusion

Droplet deposition modeling allows obtaining ibuprofen-loaded 3D printed PLGA implants with different filling densities. Thus, the variation of the filling density is an effective tool to adjust desired absolute and relative release kinetics. The obtained implants exhibit a triphasic release pattern: with a burst release from 5 to 10% during the first days of exposure to the release medium, followed by the drug, and a lag phase up to day 5 or 9 depending on the filling density of the implants. The decrease in the *relative* drug release rate with increasing implant filling can be attributed to the longer diffusion pathways to be overcome. The onset of the final rapid drug release phase was delayed, because the larger polymer matrices are mechanically more stable, retarding the onset of substantial entire implant swelling, which facilitates drug release.

VIII.6. Acknowledgements

This project has received funding from the Interreg 2 Seas programme 2014-2020 co-funded by the European Regional Development Fund under subsidy contract No 2S04-014 3DMed. The authors are very grateful for this support. They would also like to thank Mr. A. Fadel from the “Centre Commun de Microscopie” of the University of Lille (“Plateau technique de la Federation Chevreul CNRS FR 2638”) for his valuable technical help with the SEM pictures.

VIII.7. Author statement

C. Bassand	Investigation; Methodology; Validation; Conceptualization; Writing - Original Draft; Visualization
L. Benabed	Investigation; Methodology; Validation
J. Verin	Investigation; Methodology; Validation
J. Freitag	Investigation
S. Charlon	Investigation, Visualization; Project administration
F. Siepmann	Conceptualization; Methodology; Supervision; Resources; Writing - Review & Editing; Visualization; Project administration; Funding acquisition
J. Soulestin	Conceptualization; Methodology; Supervision; Resources; Writing - Review & Editing; Visualization; Project administration; Funding acquisition

J. Siepmann

Conceptualization; Methodology; Supervision; Resources; Writing -
Review & Editing; Visualization; Project administration; Funding
acquisition

VIII.8. References

1. Lim SH, Kathuria H, Tan JJY, Kang L. 3D printed drug delivery and testing systems - a passing fad or the future? *Adv Drug Deliv Rev.* 2018 May 18;
2. Pravin S, Sudhir A. Integration of 3D printing with dosage forms: A new perspective for modern healthcare. *Biomed Pharmacother Biomedecine Pharmacother.* 2018 Nov;107:146–54.
3. Spritam--a new formulation of levetiracetam for epilepsy. *Med Lett Drugs Ther.* 2016 Jun 20;58(1497):78–9.
4. Jacob J, COYLE N, West TG, Monkhouse DC, Surprenant HL, Jain NB. Rapid disperse dosage form containing levetiracetam [Internet]. WO2014144512A1, 2014 [cited 2021 Jul 8]. Available from: <https://patents.google.com/patent/WO2014144512A1/en>
5. Yu D-G, Branford-White C, Ma Z-H, Zhu L-M, Li X-Y, Yang X-L. Novel drug delivery devices for providing linear release profiles fabricated by 3DP. *Int J Pharm.* 2009 Mar 31;370(1–2):160–6.
6. Shin D, Hyun J. Silk fibroin microneedles fabricated by digital light processing 3D printing. *J Ind Eng Chem.* 2021 Mar 25;95:126–33.
7. Martinez PR, Goyanes A, Basit AW, Gaisford S. Fabrication of drug-loaded hydrogels with stereolithographic 3D printing. *Int J Pharm.* 2017 Oct 30;532(1):313–7.
8. Karakurt I, Aydoğdu A, Çıkrıkçı S, Orozco J, Lin L. Stereolithography (SLA) 3D printing of ascorbic acid loaded hydrogels: A controlled release study. *Int J Pharm.* 2020 Jun 30;584:119428.
9. Bloomquist CJ, Mecham MB, Paradzinsky MD, Januszewicz R, Warner SB, Luft JC, et al. Controlling release from 3D printed medical devices using CLIP and drug-loaded liquid resins. *J Controlled Release.* 2018 May 28;278:9–23.
10. Awad A, Fina F, Goyanes A, Gaisford S, Basit AW. Advances in powder bed fusion 3D printing in drug delivery and healthcare. *Adv Drug Deliv Rev.* 2021 Jul 1;174:406–24.
11. Fina F, Goyanes A, Gaisford S, Basit AW. Selective laser sintering (SLS) 3D printing of medicines. *Int J Pharm.* 2017 Aug 30;529(1):285–93.
12. Hassanin H, Finet L, Cox SC, Jamshidi P, Grover LM, Shepherd DET, et al. Tailoring selective laser melting process for titanium drug-delivering implants with releasing micro-channels. *Addit Manuf.* 2018 Mar 1;20:144–55.
13. Bezuidenhout MB, Booyesen E, van Staden AD, Uheida EH, Hugo PA, Oosthuizen GA, et al. Selective Laser Melting of Integrated Ti6Al4V ELI Permeable Walls for Controlled Drug Delivery of Vancomycin. *ACS Biomater Sci Eng.* 2018 Dec 10;4(12):4412–24.
14. Vaithilingam J, Kilsby S, Goodridge RD, Christie SDR, Edmondson S, Hague RJM. Functionalisation of Ti6Al4V components fabricated using selective laser melting with a bioactive compound. *Mater Sci Eng C.* 2015 Jan 1;46:52–61.

15. Goyanes A, Robles Martinez P, Buanz A, Basit AW, Gaisford S. Effect of geometry on drug release from 3D printed tablets. *Int J Pharm.* 2015 Oct 30;494(2):657–63.
16. Goyanes A, Allahham N, Trenfield SJ, Stoyanov E, Gaisford S, Basit AW. Direct powder extrusion 3D printing: Fabrication of drug products using a novel single-step process. *Int J Pharm.* 2019 Aug 15;567:118471.
17. Welsh NR, Malcolm RK, Devlin B, Boyd P. Dapivirine-releasing vaginal rings produced by plastic freeforming additive manufacturing. *Int J Pharm.* 2019 Dec 15;572:118725.
18. Khaled SA, Burley JC, Alexander MR, Roberts CJ. Desktop 3D printing of controlled release pharmaceutical bilayer tablets. *Int J Pharm.* 2014 Jan 30;461(1):105–11.
19. Khaled SA, Burley JC, Alexander MR, Yang J, Roberts CJ. 3D printing of tablets containing multiple drugs with defined release profiles. *Int J Pharm.* 2015 Oct 30;494(2):643–50.
20. Muwaffak Z, Goyanes A, Clark V, Basit AW, Hilton ST, Gaisford S. Patient-specific 3D scanned and 3D printed antimicrobial polycaprolactone wound dressings. *Int J Pharm.* 2017 Jul 15;527(1):161–70.
21. Grottkau BE, Hui Z, Pang Y. A Novel 3D Bioprinter Using Direct-Volumetric Drop-On-Demand Technology for Fabricating Micro-Tissues and Drug-Delivery. *Int J Mol Sci.* 2020 Jan;21(10):3482.
22. Clark EA, Alexander MR, Irvine DJ, Roberts CJ, Wallace MJ, Sharpe S, et al. 3D printing of tablets using inkjet with UV photoinitiation. *Int J Pharm.* 2017 Aug 30;529(1–2):523–30.
23. Patel SK, Khoder M, Peak M, Alhnan MA. Controlling drug release with additive manufacturing-based solutions. *Adv Drug Deliv Rev.* 2021 Jul 1;174:369–86.
24. Quodbach J. Modulating Drug Release from 3D Printed Pharmaceutical Products. In: *3D and 4D Printing in Biomedical Applications* [Internet]. John Wiley & Sons, Ltd; 2018 [cited 2019 Nov 5]. p. 185–209. Available from: <https://onlinelibrary.wiley.com/doi/abs/10.1002/9783527813704.ch8>
25. Zidan A, Alayoubi A, Coburn J, Asfari S, Ghamraoui B, Cruz CN, et al. Extrudability analysis of drug loaded pastes for 3D printing of modified release tablets. *Int J Pharm.* 2019 Jan 10;554:292–301.
26. Zhang B, Gleadall A, Belton P, McDonagh T, Bibb R, Qi S. New insights into the effects of porosity, pore length, pore shape and pore alignment on drug release from extrusionbased additive manufactured pharmaceuticals. *Addit Manuf.* 2021 Oct 1;46:102196.
27. Yi H-G, Choi Y-J, Kang KS, Hong JM, Pati RG, Park MN, et al. A 3D-printed local drug delivery patch for pancreatic cancer growth suppression. *J Controlled Release.* 2016 Sep 28;238:231–41.

VIII. PLGA BASED 3D PRINTED IMPLANTS – IMPACT OF FILLING DENSITY ON DRUG RELEASE

28. Wu G, Wu W, Zheng Q, Li J, Zhou J, Hu Z. Experimental study of PLLA/INH slow release implant fabricated by three dimensional printing technique and drug release characteristics in vitro. *Biomed Eng Online*. 2014 Jul 19;13:97.
29. Lai Y, Li Y, Cao H, Long J, Wang X, Li L, et al. Osteogenic magnesium incorporated into PLGA/TCP porous scaffold by 3D printing for repairing challenging bone defect. *Biomaterials*. 2019 Mar 1;197:207–19.
30. Kwon B-J, Seon GM, Lee MH, Koo M-A, Kim MS, Kim D, et al. Locally delivered ethyl-2,5-dihydroxybenzoate using 3D printed bone implant for promotion of bone regeneration in a osteoporotic animal model. *Eur Cell Mater*. 2018 12;35:1–12.
31. Lin S, Cui L, Chen G, Huang J, Yang Y, Zou K, et al. PLGA/ β -TCP composite scaffold incorporating salvianolic acid B promotes bone fusion by angiogenesis and osteogenesis in a rat spinal fusion model. *Biomaterials*. 2019 Mar 1;196:109–21.
32. Jakus AE, Geisendorfer NR, Lewis PL, Shah RN. 3D-printing porosity: A new approach to creating elevated porosity materials and structures. *Acta Biomater*. 2018 May 1;72:94–109.
33. Carlier E, Marquette S, Peerboom C, Denis L, Benali S, Raquez J-M, et al. Investigation of the parameters used in fused deposition modeling of poly(lactic acid) to optimize 3D printing sessions. *Int J Pharm*. 2019 Jun 30;565:367–77.
34. Carlier E, Marquette S, Peerboom C, Amighi K, Goole J. Development of mAb-loaded 3D-printed (FDM) implantable devices based on PLGA. *Int J Pharm*. 2021 Mar 15;597:120337.
35. Park K, Skidmore S, Hadar J, Garner J, Park H, Otte A, et al. Injectable, long-acting PLGA formulations: Analyzing PLGA and understanding microparticle formation. *J Controlled Release*. 2019 Jun 28;304:125–34.
36. Sharifi F, Otte A, Yoon G, Park K. Continuous in-line homogenization process for scale-up production of naltrexone-loaded PLGA microparticles. *J Controlled Release*. 2020 Sep 10;325:347–58.
37. Shi N-Q, Zhou J, Walker J, Li L, Hong JKY, Olsen KF, et al. Microencapsulation of luteinizing hormone-releasing hormone agonist in poly (lactic-co-glycolic acid) microspheres by spray-drying. *J Controlled Release*. 2020 May 10;321:756–72.
38. Anderson J, Shives M. Biodegradation and biocompatibility of PLA and PLGA microspheres. *Adv Drug Deliv Rev*. 1997 Oct 13;28(1):5–24.
39. Arrighi A, Marquette S, Peerboom C, Denis L, Goole J, Amighi K. Development of PLGA microparticles with high immunoglobulin G-loaded levels and sustained-release properties obtained by spray-drying a water-in-oil emulsion. *Int J Pharm*. 2019 Jul 20;566:291–8.
40. Parent M, Clarot I, Gibot S, Derive M, Maincent P, Leroy P, et al. One-week in vivo sustained release of a peptide formulated into in situ forming implants. *Int J Pharm*. 2017 Apr 15;521(1):357–60.

41. Ravivarapu HB, Burton K, DeLuca PP. Polymer and microsphere blending to alter the release of a peptide from PLGA microspheres. *Eur J Pharm Biopharm.* 2000 Sep 1;50(2):263–70.
42. Wischke C, Schwendeman SP. Principles of encapsulating hydrophobic drugs in PLA/PLGA microparticles. *Int J Pharm.* 2008 Dec 8;364(2):298–327.
43. Acharya G, Shin CS, Vedantham K, McDermott M, Rish T, Hansen K, et al. A study of drug release from homogeneous PLGA microstructures. *J Controlled Release.* 2010 Sep 1;146(2):201–6.
44. Fang Y, Zhang N, Li Q, Chen J, Xiong S, Pan W. Characterizing the release mechanism of donepezil-loaded PLGA microspheres in vitro and in vivo. *J Drug Deliv Sci Technol.* 2019 Jun 1;51:430–7.
45. Kempe S, Mäder K. In situ forming implants - an attractive formulation principle for parenteral depot formulations. *J Controlled Release.* 2012 Jul 20;161(2):668–79.
46. Ochi M, Wan B, Bao Q, Burgess DJ. Influence of PLGA molecular weight distribution on leuprolide release from microspheres. *Int J Pharm.* 2021 Apr 15;599:120450.
47. Kraus VB, Conaghan PG, Aazami HA, Mehra P, Kivitz AJ, Lufkin J, et al. Synovial and systemic pharmacokinetics (PK) of triamcinolone acetonide (TA) following intra-articular (IA) injection of an extended-release microsphere-based formulation (FX006) or standard crystalline suspension in patients with knee osteoarthritis (OA). *Osteoarthritis Cartilage.* 2018 Jan;26(1):34–42.
48. Klose D, Siepmann F, Elkharraz K, Krenzlin S, Siepmann J. How porosity and size affect the drug release mechanisms from PLGA-based microparticles. *Int J Pharm.* 2006 May 18;314(2):198–206.
49. Kohno M, Andhariya JV, Wan B, Bao Q, Rothstein S, Hezel M, et al. The effect of PLGA molecular weight differences on risperidone release from microspheres. *Int J Pharm.* 2020 May 30;582:119339.
50. Lin X, Yang H, Su L, Yang Z, Tang X. Effect of size on the in vitro/in vivo drug release and degradation of exenatide-loaded PLGA microspheres. *J Drug Deliv Sci Technol.* 2018 Jun 1;45:346–56.
51. Hamoudi-Ben Yelles MC, Tran Tan V, Danede F, Willart JF, Siepmann J. PLGA implants: How Poloxamer/PEO addition slows down or accelerates polymer degradation and drug release. *J Control Release Off J Control Release Soc.* 2017 May 10;253:19–29.
52. Ramazani F, Chen W, van Nostrum CF, Storm G, Kiessling F, Lammers T, et al. Strategies for encapsulation of small hydrophilic and amphiphilic drugs in PLGA microspheres: State-of-the-art and challenges. *Int J Pharm.* 2016 Feb 29;499(1):358–67.
53. Wan F, Yang M. Design of PLGA-based depot delivery systems for biopharmaceuticals prepared by spray drying. *Int J Pharm.* 2016 Feb 10;498(1):82–95.

VIII. PLGA BASED 3D PRINTED IMPLANTS – IMPACT OF FILLING DENSITY ON DRUG RELEASE

54. Gèze A, Venier-Julienne MC, Mathieu D, Filmon R, Phan-Tan-Luu R, Benoit JP. Development of 5-iodo-2'-deoxyuridine milling process to reduce initial burst release from PLGA microparticles. *Int J Pharm.* 1999 Feb 15;178(2):257–68.
55. Feuerbach T, Callau-Mendoza S, Thommes M. Development of filaments for fused deposition modeling 3D printing with medical grade poly(lactic-co-glycolic acid) copolymers. *Pharm Dev Technol.* 2019 Apr 21;24(4):487–93.
56. Madla CM, Trenfield SJ, Goyanes A, Gaisford S, Basit AW. 3D Printing Technologies, Implementation and Regulation: An Overview. In: Basit AW, Gaisford S, editors. *3D Printing of Pharmaceuticals* [Internet]. Cham: Springer International Publishing; 2018 [cited 2021 Jul 6]. p. 21–40. (AAPS Advances in the Pharmaceutical Sciences Series). Available from: https://doi.org/10.1007/978-3-319-90755-0_2
57. Stavropoulos P, Foteinopoulos P. Modelling of additive manufacturing processes: a review and classification. *Manuf Rev.* 2018;5:2.
58. Guessasma S, Nouri H, Roger F. Microstructural and Mechanical Implications of Microscaled Assembly in Droplet-based Multi-Material Additive Manufacturing. *Polymers.* 2017 Aug 18;9(8):372.
59. Lizambard M, Menu T, Fossart M, Bassand C, Agossa K, Huck O, et al. In-situ forming implants for the treatment of periodontal diseases: Simultaneous controlled release of an antiseptic and an anti-inflammatory drug. *Int J Pharm.* 2019 Dec 15;572:118833.
60. Bassand C, Benabed L, Verin J, Danede F, Willart J-F, Siepmann F, et al. Hot melt extruded ibuprofen-loaded PLGA implants: Importance of heat exposure. *Journal of Drug Delivery Science and Technology* - Submitted. 2021;

IX. GENERAL CONCLUSION AND DISCUSSION

IX. GENERAL CONCLUSION AND DISCUSSION

IX.1. General conclusion

PLGA is a first category choice for polymer-based parenteral controlled drug delivery systems due to its excellent biocompatibility, biodegradability, and use in several FDA-approved products. However, establishing an in vitro in vivo correlation regarding drug release of such devices is challenging as many different mechanisms are involved in drug release. Thus, it is of great importance to properly characterize the devices, to identify the release mechanism by which the API is released from the device.

In the past few years, 3D printing technologies have revolutionized the development of new controlled drug release devices. These technologies allow to precisely control the size, shape, internal and external porosity of the device, and so the release rate of the API.

In this context the research objectives of this thesis were divided into two parts:

- (i) Development of experimental set-ups for in vitro drug release measurement for implants administrated to the subcutis, and investigation on the impact of several implants attribute on in vitro drug release;
- (ii) Development of PLGA based controlled drug release implants using 3D printing technologies, and investigation of the impact of the structure of the implant on in vitro drug release.

The research results of this Ph.D. thesis had been described in seven parts corresponding to scientific papers that have either been submitted in scientific journals or plan to be. Those investigated led to the following conclusions:

1. *How hydrogels surrounding PLGA implants limit swelling and slow down drug release:*

The presence of an agarose gel surrounding PLGA implants significantly hinders polymer swelling (sterically) and slows down drug release (due to delayed penetration of substantial amounts of water into the system). In vivo it can be expected that surrounding tissue has a similar mechanical effect. However, yet it is unknown how important the impact of mechanical stress caused by body movements (e.g., muscle contractions) for the fate of a degrading PLGA implant is. The results presented in this study can help developing more realistic in vitro drug release set-ups for parenteral drug delivery systems. They also strengthen the hypothesis that implant *swelling* plays an orchestrating role for the control of drug release from PLGA-based drug delivery systems.

2. *Hot-melt extruded ibuprofen-loaded PLGA implants: Importance of heat exposure:*

Hot melt extrusion offers an interesting potential for the preparation of PLGA-based implants. However, the exposure to heat can decrease the average polymer molecular weight and alter the physical state of the drug in the polymeric matrix (and of course, thermally degrade heat sensitive drugs). The drug might be present in the form of individual molecules/ions distributed throughout the PLGA network (“dissolved”), or dispersed in the form of crystalline or amorphous tiny particles. It is worth to monitor the state of the drug and potential transformations during implant manufacturing. For instance, increasing exposure times to heat might increase the relative amount of drug, which is dissolved in the PLGA, altering the importance of the initial “burst release”. In the present study this phenomenon could be monitored, but its importance on drug release was limited. However, the impact for other drugs or other polymers might be much more pronounced and certain systems might be much less robust and “forgiving”.

3. *PLGA implants for controlled drug release: Impact of the diameter:*

The variation of the diameter of a PLGA implant is an effective tool to adjust desired absolute and relative release kinetics. In the case of hot melt extruded ibuprofen-loaded implants, bi-phasic release patterns were observed: A zero order release phase was followed by a rapid, final drug release phase (accounting for 80-90 % drug). The decrease in the relative drug release rate with increasing system diameter can be attributed to the longer diffusion pathways to be overcome. The onset of the final rapid drug release phase was delayed, because the larger polymer matrices are mechanically more stable, retarding the onset of substantial entire implant swelling, which facilitates drug release.

4. *How bulk fluid renewal can affect drug release from PLGA implants:*

Great caution has to be paid when defining the conditions for in vitro drug release measurements from PLGA implants: The systems become highly fragile once substantial polymer swelling sets on. The renewal of important parts of the release medium can cause partial damage of the highly fragile polymeric systems, accelerating device disintegration and decreasing the length of the diffusion pathways for the drug to be overcome. Embedding implants into agarose gels and limiting the sampling volume can limit these effects. In any case, it must not be forgotten that, once substantial system swelling sets on, the devices become highly fragile.

5. 3D printing of ibuprofen loaded controlled release implants with PLGA – Proof of concept and impact filling pattern:

3D printing by FFF is an interesting tool for the manufacturing of PLGA based control drug delivery devices. The polymer demonstrated viscoelastic properties compatible with the 3D printing technologies. The use of hot-melt extrusion made possible the manufacturing of Ibuprofen-loaded PLGA filament with diameters allowing 3D printing by FFF. Moreover, those filaments were printable without any substantial loss of molecular weight of the polymer nor ibuprofen up to 150°C. 3D printing of implants containing ibuprofen, with three different internal structures was achievable. This leading to the obtention of implants allowing to maintain the release of ibuprofen for up to 9 days, with a monophasic release pattern.

6. PLGA based 3D printed mesh – the impact of the 3D printed technology on drug release:

3D printing has many advantages, such as the flexibility of dosages or the possibility of creating complex structures. However, the choice of printing technology and settings can greatly influence product performance. The objective of this research was, to study and compare the impact of two printing processes on the physicochemical properties of PLGA and the in vitro performance of the implants obtained. For this, two sets of implants were printed using DDM and FFF technology. Both technologies appear to have advantages and disadvantages regarding the production of 3D printing PLGA based control drug delivery devices. DDM technology allows to easily obtain homogeneous drug-loaded implants as the printing is done from a statistical mixture of pellets. Another advantage of this technology is that it allows avoiding the challenging development needed with FFF for the obtention of filament homogeneous in diameter. However, this technology exposes the polymer and the drug substance to high mechanical stress compared to FFF technology. The implants printed by DDM have a three-phase in vitro release profile with a “burst” effect, then a slower release phase, and finally a final rapid release phase due to the significant swelling of the PLGA. FFF-printed implants exhibit a two-phase in vitro release profile. This difference is mainly due to the difference in structure obtained, leading to heavier implants by DDM, and to a longer diffusion pathway for the drug substance.

7. PLGA based 3D printed mesh – the impact of filling density on drug release:

Droplet deposition modeling allows obtaining ibuprofen-loaded 3D printed PLGA implants with different filling densities. Thus, the variation of the filling density is an effective tool to

adjust desired absolute and relative release kinetics. The obtained implants exhibit a triphasic release pattern: with a burst release from 5 to 10% during the first days of exposure to the release medium, followed by the drug, and a lag phase up to day 5 or 9 depending on the filling density of the implants. The decrease in the relative drug release rate with increasing implant filling can be attributed to the longer diffusion pathways to be overcome. The onset of the final rapid drug release phase was delayed, because the larger polymer matrices are mechanically more stable, retarding the onset of substantial entire implant swelling, which facilitates drug release.

IX.2. Future perspectives

In this context, multiples perspectives could be imagined to this project. Some of them would be listed below, regarding the two main objectives of this thesis:

(i) Development of experimental set-ups for *in vitro* drug release measurement for implants administrated to the subcutis, and investigation on the impact of several implants attribute on *in vitro* drug release:

- Investigation of biosimilar release medium, taking into consideration the protein and lipid content in the subcutis,
- Taking into consideration the possible changes *in vivo* after administration (inflammation, etc...) and how it could be mimic *in vitro*,
- Investigation of the impact of mechanical stress on *in vitro* performances.

(ii) Development of PLGA based controlled drug release implants using 3D printing technologies, and investigation of the impact of the structure of the implant on *in vitro* drug release:

- Investigate different shapes, geometry size of devices,
- Improving the printing quality of PLGA by DDM,
- Find a correlation between the *in vitro* performances and the morphological characteristics of the 3D printed implants.

SUMMARY

This thesis was driven by two main axes:

On one hand, poly (lactic-co-glycolic) acid (PLGA) is a first category choice for polymer-based parenteral controlled drug delivery systems due to its excellent biocompatibility, biodegradability, and use in several FDA-approved products for decades (microparticles, implants, *in situ* forming implants). However, establishing an *in vitro* *in vivo* correlation regarding drug release of such devices is challenging as many different mechanisms are involved in drug release. Thus, it is of great importance to properly characterize those kinds of devices, to identify the release mechanism by which the API is released from the device.

On the other hand, in the past few years, three -dimension (3D) printing technologies have revolutionized the development of controlled drug release devices. These technologies allow to precisely control the size, shape, porosity of the device, and so the release rate of the API.

In this context, the two objectives of this thesis were:

- (i) To develop an experimental set-up for *in vitro* drug release measurement for implants aimed to be administrated to the subcutis, and investigate the impact of several implants attribute on *in vitro* drug release;
- (ii) To develop PLGA based controlled drug release implants using 3D printing technologies.

As subcutaneous environment behaves more like a gel than a fluid, two *in vitro* set-up involving agarose gel to mimic the subcutis have been developed. The impact of those set-ups, on the behavior or hot melt extruded ibuprofen loaded PLGA based implants have been investigated.

Through this investigation, the following conclusions have been drawn:

- The presence of an agarose gel surrounding PLGA implants significantly hinders polymer swelling (sterically) and slows down drug release (due to delayed penetration of substantial amounts of water into the system).
- Increasing exposure times to heat might increase the relative amount of drug, which is dissolved in the PLGA, altering the importance of the initial “burst release”.
- The variation of the diameter of a PLGA implant is an effective tool to adjust desired absolute and relative release kinetics.
- Great caution has to be paid when defining the conditions for *in vitro* drug release measurements from PLGA implants.

Then, the impact of the heating treatment on PLGA ibuprofen mixture rheological behavior to access its printability have been investigated. Ibuprofen loaded PLGA based implants have been printed using: Fused Filament Fabrication (FFF), and Droplet Deposition Modeling (DDM). The impact of the 3D printed technology, the filling pattern, and the filling density of the implants on their in vitro performances have been investigated. By investigating those parameters, the following conclusions have been drawn:

- Ibuprofen loaded PLGA filaments were printable without any substantial loss of molecular weight of the polymer nor ibuprofen up to 150°C, and their viscoelastic behavior are compatible with 3D printing.
- 3D printing of implants containing ibuprofen, with three different internal structures was achievable. This leading to the obtention of implants allowing to maintain the release of ibuprofen for up to 9 days, with a monophasic release pattern.
- DDM technology allows to easily obtain homogeneous drug-loaded implants as the printing is done from a statistical mixture of pellets, allowing to avoid the challenging development of filament with constant diameter. However, this technology exposes the polymer and the drug substance to high mechanical stress compared to FFF technology.
- The variation of the filling density is an effective tool to adjust desired absolute and relative release kinetics. The obtained implants exhibit a triphasic release pattern: with relative higher burst release and shorter lag phase for the lowest filling density implants. The decrease in the relative drug release rate with increasing implant filling can be attributed to the longer diffusion pathways to be overcome.

Keywords: PLGA, in vitro set-up, agarose gel, swelling, 3D printing, fused filament fabrication, droplet deposition modeling.

RESUME

Cette thèse s'est articulée autour de deux axes principaux :

D'une part, le copolymère d'acides lactique et glycolique (PLGA) est un choix de première ligne en matière de libération contrôlée pour la voie parentérale. Sa biocompatibilité, et biodégradabilité ont menées à son utilisation dans plusieurs produits approuvés par la FDA. De nombreux mécanismes sont impliqués dans la libération de substance active (SA) à partir de ces systèmes.

D'autre part, au cours des dernières années, les technologies d'impression en trois dimensions (3D) ont révolutionné le développement de nouveaux médicaments à libération contrôlée. Ces nouvelles technologies permettent de contrôler précisément la taille, la forme, la porosité des formes galéniques produites, et ainsi de contrôler le taux de libération de la SA.

Dans ce contexte, les deux principaux objectifs de cette thèse étaient :

- (i) La mise au point d'une méthode de mesure de la libération de SA in vitro pour des implants destinés à être administrés par voie sous cutanée, et l'étude de l'impact de plusieurs attributs d'implants sur la libération de SA in vitro ;
- (ii) Le développement d'implants à libération contrôlée de médicaments à base de PLGA à l'aide de technologies d'impression 3D.

Le tissu sous-cutané se comportant davantage comme un gel que comme un fluide, deux méthodes d'évaluation de la libération in vitro de SA impliquant du gel d'agarose pour mimer les propriétés du tissu sous-cutané ont été développés. Leur impact, sur le comportement d'implants à base d'ibuprofène obtenu par extrusion à chaud ont été étudiés. Cette étude a permis de tirer les conclusions suivantes :

- La présence d'un gel d'agarose autour des implants PLGA entrave le gonflement du polymère et ralentit la libération de la SA.
- L'augmentation du temps d'exposition à la chaleur pourrait augmenter la quantité relative de SA, qui est dissoute dans la matrice de PLGA, ce qui modifierait l'importance de l'effet « *burst* » initial.
- La variation du diamètre d'un implant PLGA est un outil efficace pour ajuster la cinétique de libération absolue et relative désirée.
- La définition des conditions pour les mesures de libération de substance active in vitro à partir d'implants PLGA doit être faite avec attention.

L'impact du traitement thermique sur le comportement rhéologique du mélange d'ibuprofène PLGA a également été étudié. Des implants à base de PLGA chargés en ibuprofène ont été imprimés par : fabrication de filaments fondu (FFF) et dépôt de gouttelettes (DDM). L'impact de la technologie d'impression 3D, du motif de remplissage et de la densité de remplissage des implants sur leurs performances in vitro a été étudié. Les conclusions suivantes ont été tirées :

- Des filaments PLGA chargés d'ibuprofène ont pu être utilisés pour être imprimés sans impacter de façon significative le poids moléculaire du polymère pour des températures allant jusqu'à 150 °C, leur comportement viscoélastique est compatible avec l'impression 3D.
- Il a été possible d'imprimer des implants contenant de l'ibuprofène, avec trois structures internes différentes. Ceux-ci permettant de maintenir la libération de l'ibuprofène jusqu'à 9 jours, avec un profil monophasique.
- La technologie DDM permet d'obtenir facilement des implants chargés homogènement en SA et permet d'éviter l'étape de développement de filament nécessaire pour l'impression par FFF. Toutefois, cette technologie expose le polymère et la SA à un stress mécanique élevé par rapport à la technologie FFF.
- La variation de la densité de remplissage est un outil efficace pour ajuster la cinétique de libération de la SA. Les implants qui ont été imprimés avec différentes densités de remplissage, présentent un schéma de libération triphasique : avec une libération « burst » relativement plus élevée et une phase de plateau plus courte pour les implants de densité de remplissage la plus faible. La diminution du taux relatif de libération de SA avec l'augmentation de la densité de remplissage de l'implant est due à des chemins de diffusion allongés.

Mots-clés : PLGA, dispositif d'évaluation de la libération de substance active, gel d'agarose, gonflement, impression 3D, fabrication de filaments fusionnés, dépôt de gouttelettes.

LIST OF PUBLICATIONS

LIST OF PUBLICATIONS

Research Articles

Bassand C, Benabed L, Verin J, Freitag J, Charlon S, Siepmann F, Soulestin J, Siepmann J. PLGA based 3D printed implants – Impact of filling density on drug release, **2021** – To be reviewed by the co-authors

Bassand C, Benabed L, Charlon S, Verin J, Siepmann F, Soulestin J, Siepmann J. PLGA based 3D printed implant – Impact of the 3D printed technology on drug release, **2021** – To be reviewed by the co-authors

Bassand C, Benabed L, Charlon S, Nagalakshmaiah M, Samuel C, Siepmann F, Soulestin J, Siepmann J. 3D printing of ibuprofen loaded controlled release implants with PLGA – Proof of concept and impact of filling pattern, **2021** – To be reviewed by the co-authors

Bassand C, Benabed L, Freitag J, Verin J, Siepmann F, Siepmann J. How bulk fluid renewal can affect drug release from PLGA implants, *AAPS PharmSci Tech* **2021** – To be submitted

Bassand C, Freitag J, Benabed L, Verin J, Siepmann F, Siepmann J. PLGA implants for controlled drug release: Impact of the diameter, *EJPB* **2021**– To be submitted

Bassand C, Benabed L, Verin J, Danede F, Lefol L.A, Willart J.F, Siepmann F, Siepmann J. Hot-melt extruded ibuprofen-loaded PLGA implants: Importance of heat exposure, *JDDST* **2021** – To be submitted

Bassand C, Verin,J, Lamatsch M, Siepmann F, Siepmann J. How hydrogels surrounding PLGA implants limit swelling and slow down drug release, *JCR* **2021** – Submitted

Tamani F, **Bassand C**, Hamoudi MC, Siepmann F, Siepmann J. Mechanistic explanation of the (up to) 3 release phases of PLGA microparticles: Monolithic dispersions studied at lower temperatures. *Int J Pharm.* **2021** Mar 1;596:120220.

Tamani F, **Bassand C**, Hamoudi MC, Danede F, Willart JF, Siepmann F, et al. Mechanistic explanation of the (up to) 3 release phases of PLGA microparticles: Diprophylline dispersions. *Int J Pharm.* **2019** Dec 15;572:118819.

Lizambard M, Menu T, Fossart M, **Bassand C**, Agossa K, Huck O, et al. In-situ forming implants for the treatment of periodontal diseases: Simultaneous controlled release of an antiseptic and an anti-inflammatory drug. *Int J Pharm.* **2019** Dec 15;572:118833.

Ousset A, **Bassand C**, Chavez P-F, Meeus J, Robin F, Schubert MA, et al. Development of a small-scale spray-drying approach for amorphous solid dispersions (ASDs) screening in early drug development. *Pharm Dev Technol.* **2019** Jun;24(5):560–74.

Bassand C, Abdel-Mottaleb MMA. Penetration Enhancer Containing Vesicles (PEVs) as Carriers for Enhancing the Dermal Deposition of Thymoquinone. *IJPPR.* **2016** 7:13.

Oral communications

Bassand C, Lamatsch M, Verin J, Siepmann F, Siepmann J. Impact of the in vitro release set-up on drug release from PLGA implants. 12th PBP World Meeting **2021**.

Bassand C, Gautier H, Samuel C, Verin J, Nagalakshmaiah M, Siepmann F, Soulestin J, Siepmann J. Is PLGA suitable for 3D printing of controlled release implants? 14th PSSRC Annual Meeting **2020**.

Bassand C, Lamatsch M, Verin J, Siepmann F, Siepmann J. Impact of the in vitro release set-up on ibuprofen release from PLGA implants. 14th PSSRC Annual Meeting **2020**.

Tamani F, **Bassand C**, Hamoudi M-C, Siepmann F, Siepmann J. Drug release from single PLGA microparticle. 12th PSSRC Annual Meeting **2018**.

Poster presentations

Bassand C, Charlon S, Freitag J, Siepmann F, Siepmann J, Soulestin J. 3D printed PLGA implants loaded with ibuprofen – Proof of concept. 12th PBP World Meeting **2021**.

Bassand C, Freitag J, Siepmann F, Siepmann J. Importance of the diameter of PLGA implants for system swelling and drug release. 12th PBP World Meeting **2021**.

Bassand C, Fossart M, Siepmann F, Siepmann J. Importance of the sampling procedure and drug loading for ibuprofen release from PLGA implants. 12th PBP World Meeting **2021**.

Bassand C, Lamatsch M, Verin J, Siepmann F, Siepmann J. Impact of the in vitro release set-up on drug release from PLGA implants. 12th PBP World Meeting **2021**.

Bassand C, Nagalakshmaiah M, Siepmann F, Soulestin F, Siepmann J. Is PLGA 503H a potentially suitable matrix former for 3D printing of controlled release implants? 12th PBP World Meeting **2021**.

Bassand C, Lamatsch M, Verin J, Siepmann F, Siepmann J. Dynamic changes of the pH inside and outside PLGA implants prepared by HME. 12th PBP World Meeting **2021**.

Bassand C, Gautier H, Samuel C, Verin J, Siepmann F, Soulestin F, Siepmann J. Rheology of ibuprofen-PLGA blends. 12th PBP World Meeting **2021**.

Bassand C, Verin J, Siepmann F, Siepmann J. Impact of the HME manufacturing process on the burst release of ibuprofen from PLGA implants. 12th PBP World Meeting **2021**.

Tamani F, Hamoudi M C, **Bassand C**, Siepmann F, Siepmann J. Drug release from PLGA microparticles: the orchestrating role of polymer swelling and "accidental" release. 3rd European Conference on Pharmaceutics **2019**.

Tamani F, **Bassand C**, Hamoudi M-C, Willart J-F, Danède F, Siepmann F, Siepmann J. How single PLGA microparticles behave. 3rd European Conference on Pharmaceutics **2019**.

Tamani F, **Bassand C**, Hamoudi M-C, Siepmann F, Siepmann J. Impact of the temperature on diprophylline release from ensembles of PLGA microparticles. 3rd European Conference on Pharmaceutics **2019**.

Tamani F, **Bassand C**, Hamoudi M-C, Siepmann F, Siepmann J. How differently do single PLGA microparticles behave? APGI formulation days **2019**.

LIST OF PUBLICATIONS

CURRICULUM VITAE

Curriculum vitae

Name Céline Bassand
Birth October 27th, 1993 in Besançon, France
Nationality French

Career

Since July 2021 Post-Doc at Novartis, Basel, Switzerland
Development of dissolution set-up for in vitro in vivo correlation of long acting injectables

2018 – 2021 Ph.D. Student at the Université de Lille, France
(3 years) Subject: *In vitro* drug release from 3D printed dosage forms
Supervisor: Pr. Juergen Siepmann
Laboratory: INSERM U1008 Controlled Drug Delivery Systems and Biomaterials

2018 M.Sc. Internship at the Université de Lille, France
(6months) Subject: Towards a better understanding of the drug release mechanisms in PLGA microparticles
Supervisor: Dr. Fahima Tamani, Pr. Florence Siepmann
Laboratory: INSERM U1008 Controlled Drug Delivery Systems and Biomaterials

2017 Pharmacy internship at UCB Pharma, Braine l'Alleud, Belgium
(5 months) Subject: Development of a small-scale spray-drying approach for amorphous soli dispersions screening in early drug development
Supervisor: Dr. Aymeric Ousset
Laboratory: Formulation and process development

2016-2017 Pharmacy internship at CHU Besançon, France
(6 months) Subject: Analytical Development for total blood and plasma analysis

using HPLC-UV and LC-MS-MS

Supervisor: Dr. Bernard Royer

Laboratory: Clinical pharmacology and toxicology

2016

Pharmacy internship at Universität Bonn, Germany

(3 months)

Subject: Penetration enhancer-containing vesicles as carriers for cutaneous delivery of Thymoquinone

Supervisor: Dr. Mona Abdel-Mottaleb

Laboratory: Pharmaceutical Technology and Biopharmacy

Education

2018 – 2021

Doctor of Philosophy (Ph.D.), Université de Lille, France

Subject: *In vitro* drug release from 3D printed dosage forms

2011 – 2018

Doctor of Pharmacy (Pharm.D.), Université de Franche-Comté, France

Subject: PLGA based microparticles

Obtained with first class honors

2017 – 2018

Master of Science (M.Sc.), Université Paris-Saclay, France

Pharmaceutical technology and biopharmaceutics

Obtained with first class honors - Valedictorian

Attending international conferences

2021

3rd SOTAX Congress - Online

2021

15th PSSRC Annual meeting– Online

2021

12th PBP World meeting – Online

2020

14th PSSRC Annual meeting – Chair session – Online

2019

3rd European Conference on Pharmaceutics – Bologna, Italy

2018

11th PBP World meeting – Grenada, Spain

Reviewer for scientific journals

International Journal of Pharmaceutics

Journal of Drug Delivery Science and Technology

Training of students

Lydia Benabed	Université Paris Saclay, France Master student, pharmacist (6 months)
Jana Freitag	Universität Regensburg, Germany Erasmus student, pharmacist (5 months)
Cedric Guyot	Université de Lille, France Internship student, pharmacist (1 week)
Hana Gautier	Université Paris Descartes, France Master student (5 months)
Martin Lamatsch	Freie Universität Berlin, Germany Erasmus student, pharmacist (5 months)
Celia Dewailly	Université de Lille, France Master student, pharmacist (7 weeks)
Clotilde Terrier	Université de Lille, France Internship student, pharmacist (3 weeks)